

BL DIG ✓

FOR REFERENCE ONLY

11 FEB 1999

41 0600978 1



ProQuest Number: 10290090

All rights reserved

INFORMATION TO ALL USERS

The quality of this reproduction is dependent upon the quality of the copy submitted.

In the unlikely event that the author did not send a complete manuscript and there are missing pages, these will be noted. Also, if material had to be removed, a note will indicate the deletion.



ProQuest 10290090

Published by ProQuest LLC (2017). Copyright of the Dissertation is held by the Author.

All rights reserved.

This work is protected against unauthorized copying under Title 17, United States Code
Microform Edition © ProQuest LLC.

ProQuest LLC.
789 East Eisenhower Parkway
P.O. Box 1346
Ann Arbor, MI 48106 – 1346

**THE SYNTHESIS AND PROPERTIES OF
CERTAIN HETEROCYCLIC
MESOGENS**

SANDRA SAINT

A thesis submitted in partial fulfilment of the
requirements of The Nottingham Trent University
for the degree of Doctor of Philosophy

This research programme was carried out
in collaboration with Central Research Laboratories (CRL)

July 1998

THE SYNTHESIS AND PROPERTIES OF CERTAIN HETEROCYCLIC MESOGENS

Summary of a thesis submitted for the degree of
Doctor of Philosophy

by

Sandra Saint

Abstract

This thesis reports the synthesis and properties of three-ring thiophene- and pyrimidine-based liquid crystals in order to evaluate their usefulness as potential additives in commercial liquid crystal mixtures. Confidentiality restricts the reporting of actual measurements evaluated during the mixture investigations. Two homologous series, namely: 5-*n*-alkanoyl-5''-*n*-alkyl-2,2':5',2''-terthienyls (**series I**) and their corresponding reduced homologues 5,5''-di-*n*-alkyl-2,2':5',2''-terthienyls (**series II**) were prepared.

Members of **series I** exhibit the S_A phase alone whereas members of **series II** exhibit the CrG phase. Unfortunately, when incorporated in commercial mixtures, members of **series I** and **II** cause photochemical degradation. The thiophene strategy was abandoned and new work focused on three-ring pyrimidine-based compounds.

Twelve series of fluorinated three-ring pyrimidine-based compounds were successfully prepared via palladium-catalysed boronic acid cross-coupling technology utilising 5-bromo-2-iodopyrimidine (**41**) as a key intermediate. However, initially the first pyrimidine compound, i.e., 2-(4-*n*-hexyloxyphenyl)-5-(2,3-difluoro-4-*n*-heptylphenyl)pyrimidine (**38c**) was prepared utilising the classical ring closure/condensation technique which was extremely troublesome.

| | |
|--------------------------|--|
| (series IIIa-c) | 2-(4- <i>n</i> -alkoxyphenyl)-5-(2,3-difluoro-4- <i>n</i> -alkylphenyl)pyrimidines |
| (series IV) | 2-(2,3-difluoro-4- <i>n</i> -alkoxyphenyl)-5-(4- <i>n</i> -alkylphenyl)pyrimidines |
| (series V) | 2-(4- <i>n</i> -alkylphenyl)-5-(2,3-difluoro-4- <i>n</i> -alkoxyphenyl)pyrimidines |
| (series VI) | 2-(2,3-difluoro-4- <i>n</i> -alkylphenyl)-5-(4- <i>n</i> -alkoxyphenyl)pyrimidines |
| (series VII) | 2-(4- <i>n</i> -alkylphenyl)-5-(2,3-difluoro-4- <i>n</i> -alkylphenyl)pyrimidines |
| (series VIII) | 2-(2,3-difluoro-4- <i>n</i> -alkylphenyl)-5-(4- <i>n</i> -alkylphenyl)pyrimidines |
| (series IX) | 2-(4- <i>n</i> -alkoxyphenyl)-5-(2-fluoro-4- <i>n</i> -alkylphenyl)pyrimidines |
| (series X) | 2-(2-fluoro-4- <i>n</i> -alkoxyphenyl)-5-(4- <i>n</i> -alkylphenyl)pyrimidines |
| (series XI) | 2-(4- <i>n</i> -alkylphenyl)-5-(2-fluoro-4- <i>n</i> -alkoxyphenyl)pyrimidines |
| (series XII) | 2-(2-fluoro-4- <i>n</i> -alkylphenyl)-5-(4- <i>n</i> -alkoxyphenyl)pyrimidines |
| (series XIII) | 2-(4- <i>n</i> -alkylphenyl)-5-(2-fluoro-4- <i>n</i> -alkylphenyl)pyrimidines |
| (series XIV) | 2-(2-fluoro-4- <i>n</i> -alkylphenyl)-5-(4- <i>n</i> -alkylphenyl)pyrimidines |

The mesomorphic properties are dependant upon: the number of fluoro-substituents; nature of the terminal groups and; disposition of the pyrimidine ring within the central molecular core. High order crystal smectic phases are not observed and the phase types are restricted to N, S_A and S_C. Generally, dialkyl compounds do not exhibit the S_C phase.

Acknowledgements

I would like to thank Dr. A.S. Matharu and Dr. R.C. Wilson for their invaluable advice and excellent supervision throughout the course of this work.

The author is indebted to Central Research Laboratories for their sponsorship and would like to thank Dr. L.K.M. Chan for his support and guidance.

Thanks are also due to The Nottingham Trent University for the award of a Research Studentship.

*'Let your life flow like a river. A river takes in all it passes over
and is absorbed by all it touches.'* Lao Tzu.

I would like to express my sincerest thanks to my parents, Olive and Alec, and my parents-in-law, John and Jean, for their encouragement and support over the years for without which this thesis would not have been completed.

HOW TO USE THIS THESIS

The thesis is divided into four sections, namely:

1. INTRODUCTION AND AIMS

This section details the historical development of liquid crystals from its origin in 1888 to the present date. It discusses the various textures and optical characterisation together with applications of liquid crystals. As a lead into the subsequent sections, it finishes with general aims since two distinct areas of work have been investigated.

2. THIOPHENE-BASED LIQUID CRYSTALS

This is a self-contained section which includes an introduction on thiophene and thiophene liquid crystals, specific aims, results and discussion and, experimental.

3. PYRIMIDINE-BASED LIQUID CRYSTALS

This is also a self-contained section which includes an introduction on pyrimidine and pyrimidine liquid crystals, specific aims, results and discussion and, experimental. An in-depth comparative study is reported between pyrimidine-based compounds and also with their non-heterocyclic counterparts.

4. REFERENCES

This contains all the references cited in the previous sections.

Reagents, solvents and equipment used during this work

Acetone and dichloromethane (DCM) were dried over granular calcium chloride. Diethyl ether (ether) was dried over sodium wire. Dry tetrahydrofuran (THF) was prepared by continuously heating the solvent under reflux with sodium metal and benzophenone. *N,N*-Dimethylformamide (DMF) was distilled from calcium hydride and stored over molecular sieves. Ethanol and toluene were dried over molecular sieves. Titanium(IV) chloride (TiCl_4), anhydrous aluminium chloride (AlCl_3), dimethoxyethane (DME) and 1.6M *n*-butyllithium (solution in hexane) were used as supplied. All commercial starting materials and reagents were supplied by either the Aldrich Chemical Company Ltd. or Lancaster Synthesis Ltd.


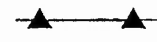
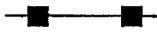
Structural confirmation of the intermediates and the products was obtained by ^1H NMR spectroscopy (JEOL FX60Q 270 MHz spectrometer) and infra-red spectroscopy (Perkin-Elmer FT 1605 spectrophotometer). Measurements of transition temperatures and microscopic observations of mesophase textures were made using an Olympus BH-2 polarising microscope in conjunction with a Mettler FP52 hot stage and FP5 control unit. The transition temperatures were confirmed by thermal analysis carried out using a Perkin-Elmer DSC7 differential scanning calorimeter at heating and cooling rates of $10^\circ\text{C min}^{-1}$. Elemental analyses were performed by the microanalysis department at The University of Nottingham.

Column chromatography was performed using silica gel (silica gel 60, 220-440 mesh size) and the progress of reactions was monitored by t.l.c. using silica gel coated on glass plates (silica gel 60, 250 μm layer thickness).

Abbreviations used in the results and discussion sections

Symbols have their usual meaning: K, crystal; CrG, crystal G; S_C, smectic C; S_A, smectic A; N, nematic; I, isotropic liquid. Thus K-N indicates the temperature (m.p.) at which the crystal (K) melts to the nematic phase (N). Values in parentheses are for monotropic transitions.

All compounds, Figures, Tables and Plates are numbered sequentially (continuously). A key to the graphs (*Figures 22 to 27* inclusive) is as follows:

-  Mesophase to mesophase or mesophase to isotropic liquid transition temperature.
-  Crystal to mesophase or crystal to isotropic liquid transition temperature.
-  Mesophase to crystal transition temperature.

CONTENTS

| | Page |
|---|------|
| 1. INTRODUCTION AND AIMS | 1 |
| 1.1 HISTORICAL REVIEW | 1 |
| 1.2 CLASSIFICATION AND MOLECULAR STRUCTURE OF LIQUID CRYSTALS | 6 |
| 1.2.1 Classification | 6 |
| 1.2.2 Molecular Structure..... | 7 |
| 1.3 MESOPHASE FORMATION | 9 |
| 1.4 OPTICAL CHARACTERISATION AND MESOPHASE TYPES | 12 |
| 1.4.1 Optical Characterisation | 12 |
| 1.4.2 Mesophase Types | 13 |
| 1.4.2.1 Nematic Mesophase (N)..... | 13 |
| 1.4.2.2 Cholesteric Mesophase (Ch or N*)..... | 14 |
| 1.4.2.3 Smectic Mesophase (S)..... | 16 |
| 1.4.2.3.1 Smectic Polymorphism..... | 17 |
| 1.5 THE CORRELATION BETWEEN MOLECULAR STRUCTURE AND LIQUID CRYSTALLINE BEHAVIOUR | 29 |
| 1.5.1 Influence of Terminal Substituents..... | 30 |
| 1.5.1.1 Homologation..... | 30 |
| 1.5.2 Influence of the Central Linking Group..... | 33 |
| 1.5.3 Influence of Lateral Substituents..... | 34 |
| 1.5.3.1 Lateral Fluorination..... | 36 |
| 1.6 ELECTRO-OPTIC APPLICATIONS OF LIQUID CRYSTALS | 38 |
| 1.6.1 Twisted Nematic and Supertwisted Nematic Displays | 39 |
| 1.6.2 Surface Stabilised Ferroelectric Displays..... | 40 |
| 1.7 AIMS | 45 |

| | | |
|---------|--|----|
| 2. | THIOPHENE-BASED LIQUID CRYSTALS | 47 |
| 2.1 | INTRODUCTION | 47 |
| 2.2 | RESULTS AND DISCUSSION | 49 |
| 2.2.1 | Optical and Thermal (DSC) Characterisation | 49 |
| 2.2.2 | Comparative Study of Series II with Analogous 4,4''-Disubstituted-1,1':4',1''-terphenyls | 54 |
| 2.3 | EXPERIMENTAL | 56 |
| 2.3.1 | The Synthesis of 5- <i>n</i> -Alkanoyl-5''- <i>n</i> -alkyl- (series I) and 5,5''-Di- <i>n</i> -alkyl-2,2':5',2''- terthienyls (series II) | 56 |
| 2.3.1.1 | Synthetic Overview | 56 |
| 2.3.1.2 | Experimental Procedures..... | 59 |
| 3. | PYRIMIDINE-BASED LIQUID CRYSTALS | 64 |
| 3.1 | INTRODUCTION | 64 |
| 3.2 | RESULTS AND DISCUSSION | 67 |
| 3.2.1 | 2-(4- <i>n</i> -Alkoxyphenyl)-5-(2,3-difluoro-4- <i>n</i> -alkylphenyl)- pyrimidines (series IIIa-d)..... | 67 |
| 3.2.2 | 2-(2,3-Difluoro-4- <i>n</i> -alkoxyphenyl)-5-(4- <i>n</i> -alkylphenyl)- pyrimidines (series IV) | 76 |
| 3.2.3 | 2-(4- <i>n</i> -Alkylphenyl)-5-(2,3-difluoro-4- <i>n</i> -alkoxyphenyl)- pyrimidines (series V)..... | 79 |
| 3.2.4 | 2-(2,3-Difluoro-4- <i>n</i> -alkylphenyl)-5-(4- <i>n</i> -alkoxyphenyl)- pyrimidines (series VI) | 82 |
| 3.2.5 | 2-(4- <i>n</i> -Alkylphenyl)-5-(2,3-difluoro-4- <i>n</i> -alkylphenyl)- ... pyrimidines (series VII)..... | 84 |
| 3.2.6 | 2-(2,3-Difluoro-4- <i>n</i> -alkylphenyl)-5-(4- <i>n</i> -alkylphenyl)- ... pyrimidines (series VIII) | 87 |
| 3.2.7 | 2-(4- <i>n</i> -Alkoxyphenyl)-5-(2-fluoro-4- <i>n</i> -alkylphenyl)- pyrimidines (series IX) | 89 |
| 3.2.8 | 2-(2-Fluoro-4- <i>n</i> -alkoxyphenyl)-5-(4- <i>n</i> -alkylphenyl)- pyrimidines (series X)..... | 91 |
| 3.2.9 | 2-(4- <i>n</i> -Alkylphenyl)-5-(2-fluoro-4- <i>n</i> -alkoxyphenyl)- pyrimidines (series XI) | 94 |

| | | |
|------------|---|------------|
| 3.2.10 | 2-(2-Fluoro-4- <i>n</i> -alkylphenyl)-5-(4- <i>n</i> -alkoxyphenyl)- pyrimidines (series XII)..... | 96 |
| 3.2.11 | 2-(4- <i>n</i> -Alkylphenyl)-5-(2-fluoro-4- <i>n</i> -alkylphenyl)-..... pyrimidines (series XIII) | 99 |
| 3.2.12 | 2-(2-Fluoro-4- <i>n</i> -alkylphenyl)-5-(4- <i>n</i> -alkylphenyl)- pyrimidines (series XIV) | 101 |
| 3.3 | COMPARATIVE STUDY OF FLUORINATED THREE- RING PYRIMIDINE-BASED COMPOUNDS WITH ANALOGOUS NON-HETEROCYCLIC COMPOUNDS.... | 103 |
| 3.4 | SUMMARY | 107 |
| 3.5 | EXPERIMENTAL..... | 108 |
| 3.5.1 | The Synthesis of 2-(4- <i>n</i> -Alkoxyphenyl)-5-(2,3-difluoro- 4- <i>n</i> -alkylphenyl)pyrimidines (series IIIa-d)..... | 108 |
| 3.5.1.1 | Ring Closure Techniques - Synthetic Overview .. | 108 |
| 3.5.1.1.1 | Ring Closure Techniques - Experimental Procedures | 114 |
| 3.5.1.2 | Boronic Acid Cross-coupling - Synthetic Overview | 126 |
| 3.5.1.2.1 | Boronic Acid Cross-coupling - Experimental Procedures | 133 |
| 3.5.2 | The Synthesis of 2-(2,3-Difluoro-4- <i>n</i> -alkoxyphenyl)-5- (4- <i>n</i> -alkylphenyl)pyrimidines (series IV)..... | 140 |
| 3.5.2.1 | Experimental Procedures | 142 |
| 3.5.3 | The Synthesis of 2-(4- <i>n</i> -Alkylphenyl)-5-(2,3-difluoro- 4- <i>n</i> -alkoxyphenyl)pyrimidines (series V)..... | 147 |
| 3.5.3.1 | Experimental Procedures | 149 |
| 3.5.4 | The Synthesis of 2-(2,3-Difluoro-4- <i>n</i> -alkylphenyl)-5- (4- <i>n</i> -alkoxyphenyl)pyrimidines (series VI)..... | 151 |
| 3.5.4.1 | Experimental Procedures | 151 |
| 3.5.5 | The Synthesis of 2-(4- <i>n</i> -Alkylphenyl)-5-(2,3-difluoro- 4- <i>n</i> -alkylphenyl)pyrimidines (series VII)..... | 154 |
| 3.5.5.1 | Experimental Procedures | 154 |

| | | |
|----------|---|-----|
| 3.5.6 | The Synthesis of 2-(2,3-Difluoro-4- <i>n</i> -alkylphenyl)-5-(4- <i>n</i> -alkylphenyl)pyrimidines (series VIII) | 156 |
| 3.5.6.1 | Experimental Procedures | 158 |
| 3.5.7 | The Synthesis of 2-(4- <i>n</i> -Alkoxyphenyl)-5-(2-fluoro-4- <i>n</i> -alkylphenyl)pyrimidines (series IX) | 159 |
| 3.5.7.1 | Experimental Procedures | 161 |
| 3.5.8 | The Synthesis of 2-(2-Fluoro-4- <i>n</i> -alkoxyphenyl)-5-(4- <i>n</i> -alkylphenyl)pyrimidines (series X) | 167 |
| 3.5.8.1 | Experimental Procedures | 169 |
| 3.5.9 | The Synthesis of 2-(4- <i>n</i> -Alkylphenyl)-5-(2-fluoro-4- <i>n</i> -alkoxyphenyl)pyrimidines (series XI) | 173 |
| 3.5.9.1 | Experimental Procedures | 173 |
| 3.5.10 | The Synthesis of 2-(2-Fluoro-4- <i>n</i> -alkylphenyl)-5-(4- <i>n</i> -alkoxyphenyl)pyrimidines (series XII) | 175 |
| 3.5.10.1 | Experimental Procedures | 177 |
| 3.5.11 | The Synthesis of 2-(4- <i>n</i> -Alkylphenyl)-5-(2-fluoro-4- <i>n</i> -alkylphenyl)pyrimidines (series XIII) | 178 |
| 3.5.11.1 | Experimental Procedures | 180 |
| 3.5.12 | The Synthesis of 2-(2-Fluoro-4- <i>n</i> -alkylphenyl)-5-(4- <i>n</i> -alkylphenyl)pyrimidines (series XIV) | 181 |
| 3.5.12.1 | Experimental Procedures | 181 |

| | | |
|----|-------------------------|-----|
| 4. | REFERENCES | 184 |
|----|-------------------------|-----|

INTRODUCTION AND AIMS

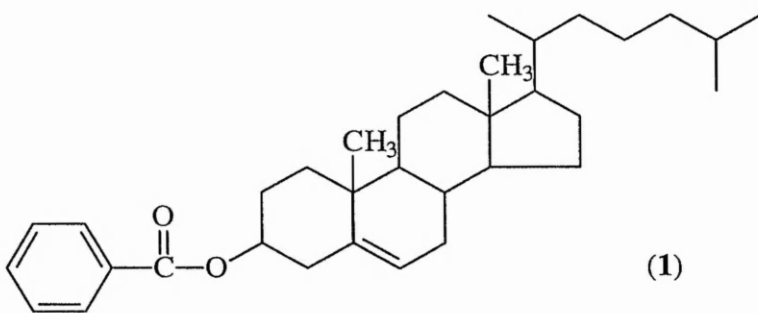
1. INTRODUCTION AND AIMS

*The terms solid, liquid and gas describe the three conventional states of matter. On heating the crystalline solid, at a particular temperature defined as its melting point, 3-dimensional order is lost and the isotropic liquid is formed. Conversely, as the isotropic liquid is cooled, 3-dimensional order is restored and the crystalline solid is reformed. However, certain compounds on heating the crystalline solid neither convert directly to the isotropic liquid nor, on cooling the isotropic liquid, do they convert back to the crystalline solid but display an intermediate state of matter which resembles both the crystalline solid and the isotropic liquid. Compounds which exhibit this phenomenon are termed **liquid crystals**, **liquid crystalline**, **mesogenic** or **mesomorphic** and the intermediate state of matter is termed the **mesophase**. In fact, the liquid crystalline state can be considered as the fourth state of matter.*

1.1 HISTORICAL REVIEW

In 1888 Reinitzer,¹ an Austrian botanist and chemist of the University of Graz, unwittingly made the first observation of a liquid crystalline compound. He noted the rather unusual melting behaviour of cholesteryl benzoate (**1**) which transformed sharply at 145.5°C into an opaque turbid liquid and then cleared to the isotropic liquid at 178.5°C. However, at the time Reinitzer was unable to elucidate this extraordinary phenomenon which he termed 'double melting'.

In 1890 Lehmann,² of the Technical High School of Karlsruhe, reported that when thin samples of cholesteryl benzoate (**1**) sandwiched between glass substrates were



viewed using a light polarising microscope, they exhibited an iridescent colour effect, i.e., a birefringent texture. Lehmann also reported similar effects in samples of ammonium oleate and *p*-azoxyanisole. Since these turbid states were somewhat fluid-like whilst exhibiting anisotropic properties he realised that these compounds showed characteristics of both the crystalline solid and the isotropic liquid. Hence, Lehmann introduced the terms *fliessende krystalle* (flowing crystal) and *flüssige krystalle* (*liquid crystal*) to describe such compounds. Quincke,³ Tamman,⁴ and Nernst⁵ proposed that either impurities or colloidal effects may be responsible for this unusual melting behaviour. However, the very nature of the sharp transitions between the solid and the birefringent melt and of the birefringent melt to the isotropic liquid rendered this proposal unacceptable.

At the turn of the century, hundreds of compounds exhibiting liquid crystalline behaviour were synthesised. Vorländer,⁶ of the University of Halle, carried out a methodical synthetic study of such compounds to establish a relationship between liquid crystallinity and molecular structure. By 1908 he concluded that compounds which exhibit liquid crystalline behaviour require a linear structure.

In 1922 Friedel,⁷ of the University of Strasbourg, introduced the term

mesophase (derived from the Greek words *mesos* and *phasis* meaning intermediate and phase, respectively) to describe the intermediate state of matter which exists between the crystalline solid and the isotropic liquid. Furthermore, he was able to distinguish categorically three distinct types of mesophase: smectic; nematic and; cholesteric. A description of these phase types is given in section 1.4.2, p. 13. It is important to note that Friedel did not ascertain the possibility of more than one type of smectic phase (smectic polymorphism) which was discovered earlier by Vorländer and Wilke.⁸

During this period, the busy history of liquid crystals was not confined solely to the synthesis and textural characterisation of compounds. Two mathematical theories were put forward to elucidate and describe the nematic phase, namely the *swarm theory* and the *continuum theory*.

The swarm theory was proposed by Bose⁹ in 1909 and refined further by Ornstein and Zernicke¹⁰ in 1919. It proposes the liquid crystalline state as being the result of intermolecular interactions which aligns the molecules, in a near parallel arrangement, in swarms or clusters of 10^5 molecules. Although this theory was used as a basis for the interpretation of early experimental results it was unable to explain the unusual results obtained from electrical and magnetic experiments carried out by Zocher¹¹ in 1927. Zocher therefore proposed the continuum theory which envisages the liquid crystalline state as an anisotropic elastic medium with its own symmetry, viscosity, and elasticity parameters.

The period from the mid 1930's to shortly after the Second World War saw research virtually abandoned with a total breakdown in international communication and co-operation. Thereafter, research was slow to pick up although significant

developments were made in the United Kingdom. Of particular note in 1962, G.W.Gray's treatise of '*Molecular Structure and the Properties of Liquid Crystals*',¹² which reports the results of a systematic investigation into the relationship between molecular structure and mesomorphism, has proved to be invaluable. In recognition of Professor Gray's outstanding contribution to the field of liquid crystals, in 1995 he was awarded the Kyoto Prize for Advanced Technology by the Inamouri Foundation.

At the start of the 1970's, the synthesis and ensuing investigation into the electro-optical properties of stable organic compounds by Gray *et al.*¹³ gave rise to the first marketable liquid crystal display, i.e., TNLCD¹⁴ (Twisted Nematic Liquid Crystal Display). It was realised quickly that in certain areas, the new type of display device would surpass light-emitting diode (LED) displays because they employ low power and are portable. Globally, the liquid crystal display market is a multi-billion dollar industry and the TNLCD device is used in watches, calculators, etc. The need for faster operating devices prompted Clark and Lagerwall¹⁵ to develop the Surface Stabilised Ferroelectric Liquid Crystal (SSFLC) display device following the initial theoretical suggestions of Meyer *et al.*¹⁶ in 1975.

Recent advances in display technology include polymeric ferroelectric liquid crystals (PFLCs) for large-area flexible displays because of their good processability¹⁷ and desirable ferroelectric properties.¹⁸ The response of early PFLCs to an electric field tended to be rather slow but more recently siloxane copolymers exhibiting a wide smectic C* phase, large spontaneous polarisation and sub-millisecond response times have been reported.¹⁹ Also, following the discovery of the ferri- and antiferro-electric phase types by Chandani *et al.*,^{20,21} there is currently very strong interest in developing a

tristate switching display. The antiferroelectric state has the ability to switch between two ferroelectric states at very sharp threshold voltages.

During the last decade, new and peculiar phase types have been reported. For example, in 1988 Renn and Lubensky²² theorised that a chiral compound which exhibits a smectic A phase but possesses a very short pitch will attempt to lower its free energy by introducing twist grain boundaries at regular intervals. In fact, Goodby *et al.*²³ in 1989 experimentally proved the work of Renn and Lubensky by synthesising compounds exhibiting a *helical smectic A** phase or the Twist Grain Boundary Smectic A (TGB A) phase. A Twist Grain Boundary Smectic C (TGB C) phase has also now been observed.^{24,25}

The field of liquid crystals is a multi-disciplinary science involving collaboration between chemists, physicists, mathematicians and biologists. The author would like to draw the attention of the reader to two recent books of particular note: '*Handbook of Liquid Crystal Research*' edited by Collings and Patel²⁶ and; the '*Handbook of Liquid Crystals Vols. I-IV*' edited by Demus *et al.*²⁷

1.2 CLASSIFICATION AND MOLECULAR STRUCTURE OF LIQUID CRYSTALS

1.2.1 CLASSIFICATION

Liquid crystal compounds may be classified according to either their mode of production or structural integrity. The former are termed either *thermotropic* or *lyotropic*. Compounds which exhibit liquid crystalline phases due to the action of heat are termed thermotropic, whereas those which generate mesomorphic properties due to the action of solvents (usually water) are termed lyotropic. Liquid crystals are more satisfactorily classified as either *amphiphilic*, *amphotropic* or *non-amphiphilic* based on their structural integrity.

Amphiphilic liquid crystals are composed of molecules which contain both lipophilic and hydrophilic groups and hence confer solubility both in polar and non-polar solvents. Amphiphilic liquid crystals may be either cationic, anionic or non-ionic in character. Mesophases observed in amphiphilic compounds are not derived from the arrangement of individual molecules but on the formation of multi-molecular aggregates composed of micelles. Amphotropic liquid crystals²⁸ contain a lyotropic head group joined to a thermotropic mesogen via a flexible alkyl chain and hence exhibit both lyotropic and thermotropic properties.

Non-amphiphilic liquid crystals are predominantly non-polar or moderately polar organic compounds which are readily soluble in organic solvents. Non-amphiphilic mesophases formed either on heating or cooling are reliant upon the arrangement of individual lath- or disc-like molecules.

The work contained in this thesis deals solely with the synthesis and properties of non-amphiphilic liquid crystals and hence amphiphilic and amphotropic liquid crystals will not be mentioned further.

1.2.2 MOLECULAR STRUCTURE

In general compounds which possess a characteristic elongated, lath-like molecular structure, i.e., geometrically anisotropic, exhibit liquid crystalline properties. Such compounds are termed *calamitic* liquid crystals. *Figure 1* depicts a schematic representation of a calamitic liquid crystal where: A and B are terminal groups which lengthen the long molecular axis of the molecule; the rectangles are often rigid polarisable units which are connected by a central linking group (X) and serve to keep the molecule rigid and linear and; Y and Y' represent lateral substituents which, with the exclusion of hydrogen, increase molecular breadth.

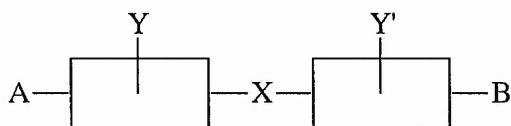
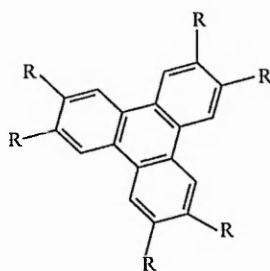


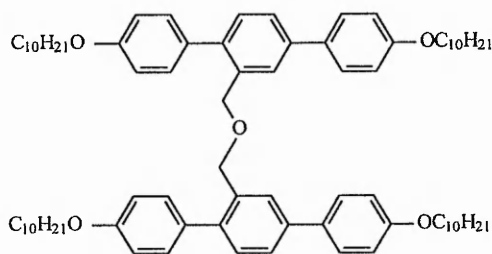
Figure 1 Schematic representation of a calamitic liquid crystal.

However, particular compounds, as shown by structures (2-6) depicted in *Figure 2*, deviate quite drastically from the classical calamitic shape but still retain liquid crystallinity. Of particular note are the *discotic* compounds (2)²⁹ which were first reported by Chandrasekhar.³⁰ Other types include: *twin* or *siamese twin* mesogens (3)³¹ and; *polycatenar*³² mesogens - these embrace two or more flexible chains, e.g., swallow-tailed compounds (4),³³ bi-forked compounds (5)³⁴ and phasmidic compounds (6).³⁵

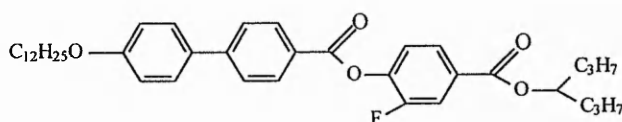


where $R = C_6F_{13}C_2H_4OCOCH_2O$

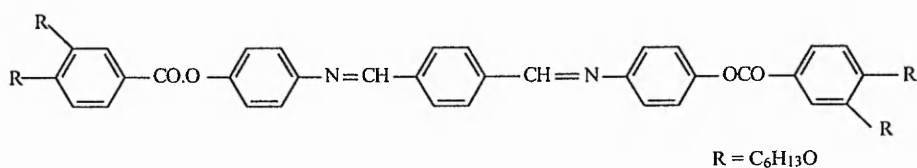
(2) Discotic
Cr 30 D_h 210 decomp



(3) Siamese twin
Cr 99 S_C 128 S_A 168 I

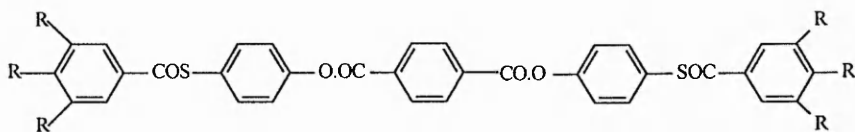


(4) Swallow-tailed
I 72.9 S_A 56.8 S_{Calt} K



$R = C_6H_{13}O$

(5) Biforked
K 160 S_C 200 N 240 I



$R = C_{12}H_{25}O$

(6) Phasmidic
K 59 hexagonal columnar 82 I

Figure 2 Examples of a variety of liquid crystalline structures.

1.3 MESOPHASE FORMATION

The geometrical anisotropy of the molecule leads to anisotropy of the intermolecular forces which hold the molecules together in the crystal lattice. The formation of mesophases may be related directly to changes in magnitude of the anisotropy of intermolecular forces either on heating the crystalline solid or on cooling the isotropic liquid. Two principle forces operate: lateral intermolecular cohesive forces which interact between the sides of molecules and; terminal intermolecular cohesive forces which interact between the ends of the molecules. The lateral cohesive forces are stronger than the terminal cohesive forces, i.e., anisotropy of intermolecular forces. To achieve an intermediate state of matter there must be a gradual breakdown of the intermolecular forces on heating the crystalline solid.

In 1933 Bernal and Crowfoot³⁶ carried out X-ray investigations on the crystal structure of numerous liquid crystal compounds and established two types of crystal lattice: *layer lattice* and; *non-layer lattice*. A layer crystal lattice comprises molecules which are arranged with their long axes parallel and their ends lying in the same plane. In a non-layer lattice the ends of any particular molecule lie about halfway along the length of any adjacent molecules, i.e., imbricated or inter-digitated structure (*Figure 3*).

On heating a crystal with a layer lattice to a temperature, T_1 , the weaker terminal forces break allowing the layers to slide and rotate over each other. The resultant structure equates to the smectic phase and is stabilised by the 'unaffected' lateral cohesive forces and residual terminal forces. A detailed account of the smectic phase is given later in section 1.4.2.3, p. 16. On further heating two possibilities may arise: firstly, at T_2 , the lateral forces may weaken so that the molecules slide out of the layers

to resemble a structure similar to the nematic phase which on heating to a higher temperature, T_3 , converts to the isotropic liquid. A detailed account of the nematic phase is given in section 1.4.2.1, p. 13; alternatively, the smectic phase may convert directly to the isotropic liquid on heating to temperature T_4 . In addition, T_5 shows the possibility for the formation of the nematic phase directly from the crystal due to simultaneous breakdown of both lateral and terminal cohesive forces.

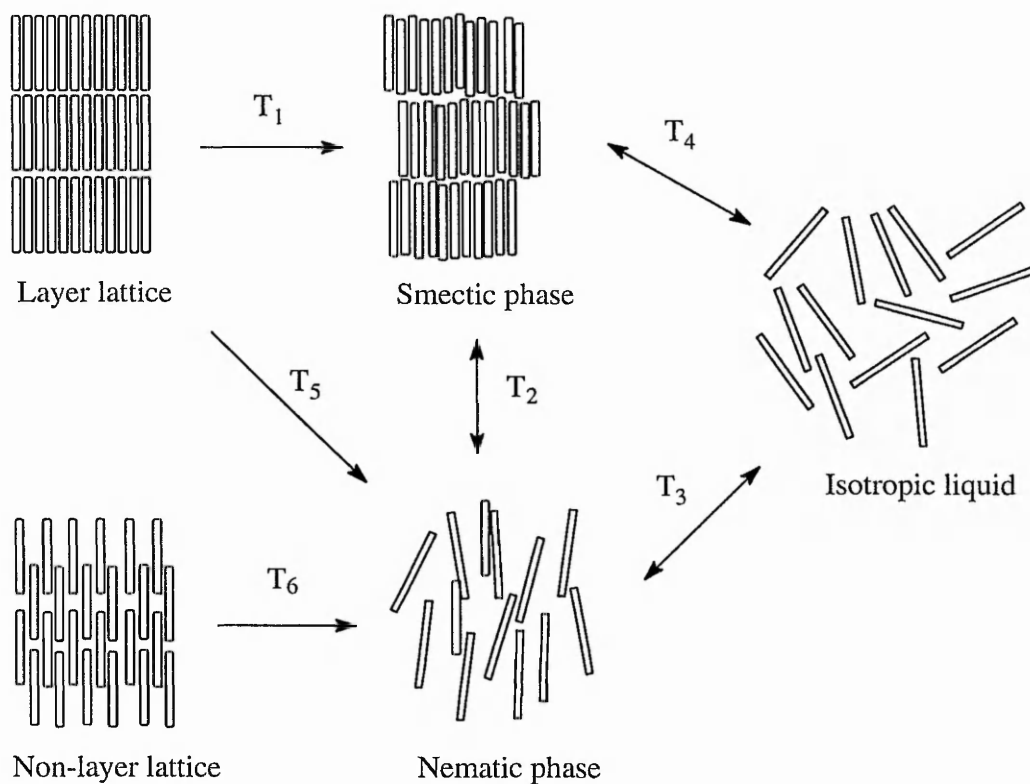


Figure 3 Diagrammatic representation of molecular rearrangements which may occur on heating a crystalline solid consisting of either a layer or non-layer lattice.

It was originally thought that a non-layer lattice would only give rise to a nematic phase, T_6 , and further heating, T_3 , would result in the formation of the isotropic

liquid. However, it has been shown by Leadbetter *et al.*³⁷ that certain members of an homologous series of 4'-*n*-alkyl- and 4'-*n*-alkoxy-4-cyanobiphenyls (K and M series) exhibit a smectic A phase despite possessing a non-layer lattice crystal structure.

Apart from the melting point (crystal to mesophase transition) and crystallisation (mesophase to crystal transition), liquid crystal phase transitions (smectic to smectic; smectic to nematic; smectic to isotropic liquid and; nematic to isotropic liquid) are reversible. The transition from a mesophase to the isotropic liquid is defined as the clearing point. In compounds which exhibit both the smectic and nematic phase, the latter appears at a higher temperature. Mesophases which are observed above the melting point are termed *enantiotropic* whereas those observed on cooling only below the melting point are termed *monotropic*.

1.4 OPTICAL CHARACTERISATION AND MESOPHASE TYPES

1.4.1 OPTICAL CHARACTERISATION

The use of optical polarising microscopy is an invaluable method for the study of mesophases, being both convenient and uncomplicated. The visual characteristics or *optical textures* of a mesogenic material are readily detected when a thin film, sandwiched between two glass surfaces, is examined between crossed polarisers. A knowledge of the molecular alignment, either homeotropic or homogeneous, of the mesogenic material on the supporting surface (*Figure 4*) is useful in the identification of mesophase types.

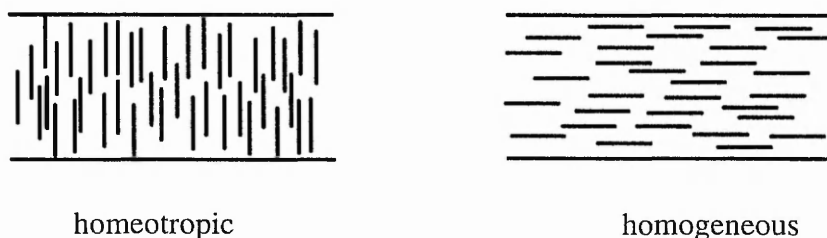


Figure 4 Molecular alignment of the homeotropic and homogeneous optical textures.

The homeotropic alignment occurs when the long axes of the molecules lie normal to the glass slide and can be induced by the use of surfactants such as lecithin.³⁸ In the homogeneous alignment the molecules are arranged with their long axes parallel to the supporting surface and is achieved by rubbing the supporting surface in a single direction. For the identification of many optical textures it is best if both homogeneous and homeotropic areas appear together on the same glass slide.

Alternatively, some mesophase types are more readily identified when viewed as a free standing film through crossed polarisers. This technique involves drawing the sample (in either the S_A or S_C phase) over a small hole (1-2 mm) in an aluminium plate

so that it is suspended freely (absence of surface interactions). In this situation, the layers are perpendicular with respect to the optic axis such that the S_A phase would appear optically extinct. The author would like to direct the reader to the following texts: '*Smectic Liquid Crystals*', by Gray and Goodby³⁹ and; '*Textures of Liquid Crystals*', by Demus and Richter⁴⁰ which are invaluable for the purpose of phase identification.

1.4.2 MESOPHASE TYPES

In 1922 Friedel⁷ proposed three structurally diverse liquid crystalline phase types, namely: nematic; smectic and cholesteric. In recent years distinct new phase types have been discovered such as Twist Grain Boundary phases,²³ ferri- and antiferroelectric phases,^{20,21} and blue phases.⁴¹ The following sections provide an insight into the structure and optical textures of each phase type.

1.4.2.1 NEMATIC MESOPHASE (N)

The term nematic is derived from the Greek word 'nematos' meaning 'thread-like' and refers to the thread-like texture which is observed when a thin sample of a nematic phase, sandwiched between two glass substrates, is viewed between crossed polarisers. *Figure 5* depicts the structure of the nematic phase in which the long axes of the molecules remain essentially parallel although the centres of mass are disorganised, i.e., long range orientational order but zero positional order. The direction of alignment is given by the director, n , and the extent of parallel ordering is determined by the order parameter, S . The molecules are free to rotate and the phase is said to be 'fluid-like'. Not surprisingly, X-ray diffraction patterns, initially investigated by Hückel,⁴² show a

substantial likeness to those for the isotropic liquid.

The nematic phase is most easily identified on cooling from the optically extinct isotropic liquid due to the appearance of highly coloured, small circular droplets known as nematic droplets which then coalesce to give further distinct textures.

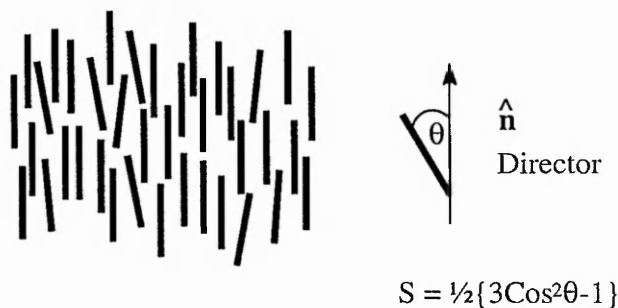


Figure 5 Idealised nematic structure.

The planar or homogeneous alignment gives the threaded and marbled textures. The latter is characterised by its rock-like appearance. Sometimes the schlieren texture is observed which is identified by the appearance of dark brushes (two and four) emanating from point singularities. If the molecules adopt the homeotropic alignment then the field of view appears dark. However, this phase can be characterised by displacing the cover slip which results in bright ‘flashes’ being observed.

1.4.2.2 CHOLESTERIC MESOPHASE (Ch or N*)

The term cholesteric is used mainly for historical reasons because it was first observed in derivatives of cholesterol. However, it is now known that compounds which exhibit this mesophase possess a chiral group and hence the cholesteric phase is also termed the chiral nematic phase (N*). The cholesteric phase may be visualised as a ‘layered’ nematic structure which adopts a helical conformation due to changes in the

director pattern (*Figure 6*).

The distance required by the director, n , to turn through 360° is known as the pitch, p , of the helix. The pitch is much longer than the molecular length, l , and its magnitude is comparable to the wavelength of light (a few thousand Ångströms) such that the cholesteric phase undergoes selective reflection of light. The direction of twist is reliant on the chirality of the compound whilst the pitch of the helix is temperature dependant.

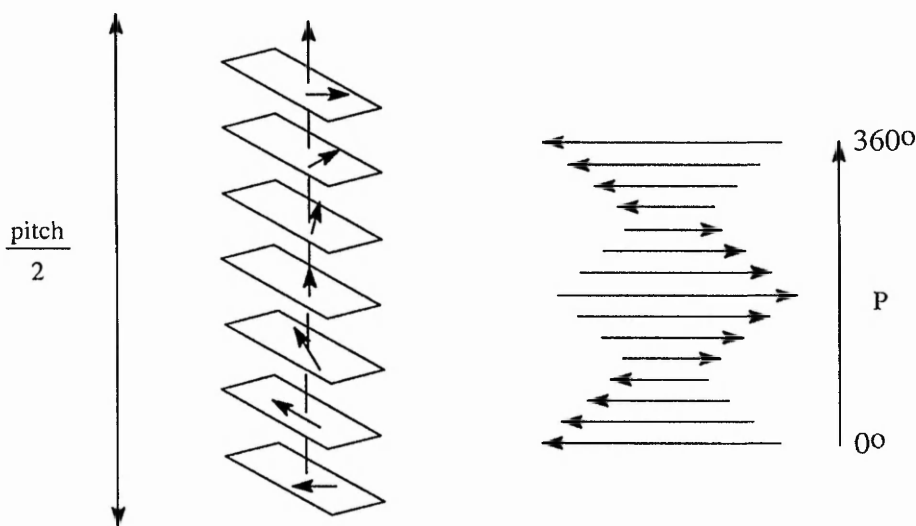


Figure 6 Diagrammatic representations of the cholesteric phase.

If a small electric or magnetic field is applied, the director in each layer will turn to face in the same direction thus giving an ordinary nematic phase. It is also possible, by interaction with the surrounding walls, to impose a mechanical twist to the nematic phase to give a pseudo-cholesteric phase. The following observations confirm the similarity between the nematic and the cholesteric mesophases:

- a) X-ray diffraction patterns are very similar;
- b) both phases are completely miscible and;

- c) a cholesteric racemic mixture (equal parts of each optical isomer) possesses an infinite pitch and is therefore nematic.

The cholesteric mesophase mainly exhibits two different textures which are dependant upon the alignment of the helices on the supporting surface (*Figure 7*) with respect to the optical axis:

- a) the focal-conic or undisturbed texture - forms upon cooling the isotropic liquid. This texture is birefringent but optically inactive. The helices lie perpendicular to the incident light and;

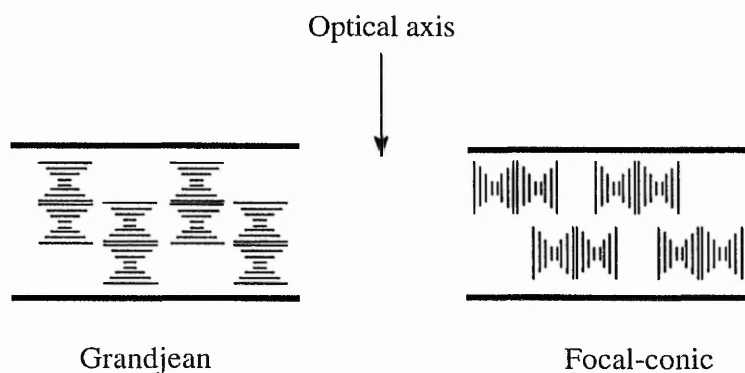


Figure 7 Helical orientation for Grandjean and focal-conic textures.

- b) the Grandjean (planar or disturbed) texture - the helical axes are parallel to the light path. This texture is quite outstanding having a bright coloured background interlaced with 'streams' which give a flowing appearance and is formed by mechanical shear of the focal-conic texture.

1.4.2.3 SMECTIC MESOPHASE (S)

The term smectic is derived from the Greek word 'smectos' meaning 'soap-like' and is used to denote mesophases which have their molecules stratified and confined in

layers, i.e., contain orientational and positional order. As shown in **Figure 8**, the long axes of the calamitic molecules may align either perpendicular (orthogonal) or at an angle (tilted) with respect to the layer planes. X-Ray diffraction patterns of the smectic phase are generally composed of two rings, namely:

- a) an inner ring at a small Bragg angle corresponding to the layer spacing and;
- b) an outer ring at a larger Bragg angle characteristic of the lateral distribution of parallel molecules within each layer.

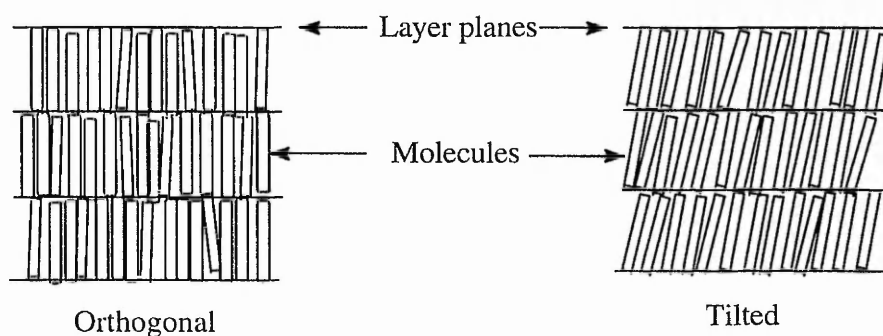


Figure 8 Idealised smectic structures.

Depending on the extent of both orientational and positional order several smectic types (smectic polymorphism) are possible (S_A, S_B, \dots, S_K). The S denotes smectic and the subscript represents the specific phase type. Letters of the alphabet are used to describe the order in which they were discovered.

1.4.2.3.1 Smectic Polymorphism

Smectic polymorphism may be defined as the transformation from one smectic mesophase to another due to subtle changes in molecular ordering under the influence of temperature. Originally Sackmann and Demus⁴³ identified and classified seven

polymorphs, each polymorph being coded as outlined previously (S_A, S_B, \dots, S_G), based on the *miscibility rule* which states 'Liquid crystalline modifications which exhibit an uninterrupted series of mixed crystals in binary systems without contradiction can be marked with the same symbol'.

To date, twelve different smectic polymorphs are known which, upon cooling from the isotropic liquid, can be arranged in order of thermodynamic stability as shown below.

Isotropic liquid, N, S_A , S_D , S_C , S_B^h , S_I , S_B^c , S_F , S_J , S_G , S_E , S_K , S_H , crystal.

Thermodynamic sequence of phases.

Mesophases which possess a high degree of order, i.e., closely resemble the crystalline solid, are now termed smectic crystal phases as opposed to the less ordered polymorphs which are termed smectic liquid crystal phases. There is also the curious smectic D phase which is now designated solely as the D phase. The structure of the D phase is discussed briefly on p. 27. Hence, the thermodynamic sequence of phases is now better expressed as shown below.

Isotropic liquid, N, S_A , D, S_C , S_B , S_I , CrB, S_F , CrJ, CrG, CrE, CrK, CrH, crystal.

Revised thermodynamic sequence of phases.

Unfortunately, this order does not always hold true due to the phenomenon of *re-entrant* phases.⁴⁴ This is where a phase reappears on cooling further down the sequence. For example, Byron *et al.*⁴⁵ have reported a re-entrant S_A phase which reappears on cooling below an S_C phase.

Smectic A phase, S_A

The smectic A phase is the least ordered of the smectic mesophases. *Figure 9* shows the arrangement of molecules in 'diffuse layers' with their long axes perpendicular with respect to the 'diffuse layer planes'. The terms diffuse layers and diffuse layer planes are used because the molecules are in continual motion due to translational and rotational freedom.⁴⁶ Evidence for the perpendicular arrangement is provided by X-ray diffraction studies⁴⁷ which reveals that the lamellar spacing (d) is approximately equal to the molecular length (l). However, in some cases the lamellar spacing (d) is shorter than the molecular length (l). For example, a ratio 0.8:1 ($d:l$) has been attributed to either flexing of the fluid-like alkyl chains or the combination of random tilting of the core coupled with chain flexing.³⁹

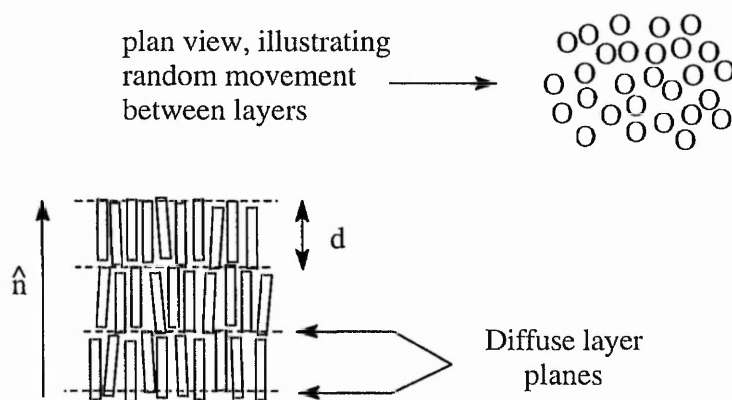


Figure 9 Schematic representation of the S_A phase.

In certain compounds, notably the 4'- n -alkyl-4-cyanobiphenyls¹³ (K series), X-ray scattering data reveals that the lamellar spacing (d) is greater than the molecular length (l) such that the $d:l$ ratio is 1.4:1. This result has been interpreted in terms of an interdigitated bilayer arrangement of molecules (*Figure 10*) and the phase

type is classified as S_{Ad} .

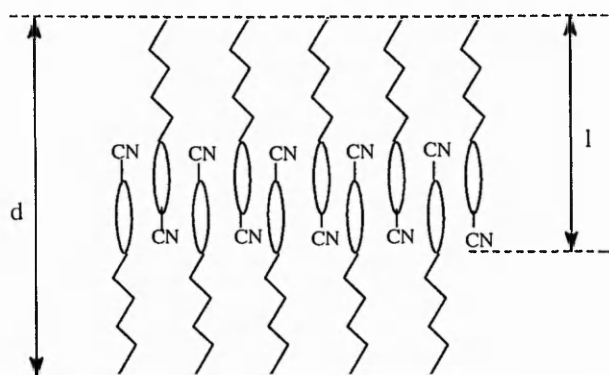


Figure 10 Schematic illustration of the interdigitated bilayer S_{Ad} phase in the 4'-*n*-alkyl-4-cyanobiphenyls (K series).

The S_A phase is characterised by two optical textures:

- a) the focal-conic fan texture which emerges from either the isotropic liquid or the nematic phase in the form of elongated rod-like protrusions termed bâtonnets which coalesce to give the characteristic focal-conic fans. The polygonal texture, being a particular form of the focal-conic fan texture, is observed in thicker preparations and;
- b) the homeotropic texture which is optically extinct since the molecules align parallel with respect to the optic axis.

Smectic B phase, S_B , and Crystal B phase, CrB

In both types of B phase, the molecules arrange themselves in hexagonal close-packed nets with their molecular long axes perpendicular with respect to the layer planes (**Figure 11**). Consequently, free rotation of the molecules is not possible. However, rotation is possible but in a co-operative manner only,⁴⁸ i.e., molecules within each

hexagonal net are packed neatly together like ball bearings such that rotation of an individual molecule will cause the remainder to rotate as well.

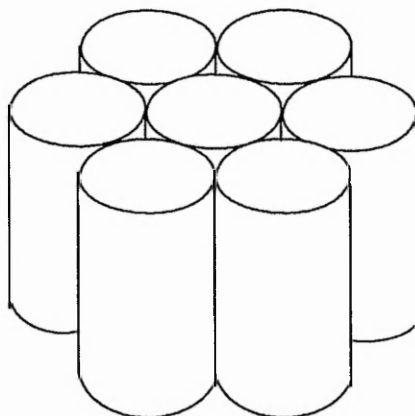
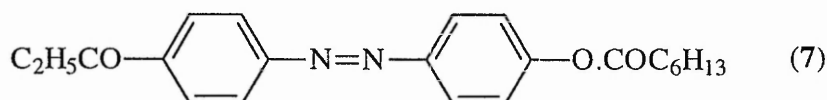


Figure 11 Hexagonal close-packed arrangement of the molecules in the B phase.

Initially, the notion of two types of B phase was not well received because no example was available. However in 1979, Goodby⁴⁹ synthesised 4-propionyl-4'-heptanoyloxyazobenzene (7) and phase characterisation revealed the presence of both types. The existence of these two types can be attributed to the varying degree of inter-layer correlation between the hexagonal nets. The crystal B (CrB) phase has extensive long range inter-layer correlations whereas in the smectic B (S_B) phase inter-layer positional correlations are absent.



I 142.5°C N 141.7°C S_A 90.3°C S_B 86.0°C CrB

Two natural textures[†] are exhibited by both types of B phase (the homeotropic and mosaic textures) and one paramorphotic texture[‡] (the focal-conic fan texture). The latter is useful for determining the type of B phase that is formed on cooling below the S_A phase. For example, at the transition from the S_A phase to the CrB phase, lines or *transition bars*⁵⁰ appear briefly across the back of the fans which then disappear to leave particularly smooth backs. On reversal of this transition, i.e., from CrB to S_A , the fans display parabolic ‘wish-bone’ defects. In contrast, at the S_A to S_B phase transition, the transition bars are not usually seen. The mosaic texture emerges from the isotropic liquid in the form of oblong sheets or platelets. These characteristically ‘H’ shaped mosaic areas are commonly encircled by homeotropic regions.

Smectic C phase, S_C

The smectic C phase is similar to the smectic A phase, except that the molecules are tilted with respect to the layer planes (*Figure 12*). The tilt angle, θ , defined as the

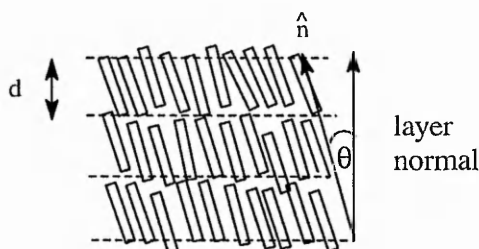


Figure 12 Schematic representation of the S_C phase.

[†] Natural textures appear on cooling from either the isotropic liquid or nematic phase.

[‡] Paramorphotic textures appear on cooling from a previous smectic phase.

angle between the molecule and the layer normal, is temperature dependent. X-Ray scattering studies show the layer thickness, d , to be significantly less than the molecular length, l , which accounts for the tilted arrangement of the molecules.

The S_C phase exhibits two optical textures:

- a) the schlieren texture which commonly forms preferentially from the isotropic liquid or the nematic phase and shows four-brush point singularities (as opposed to two or four brushes seen in the nematic phase) and;
- b) the broken focal-conic fan texture formed when cooling from the S_A phase. It is characterised by the shattering of the fans combined with the development of the schlieren texture in the previously homeotropic regions. This texture can also be observed upon cooling from the isotropic liquid or the nematic phase and therefore occurs either naturally or paramorphotically.

Crystal E phase, CrE

The CrE phase is similar to the CrB phase in that the molecules have an orthogonal arrangement and extensive inter-layer correlations, although overall it has a higher level of ordering. Within the layers of the CrE phase the molecules adopt a chevron-like or orthorhombic symmetry (*Figure 13*) which prevents co-operative rotation about their long axis but allows a long range co-operative 'flapping' motion through a limited angle ($<180^\circ$) to occur.

Commonly, the paramorphotic focal-conic fan texture emerges from the preceding S_A or B phase fan texture and is recognised by the formation of permanent,

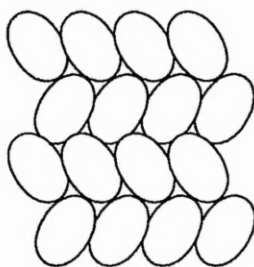


Figure 13 A cross-section of the CrE phase looking down the long molecular axes showing the chevron packing of the molecules.

unbroken concentric arcs over the backs of the fans. A semi-transparent platelet texture also forms in the previously homeotropic areas. The natural texture of the CrE phase, which is described as mosaic, is not frequently observed.

Smectic F phase, S_F

X-Ray diffraction studies⁵¹ reveal that molecules within the S_F phase are packed in layers with virtually no inter-layer correlation. The molecules are arranged in pseudo-hexagonal nets (**Figure 14**) with an approximate tilt angle of 25° towards one *side*.



Figure 14 The molecular arrangement in the S_F phase.

On rare occasions the S_F phase originates directly from the isotropic liquid and displays two natural textures, i.e., the schlieren-mosaic texture (schlieren brushes and

fine mosaic lines) and the broken focal-conic fan texture. The S_F phase is optically very similar to the S_I phase but close examination of their schlieren textures affords identification. The S_F phase exhibits schlieren brushes with a sharp focusable image whereas in the S_I phase the image appears slightly blurred. On cooling from various other smectic phases the S_F phase forms a number of paramorphic textures but again is best identified by close examination of the schlieren-mosaic areas.

Crystal G phase, CrG

The crystal G phase is a highly ordered crystal-like structure having a tilted pseudo-hexagonal arrangement of molecules (*Figure 15*), analogous with the S_F phase, but differing in that it possesses widespread inter-layer correlation.

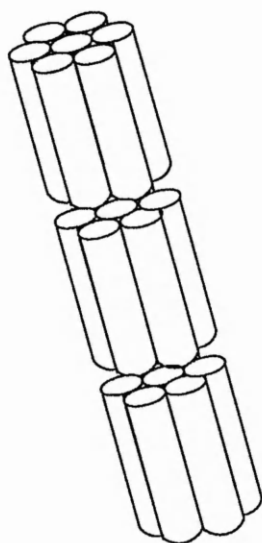


Figure 15 Molecular structure of the Crystal G phase.

Typically, on cooling from the previous homeotropic or schlieren textures the onset of the CrG phase is characterised by the formation of dendrites (branch-like projections) which rapidly coalesce to form the classical mosaic texture. Paramorphic

textures of the focal-conic fan type are also observed, the fans are usually broken and on cooling from a B phase they exhibit concentric arcs similar in texture to the CrE phase.

Crystal H phase, CrH

The crystal H phase is a tilted analogue of the CrE phase (*Figure 16*) where the molecules are arranged in a contracted hexagonal or orthorhombic arrangement which is tilted towards one *side* of the distorted hexagonal array with respect to the layer normal.

The CrH phase is most readily identified upon cooling the mosaic texture of the CrG phase. At the point of transformation, zigzag cross-hatched lines are observed within the mosaic areas, which may either prevail throughout the temperature range of the phase or disappear immediately upon phase formation.

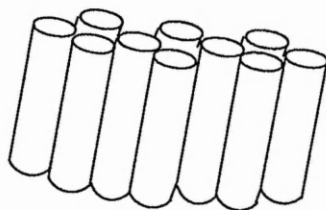


Figure 16 Structure of the Crystal H phase.

Smectic I phase, S_I

The structure of the smectic I phase is similar to the structure to the S_F phase as discussed earlier (p. 24), i.e., molecules arranged in hexagonal nets, except for the tilt direction of the hexagonal net (*Figure 17*). In the S_I phase the tilt direction is towards the *apex* of the hexagonal net as opposed to one *side* in the S_F phase.

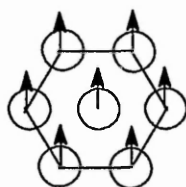


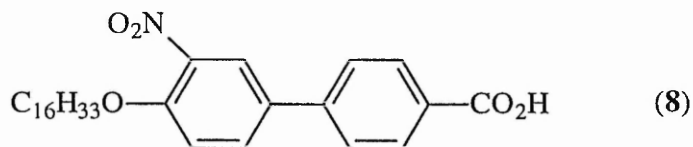
Figure 17 Structure of the S_1 phase - the arrows showing the tilt direction towards the apex of the hexagonal net.

Crystal J phase, CrJ and Crystal K phase, CrK

The structures of the crystal J and crystal K phases⁵² are analogous to those of the CrG and CrH phases, respectively, except for the tilt direction which is towards one *apex* of either the hexagonal array (CrJ) or the orthorhombic array (CrK) as opposed to the *side* of the nets. Recently, the first observation of a natural CrK texture has been reported by Bowden *et al.*⁵³

The D phase, D

Although the D phase was first detected in 1957 by Gray *et al.*,⁵⁴ however to date, there are still relatively few examples which exhibit this phase. Generally, materials which exhibit the D phase possess a dimeric structure composed of long terminal alkoxy chains and are able to form strong intermolecular interactions, e.g., 4'-*n*-hexadecyloxy-3'-nitrophenyl-4-carboxylic acid (**8**).⁵⁵



K 126.8°C S_C 171.0°C S_D 197.2°C S_A 201.9°C I

The structure of the D phase is somewhat unusual with a suggested model based on a body centred cubic (BCC)⁵⁶ lattice in which the aromatic cores of the molecules form spherical micelles which themselves form the lattice. An alternative model has also been suggested⁵⁷ and is based on dimeric molecules aggregated in discs which stack in the same manner as discotic mesogens to form columns. When of a specific length the individual columnar units pack closely together to form a regular infinite lattice with an overall cubic symmetry. Recent investigations on the D phase of the 3'-substituted-4'-*n*-alkoxybiphenyl-4-carboxylic acids, carrying either a nitro- or a cyano-group, have shown that the cubic structure varies with the lateral group substituted on the biphenyl core.⁵⁸

The D phase is optically isotropic but can be distinguished from the isotropic liquid or the homeotropic phases since it nucleates in the birefringent S_C phase as dark squares, hexagons and rectangles.

1.5 THE CORRELATION BETWEEN MOLECULAR STRUCTURE AND LIQUID CRYSTALLINE BEHAVIOUR

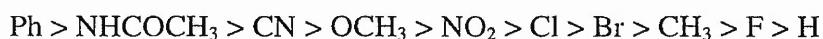
Researchers working in the field of liquid crystals need to understand the relationship between molecular structure and mesomorphic properties in order to design useful novel liquid crystalline materials. The formation of thermotropic mesophases is controlled by two factors: the anisotropy of molecular shape and; the anisotropy of intermolecular forces, as mentioned earlier in section 1.3, p. 9.

Calamitic liquid crystals are constructed of a rigid polarisable aromatic core which is elongated by the introduction of terminal groups. In addition, the aromatic core units may be connected by a central linking group and/or may possess lateral substituents (see *Figure 1*, p. 7). The mesophase thermal stability, i.e., transition temperature from the nematic to isotropic liquid (T_{N-I}), smectic to nematic mesophase (T_{S-N}) or smectic to isotropic liquid (T_{S-I}) may be increased, reduced or eliminated completely by judicious selection of the groups comprising a calamitic liquid crystal.

The mesophase thermal stability may be related to the anisotropy of molecular polarisability, $\Delta\alpha$, which is defined as 'the difference in polarisability of the molecule along the molecular long axis with respect to the polarisability along the short molecular axis'. An increase in mesophase thermal stability is usually associated with an increase of $\Delta\alpha$. An extensive study of structure-property relationships is beyond the scope of this thesis and a brief insight follows. However, the author would like to draw the attention of the reader to the comprehensive studies by Demus⁵⁹ and Toyne⁶⁰ cited in the literature.

1.5.1 INFLUENCE OF TERMINAL SUBSTITUENTS

Terminal substituents tend to extend the linearity of the molecule. The mesophase thermal stability will be enhanced if the terminal groups can conjugate with the aromatic core, thus increasing the polarisability along the long molecular axis and correspondingly increasing the value of $\Delta\alpha$. For example, Gray *et al.*⁶¹ have proposed the following average group efficiency order for nematic thermal stability (T_{N-I}):



Group efficiency order

A similar efficiency order was also proposed by Gray for the improvement of the smectic to isotropic liquid transition temperature (T_{S-I}). Replacement of the terminal H by another substituent is generally beneficial to mesophase thermal stability.

1.5.1.1 HOMOLOGATION

Structure-property relationships are more apparent when the terminal substituent consists of either an alkyl or alkoxy chain. Gray *et al.*⁶² showed that if the transition temperatures are plotted against the number of carbon atoms, n , in either the alkyl or alkoxy terminal chain for the members of an homologous series, i.e., transition temperature plot, (*Figure 18*), several conclusions regarding structure-property relationships may be drawn:

- a) there is no correlation between the melting point and the crystal structure;
- b) the nematic phase alone is exhibited by the early homologues. The thermal stability of the nematic phase is mainly determined by terminal attractions between molecules that are in parallel arrangement and as the chain length

increases these terminal attractions are gradually lost due to the increasing flexibility of these chains;

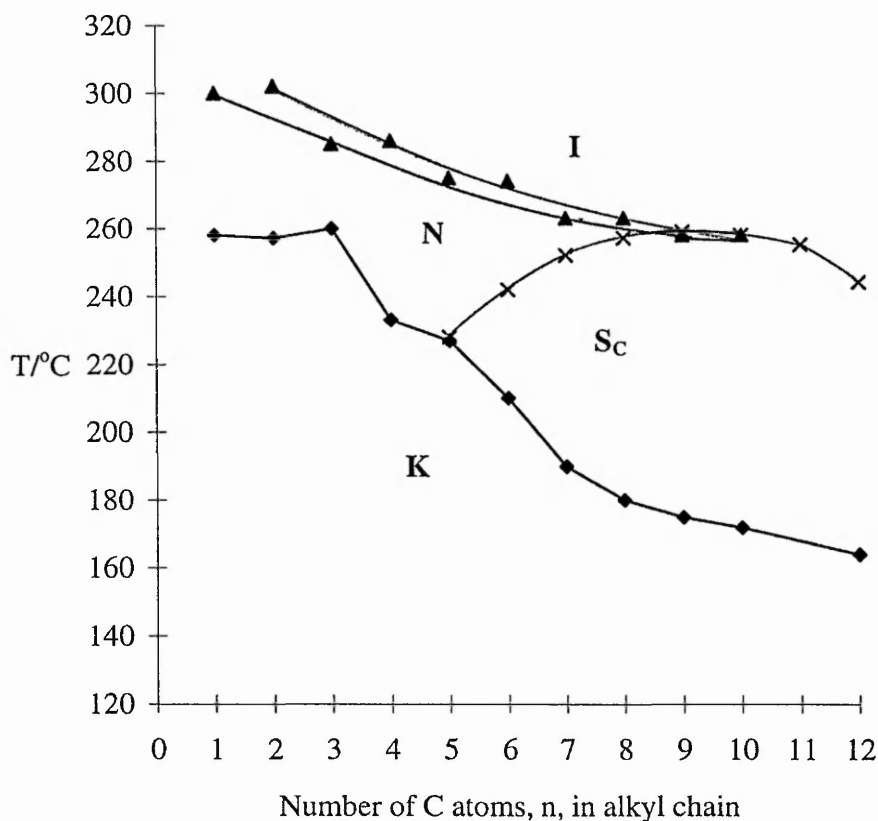
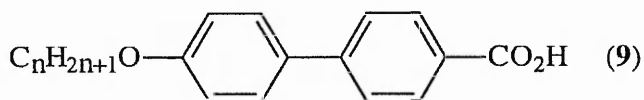
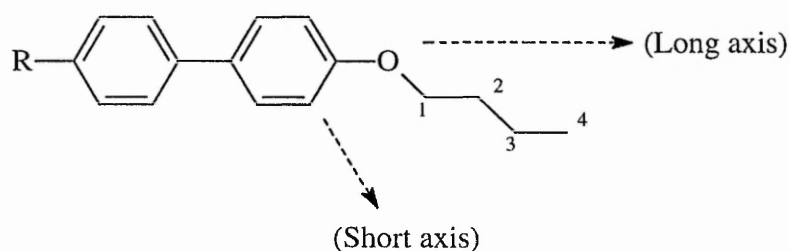


Figure 18 Plot of transition temperatures for an homologous series of 4'-*n*-alkoxybiphenyl-4-carboxylic acids (9).

- c) the points for the N-I transition temperatures may be correlated by two smooth curves. This phenomenon is known as the *odd-even effect* and correlates to the number of C-C bonds directed along the long molecular axis with respect to the

number directed along the short molecular axis.

For alkoxy terminal substituents, the points for the N-I transition temperature for even-n homologues may be correlated by a smooth curve which lies above a similar smooth curve for the odd-n homologues. The even-n homologues have more bonds directed along the long molecular axis than along the short molecular axis which increases the anisotropy of molecular polarisability.

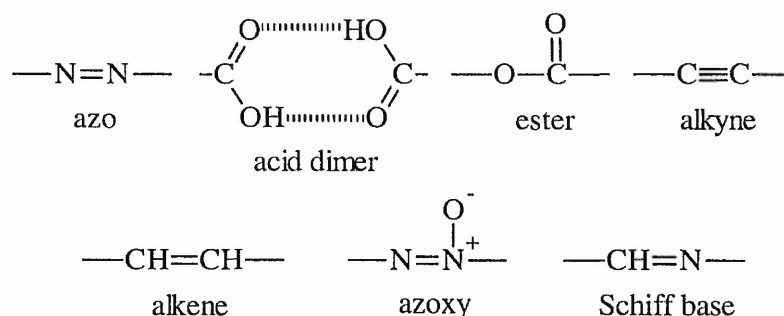


This trend is reversed for compounds with terminal alkyl groups assuming that the oxygen atom is stereochemically equivalent to a methylene group;

- d) for intermediate homologues both smectic and nematic phases may be observed. As the chain length increases the thermal stability of the smectic phase will increase at the expense of the nematic or cholesteric phase due to very weak terminal intermolecular attractive forces caused by the conformational changes (flexing) of the long terminal alkyl chains and;
- e) for higher homologues the nematic phase can disappear entirely and smectic phases alone may be formed. The thermal stability of smectic phases is decided by lateral intermolecular attractions.

1.5.2 INFLUENCE OF THE CENTRAL LINKING GROUP

Although the presence of a central linking group is not essential, the purpose of this unit is to connect aromatic fragments by extending the conjugation in a molecular core. Commonly, sp^2 hybridised groups are chosen because they are essentially flat (planar) and prevent free rotation about the single bond thus enabling close packing between adjacent molecules. Such moieties increase mesophase thermal stability because they are able to extend conjugation when placed between two aromatic units and enhance the rigidity of the molecule. A wide variety of central linking groups may be employed as shown below.

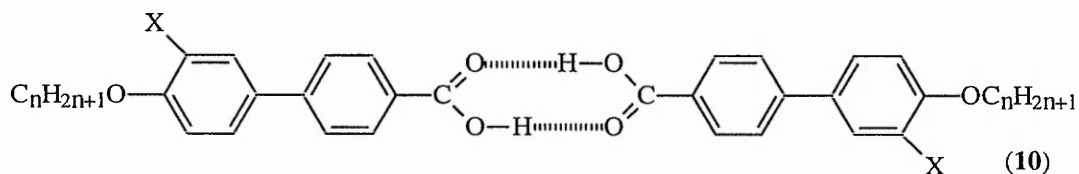


Some of the earliest linking groups included the Schiff base (-CH=N-), azo (-N=N-), and azoxy linkages. However, these types are not commercially advantageous for display devices because they are sensitive to moisture and/or are photochemically unstable. Gray and McDonnell⁶³ have shown that certain flexible central linking groups such as dimethylene (-CH₂CH₂-) and oxymethylene (-CH₂O-), which neither allow conjugation nor enhance rigidity, can be employed successfully to give liquid crystalline compounds with high clearing points.

1.5.3 INFLUENCE OF LATERAL SUBSTITUENTS

Mesophase thermal stability is influenced directly by the addition of lateral substituents because they increase the molecular breadth and thus disrupt the close molecular packing arrangement. The molecular breadth may be defined as 'the diameter of the smallest cylinder through which the molecule may pass'.

Initial studies on the influence of lateral substituents were undertaken by Gray and Worrall⁶⁴ who introduced a variety of lateral substituents in the 3'-position of a series of 3'-substituted 4'-*n*-alkoxybiphenyl-4-carboxylic acids (**10**).

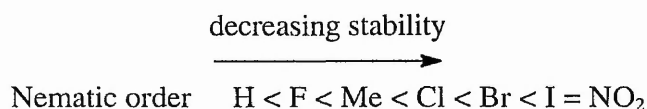


The substituent X has two opposing effects:

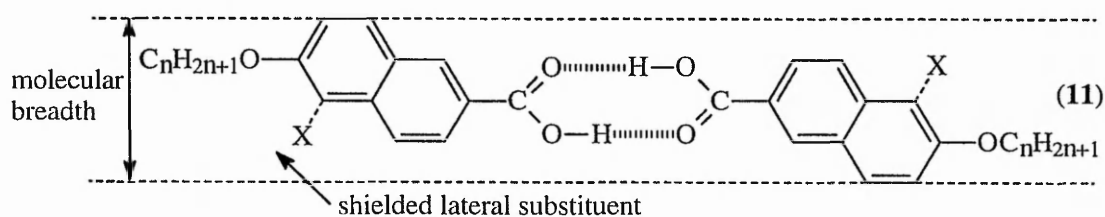
- a) the substituent may force the long molecular axes apart reducing the intermolecular forces of attraction and therefore lowering mesophase thermal stability. Smectic mesophase thermal stability is the most likely to be affected and;
- b) the replacement of a ring hydrogen by a ring X substituent will increase the molecular polarisability and possibly the dipolarity of the molecule. In this event liquid crystal thermal stability should be enhanced by the increase in lateral intermolecular attractions, in particular the smectic mesophase.

In all instances there was a decrease in smectic and nematic thermal stability suggesting that the size of the substituent rather than the magnitude of its polarity is

more important, i.e., thermal stability decreases as the size of the substituent increases.



The position and number of lateral substituents is also significant. For example, if the substituent X is moved from the 3'-position to the 2'-position in compound (10), then the mesophase thermal stability may decrease further. In this instance, the two phenyl rings can no longer lie co-planar because of steric hindrance which causes twisting about the 1,1'-inter-ring bond and reduces inter-ring conjugation. Also if the number of lateral substituents is increased, the thermal stability decreases accordingly, i.e., an additive effect is observed.



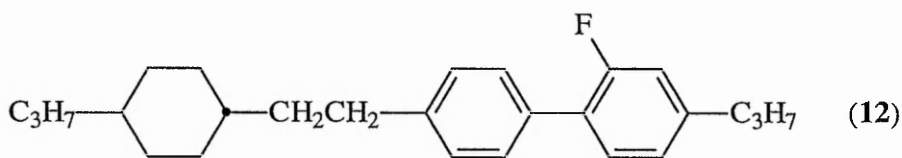
In some mesogenic compounds the introduction of a lateral substituent may have little or no effect on the thermal stability of the compound because it may be shielded by the overall molecular structure. For example, introduction of a lateral substituent (X) in the 5-position in a series of 6-*n*-alkoxy-2-naphthoic acids (11)⁶⁵ actually increases mesophase thermal stability. However, very large substituents such as iodo-, tend to extend the molecular perimeter and hence mesophase thermal stability is lowered.

As a general rule, the introduction of lateral substituents is detrimental to mesophase thermal stability. However, small substituents may be tolerated and now

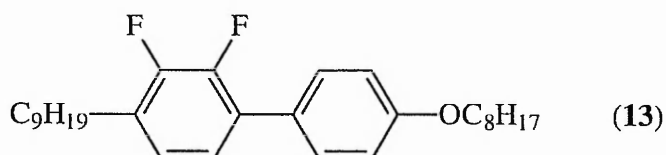
lateral substitution plays a vital role in the design and synthesis of new low melting, room temperature liquid crystalline compounds for commercial application. Of particular interest are the laterally fluorinated bi- and ter-phenyls⁶⁶ as outlined in the next section.

1.5.3.1 LATERAL FLUORINATION

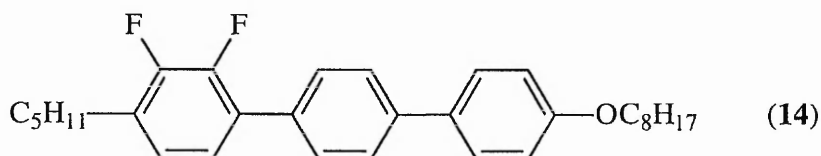
Numerous compounds containing lateral fluoro-substituents have been synthesised⁶⁶⁻⁷⁴ enabling researchers to build up an understanding of the effect of such substitution on mesophase type and mesophase thermal stability. Specific examples include the I-compounds (**12**) reported by Balkwill *et al.*⁷¹ and more recently the 2,3-difluorobi- (e.g. **13**) and 2,3-difluoroter-phenyls (e.g. **14**).⁶⁶



K 40°C N 108°C I



K 25.0°C S_C (11.5°C) S_A 33.0°C N 34.0°C I



K 89.0°C S_C 155.5°C S_A 165.0°C N 166.0°C I

The inclusion of a lateral fluoro-substituent may either enhance nematic or smectic properties and at the same time reduce the melting point. The lateral fluoro-substituent is readily used as opposed to other substituents because it imparts the following advantages:

- a) fluorine is the smallest substituent possible (the van der Waals radii of fluorine and hydrogen are 1.35-1.47Å and 1.2Å, respectively) thus causing the minimum amount of disruption to the packing arrangement of the molecules;
- b) the introduction of a highly electronegative fluoro-substituent gives rise to a moderately polar C-F bond directed across the long molecular axis. The result is a lateral dipole which allows the design of mesogenic materials with either a negative⁶⁶ or positive⁷² dielectric anisotropy ($\Delta\epsilon$), where the dielectric anisotropy is defined as 'the difference between the dielectric permittivity values measured parallel (ϵ_{\parallel}) and perpendicular (ϵ_{\perp}) to the molecular director' thus providing a measure of the strength of interaction between a liquid crystal and an applied field, and;
- c) the lateral dipole produced by the C-F bond can either induce the formation of or stabilise tilted smectic mesophases.^{66,73,74}

1.6 ELECTRO-OPTIC APPLICATIONS OF LIQUID CRYSTALS

The demand for flat-panel, portable, light-weight display devices with low power consumption, good viewing angle and sharp contrast results in ever increasing complexity of display devices. Such devices are required both for indoor and outdoor usage and have created the need for a high degree of refinement in liquid crystal materials. The parameters required by these materials include a wide range of physical properties such as wide nematic or S_C^* range, low viscosity, good solubility, suitable optical and dielectric anisotropies, acceptable elastic deformation characteristics and high multiplexibility, i.e., sharp threshold response, low temperature dependence of threshold voltage, low $\Delta\epsilon/\epsilon_{\perp}$, etc.⁷⁵

The geometric anisotropy of a liquid crystal gives rise to anisotropic electromagnetic properties. The electric and magnetic susceptibilities are different parallel to the director and perpendicular to the director. This anisotropy is crucial in that, depending on which susceptibility is larger, it is responsible for the director of the liquid crystal either aligning itself parallel or perpendicular to an applied field.

At present there is no single liquid crystalline material which is able to fulfil all the parameters referred to above and in fact most display devices comprise a multi-component liquid crystal mixture. The search for better materials is an important aspect of liquid crystal research and applies to both additives, materials which perform a specific function in the mixture such as reducing viscosity, raising the clearing point temperature or increasing multiplexing capability of the mixture, and to new host materials which satisfy as many of the device parameters as possible.

1.6.1 TWISTED NEMATIC AND SUPERTWISTED NEMATIC DISPLAYS

There are numerous types of liquid crystal display (LCD) devices on the market, notably the *Twisted Nematic*¹⁴ (TN) and *Supertwisted Nematic*⁷⁶ (STN) which are in abundant use in calculators, cash registers, electronic test equipment, etc. *Figure 19* shows the basic assembly of a nematic liquid crystal device which consists of a thin layer of nematogenic material sandwiched between two glass substrates approximately 5-10 μm apart. The inner surface of each glass substrate is coated with a transparent indium-tin oxide (ITO) conductive layer and a surfactant layer which is rubbed in a single direction. The latter has a two-fold effect: provides the planar or homogeneous

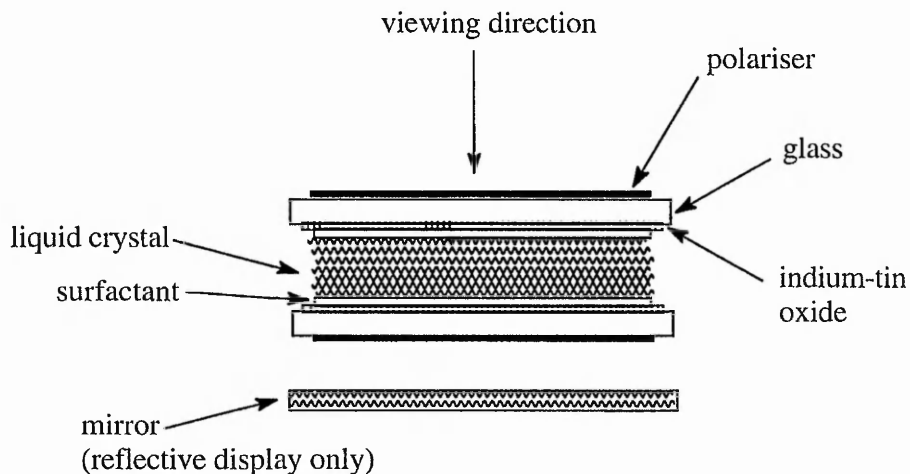


Figure 19 Twisted nematic liquid crystal display device.

alignment and; orients the molecules in a given direction. However, the rubbing direction of the second glass slide is perpendicular with respect to the first glass slide and this results in the director rotating through 90° and hence the name 'twisted nematic'. A polarising film is added to the outside of each glass substrate. In the presence of crossed polarisers and in the absence of an applied electric field, light

entering through the top polariser, rotates with the director (wave-guided) as it passes through the liquid crystal and therefore passes through the bottom polariser. In this situation a bright field of view is observed. On application of a small voltage across the plates, the liquid crystal material adopts the homeotropic alignment, i.e., molecules align orthogonal with respect to the substrate. In this situation, light entering through the top polariser propagates along the director unaffected and hence is extinguished by the second polariser thus giving a dark field of view. When the field is removed the molecules revert to the homogeneous alignment due to the natural elasticity of the nematic phase. The whole switching process is on the millisecond time scale.

The supertwisted nematic display device⁷⁶ is an advancement of the TN display affording improvements in contrast and viewing angle characteristics. The mode of operation is basically the same but in this display the director rotates through 270° between the two glass slides instead of 90° as in the TN display.

1.6.2 SURFACE STABILISED FERROELECTRIC DISPLAYS

The requirement for faster operating display devices prompted the development of the *Surface Stabilised Ferroelectric Liquid Crystal* (SSFLC) display device.¹⁵ To understand fully how the SSFLC device operates one needs an insight into the origin of ferroelectricity.

The term ferroelectric is applied to any material which possesses either a permanent or spontaneously polarised dipole moment. The ferroelectric effect was first observed indirectly by Valasek⁷⁷ in 1921 during experiments on crystals of Rochelle salt. Upon the application of mechanical stress the crystals exhibit an induced polarisation

due to a reduction of symmetry elements. This phenomenon is actually termed piezoelectricity and not ferroelectricity.

In 1975 Meyer *et al.*¹⁶ argued that certain liquid crystal phase types could possess reduced symmetry elements and, in the presence of an applied electric field rather than mechanical stress, induce polarisation, i.e, exhibit ferroelectricity. Meyer stated that the following prerequisites must be satisfied for any liquid crystal phase to be considered as being ferroelectric:

- a) tilted phase, i.e., possesses monoclinic symmetry;
- b) the molecules must be chiral;
- c) molecules must occur in layers. Therefore it is confined to smectic phases, and;
- d) the molecules must possess a strong transverse dipole moment.

There are numerous smectic phases which meet the above requirements (S_C^* , S_F^* , S_I^*), however, the S_C^* phase was utilised by Clark and Lagerwall¹⁵ when developing the first ferroelectric electro-optic display device. In the S_C^* phase, (*Figure 20*), the chiral molecules occur in layers and are tilted with respect to the layer planes. The tilt direction in each layer is constant, however, the director rotates in a helical manner through successive layers. Each layer in the helix has a spontaneous polarisation associated with it, however due to the helical stacking arrangement, the overall polarisation averages out to zero. The phase is consequently described as *helielectric*.

Clark and Lagerwall¹⁵ realised that by suppression of the helix, the molecules would align in a given direction and hence give a ferroelectric state. To this effect, they

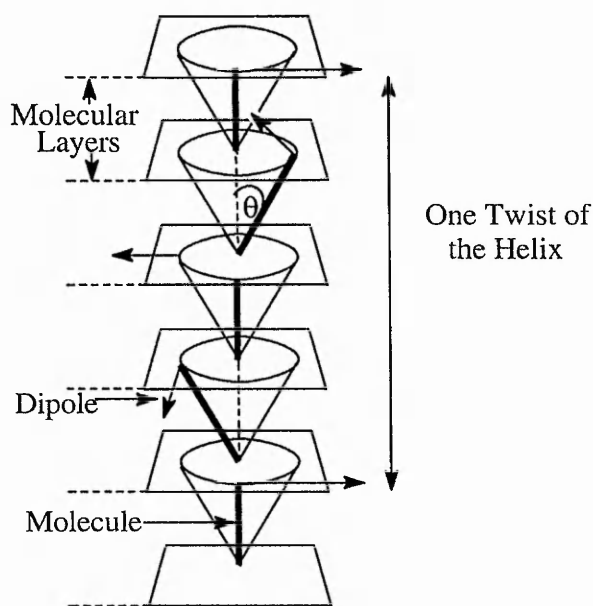


Figure 20 Helielectric structure of the chiral smectic C phase.

developed the Surface Stabilised Ferroelectric Liquid Crystal (SSFLC) display in which the helix of the chiral smectic phase is suppressed by sandwiching the phase between two glass substrates in a very thin cell (1-2 μm). The molecules are aligned in special geometry whereby the layers are perpendicular with respect to the glass substrates (bookshelf geometry). Strong surface or boundary interactions (surface stabilisation) cause the helix to unwind and the molecules lie parallel with respect to the surface whereas the strong dipole moment (associated with the chiral centre) rests perpendicular with respect to the surface. On the application of a small DC potential across the plates, the polarisation direction can be switched (reversed). The reversal of polarisation causes the molecules to rotate about a degenerate energy cone by an angle of 2θ (**Figure 21**) (the optimum molecular tilt angle, (θ) , for the cell is 22.5°) and the molecules therefore undergo a change in tilt angle of 45° . If the cell is placed between crossed polarisers so

that the top polariser lies parallel with the director, then in the off state light entering the display device is polarised along the director until it is extinguished by the bottom polariser thus giving a dark field of view. However, when the electric field is reversed, i.e., in the on state the light polarised by the top polariser is at 45° to the director. The cell thickness is carefully allied to the birefringence of the liquid crystal medium and

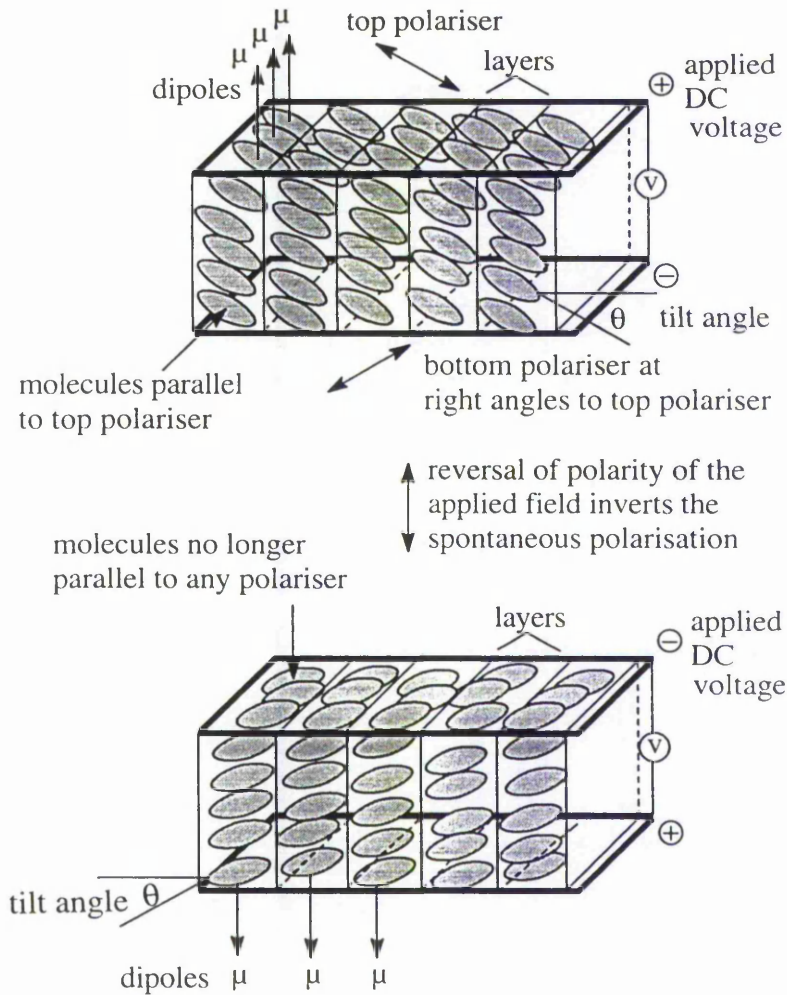


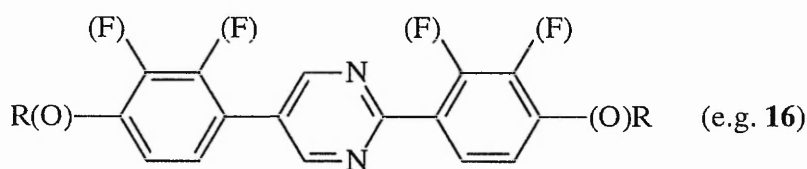
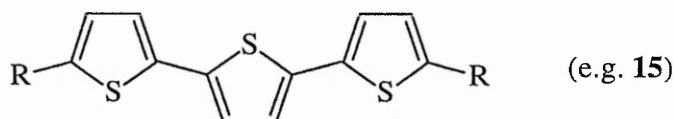
Figure 21 Optical transmission in a surface stabilised ferroelectric liquid crystal display. The top cell demonstrates light transmission and the bottom cell demonstrates light extinction.

hence the cell acts as a half-wave plate allowing light to pass through the bottom polariser, i.e., field of view appears bright (*Figure 21*). Both polarisation states are stable upon removal of an applied electric field and the ferroelectric device is said to be bistable. The optimum switching angle (45°) is smaller than for the TN display (90°) and the ferroelectric device operates on the microsecond time scale. This type of display device is constantly being updated due to its unique properties of faster switching speeds of 10-100 μs (c.f. conventional twisted nematic cell with switching speeds of 10 ms), bistability and good viewing angle which are all important requirements for use in high-resolution video liquid crystal displays of the future.

1.7 AIMS

Commercial ferroelectric mixtures exhibit the following phase sequence: I-N-S_A-S_C*. Obviously, the S_C* phase is vitally important, but most commercial mixtures are composed of achiral materials which exhibit the non-chiral S_C phase and chirality is induced by the addition of a chiral dopant. The commercial mixture must then display a wide S_C* temperature range, usually from -30 to 70°C, a large spontaneous polarisation (P_S) and low viscosity. At present, industry is striving to design novel mixtures which exhibit the desired properties mentioned above.

The general aims of the research concentrate on the design and synthesis of novel heterocyclic-based compounds (e.g. **15**) and (e.g. **16**) in order to evaluate their



potential usefulness as additives in commercial ferroelectric mixtures. Initial studies focused on the synthesis of three-ring thiophene-based compounds comprising suitably 2,5-disubstituted thienyl units (**15**). The results of this study are reported in chapter 2 (p. 47 to p. 63). Following this short study, the research effort then concentrated on the synthesis of fluorinated three-ring pyrimidine compounds (**16**). The results of this major study are reported in chapter 3 (p. 64 to p. 183).

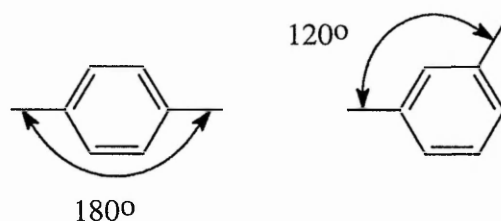
Synthesis and preliminary characterisation of mesomorphic properties (optical microscopy and DSC) were undertaken at Nottingham Trent whilst evaluation of their physical properties as additives in commercial mixtures was studied in collaboration with Dr. Chan of Central Research Laboratories (CRL) U.K. The latter work is confidential and hence actual evaluation results, i.e., measurement of P_S , viscosity, etc., cannot be disclosed.

THIOPHENE-BASED LIQUID CRYSTALS

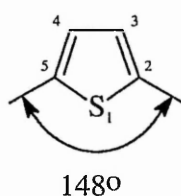
2. THIOPHENE-BASED LIQUID CRYSTALS

2.1 INTRODUCTION

Conventional liquid crystals are based on suitably substituted 1,4-phenylene units (bond angle = 180°) because they give rise to an elongated and lath-like molecular geometry, i.e., calamitic liquid crystals. The introduction of a bend or 'kink' in the system is thought to be detrimental to mesophase thermal stability such that molecules comprising 1,3-phenylene units are, generally, not liquid crystalline. The 1,3-disposition



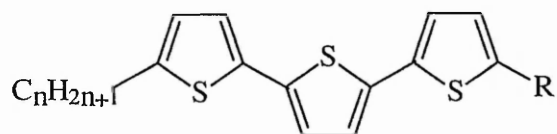
generates an exocyclic bond angle of 120° which confers a strong bend in the geometry of the molecule and hence disrupts the lamellar packing arrangement conducive for liquid crystal formation. The liquid crystal group at Nottingham Trent, however, has a strong tradition in the synthesis of non-linear compounds which exhibit mesomorphic properties with particular expertise in thiophene-based liquid crystals.



Thiophene is a five-membered aromatic heterocycle comprising sulphur. The chemistry of thiophene is dominated by electrophilic aromatic substitution reactions because it contains six π -electrons distributed over five atomic orbitals and is said to be

π -excessive. Electrophilic substitution takes place preferentially at the α -positions (C2- and C5-) rather than the β -positions (C3- and C4-).

2,5-Disubstituted thiophene is an interesting unit because it possesses an exocyclic bond angle of 148° which is intermediate between that for 1,4-phenylene (180°) and 1,3-phenylene (120°). The partially 'bent' or 'kinked' nature of 2,5-disubstituted thiophene is thought to cause minimal disruption to the linear packing arrangement of the molecules such that mesomorphic properties should be retained. Low melting materials which exhibit tilted phases are to be expected. In addition, the electronegative sulphur atom provides a strong lateral dipole thus eliminating the need for lateral substituents. The latter, although very useful as discussed earlier (p. 34), tend to increase viscosity which subsequently slows the response time. Hence, 2,5-disubstituted thiophene appears to be a reasonable moiety for generating some of the desired features required for a commercial ferroelectric mixture. The following sections of this chapter now report the results of a short study on the synthesis and mesomorphic properties of suitably 5,5"-disubstituted 2,2':5',2"-terthienyls (**20a-d** and **21a-d** or **series I** and **II**, respectively).



$R = \text{COC}_m\text{H}_{2m+1}$ (**20a-d** or **series I**)

$\text{C}_n\text{H}_{2n+1}$ (**21a-d** or **series II**)

where $m=n-1$

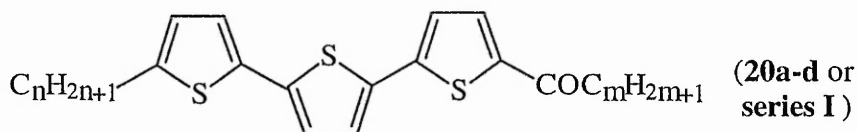
2.2 RESULTS AND DISCUSSION

The introduction of either alkyl or acyl substituent(s) to the 5- and 5''-positions of the terthienyl core is effective in producing liquid crystalline behaviour since all members of the 5-*n*-alkanoyl-5''-*n*-alkyl-2,2':5',2''-terthienyls (**series I**) and the corresponding 5,5''-di-*n*-alkyl-2,2':5',2''-terthienyls (**series II**) are mesomorphic. It appears, therefore, that the disposition of the three thiophene rings affords a suitably linear molecular geometry conducive for liquid crystal formation.

2.2.1 OPTICAL AND THERMAL (DSC) CHARACTERISATION

The mesophase transition temperatures and thermodynamic data for the members of **series I** are listed in *Table 1* and are represented graphically in *Figure 22* as a plot against the number of carbon atoms, *n*, in the alkyl chain.

Table 1. Transition temperatures (°C) (**in bold**) and enthalpies ($\Delta H/\text{kJ mol}^{-1}$) (*in italics*) for the 5-*n*-alkanoyl-5''-*n*-alkyl-2,2':5',2''-terthienyls (**series I**).



| No. | <i>n</i> | <i>m</i> | I-S _A | S _A -K | K-S _A |
|------------|----------|----------|------------------------------|------------------------------|------------------------------|
| 20a | 3 | 2 | 166.5 <i>7.60</i> | 145.0 <i>21.78</i> | 155.5 <i>20.96</i> |
| 20b | 4 | 3 | 155.7 <i>7.64</i> | 136.9 <i>21.41</i> | 148.3 <i>24.58</i> |
| 20c | 5 | 4 | 163.0 <i>6.36</i> | 130.5 <i>14.74</i> | 137.2 <i>15.57</i> |
| 20d | 6 | 5 | 162.0 <i>10.70</i> | 132.9 <i>24.69</i> | 138.4 <i>25.86</i> |

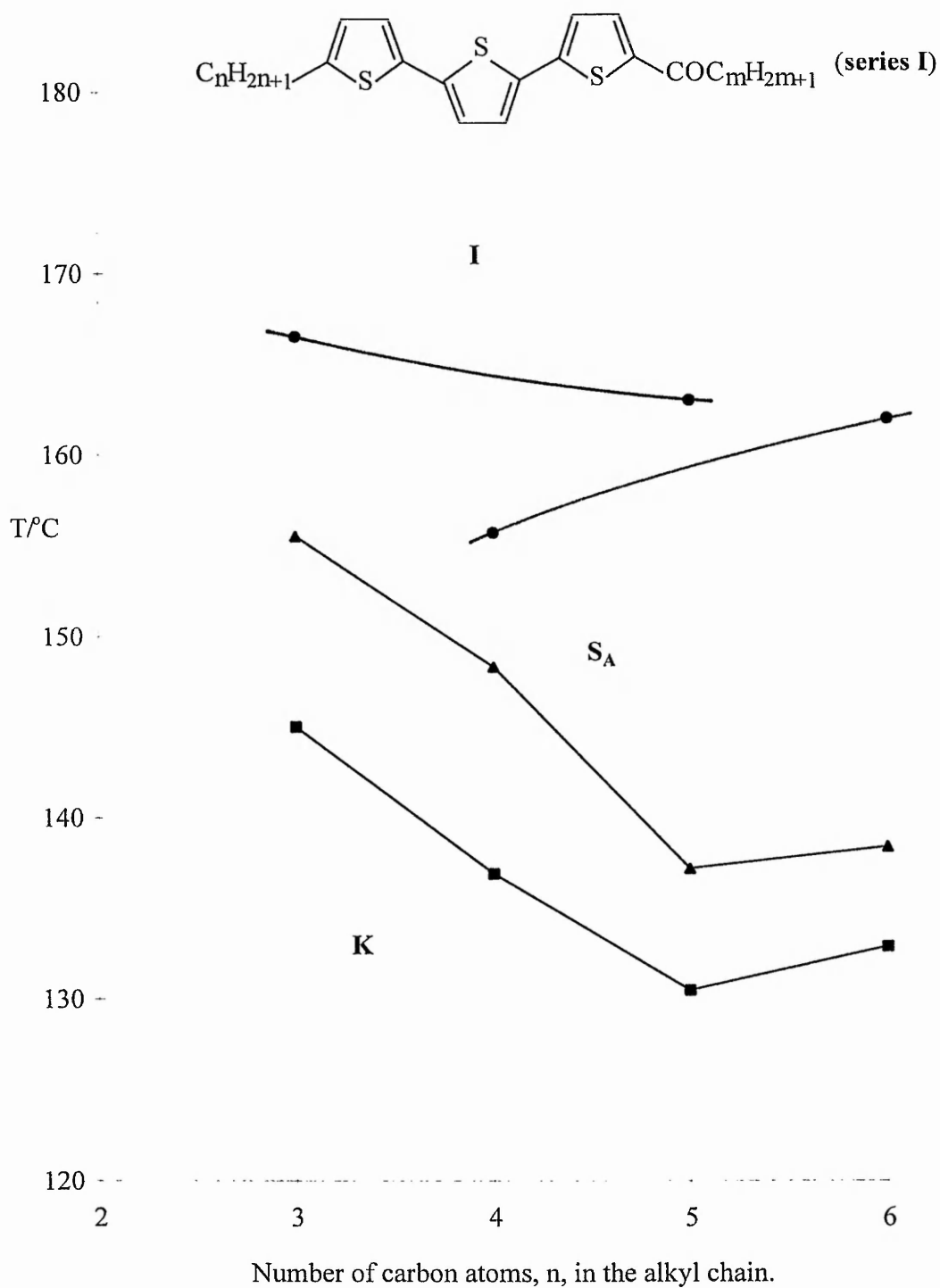


Figure 22. Plot of transition temperatures for certain 5-*n*-alkanoyl-5'-*n*-alkyl-2,2':5',2''-terthienyls (series I).

All the members ($n=3-6$) of an homologous series of 5- n -alkanoyl-5''- n -alkyl-2,2':5',2''-terthienyls (**series I**), exhibit an S_A phase (*Plate 1*) which, on cooling from the isotropic liquid, is characterised by the formation of bâtonnets which coalesce to fashion an elongated focal-conic fan texture interspersed with homeotropic regions. Although only four members have been prepared the points for the I- S_A transition temperatures alternate, i.e., exhibit an odd-even effect, with the odd- n homologues lying uppermost.

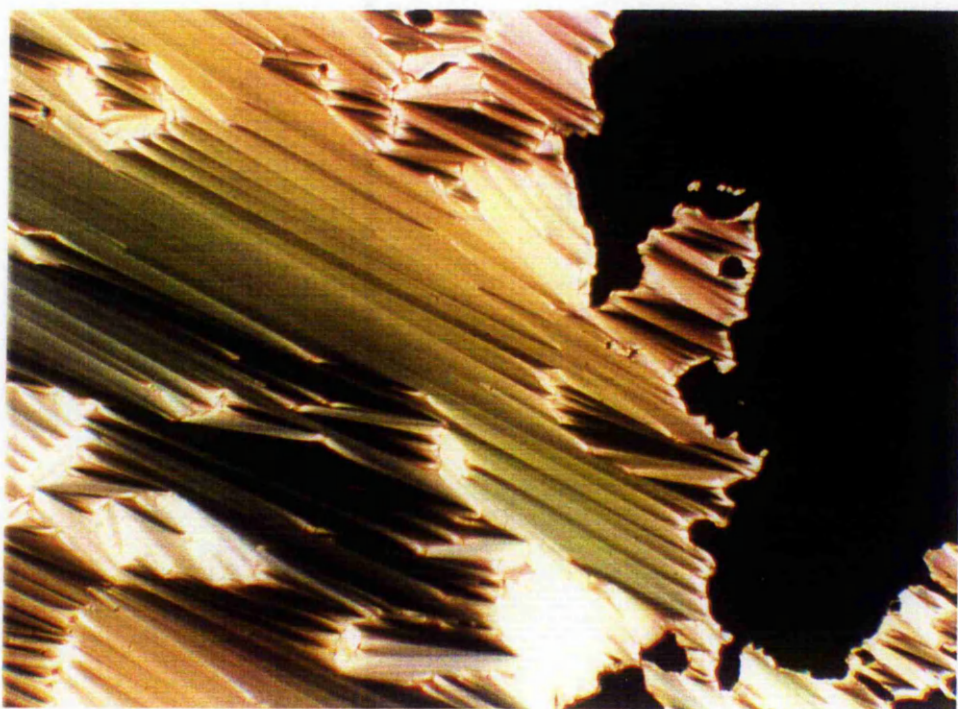
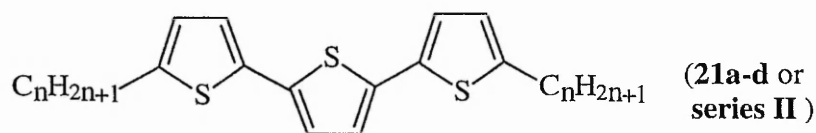


Plate 1. The focal-conic fan texture of the 5- n -hexanoyl-5''- n -hexyl-2,2':5',2''-terthienyl (**20d**).

The mesophase transition temperatures and thermodynamic data for the members of **series II** are listed in *Table 2* and are represented graphically in *Figure 23* as a plot against the number of carbon atoms, n , in the alkyl chain.

Table 2. Transition temperatures ($^{\circ}\text{C}$) (**in bold**) and enthalpies ($\Delta\text{H}/\text{kJ mol}^{-1}$) (*in italics*) for the 5,5"-di-*n*-alkyl-2,2':5',2"-terthienyls (**series II**).



| No. | n | I-CrG | CrG-K | K-CrG |
|------------|---|--------------|--------------|--------------|
| 21a | 3 | 74.6 | 20.0 | 50.0 |
| | | <i>12.38</i> | <i>2.76</i> | <i>18.01</i> |
| 21b | 4 | 75.1 | 28.0 | 48.5 |
| | | <i>16.32</i> | <i>17.85</i> | <i>20.99</i> |
| 21c | 5 | 78.0 | 30.6 | 54.2 |
| | | <i>12.37</i> | <i>9.65</i> | <i>22.07</i> |
| 21d | 6 | 80.1 | 38.90 | 51.9 |
| | | <i>19.94</i> | <i>20.44</i> | <i>20.15</i> |

Reduction of the carbonyl group in **series I** to afford members of an homologous series of 5,5"-di-*n*-alkyl-2,2':5',2"-terthienyls (**series II**) lowers the melting point considerably and also dramatically alters the mesomorphic properties. The S_A phase is no longer observed but is replaced by a high order crystal G phase. On cooling from the isotropic liquid it first appears that crystallisation is occurring, particularly as the allied enthalpy of transition is large ($>10 \text{ kJ mol}^{-1}$). However, on cooling at $0.2^{\circ}\text{C min}^{-1}$ growth of dendrites can be discerned which on further cooling give a mosaic texture which has irregularly shaped and sized constituents, mostly angular and sharp-cornered in appearance, which are characteristic of the CrG phase (*Plate 2*).

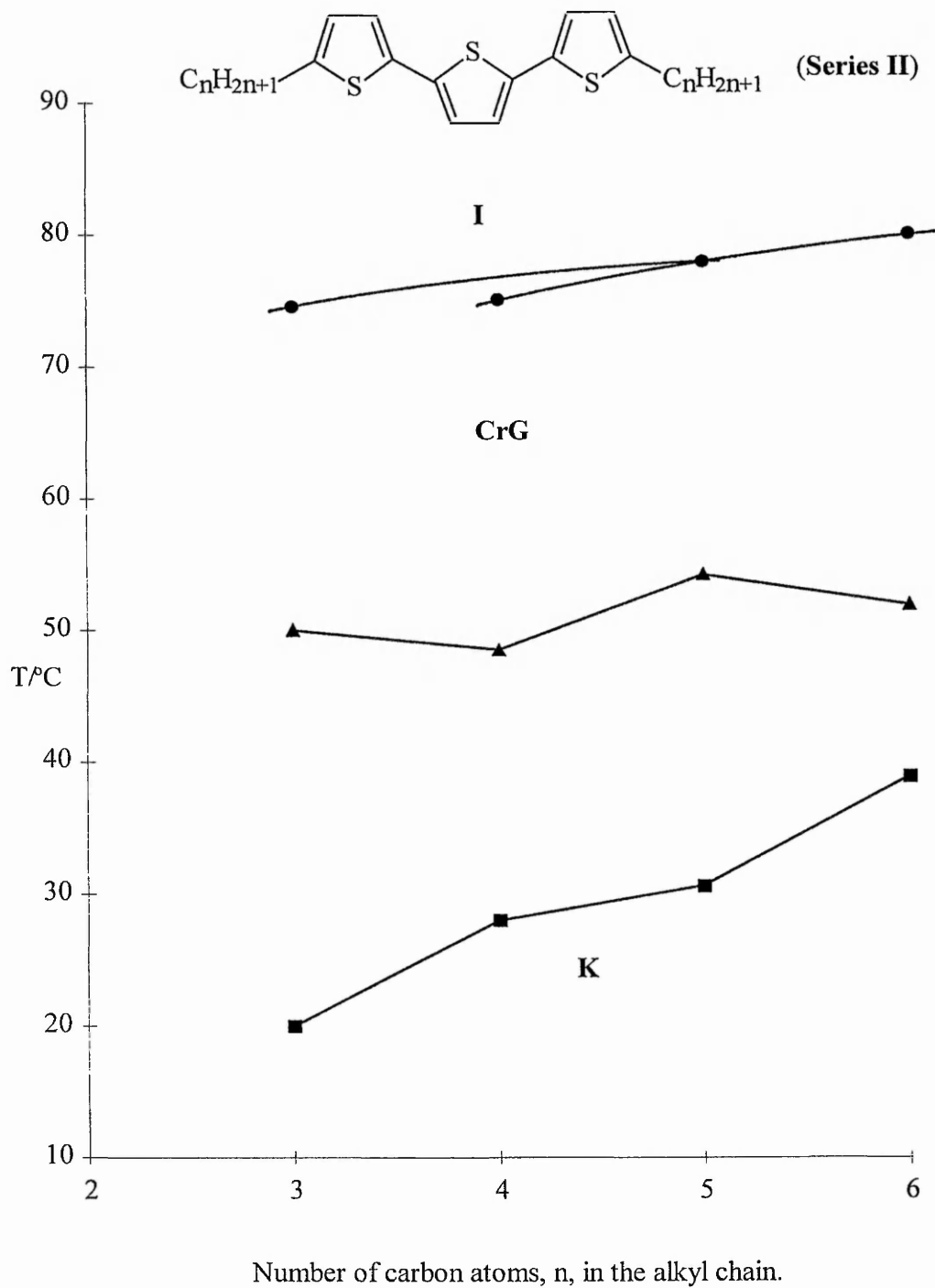


Figure 23. Plot of transition temperatures for certain 5,5''-di-*n*-alkyl-2,2':5',2''-terthienyls (**series II**).

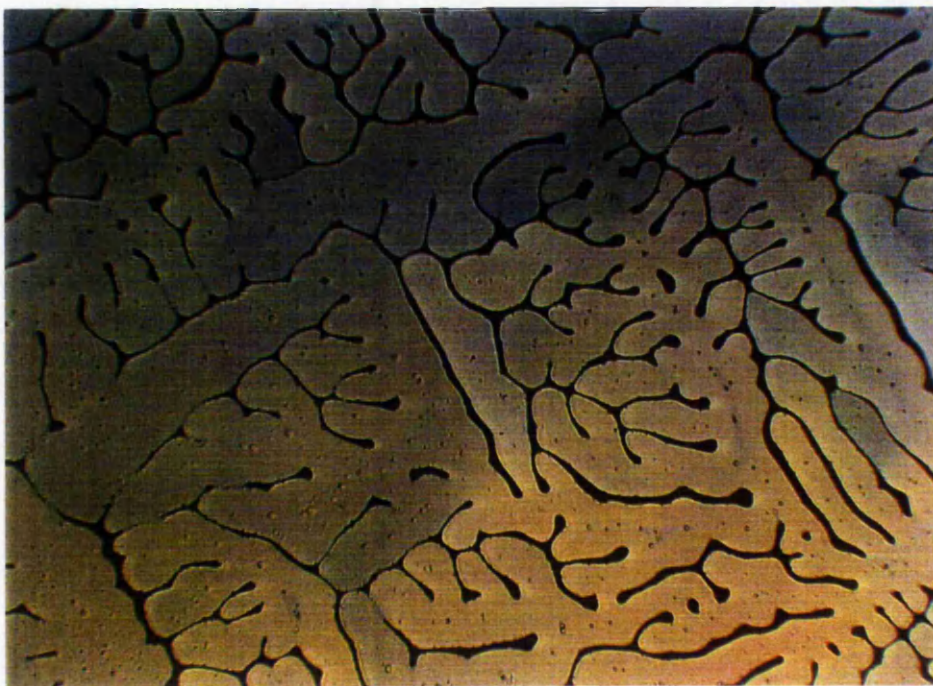


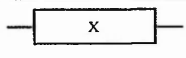
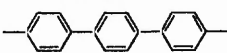
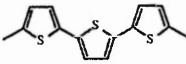
Plate 2. Dendritic growth of the CrG phase in the isotropic liquid of 5,5''-di-*n*-pentyl-2,2':5',2''-terthienyl (**21c**).

2.2.2 COMPARATIVE STUDY OF **SERIES II** WITH ANALOGOUS 4,4''-DISUBSTITUTED-1,1':4',1''-TERPHENYLS

An appraisal of the mesomorphic properties of the compounds containing the 2,2':5',2''-terthienyl core, i.e., **series II**, can be concluded by comparison with their corresponding non-heterocyclic counterparts, i.e., 4,4''-disubstituted-1,1':4',1''-terphenyls.⁷⁸

Table 3 shows the average melting point and clearing point temperature, i.e., thermal stability, for the members of **series II** and their corresponding terphenyl analogues. The replacement of the terphenyl core with the terthienyl core greatly lowers both the average melting point (average reduction of 152.4°C) and the average mesophase thermal stability (average reduction of 142.3°C). These results may be

Table 3. Average melting point, clearing point and phase range ($^{\circ}\text{C}$) for members ($n=3-6$) of an homologous series of 5,5''-di- n -alkyl-2,2':5',2''-terthienyls (**series II**) and their corresponding terphenyl analogues.⁷⁸

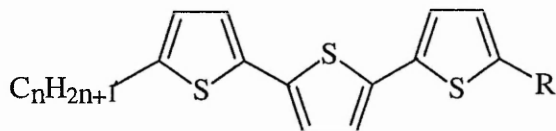
|  | Average melting point | Average clearing point | Average phase range |
|---|-----------------------|------------------------|---------------------|
|  | 203.5 | 219.2 | 15.7 |
|  | 51.1 | 76.9 | 25.8 |

associated with the significant deviation from linearity within the terthienyl core which disrupts the lamellar packing arrangement of the molecules with respect to their terphenyl analogues. Nevertheless, the average phase range, i.e., melting point to clearing point temperature range, of the three-ring thiophene compounds is wider than their phenylene analogues by 10.1°C .

Unfortunately, neither members of **series I** nor members of **series II** exhibit the desired smectic C phase despite their non-linear geometry. Members of **series I** exhibit the S_A phase alone whereas members of **series II** exhibit the CrG phase alone. This is even more surprising for members of **series I** which also contain a strong terminal dipole, i.e., carbonyl moiety which is thought desirable for generating the S_C phase. Despite their poor mesogenic behaviour, the compounds were sent to Central Research Laboratories for further specialist evaluation. Unfortunately, a second and major setback was encountered in that when these compounds were added to commercial mixtures, they were found to be highly unstable due to rapid photochemical degradation. Hence the thiophene strategy was abandoned and new work was focused on a different heterocyclic core, namely pyrimidine (see chapter 3, p. 64).

2.3 EXPERIMENTAL

2.3.1 THE SYNTHESIS OF 5-*n*-ALKANOYL-5''-*n*-ALKYL- (series I) AND 5,5''-DI-*n*-ALKYL-2,2':5',2''-TERTHIENYLS (series II)



R = COC_mH_{2m+1} (**20a-d** or series I)

C_nH_{2n+1} (**21a-d** or series II)

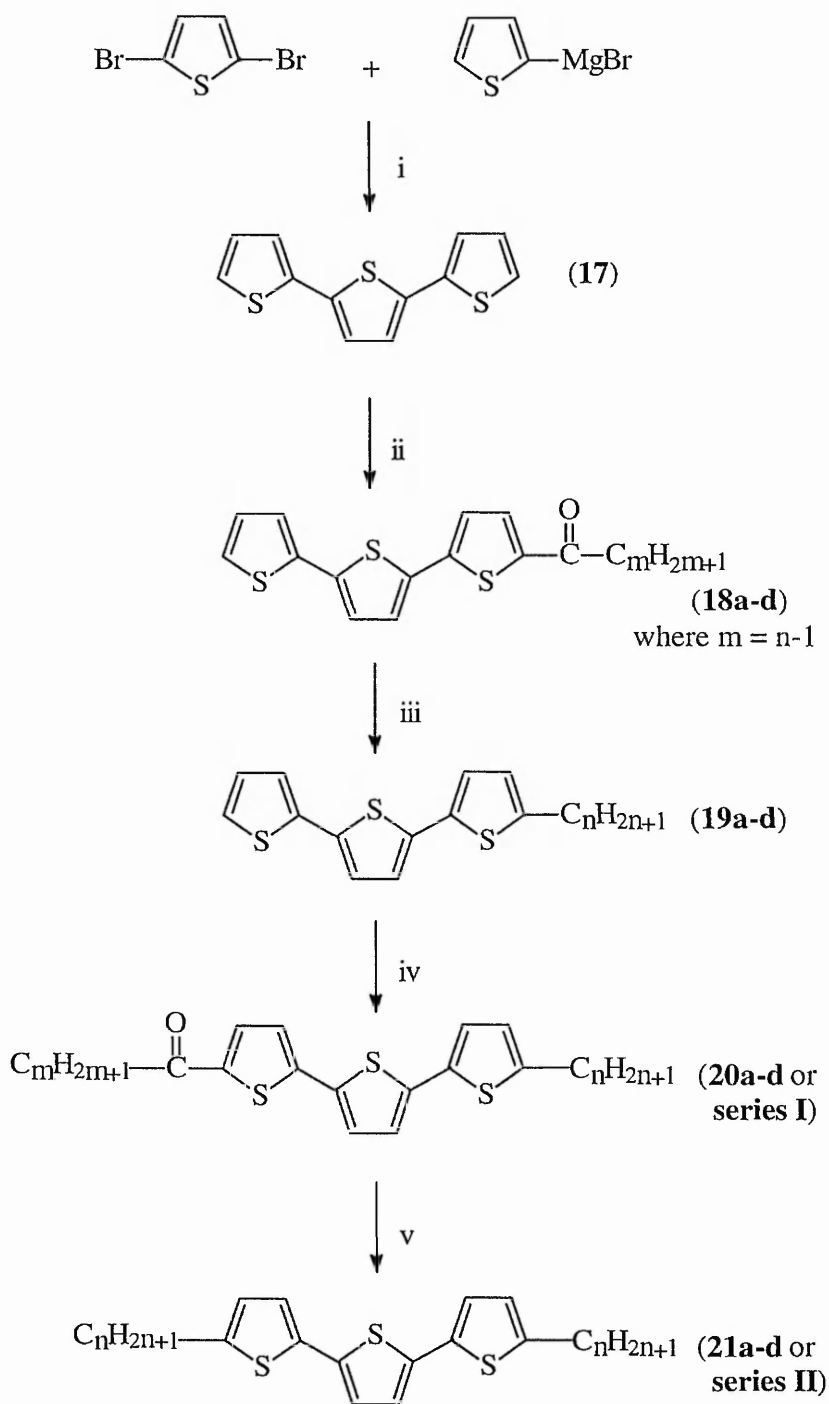
where m=n-1

2.3.1.1 SYNTHETIC OVERVIEW

The preparative route leading to members of an homologous series of 5-*n*-alkanoyl-5''-*n*-alkyl-2,2':5',2''-terthienyls (**series I**) and their corresponding 5,5''-di-*n*-alkyl-2,2':5',2''-terthienyls (**series II**) is outlined in **scheme 1** (p. 57).

2,2':5',2''-Terthienyl (**17**) may be prepared via several methods.⁷⁹⁻⁸³ However, the nickel-catalysed cross-coupling reaction reported by Tamao *et al.*⁸⁴ was employed because of its high yield and ease of purification. Hence, 2,2':5',2''-terthienyl (**17**) was prepared by coupling the Grignard reagent of 2-bromothiophene with 2,5-dibromothiophene in the presence of [1,3-*bis*(diphenylphosphino)propane]nickel(II) chloride, as catalyst.

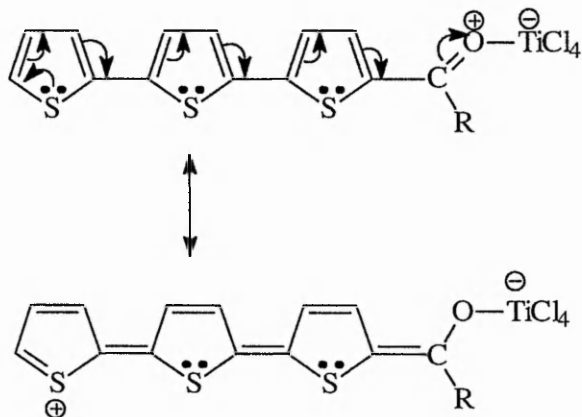
Subsequently, Friedel-Crafts acylation of (**17**) with the appropriate alkanoyl chloride, catalysed by titanium(IV) tetrachloride, afforded the mono-acylated terthiophene (**18a-d**). TiCl₄ was used in preference to AlCl₃ as choice of catalyst because the latter causes the polymerisation of thiophene to give intractable tars. Polyacylation of the terthienyl core does not occur because once the ketone-catalyst complex



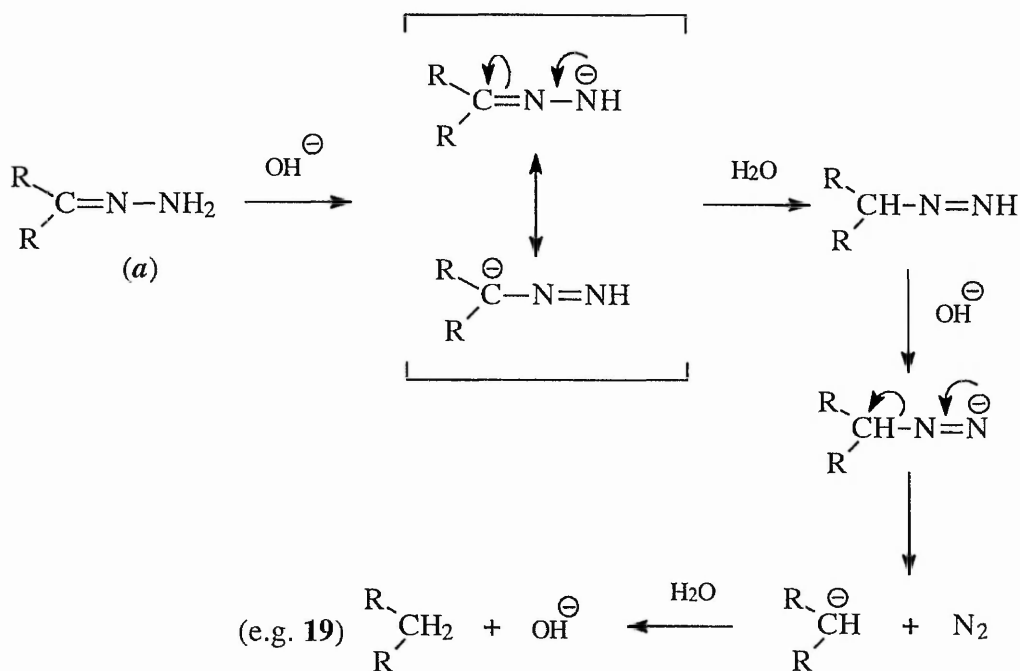
- i. $[(\text{C}_6\text{H}_5)_2\text{P}(\text{CH}_2)_3\text{P}(\text{C}_6\text{H}_5)_2]\text{NiCl}_2$, ether, reflux.
 ii. and iv. $\text{C}_m\text{H}_{2m+1}\text{COCl}$, TiCl_4 , CH_2Cl_2 .
 iii. and v. $\text{NH}_2\text{NH}_2 \cdot \text{H}_2\text{O}$, KOH , diethylene glycol, reflux.

Scheme 1

reacts at a vacant α -position the remainder of the molecule is deactivated towards further electrophilic substitution due to the powerful $-M$ effect of the ketone which withdraws electron density from the aromatic core as shown below.



The 5-*n*-alkanoyl-2,2':5',2''-terthienyls (**18a-d**) were then reduced to the corresponding 5-*n*-alkyl-2,2':5',2''-terthienyls (**19a-d**) using the Huang-Minlon modification⁸⁵ of the Wolff-Kishner reduction which employs a high boiling solvent



(diethylene glycol). The mechanism shown overleaf involves the formation of a hydrazone intermediate (*a*) which undergoes base-catalysed proton elimination with double-bond migration (tautomerism), followed by loss of nitrogen gas to give the desired alkane product (e.g. **19**).

A second Friedel-Crafts acylation of the appropriate mono-alkyl terthienyls (**19a-d**) with the appropriate alkanoyl chloride afforded the members of the 5-*n*-alkanoyl-5'-*n*-alkyl-2,2':5',2''-terthienyls (**20a-d**), i.e., members of **series I**. Subsequent reduction of the members of **series I** gave the corresponding 5,5''-di-*n*-alkyl-2,2':5',2''-terthienyls (**21a-d**), i.e., members of **series II**.

2.3.1.2 EXPERIMENTAL PROCEDURES

2,2':5',2''-Terthienyl (**17**) (scheme 1)

In an atmosphere of nitrogen, a solution of 2-bromothiophene (60.0 g, 0.368 mol) in dry diethyl ether (ether) (200 ml) was added, dropwise, to a mixture of magnesium turnings (9.8 g, 0.404 mol) and dry ether (100 ml) at such a rate that the ether boiled gently. After the addition was complete, the reaction mixture was heated under reflux for 1 h., cooled to 0°C and then added, dropwise, under an atmosphere of nitrogen, to a stirred mixture of 2,5-dibromothiophene (40.0 g, 0.165 mol), [1,3-*bis*(diphenylphosphino)propane]nickel(II) chloride (1.0 g, 0.0018 mol) and dry ether (200 ml) at 0°C. The reaction mixture was stirred under reflux for 10 h., then cooled and poured on to ice-cold saturated ammonium chloride solution (200 ml). The crude product was extracted with ether (4 x 150 ml) and the combined organic extract was washed with

water (3 x 100 ml), dried (MgSO₄) and the solvent removed *in vacuo*. The crude residue was purified by recrystallisation from ethanol to furnish the pure 2,2':5',2''-terthienyl (**17**), 30.0 g (73%), m.p. 92-94°C (Lit.⁸⁴ 93-95°C), as a yellow solid.

¹H NMR (CDCl₃) δ: 7.0-7.3 (8H, m, ThH) ppm.

i.r. ν_{\max} (KBr): 3036, 1422, 798, 688 cm⁻¹.

5-*n*-Alkanoyl-2,2':5',2''-terthienyls (**18a-d**) (scheme 1)

A solution of 2,2':5',2''-terthienyl (**17**) (6.0 g, 0.024 mol) in dry DCM (50 ml) was added, dropwise, to a cooled (-10°C), stirred mixture of the appropriate alkanoyl chloride (0.036 mol), titanium(IV) chloride (3.9 ml, 0.036 mol) and dry DCM (100 ml). The reaction mixture was stirred for 4 h. at -10°C, allowed to warm to room temperature and then poured into concentrated hydrochloric acid/ice (200 ml) and stirred for 1 h. The organic layer was extracted with DCM, washed with saturated sodium hydrogen carbonate solution (200 ml), water (200 ml), dried (MgSO₄) and the solvent was removed under reduced pressure. The crude residue was subjected to column chromatography on silica gel using a 4:1 chloroform : light petroleum ether (b.p. 40-60°C) mixture as the eluent. The desired fractions were isolated, evaporated under reduced pressure and recrystallised from ethanol to afford the appropriate pure 5-*n*-alkanoyl-2,2':5',2''-terthienyl (**18a-d**), (50-60%), as a yellow crystalline solid. M.p.s: C₂H₅CO (**18a**), 135-137°; C₃H₇CO (**18b**), 123-125°; C₄H₉CO (**18c**), 126-128°; C₅H₁₁CO (**18d**), 132-134°C.

The following spectroscopic data refer to 5-*n*-hexanoyl-2,2':5',2''-terthienyl (**18d**) and are typical of the series:

$^1\text{H NMR}$ (CDCl_3) δ : 1.0 (3H, t, CH_3), 1.2-1.4 (4H, m, CH_2) 1.8 (2H, quint, CH_2), 2.9 (2H, t, COCH_2), 7.0-7.6 (7H, m, ThH) ppm.

i.r. ν_{max} (KBr): 3070, 2930, 2870, 1655 ($\text{C}=\text{O}$ str.), 1442, 1423, 794 cm^{-1} .

5-*n*-Alkyl-2,2':5',2''-terthienyls (**19a-d**) (scheme 1)

A mixture of the appropriate ketone (**18a-d**) (1.0 g, 0.002 mol), diethylene glycol (80 ml) and hydrazine hydrate (5 ml, 0.1 mol) was heated to reflux for 4 h. Subsequently, the excess of hydrazine hydrate was removed by atmospheric distillation and the internal temperature was raised to 210°C and then cooled to room temperature. Potassium hydroxide (5.0 g, 0.09 mol) was added and the reaction mixture was heated to reflux for 4 h. and then allowed to cool to room temperature. The reaction was quenched with concentrated hydrochloric acid/ice (100 ml), extracted with chloroform (100 ml), washed with water (100 ml), dried (MgSO_4) and the solvent removed *in vacuo*. The crude product was applied to a column of silica gel, eluting with a mixture of 1:4 chloroform : light petroleum ether (b.p. 40-60°C). The desired fraction was isolated, evaporated under reduced pressure and recrystallised from ethanol to give the appropriate pure 5-*n*-alkyl-2,2':5',2''-terthienyl (**19a-d**), (70-80%), as a pale yellow solid. M.p.s: C_3H_7 (**19a**), 56-57°; C_4H_9 (**19b**), 54-55°; C_5H_{11} (**19c**), 58-59°; C_6H_{13} (**19d**), 61-62°C.

The following spectroscopic data refer to 5-*n*-hexyl-2,2':5',2''-terthienyl (**19d**) and are typical of the series:

$^1\text{H NMR}$ (CDCl_3) δ : 0.9 (3H, t, CH_3), 1.2-1.4 (6H, m, CH_2) 1.8 (2H, quint, CH_2), 2.8 (2H, t, Th CH_2), 6.6-7.2 (7H, m, ThH) ppm.

i.r. ν_{\max} (KBr): 3065, 2919, 2854, 1450, 1427, 795, 681 cm^{-1} .

5-*n*-Alkanoyl-5''-*n*-alkyl-2,2':5',2''-terthienyls (**20a-d** or **series I**) (scheme 1)

A solution of the appropriate 5-*n*-alkyl-2,2':5',2''-terthienyl (**19a-d**) (1.5 g, 0.005 mol) in dry DCM (10 ml) was added, dropwise, to a cooled (-10°C), stirred mixture of the appropriate alkanoyl chloride (0.0077 mol), titanium(IV) chloride (0.8 ml, 0.0077 mol) and dry DCM (30 ml). The reaction was carried out as described by the method reported on p. 60 for compounds (**18a-d**). The crude residue was purified by column chromatography on silica gel eluting with 4:1 chloroform : light petroleum ether (b.p. $40-60^{\circ}\text{C}$) followed by recrystallisation from ethanol to furnish the appropriate pure 5-*n*-alkyl-2,2':5',2''-terthienyl (**20a-d**), (40-50%), as pale yellow crystals. The m.p.s and mesomorphic transition temperatures are listed in **Table 1**, section 2.2.1, p. 49.

The following spectroscopic data refer to 5-*n*-hexanoyl-5''-*n*-hexyl-2,2':5',2''-terthienyl (**20d**) and are typical of the series:

^1H NMR (CDCl_3) δ : 0.9 (6H, t, 2CH_3), 1.2-1.4 (12H, m, CH_2) 1.8 (2H, quint, CH_2), 2.8 (4H, m, COCH_2 , ThCH_2), 6.7-7.6 (6H, m, ThH) ppm.

i.r. ν_{\max} (KBr): 3070, 2923, 2857, 1651 ($\text{C}=\text{O}$ str.), 1450, 1439, 794 cm^{-1} .

5,5''-Di-*n*-alkyl-2,2':5',2''-terthienyls (**21a-d** or **series II**) (scheme 1)

The appropriate 5-*n*-alkanoyl-5''-*n*-alkyl-2,2':5',2''-terthienyl (**20a-d**) (0.7 g, 0.0014 mol) was reduced using the method described previously for compounds (**19a-d**) on p. 61. The crude residue was applied to a silica gel column and eluted with 1:9 chloroform : light petroleum ether (b.p. $40-60^{\circ}\text{C}$) to afford the appropriate pure 5,5''-di-*n*-alkyl-

2,2':5',2''-terthienyl (**21a-d**), (70-78%), as a pale yellow solid. The m.p.s and mesomorphic transition temperatures are listed in *Table 2*, section 2.2.1, p. 52.

The following spectroscopic data refer to 5,5''-di-*n*-hexyl-2,2':5',2''-terthienyl (**21d**) and are typical of the series:

¹H NMR (CDCl₃) δ: 0.9 (6H, t, 2CH₃), 1.2-1.4 (16H, m, CH₂), 2.8 (4H, t, 2ThCH₂), 6.6-7.2 (6H, m, ThH) ppm.

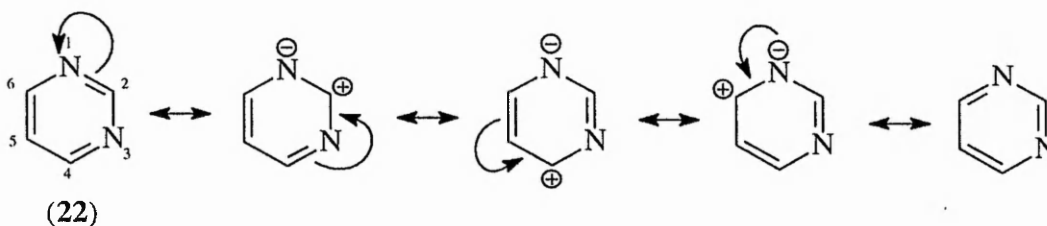
i.r. ν_{max} (KBr): 3065, 2919, 2853, 1466, 1445, 853, 793 cm⁻¹.

PYRIMIDINE-BASED LIQUID CRYSTALS

3. PYRIMIDINE-BASED LIQUID CRYSTALS

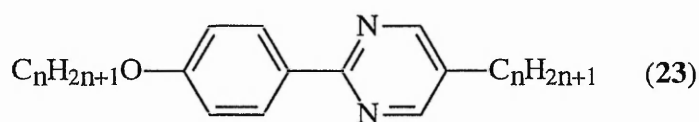
3.1 INTRODUCTION

Pyrimidine (**22**) is a six-membered heterocycle containing two nitrogen atoms and belongs to the class of compounds termed diazines. Pyrimidine is a π -deficient molecule resistant to aromatic electrophilic substitution due to the delocalisation of the π -electron cloud by the nitrogen atoms as shown below. The π -electron densities calculated for the ground state of pyrimidine at positions 2, 4 (6) and 5 are 0.776, 0.825 and 1.103 eV, respectively.⁸⁶ Hence, pyrimidine readily undergoes nucleophilic substitution at the 2-, 4- and 6-positions but attack by a nucleophile at the 5-position is not favoured because the negative charge on the intermediate cannot be delocalised onto the nitrogen atoms. The pyrimidine nucleus, however, can be activated towards electrophilic attack by employing N-oxides or pyrimidones.



The ability of pyrimidine to selectively undergo substitution at both the 2- and 5-positions allows for the synthesis of calamitic liquid crystals because the exocyclic bond angle is 180° . To this effect, the literature reports numerous examples of two-ring pyrimidine-based liquid crystals following the initial and significant work of Zschke⁸⁷

on a series of 5-*n*-alkyl-2-(4-*n*-alkoxyphenyl)pyrimidines (**23**).



The incorporation of pyrimidine in the molecular core tends to generate stable compounds with lower melting point, reduced viscosity and wide smectic C phase range when compared with their non-heterocyclic counterparts, i.e., suitably substituted biphenyls. In addition, the lone pairs on the two nitrogen atoms in the pyrimidine ring generate a strong transverse dipole moment which produces compounds with high negative dielectric anisotropy ($\Delta\epsilon$). These features make pyrimidine-based compounds highly desirable for use as additives in commercial ferroelectric mixtures.

Despite numerous reports on two-ring compounds surprisingly there are relatively few examples of three-ring pyrimidine-based compounds cited in the literature. Hence, the aim of this area of research was to investigate the synthesis and mesomorphic properties of mono- and di-fluorinated three-ring pyrimidine-based compounds, as shown by the general structure (**16**), in order to generate compounds which are likely to

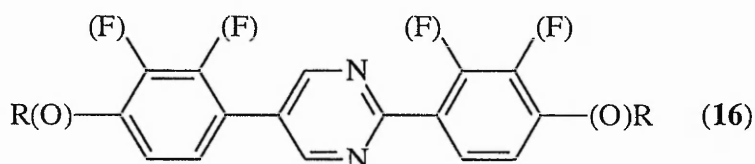
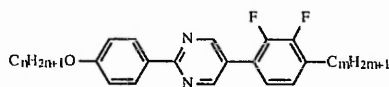
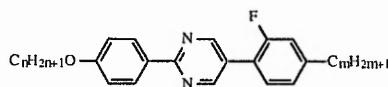


exhibit the desired phase sequence: I-N-S_A-S_C and to investigate their potential as additives in commercial ferroelectric mixtures. Both the position of the pyrimidine ring and number of fluoro-substituents will be varied (**series III-XIV**, structures shown overleaf) systematically such that a comprehensive structure-property relationship may

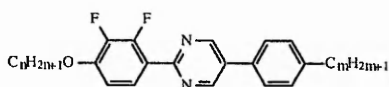
be undertaken. The inclusion of lateral fluoro-substituents is expected to depress the formation of high order smectic crystal phases whilst assisting the formation of the S_C phase. The position of the fluoro-substituent(s), situated either on the inner-edge (mono-fluorinated compounds) or on both the inner- and outer-edge (difluorinated compounds) of the phenyl ring, is anticipated to be of extreme importance. The compounds will also be compared with the monofluoro- and 2,3-difluoro-terphenyls reported by Hird *et al.*^{66,68} thus allowing an insight into the influence of replacing a 1,4-phenylene moiety with the corresponding 2,5-pyrimidyl moiety.



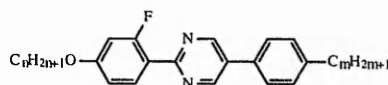
series IIIa-d



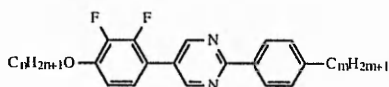
series IX



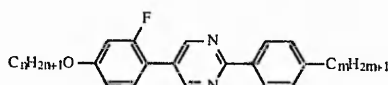
series IV



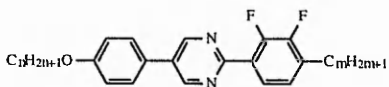
series X



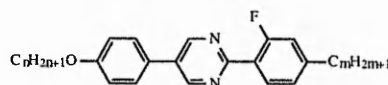
series V



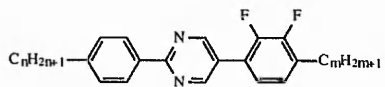
series XI



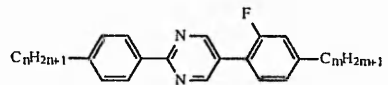
series VI



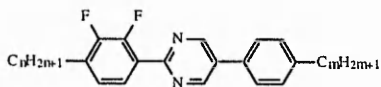
series XII



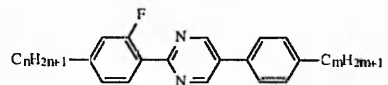
series VII



series XIII



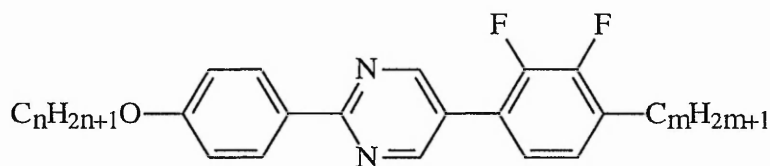
series VIII



series XIV

3.2 RESULTS AND DISCUSSION

3.2.1 2-(4-*n*-ALKOXYPHENYL)-5-(2,3-DIFLUORO-4-*n*-ALKYLPHENYL) PYRIMIDINES (series IIIa-d)

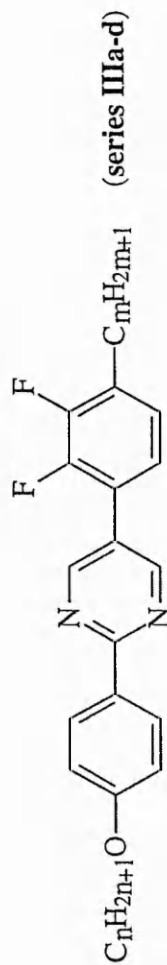


(**51a-d** or series **IIIa**) : (**52a-d** or series **IIIb**) : (**38a-e** or series **IIIc**)
(**53** or series **IIId**)

Fourteen 2-(4-*n*-alkoxyphenyl)-5-(2,3-difluoro-4-*n*-alkyl)pyrimidines which differed both in the number of carbon atoms in the alkoxy chain (*n*) and the number of carbon atoms in the alkyl chain (*m*), i.e., where *n*=4 and *m*=5-8 (**51a-d** or series **IIIa**), *n*=5 and *m*=5-8 (**52a-d** or series **IIIb**), and *n*=6 and *m*=5-9 (**38a-e** or series **IIIc**) and *n*=8 and *m*=9 (**53** or series **IIId**), were successfully prepared. Their mesomorphic transition temperatures are listed in *Table 4* (p. 68) and represented graphically as a plot against *m*, the number of atoms in the alkyl chain in *Figures 24* (series **IIIa**), *25* (series **IIIb**) and *26* (series **IIIc**).

Except for the *m*=6 homologue (**51b**) of series **IIIa** which exhibits the nematic phase alone, all the other 2-(4-*n*-alkoxyphenyl)-5-(2,3-difluoro-4-*n*-alkyl)pyrimidines exhibit the following phase sequence on cooling from the isotropic liquid: I-N-S_C-K. Unfortunately, the S_A phase was not observed. However, beneficially, unlike the thiophene systems reported earlier (chapter 2, p. 47-63), no high order smectic crystal phases were detected.

Table 4. Transition temperatures ($^{\circ}\text{C}$) (**in bold**) and enthalpies ($\Delta\text{H}/\text{kJ mol}^{-1}$) (*in italics*) for certain 2-(4-*n*-alkoxyphenyl)-5-(2,3-difluoro-4-*n*-alkyl)pyrimidines (**series IIIa-d**)



| m | n=4 (51a-d, series IIIa) | | | n=5 (52a-d, series IIIb) | | | n=6 (38a-e, series IIIc) | | | n=8 (53) | | | |
|---|--------------------------|-----------------|----------------|--------------------------|-------------------|---------------|--------------------------|-------------------|-----------------------|---------------|-----------------|-------------------|-----------------------|
| | I-N | N-Sc | N-K | K-N | S _C -K | I-N | N-Sc | S _C -K | K-N | I-N | N-Sc | S _C -K | K-N |
| 5 | 169.5 0.67 | (105.0) 1.19 | - | 110.8 18.73 | 99.9 21.99 | 154.2 0.50 | (106.5) 1.04 | 94.1 22.26 | 110.4 26.66 | 154.2 0.96 | (107.9) 0.89 | 91.8 25.47 | 110.8 26.85 |
| 6 | 150.2 0.45 | - | 105.7 29.13 | 114.8 27.57 | - | 146.2 0.58 | 110.9 1.79 | 85.1 21.73 | K-Sc 99.3 22.60 | 143.4 0.22 | 108.5 0.05 | 77.5 23.27 | K-Sc 95.6 25.24 |
| 7 | 152.4 0.74 | (102.1) 0.61 | - | 109.4 28.21 | 99.8 25.59 | 146.5 0.68 | 110.8 1.03 | 79.8 21.31 | 94.0 22.46 | 148.2 0.97 | 118.1 0.84 | 73.5 20.17† | 94.0 35.45 |
| 8 | 145.0 0.45 | (102.1) 0.60 | - | 110.0 27.66 | 93.8 28.29 | 143.8 0.59 | 115.2 1.06 | 77.7 20.94 | 92.2 21.51 | 139.5 0.77 | 115.9 0.46 | 69.6 20.98 | 88.7 38.48 |
| 9 | | | | | | | | | | 141.5 1.15 | 119.0 0.84 | 67.0 23.54 | 90.0 43.38 |
| | | | | | | | | | | 139.7 2.11 | 126.6 1.40 | 60.8 25.67 | 77.2 40.85† |

† Value includes the enthalpy of adjacent crystal-crystal transition(s).

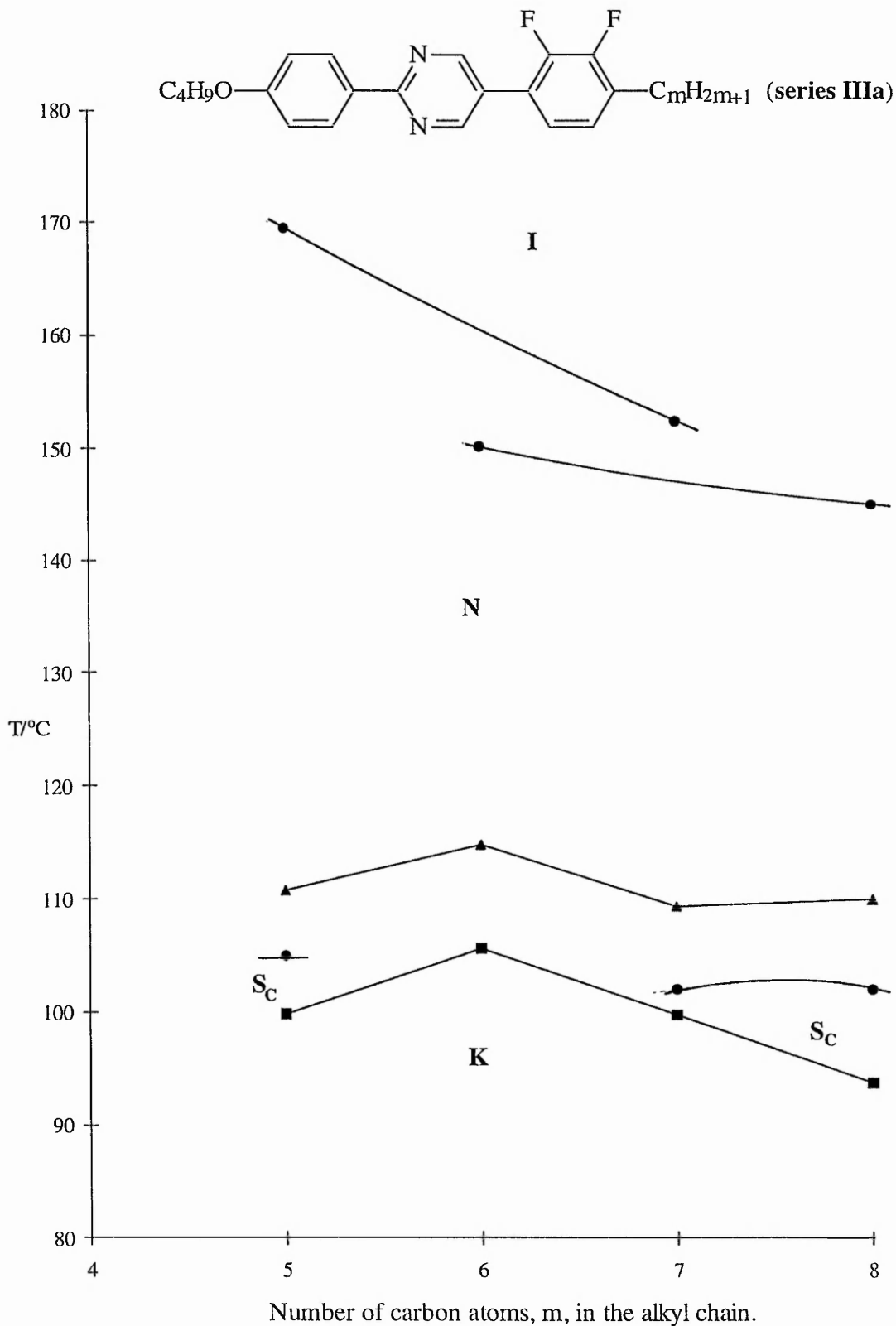


Figure 24. Plot of transition temperatures for certain 2-(4-*n*-butyloxyphenyl)-5-(2,3-difluoro-4-*n*-alkylphenyl)pyrimidines (series IIIa).

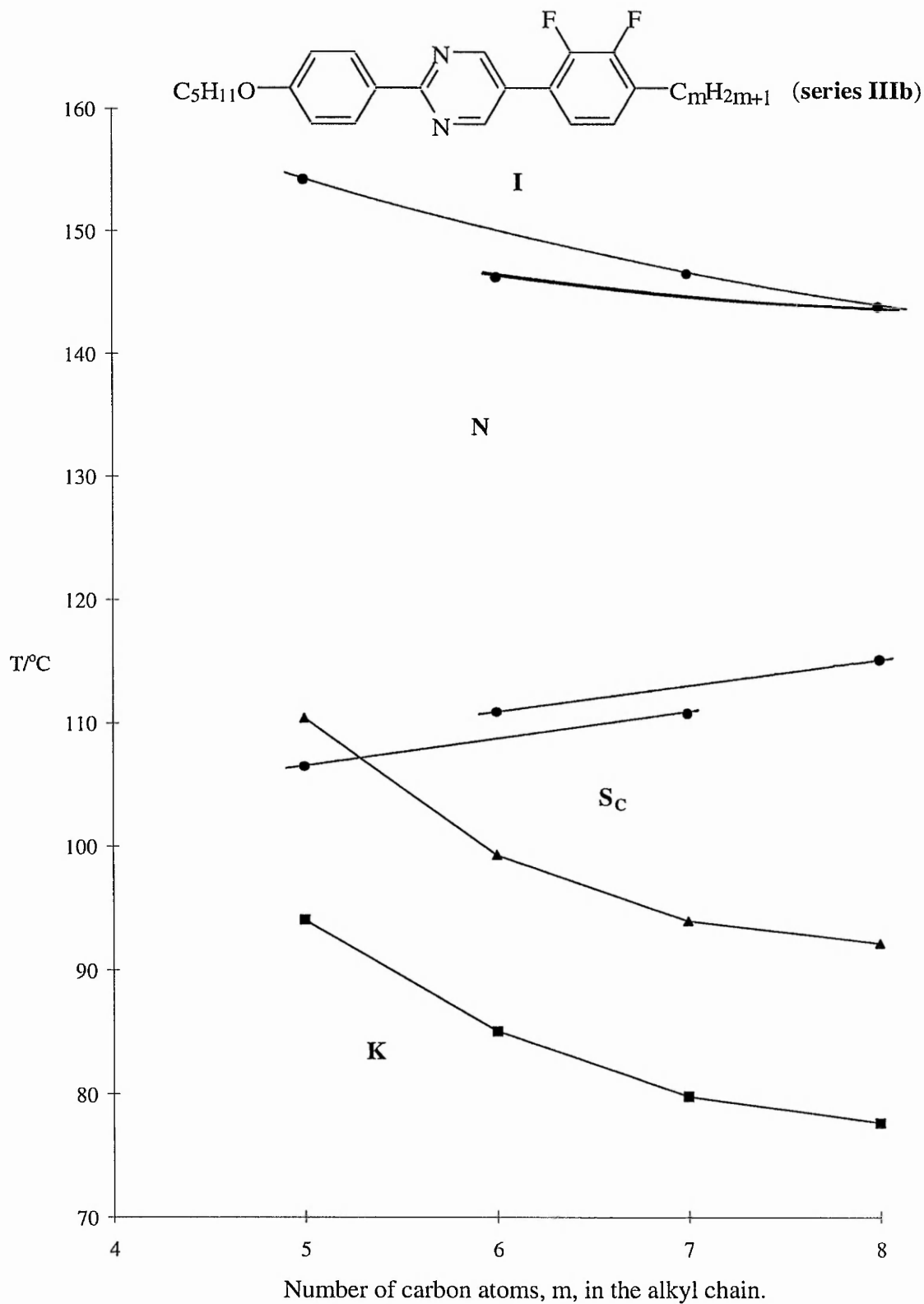


Figure 25. Plot of transition temperatures for certain 2-(4-*n*-pentyloxyphenyl)-5-(2,3-difluoro-4-*n*-alkyl)pyrimidines (series IIIb).

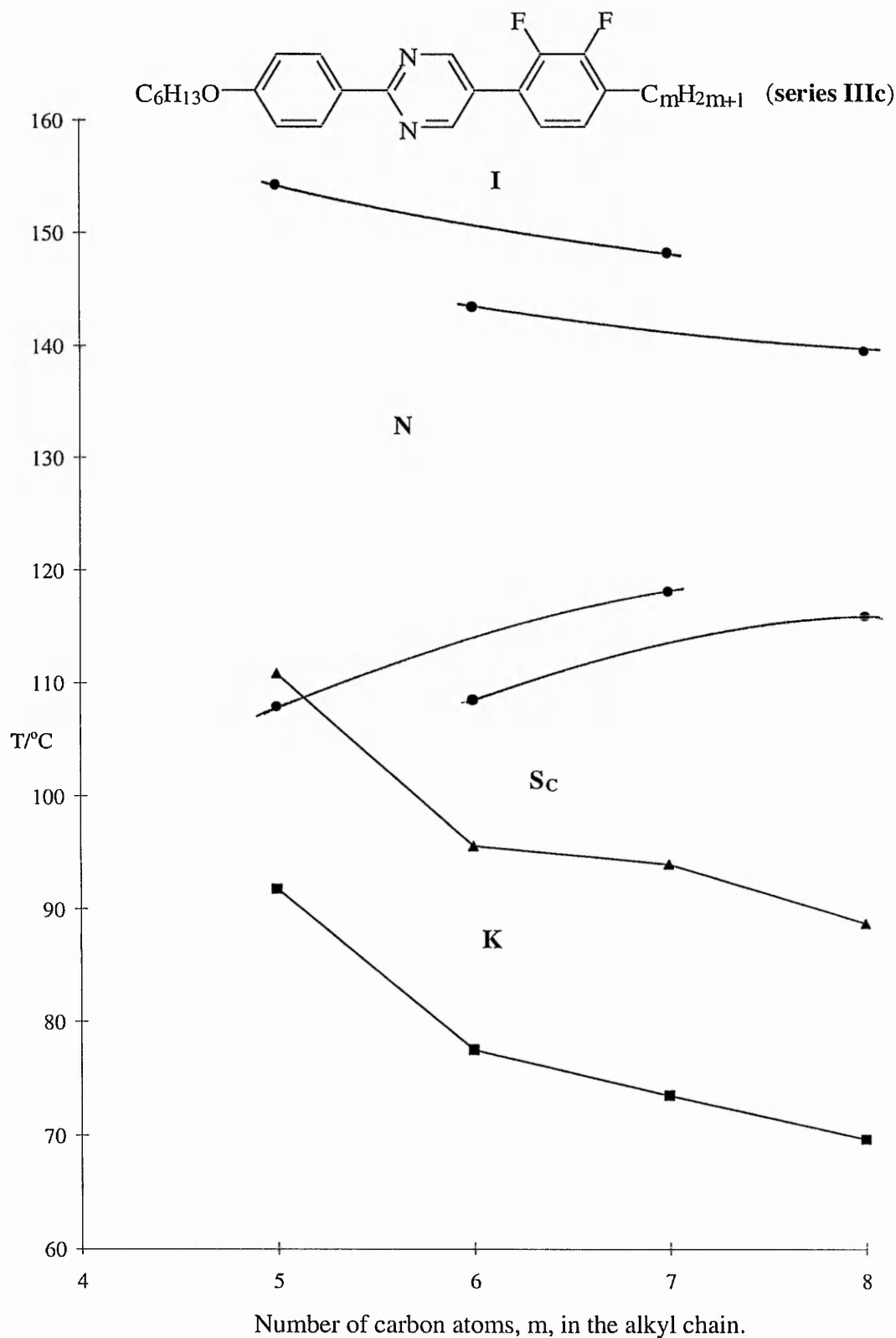


Figure 26. Plot of transition temperatures for certain 2-(4-*n*-hexyloxyphenyl)-5-(2,3-difluoro-4-*n*-alkylphenyl)pyrimidines (series IIIc).

The nematic phase was easily characterised on cooling from the isotropic liquid by the appearance of tiny droplets (nematic droplets) which then coalesced to give the classical threaded texture (*Plate 3*). At the N-S_C transition, certain regions of the threaded texture convert to the blurred schlieren texture whilst the remainder affords the broken focal-conic fan texture (*Plate 4*). The appearance of both textures (blurred schlieren and broken fan) confirms the identity of the S_C phase.



Plate 3. The nematic texture of 2-(4-*n*-octyloxyphenyl)-5-(2,3-difluoro-4-*n*-nonylphenyl)pyrimidine (**53**).

Examination of *Figures 24, 25* and *26* reveals that the points for the nematic to isotropic transition temperatures decrease with increasing chain length and may be correlated by two smooth curves. As expected, the odd-*m* homologues occur on a

decreasing smooth curve which lies above the corresponding curve which connects the even- m homologues. Both curves tend to converge towards the higher homologues.

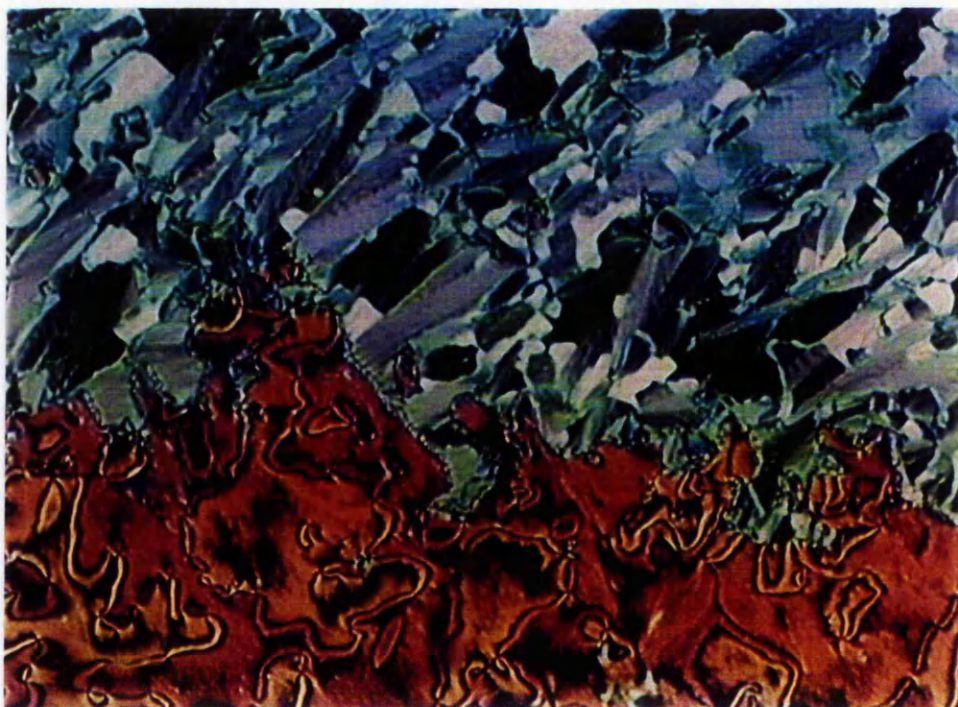


Plate 4. The broken fan and schlieren textures of the S_C phase of 2-(4- n -octyloxyphenyl)-5-(2,3-difluoro-4- n -nonylphenyl)pyrimidine (**53**).

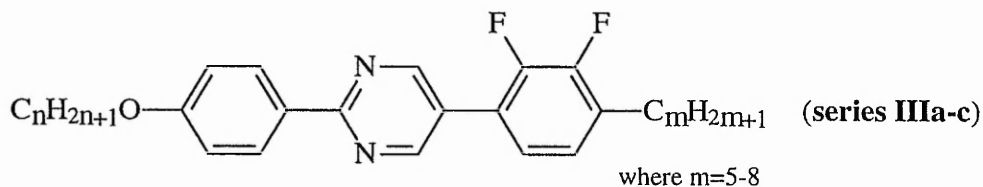
Similarly, as shown by **Figure 26**, the points for the N - S_C transition temperatures may be correlated by two rising curves, i.e., odd- m above even- m . However, there is no apparent similar trend for members of **series IIIa** (**Figure 24**) and **series IIIb** (**Figure 25**). Surprisingly, the S_C thermal stability for members of **series IIIa** appears to decrease with increasing chain length.

In order to investigate the influence of increasing the number of atoms, n , in the alkoxy chain on mesomorphic properties, **Table 5** lists the average m.p., clearing point (T_{N-I}), N - S_C transition temperature (T_{N-S_C}), nematic phase range and S_C phase range for

the m=5-8 members of **series IIIa-c**. For clarity, the average mesomorphic transition temperatures quoted in **Table 5** have been represented graphically in **Figure 27** as a plot against, n, the number of carbon atoms in the alkoxy chain.

As the number of atoms, n, in the alkoxy chain increases from four to six both the average melting point and crystallisation temperature decrease by a magnitude of 14°C and 21.7°C, respectively. However, it must be stressed that there is no correlation between either the melting point or the crystallisation temperature and crystal structure. Importantly, the average nematic to isotropic transition temperature, T_{N-I} , decreases (8°C) as the number of carbon atoms increases whereas the average nematic to S_C transition temperature, T_{N-SC} , increases (9.6°C).

Table 5. Average melting point, clearing point (T_{N-I}), N- S_C transition temperature (T_{N-SC}), nematic phase range and S_C phase range for the m=5-8 members of **series IIIa-c**.



| Average (m=5-8), °C | | | | | | | |
|---------------------|---|-------|-----------|------------|-----------------------------|---------------------|-------------------|
| series | n | m.p. | T_{N-I} | T_{N-SC} | crystallisation temperature | nematic phase range | S_C phase range |
| IIIa | 4 | 111.3 | 154.3 | 103.0 | 99.8 | 51.3 | 3.2 |
| IIIb | 5 | 99.0 | 147.7 | 110.9 | 84.2 | 36.8 | 26.7 |
| IIIc | 6 | 97.3 | 146.3 | 112.6 | 78.1 | 33.7 | 34.5 |

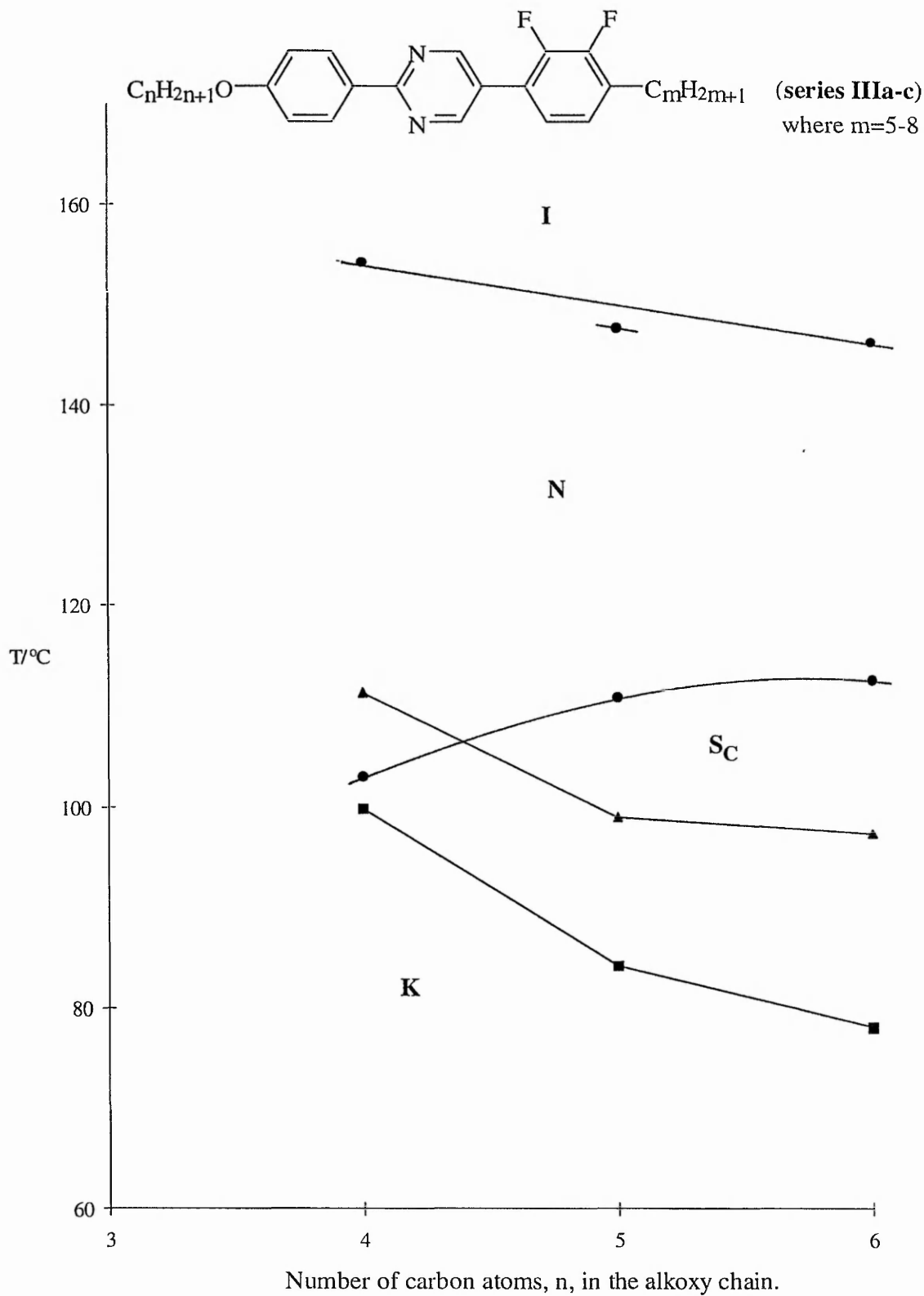
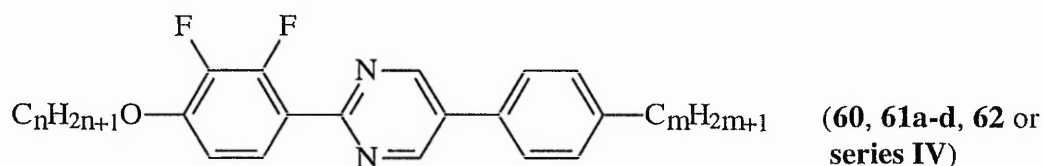


Figure 27. Plot of average transition temperatures for certain 2-(4-*n*-alkoxyphenyl)-5-(2,3-difluoro-4-*n*-alkylphenyl)pyrimidines (series IIIa-c).

Series IIIa gives the widest nematic phase range (51.3°C) whereas **series IIIc** gives the widest S_c phase range (34.5°C). These results may be explained in terms of the general features of a transition temperature plot where the nematic to isotropic transition temperatures usually decrease with increasing chain length and the smectic properties increase. Hence this leads to reduction in the nematic phase range and an increase in the smectic phase range.

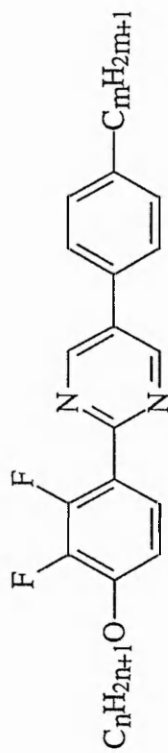
3.2.2 2-(2,3-DIFLUORO-4-*n*-ALKOXYPHENYL)-5-(4-*n*-ALKYLPHENYL) PYRIMIDINES (series IV)



In order to gauge quickly the influence of moving the difluoro-substituents from the right-hand terminal alkylphenyl-ring to the left-hand terminal alkoxyphenyl-ring selected members of a series of 2-(2,3-difluoro-4-*n*-alkoxyphenyl)-5-(4-*n*-alkylphenyl)pyrimidines which differed both in the number of carbon atoms in the alkoxy chain (*n*) and the number of carbon atoms in the alkyl chain (*m*), i.e., where *n*=4 and *m*=5 (**60**), *n*=5-8 and *m*=7 (**61a-d**) and; *n*=8 and *m*=9 (**62**) (members of **series IV**), were prepared. Their mesophase transition temperatures are listed in **Table 6** (p. 77).

The disposition of the two fluoro-substituents in the left-hand phenyl-ring is expected to lower the thermal stability because of increased steric hindrance at the inter-ring junction. In this situation, the fluoro-substituent disposed *ortho*- to the inter-ring bond is in close proximity of the nitrogen atoms of the pyrimidine ring.

Table 6. Transition temperatures ($^{\circ}\text{C}$) (**in bold**) and enthalpies ($\Delta\text{H}/\text{kJ mol}^{-1}$) (*in italics*) for certain 2-(2,3-difluoro-4-*n*-alkoxyphenyl)-5-(4-*n*-alkyl)pyrimidines (**series IV**)



(**series IV** or **60** where $n=4$: $m=5$
61a-d $n=5-8$: $m=7$
62 $n=8$: $m=9$)

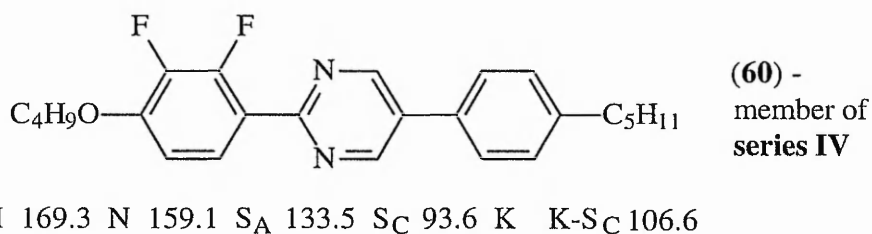
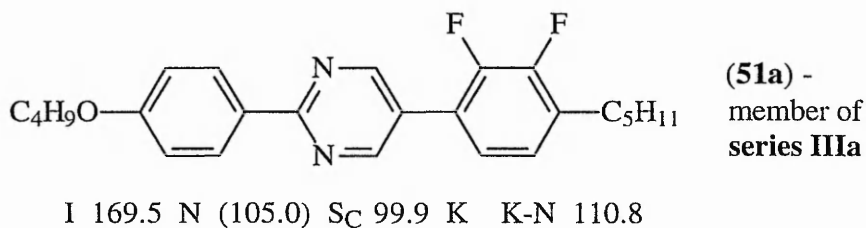
| n | m=5 (60) | | | m=7 (61a-d) | | | m=9 (62) | | | | |
|---|-----------------------------|-----------------------------|--------------------------------|-----------------------------|--------------------------------|-----------------------------|--|-----------------------------|--------------------------------|-----------------------------|-----------------------------|
| | I-N | N-S _A | S _A -S _C | I-S _A | S _A -S _C | S _C -K | K-S _C | I-S _A | S _A -S _C | S _C -K | K-S _C |
| 4 | 169.3 <i>1.10</i> | 159.1 <i>0.64</i> | 133.5 Φ | - | - | 93.6 <i>15.77</i> | 106.6 <i>18.10</i> | - | - | - | - |
| 5 | - | - | - | 162.3 <i>3.98</i> | 143.6 ϕ | - | 76.5 <i>14.86</i> | 94.1 <i>15.16</i> | - | - | - |
| 6 | - | - | - | 162.5 <i>5.09</i> | 148.8 <i>2.30</i> | - | 72.8 <i>15.56</i> | 90.2 <i>18.02</i> | - | - | - |
| 7 | - | - | - | 159.8 <i>4.86</i> | 146.5 ϕ | - | 70.0 <i>15.71</i> | 88.0 <i>24.81</i> | - | - | - |
| 8 | - | - | - | 158.5 <i>4.72</i> | 144.0 ϕ | - | 58.0 <i>11.56</i> [†] | 86.7 <i>26.19</i> | 156.4 <i>5.66</i> | 153.5 <i>0.09</i> | 88.0 <i>28.69</i> |

Φ Detected by optical microscopy and DSC, but peak too small to measure.

ϕ Transition detected by optical microscopy, but not by DSC.

[†] Value includes the enthalpy of adjacent crystal-crystal transition(s).

However, surprisingly, comparing 2-(2,3-difluoro-4-*n*-butyloxyphenyl)-5-(4-*n*-pentylphenyl)pyrimidine (**60**) with its isomeric counterpart 2-(4-*n*-butyloxyphenyl)-5-(2,3-difluoro-4-*n*-pentylphenyl)pyrimidine (**51a**) shows only a very slight decrease in



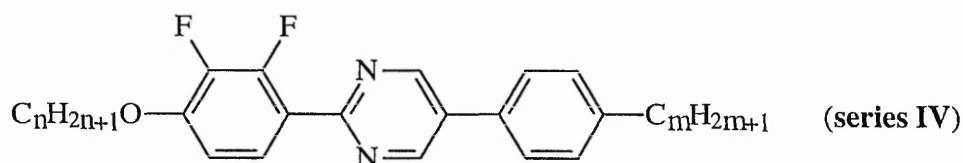
the thermal stability (0.2°C) when the position of the 2,3-difluoro-substituents is moved from the right-hand terminal alkylphenyl-ring to the left-hand terminal alkoxyphenyl-ring. In fact, the nematic phase range is drastically lowered from 64.5°C to only 10.2°C and is replaced effectively by the S_A and S_C phase types possibly due to the close proximity of the lateral dipoles which may enhance the lamellar packing arrangement by affording stronger dipole-dipole interactions between molecules. The S_C phase for (**60**) is not enantiotropic and both the S_C thermal stability and S_C phase range increase by 28.5°C and 34.8°C, respectively.

All members of the 2-(2,3-difluoro-4-*n*-alkoxyphenyl)-5-(4-*n*-alkylphenyl)pyrimidines (**60**, **61a-d**, **62** or **series IV**) exhibit the S_A and S_C phase types. The shortest homologue, i.e., *n*=4, *m*=5 (**60**), in addition, exhibits the nematic phase and hence gives the desired phase sequence: I-N-S_A-S_C. However, both its melting point and clearing

point are rather high.

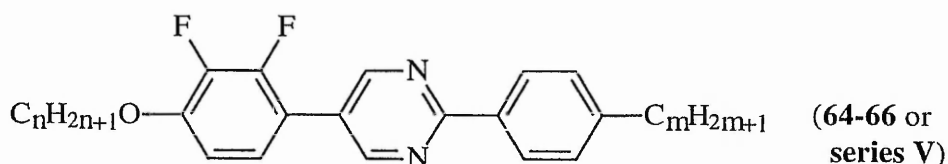
Table 7 shows the influence of increasing sequentially the length of the molecule by increasing the length of both the alkyl- and alkoxy-chain by two carbon atoms. A sequential increase in the number of carbon atoms in the terminal chains lowers both the melting point and clearing point. Unfortunately, the nematic phase is totally extinguished from the middle ($n=6, m=7$, **61b**) and longest ($n=8, m=9$, **62**) homologues.

Table 7. Transition temperatures ($^{\circ}\text{C}$) for the 2-(2,3-difluoro-4- n -alkoxyphenyl)-5-(4- n -alkylphenyl)pyrimidines (**series IV**).



| No. | n | m | I-S _A /N | N-S _A | S _A -S _C | S _C -K | K-S _C |
|------------|---|---|---------------------|------------------|--------------------------------|-------------------|------------------|
| 60 | 4 | 5 | 169.3 | 159.1 | 133.5 | 93.6 | 106.6 |
| 61b | 6 | 7 | 162.5 | | 148.8 | 72.8 | 90.2 |
| 62 | 8 | 9 | 156.4 | | 153.5 | 66.0 | 88.0 |

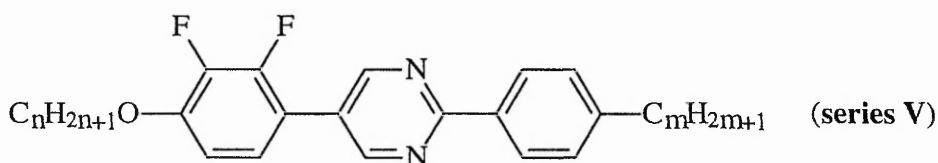
3.2.3 2-(4- n -ALKYLPHENYL)-5-(2,3-DIFLUORO-4- n -ALKOXYPHENYL) PYRIMIDINES (series V)



The next strategy was to investigate the influence of reversing the central pyrimidyl ring on mesomorphic properties. Listed in **Table 8** are the mesomorphic

properties of the members ($n=4, m=5$ (**64**); $n=6, m=7$ (**65**); $n=8, m=9$ (**66**)) of a series of 2-(4- n -alkylphenyl)-5-(2,3-difluoro-4- n -alkoxy)pyrimidines (**series V**).

Table 8. Transition temperatures ($^{\circ}\text{C}$) (**in bold**) and enthalpies ($\Delta H/\text{kJ mol}^{-1}$) (*in italics*) for the 2-(4- n -alkylphenyl)-5-(2,3-difluoro-4- n -alkoxyphenyl) pyrimidines (**series V**).



| No. | n | m | I-N | N-S _A | N-S _C | S _C -K | K-S _C |
|-----------|---|---|--------------|------------------|------------------------|-------------------|------------------|
| 64 | 4 | 5 | 161.0 | - | 111.1 | 93.3 | 103.6 |
| | | | <i>0.55</i> | - | <i>0.65</i> | <i>15.49</i> | <i>16.67</i> |
| 65 | 6 | 7 | 151.5 | - | 132.5 | 75.7 | 89.2 |
| | | | <i>0.99</i> | - | <i>0.34</i> | <i>14.50</i> | <i>15.82</i> |
| 66 | 8 | 9 | 139.9 | 135.0 | $\frac{S_A-S_C}{\Phi}$ | 57.7 | 71.0 |
| | | | <i>1.12</i> | Ψ | Φ | <i>13.16</i> | <i>14.93</i> |

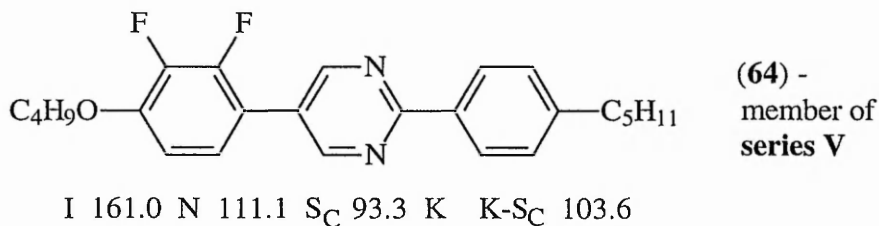
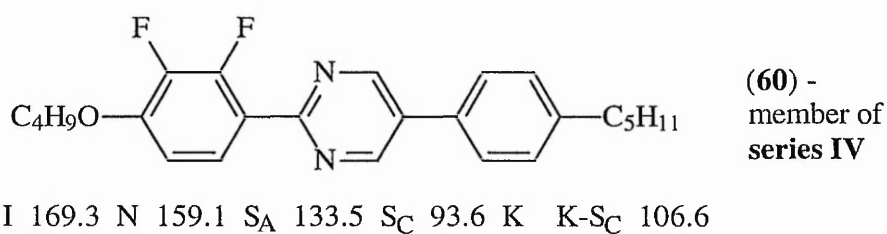
Ψ The enthalpy of transition is concealed by an adjacent transition.

Φ Detected by optical microscopy and DSC, but peak too small to measure.

Generally, a qualitative comparison of the mesomorphic properties of the members of **series V** with its isomeric counterparts, i.e., members of **series IV**, reveals that the latter possess more smectic character. All members of **series IV** exhibit the S_A and S_C phase types (the shortest homologue (**60**) also exhibits an additional nematic phase) whereas the short ($n=4, m=5$, **64**) and middle ($n=6, m=7$, **65**) homologues of

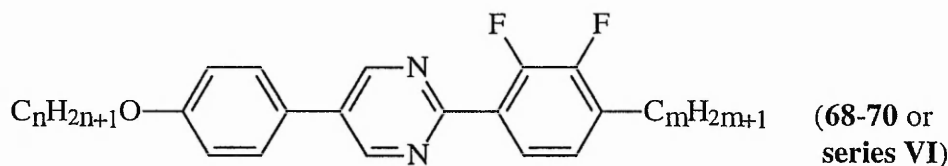
their isomeric series (**series V**) only exhibit the nematic and S_C phase types which can be explained in terms of the net dipole projecting away from the ether oxygen atom. In fact, only the longest homologue ($n=8$, $m=9$, **66**) of **series V** exhibits the same phase sequence as the shortest homologue ($n=4$, $m=5$, **60**) of **series IV**, i.e., I-N- S_A - S_C .

On a quantitative basis, the shortest homologue of each series may be compared, i.e., 2-(2,3-difluoro-4-*n*-butyloxyphenyl)-5-(4-*n*-pentyloxyphenyl)pyrimidine (**60**) versus 2-(4-*n*-pentyloxyphenyl)-5-(2,3-difluoro-4-*n*-butyloxyphenyl)pyrimidine (**64**).



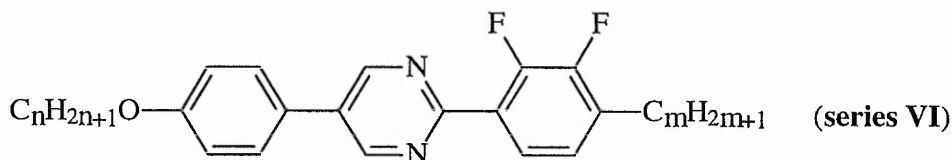
Positioning the two nitrogen atoms away from the 2,3-difluorophenyl-ring is expected to reduce inter-ring steric strain⁸⁸ and, therefore, increase thermal stability. The nematic phase range is, in fact, increased dramatically by 39.7°C whilst the S_C phase range is reduced by 21.9°C and the S_A phase is lost altogether. This analysis reveals that nematic properties dominate over smectic properties when the pyrimidyl ring is reversed. However, contrary to expectation, the clearing point decreases by 8.3°C.

3.2.4 2-(2,3-DIFLUORO-4-*n*-ALKYLPHENYL)-5-(4-*n*-ALKOXYPHENYL) PYRIMIDINES (series VI)



The next stage in the investigation led to the preparation of members of 2-(2,3-difluoro-4-*n*-alkylphenyl)-5-(4-*n*-alkoxyphenyl)pyrimidines (**series VI**) where the fluoro-substituents are transposed on to the right-hand phenyl-ring, i.e., pyrimidine is reversed so that the fluoro-substituents are now adjacent the nitrogens but away from the ether oxygen on the left-hand terminal ring. *Table 9* lists the mesomorphic transition temperatures of the members of **series VI**.

Table 9. Transition temperatures ($^{\circ}\text{C}$) (**in bold**) and enthalpies ($\Delta\text{H}/\text{kJ mol}^{-1}$) (*in italics*) for the 2-(2,3-difluoro-4-*n*-alkylphenyl)-5-(4-*n*-alkoxyphenyl) pyrimidines (**series VI**).

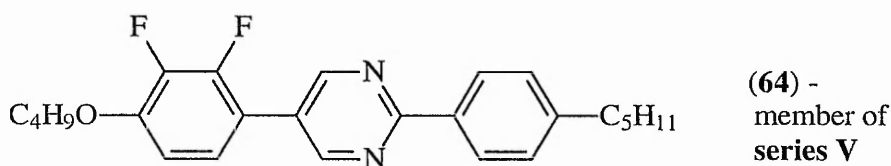


| No. | n | m | I-S _A | S _A -S _C | S _C -K | K-S _A |
|-----------|---|---|-----------------------------|--------------------------------|-----------------------------|---|
| 68 | 4 | 5 | 180.3 <i>5.08</i> | (104.3) ϕ | 95.7 <i>14.02</i> | 108.2 <i>14.93</i> |
| 69 | 6 | 7 | 171.4 <i>5.93</i> | 122.9 ϕ | 95.7 <i>14.41</i> | K-S_C 93.5 <i>15.08</i> |
| 70 | 8 | 9 | 163.3 <i>7.62</i> | 143.9 ϕ | 76.2 <i>18.95</i> | 87.3 <i>23.03</i> |

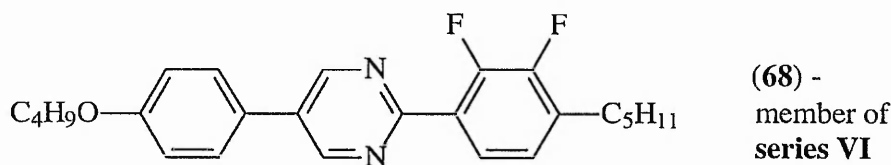
ϕ Transition detected by optical microscopy, but not by DSC.

Comparison of the mesomorphic properties of 2-(2,3-difluoro-4-*n*-alkylphenyl)-5-(4-*n*-alkoxyphenyl)pyrimidines (**series VI**) with the analogous 2-(4-*n*-alkylphenyl)-5-(2,3-difluoro-4-*n*-alkoxyphenyl)pyrimidines (**series V**) reveals that moving the fluoro-substituents to the right-hand terminal ring completely destroys all nematic properties. The S_A phase is introduced to the short (n=4, m=5, **68**) and middle (n=6, m=7, **69**) homologues. The S_C phase range is reduced and S_C thermal stability is decreased. Also, the clearing points and melting points are higher.

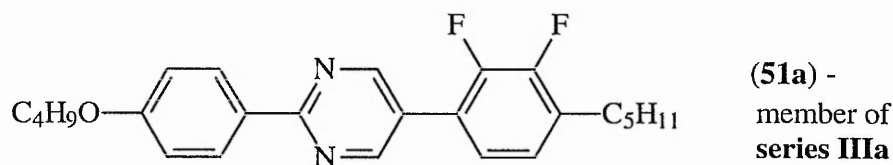
A quantitative comparison between 2-(2,3-difluoro-4-*n*-pentylphenyl)-5-(4-*n*-butyloxyphenyl)pyrimidine (**68**) and the analogous 2-(4-*n*-pentylphenyl)-5-(2,3-difluoro-4-*n*-butyloxyphenyl)pyrimidine (**64**) reveals, amazingly, that the clearing point is increased by 19.3°C and mesophase thermal stability is enhanced which once again



I 161.0 N 111.1 S_C 93.4 K K-S_C 103.6



I 180.3 S_A (104.3) S_C 95.7 K K-S_A 108.2

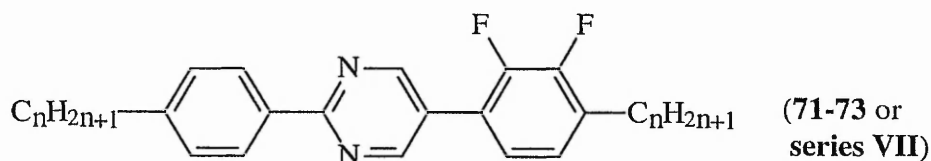


I 169.5 N (105.0) S_C 99.9 K K-S_C 110.8

shows that inter-ring twisting is not the sole factor governing mesophase thermal stability. The situation is far more complex involving subtle inter-play between many parameters, such as; directionality of dipoles, extent of conjugation, separation of charge, etc. Also, for (68) it is surprising that the S_A phase is now observed at the expense of the S_C phase (reduced phase range of 9.1°C) and S_C thermal stability is decreased by 2.3°C regardless of the extended conjugation between the ether oxygen and the pyrimidine ring.

A comparison between the 2-(2,3-difluoro-4-*n*-pentylphenyl)-5-(4-*n*-butyloxyphenyl)pyrimidine (68) and its isomeric counterpart 2-(4-*n*-butyloxyphenyl)-5-(2,3-difluoro-4-*n*-pentylphenyl)pyrimidine (51a) shows that a reversal of the pyrimidyl ring nitrogens so that their disposition is close to the fluoro-substituents, again, totally eliminates the nematic phase whilst introducing the S_A phase. The unexpected trend is continued as mesophase thermal stability is also increased. The clearing point rises by 10.8°C , enhancing mesophase thermal stability, and the S_C phase range and S_C thermal stability increase by 3.5°C and 4.2°C , respectively.

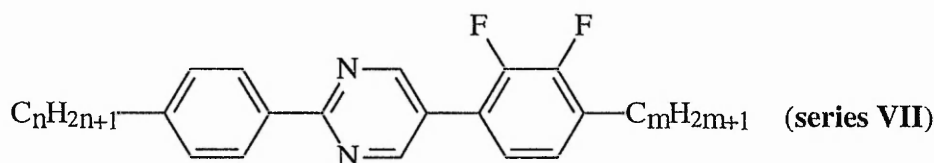
3.2.5 2-(4-*n*-ALKYLPHENYL)-5-(2,3-DIFLUORO-4-*n*-ALKYLPHENYL) PYRIMIDINES (series VII)



With the knowledge that alkyl-alkoxy three-ring pyrimidine compounds (series III-VI) give compounds with relatively high melting and clearing points it

was decided to investigate the influence of replacing the terminal alkoxy chain with an alkyl chain. Replacement of the ether oxygen with a methylene unit is expected to generate compounds with lower melting and clearing points. To this effect, a series of 2-(4-*n*-alkylphenyl)-5-(2,3-difluoro-4-*n*-alkylphenyl)pyrimidines (**71-73**, **series VII**) were prepared and their mesomorphic properties are listed in *Table 10*.

Table 10. Transition temperatures (°C) (**in bold**) and enthalpies ($\Delta H/\text{kJ mol}^{-1}$) (*in italics*) for the 2-(4-*n*-alkylphenyl)-5-(2,3-difluoro-4-*n*-alkylphenyl)pyrimidines (**series VII**).



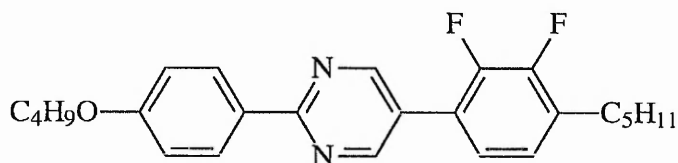
| No. | n | m | I-N | N-S _C | S _A -S _C | N-K | K-N |
|-----------|---|---|-----------------------------|---|--------------------------------|---|--|
| 71 | 5 | 5 | 129.1 <i>0.66</i> | | | 99.4 <i>20.97</i> | 106.9 <i>21.63</i> |
| 72 | 7 | 7 | 123.7 <i>1.15</i> | 105.4 <i>0.33</i> | | <u>S_C-K</u> 90.0 <i>21.53</i> | <u>K-S_C</u> 101.0 <i>23.03</i> |
| 73 | 9 | 9 | 117.8 <i>2.93</i> | <u>N-S_A</u> 115.5 <i>0.20</i> | 110.7 ϕ | 80.9 <i>22.74</i> | 94.3 <i>26.31</i> |

ϕ Transition detected by optical microscopy, but not by DSC.

All members of the series of 2-(4-*n*-alkylphenyl)-5-(2,3-difluoro-4-*n*-alkylphenyl)pyrimidines (**series VII**) exhibit the nematic phase. The shortest homologue ($n=m=5$, **71**) exhibits the nematic phase alone. The middle homologue ($n=m=7$, **72**) also

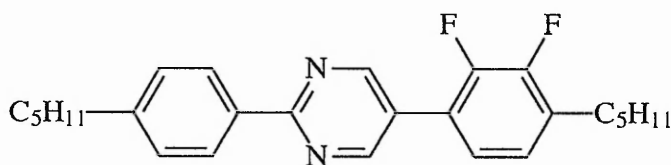
exhibits the S_C phase. Surprisingly the longest homologue ($n=m=9$, **73**) exhibits the ideal I-N- S_A - S_C phase sequence. The appearance of the S_C phase is rather surprising since according to the McMillan theory of the S_C phase, a terminal outboard dipole moment is usually a strong prerequisite. In this instance, replacement of the ether oxygen with a methylene group removes the terminal dipole. Hence, the required dipole necessary for molecular tilting must be from an association of the dipoles on the nitrogen atoms with the lateral fluoro-substituents. Unfortunately, the nematic and S_A phases are rather narrow with mesophase ranges of 2.3°C and 4.8°C , respectively.

A comparison of the 2-(4-*n*-pentylphenyl)-5-(2,3-difluoro-4-*n*-pentylphenyl)-pyrimidine (**71**) with the analogous 2-(4-*n*-butyloxyphenyl)-5-(2,3-difluoro-4-*n*-pentylphenyl)pyrimidine (**51a**) discloses that replacement of the ether oxygen with a methylene group in the left-hand terminal chain drastically reduces the clearing point by 40.4°C which may be attributed to reduced conjugation of the terminal group with the molecular core. The melting point is only very slightly lowered by a magnitude of 3.9°C .



(51a) -
member of
series **IIIa**

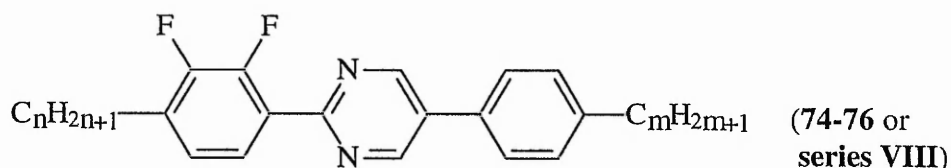
I 169.5 N (105.0) S_C 99.9 K K-N 110.8



(71) -
member of
series **VII**

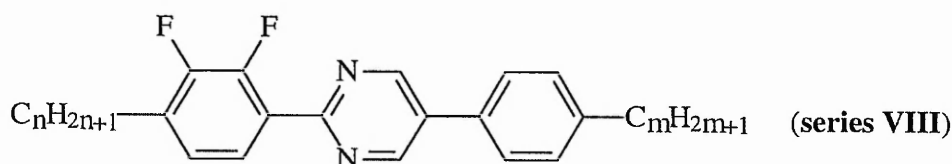
I 129.1 N 99.4 K K-N 106.9

3.2.6 2-(2,3-DIFLUORO-4-*n*-ALKYLPHENYL)-5-(4-*n*-ALKYLPHENYL) PYRIMIDINES (series VIII)



Similarly, members ($n=m=5$, (74); $n=m=7$, (75); $n=m=9$, (76)) of the isomeric series of 2-(2,3-difluoro-4-*n*-alkylphenyl)-5-(4-*n*-alkylphenyl)pyrimidines (series VIII) were prepared and their mesomorphic transition temperatures are given in *Table 11*.

Table 11. Transition temperatures ($^{\circ}\text{C}$) (**in bold**) and enthalpies ($\Delta H/\text{kJ mol}^{-1}$) (*in italics*) for the 2-(2,3-difluoro-4-*n*-alkylphenyl)-5-(4-*n*-alkylphenyl)-pyrimidines (series VIII).

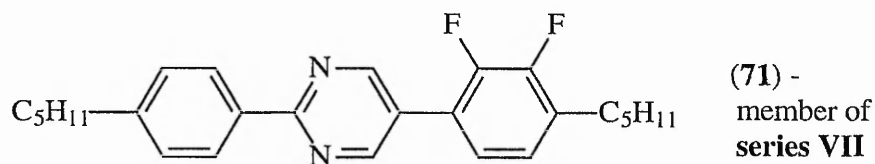


| No. | n | m | I-S _A | S _A -S _C | S _A -K | K-S _A |
|-----------|---|---|-----------------------------|--------------------------------|---|--|
| 74 | 5 | 5 | 150.8 <i>3.80</i> | | 108.1 <i>20.91</i> | 121.3 <i>22.69</i> |
| 75 | 7 | 7 | 145.6 <i>4.95</i> | | 107.6 <i>24.27</i> | 116.3 <i>24.74</i> |
| 76 | 9 | 9 | 135.9 <i>5.91</i> | 116.4 ϕ | <u>S_C-K</u> 97.9 <i>24.59</i> | <u>K-S_C</u> 106.7 <i>24.64</i> |

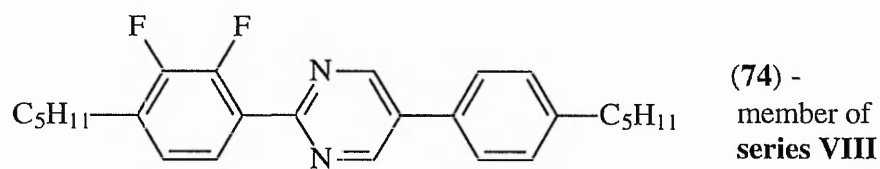
ϕ Transition detected by optical microscopy, but not by DSC.

The $n=m=5$ homologue (**74**) and $n=m=7$ homologue (**75**) exhibit the S_A phase alone on cooling from the isotropic liquid. The longest homologue, i.e., $n=m=9$, (**76**), additionally exhibits the S_C phase.

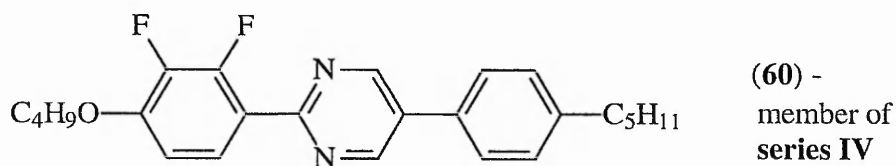
A detailed comparison may be undertaken between the 2-(2,3-difluoro-4-*n*-pentylphenyl)-5-(4-*n*-pentylphenyl)pyrimidine (**74**) and its isomeric counterpart 2-(4-*n*-pentylphenyl)-5-(2,3-difluoro-4-*n*-pentylphenyl)pyrimidine (**71**) to show the influence of moving the two fluoro-substituents on mesomorphic properties. Transposition of the two fluoro-substituents from the right-hand terminal ring (**71**) to the left-hand terminal ring (**74**) drastically alters the mesophase type and thermal stability. The nematic phase is no longer observed and the clearing point increases by 21.7°C. However, the melting point also increases by a magnitude of 14.4°C.



I 129.1 N 99.4 K K-N 106.9



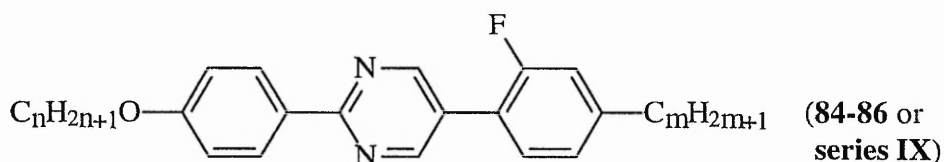
I 150.8 S_A 108.1 K K- S_A 121.3



I 169.3 N 159.1 S_A 133.5 S_C 93.6 K K- S_C 106.6

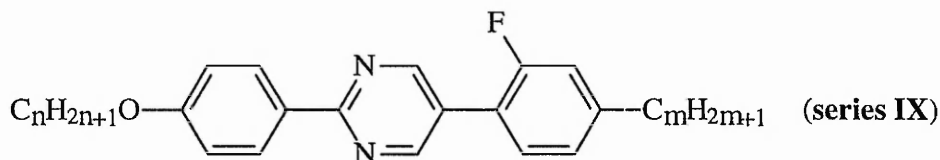
Likewise compound (74) may be compared with 2-(2,3-difluoro-4-*n*-butyloxyphenyl)-5-(4-*n*-pentylphenyl)pyrimidine (60) in order to investigate the influence of replacing the ether oxygen with a methylene unit on mesomorphic properties. The comparison reveals that the presence of an ether oxygen atom in the terminal chain is beneficial for generating nematic and smectic phases with high clearing points, i.e., phase sequence I-N-S_A-S_C. As the ether oxygen is replaced with a methylene unit, the nematic and S_C phase types are no longer observed for the reasons stated earlier. Compound (74) exhibits the S_A phase alone with a lower clearing point (difference of 18.5°C) and increased melting point (difference of 14.7°C).

3.2.7 2-(4-*n*-ALKOXYPHENYL)-5-(2-FLUORO-4-*n*-ALKYLPHENYL)-PYRIMIDINES (series IX)



In order to further investigate the mesomorphic properties of three-ring pyrimidine-based compounds, mono-fluoro-substituted compounds were prepared, i.e., 2-(4-*n*-alkoxyphenyl)-5-(2-fluoro-4-*n*-alkylphenyl)pyrimidines (84-86 or series IX). The removal of the outer edge or 'space filling' fluoro-substituent is expected to enhance nematic properties due to the reduction of intermolecular attractions and consequently their lamellar packing arrangements. Their mesomorphic properties are listed in *Table 12*.

Table 12. Transition temperatures ($^{\circ}\text{C}$) (**in bold**) and enthalpies ($\Delta\text{H}/\text{kJ mol}^{-1}$) (*in italics*) for the 2-(4-*n*-alkoxyphenyl)-5-(2-fluoro-4-*n*-alkylphenyl) pyrimidines (**series IX**).



| No. | n | m | I-N | N-S _c | S _A -S _c | N-K | K-N |
|-----------|---|---|-----------------------------|--|--------------------------------|---|---|
| 84 | 4 | 5 | 169.8 <i>0.83</i> | | | 78.0 <i>23.24</i> | 89.8 <i>23.73</i> |
| 85 | 6 | 7 | 154.9 <i>0.84</i> | 80.6 <i>0.13</i> | | <u>S_c-K</u> 53.9 <i>16.25</i> | <u>K-S_c</u> 77.4 <i>35.63</i> |
| 86 | 8 | 9 | 146.0 <i>1.23</i> | <u>N-S_A</u> 130.4 Φ | 119.6 ϕ | 47.5 <i>38.68</i> [†] | 69.1 <i>14.94</i> |

Φ Detected by optical microscopy and DSC, but peak too small to measure.

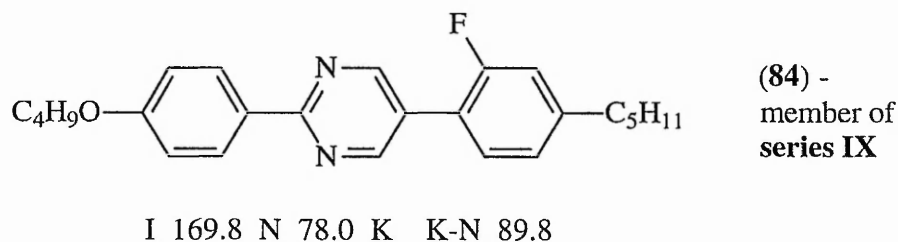
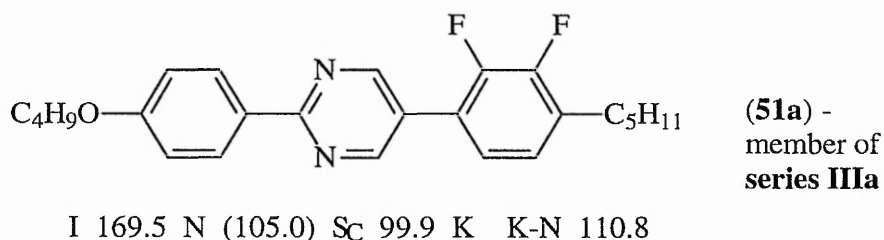
ϕ Transition detected by optical microscopy, but not by DSC.

[†] Value includes the enthalpy of adjacent crystal-crystal transition(s).

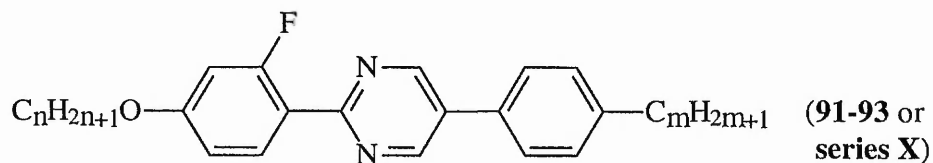
The early homologue (**84**) is nematogenic and as the chain length increases, smectic phase types are also observed, namely S_A and S_c. The longest homologue (**86**) exhibits the ideal phase sequence: I-N-S_A-S_c.

The effect of removing a single lateral fluoro-substituent, i.e., comparing (**84**) with (**51a**) does not particularly alter the clearing point. This observation can be accounted for by the removal of a 'space filling'⁶⁸ fluoro-substituent, i.e., fluoro-substituent *ortho*- to the terminal chain, since it is unlikely to cause either a significant reduction in inter-annular twisting or a reduction in molecular breadth. However, the

removal of a fluoro-substituent greatly lowers the melting point (by 21°C) thus giving rise to materials with a very wide mesophase range. Surprisingly, reducing the number of fluoro-substituents enhances nematic character at the expense of smectic character, i.e., the S_C phase is not observed for (84). Enhancement of nematic character may be due to the absence of the outer edge fluoro-substituent which results in the molecule having a stronger lateral dipole directed towards the terminal ether oxygen.



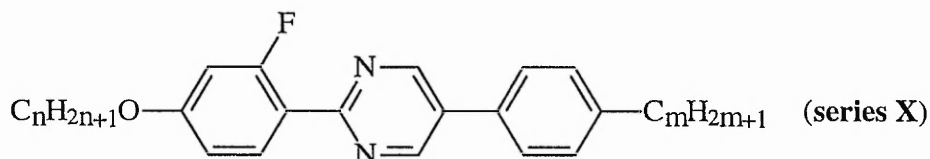
3.2.8 2-(2-FLUORO-4-*n*-ALKOXYPHENYL)-5-(4-*n*-ALKYLPHENYL)-PYRIMIDINES (series X)



To investigate the influence of moving the single fluoro-substituent from the right-hand terminal ring to the left-hand terminal ring, several members (91-93) of a

series of 2-(2-fluoro-4-*n*-alkoxyphenyl)-5-(4-*n*-alkylphenyl)pyrimidines (**series X**) were synthesised and their mesophase transition temperatures are shown in **Table 13**.

Table 13. Transition temperatures (°C) (**in bold**) and enthalpies ($\Delta H/\text{kJ mol}^{-1}$) (*in italics*) for the 2-(2-fluoro-4-*n*-alkoxyphenyl)-5-(4-*n*-alkylphenyl)pyrimidines (**series X**).



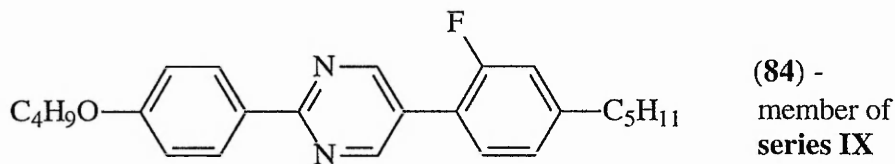
| No. | n | m | I-N | N-S _c | N-K | K-N |
|-----------|---|---|-----------------------------|-----------------------------|---|---|
| 91 | 4 | 5 | 170.2 <i>0.87</i> | | 83.8 <i>17.53</i> | 99.0 <i>14.37</i> |
| 92 | 6 | 7 | 158.4 <i>1.03</i> | 124.9 <i>0.54</i> | <u>S_c-K</u> 71.8 <i>16.37</i> | <u>K-S_c</u> 86.6 <i>16.89</i> |
| 93 | 8 | 9 | 150.4 <i>1.91</i> | 139.2 <i>0.59</i> | 65.1 <i>20.95</i> | 85.8 <i>6.90†</i> |

† Value includes the enthalpy of adjacent crystal-crystal transition(s).

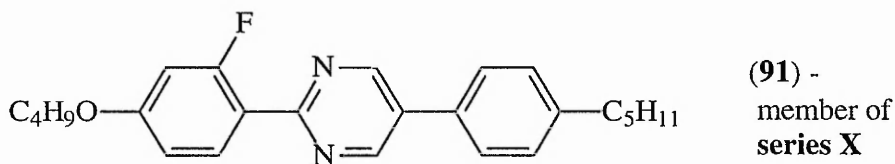
The S_A phase is not present in any of the homologues prepared. For the shortest homologue (**91**) the nematic phase alone is exhibited whereas the remaining homologues (**92**) and (**93**), in addition, exhibit the S_c phase.

A comparative study of compound (**91**) with the analogous compounds (**84**) and (**60**) allows insight into both reducing the number of fluoro-substituents (**91** vs **60**) and moving the mono-fluoro-substituent (**91** vs **84**) on mesomorphic properties. The latter

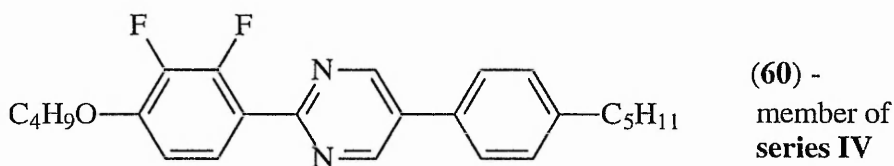
comparison shows that, once again, transposition of the fluoro-substituent from the right-hand ring (**84**) to the left-hand ring (**91**) has little or no effect on mesophase thermal stability. However, such a transposition increases the melting point by 9.2°C.



I 169.8 N 78.0 K K-N 89.8



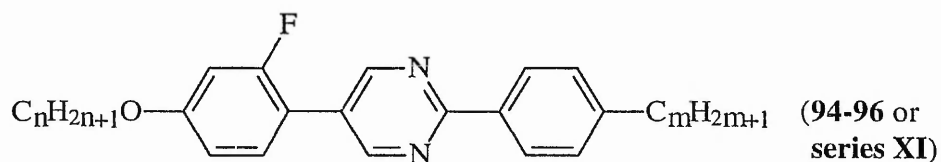
I 170.2 N 83.8 K K-N 99.0



I 169.3 N 159.1 S_A 133.5 S_C 93.6 K K-S_C 106.6

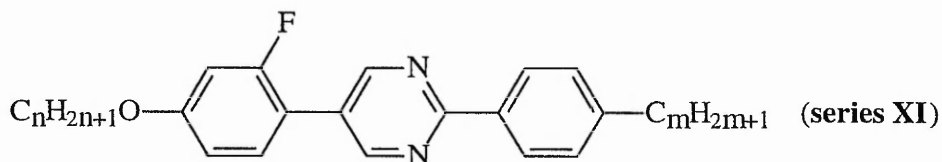
Comparing (**91**) with (**60**) reveals that reducing the number of lateral fluoro-substituents disposed on the left-hand terminal ring from two to one eliminates smectic properties and greatly extends the nematic phase range possibly due to the slightly weaker lateral dipole and the loss of the outer edge fluoro-substituent. The clearing point remains relatively unaffected and the melting point is reduced by 7.6°C.

3.2.9 2-(4-*n*-ALKYLPHENYL)-5-(2-FLUORO-4-*n*-ALKOXYPHENYL)-PYRIMIDINES (series XI)



To investigate the influence of reversing the central pyrimidine ring of three-ring pyrimidine-based compounds, three members (94-96) of a series of 2-(4-*n*-alkylphenyl)-5-(2-fluoro-4-*n*-alkoxyphenyl)pyrimidines (series XI) were prepared and their mesomorphic transition temperatures are reported in *Table 14*.

Table 14. Transition temperatures ($^{\circ}\text{C}$) (**in bold**) and enthalpies ($\Delta\text{H}/\text{kJ mol}^{-1}$) (*in italics*) for the 2-(4-*n*-alkylphenyl)-5-(2-fluoro-4-*n*-alkoxyphenyl)pyrimidines (series XI).



| No. | n | m | I-N | N-S _A | N-K | K-N |
|-----------|---|---|------------------------------|-----------------------------|---|--|
| 94 | 4 | 5 | 166.7 <i>0.53</i> | | 54.2 <i>13.63</i> | 71.2 <i>19.33</i> |
| 95 | 6 | 7 | 154.5 <i>1.12</i> | 141.1 <i>0.55</i> | <u>S_A-K</u> 40.2 <i>13.77</i> | <u>K-S_A</u> 61.9 <i>11.23†</i> |
| 96 | 8 | 9 | 147.2 <i>5.63§</i> | 146.4 <i>⊠</i> | 32.6 <i>18.03</i> | 66.0 <i>39.78</i> |

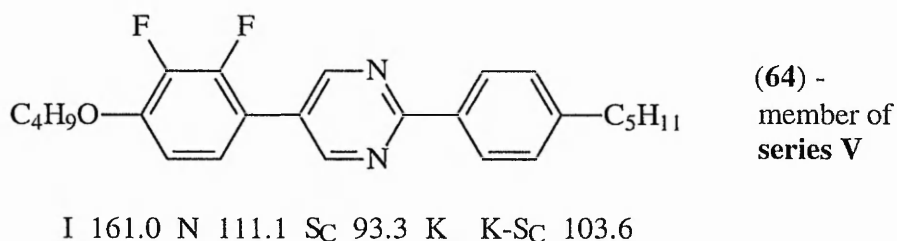
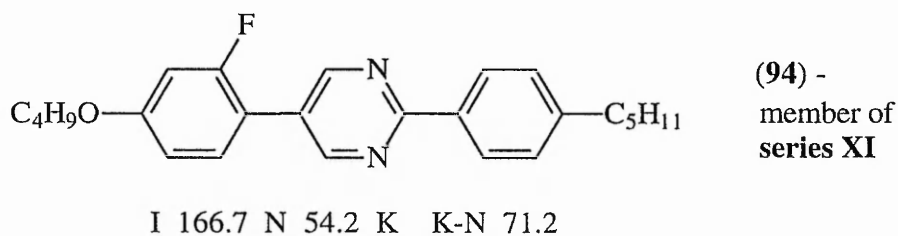
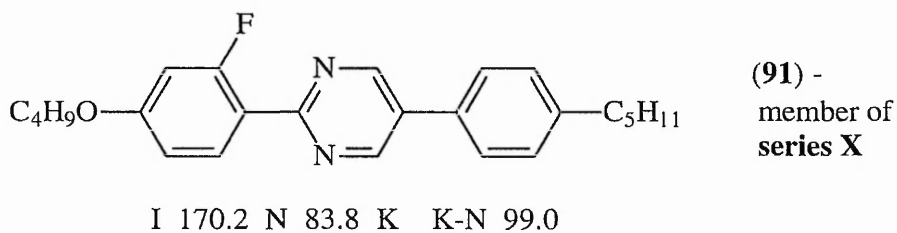
† Value includes the enthalpy of adjacent crystal-crystal transition(s).

§ Combined enthalpy value for two unresolved peaks.

⊠ The enthalpy of transition is concealed by an adjacent transition.

The middle (**95**) and higher homologues (**96**) exhibit the nematic and S_A phase types whereas the shortest homologue (**94**) is nematogenic.

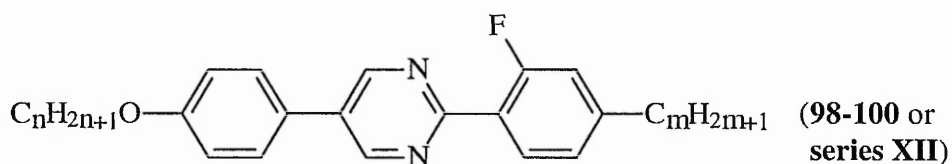
Compound (**94**) may be compared with the isomeric compound (**91**) to show the influence of reversing the central pyrimidine ring on mesomorphic properties. Similarly, (**94**) may be compared with the analogous 2,3-difluoro-substituted compound, i.e., (**64**) to investigate the influence of reducing the number of fluoro-substituents.



Reversing the central pyrimidine ring (**91** vs **94**) slightly lowers the clearing point (3.5°C) and considerably lowers the melting point (27.8°C). Regardless of the positioning of the pyrimidine ring nitrogens moderately low melting compounds with a wide nematic phase range are generated, e.g: for (**91**), phase range is 86.4°C; for (**94**), phase range is 112.5°C.

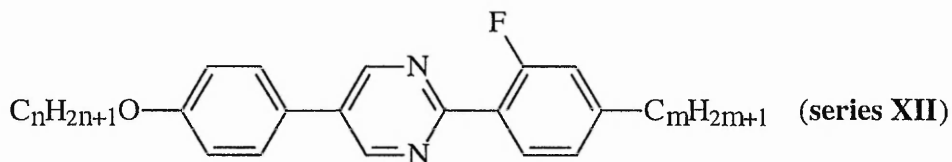
Reducing the number of lateral fluoro-substituents slightly increases the clearing point and strongly depresses the melting point (32.4°C). However, the main effect is on mesophase type. The mono-fluoro- compound (**94**) is nematogenic whereas the 2,3-difluoro- compound (**64**) exhibits the nematic and S_C phase types. Once again, this indicates the importance of the ‘space filling’ fluoro-substituent on the influence of phase types.

3.2.10 2-(2-FLUORO-4-*n*-ALKYLPHENYL)-5-(4-*n*-ALKOXYPHENYL)-PYRIMIDINES (series XII)



Further expansion of the knowledge base of mono-fluoro-substituted three-ring pyrimidine-based compounds led to the preparation of three members (**98-100**) of a series of 2-(2-fluoro-4-*n*-alkyl)-5-(4-*n*-alkoxyphenyl)pyrimidines (series **XII**). In this situation the mono-fluoro-substituent is located in the right-hand terminal ring. From the data acquired previously, for terminal alkyl and alkoxy chains when the fluoro-substituent is located on an inner edge facing the two nitrogen atoms, e.g. (**91**), coupled with reduction in the number of fluoro-substituents which leads to a reduction in smectic character, it is envisaged that compounds (**98-100**) would be nematogenic. *Table 15* lists the mesomorphic properties for members of a series of 2-(2-fluoro-4-*n*-alkyl)-5-(4-*n*-alkoxyphenyl)pyrimidines.

Table 15. Transition temperatures ($^{\circ}\text{C}$) (**in bold**) and enthalpies ($\Delta\text{H}/\text{kJ mol}^{-1}$) (*in italics*) for the 2-(2-fluoro-4-*n*-alkylphenyl)-5-(4-*n*-alkoxyphenyl)pyrimidines (**series XII**).



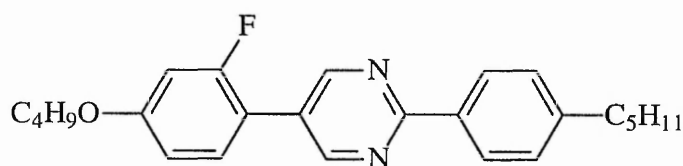
| No. | n | m | I-N | N-S _A | S _A -S _C | S _C -K | K-S _C |
|------------|---|---|---|-----------------------------|--------------------------------|-----------------------------|-----------------------------|
| 98 | 5 | 4 | 173.0 <i>0.60</i> | 132.7 ϕ | 103.2 ϕ | 79.4 <i>14.10</i> | 92.2 <i>14.79</i> |
| 99 | 7 | 6 | 162.4 <i>1.24</i> | 155.6 <i>0.71</i> | 121.7 ϕ | 74.4 <i>17.50</i> | 89.3 <i>17.80</i> |
| 100 | 9 | 8 | <u>I-S_A</u> 160.3 <i>5.35</i> | | 145.6 ϕ | 64.5 <i>14.87</i> | 81.8 <i>14.42</i> |

ϕ Transition detected by optical microscopy, but not by DSC.

The results listed in **Table 15** are rather surprising since all the homologues exhibit smectic tendency. In this situation, mono-fluoro-substitution does not eliminate smectic properties.

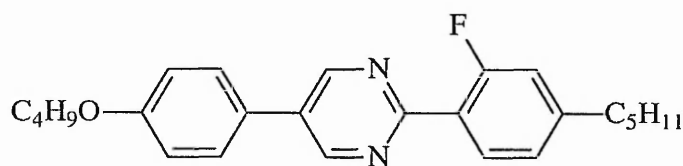
Comparison of the mesomorphic properties of 2-(2-fluoro-4-*n*-pentylphenyl)-5-(4-*n*-butyloxyphenyl)pyrimidine (**98**) with 2-(4-*n*-pentylphenyl)-5-(2-fluoro-4-*n*-butyloxyphenyl)pyrimidine (**94**) and 2-(4-*n*-butyloxyphenyl)-5-(2-fluoro-4-*n*-pentylphenyl)pyrimidine (**84**) shows the disposition of a mono-fluoro-substituent can drastically alter mesophase types.

Mono-fluoro-substituted three-ring pyrimidine-based compounds exhibit smectic properties when the fluoro-substituent is located on an inner edge facing the two nitrogen atoms of the pyrimidine ring and both the nitrogen atoms and the fluoro-substituent are on the right-hand side away from the ether oxygen in the left-hand terminal chain, e.g. (98). The extended conjugation between the ether oxygen atom and the phenyl-pyrimidine core combined with the opposing lateral dipole may compensate for the loss of the 'space filling' outer edge fluorine atom and promote smectic character.



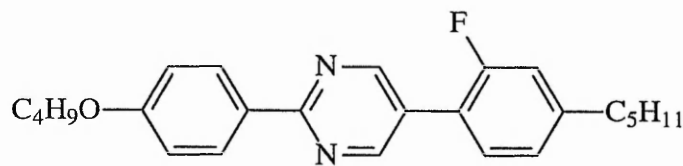
(94) -
member of
series XI

I 166.7 N 54.2 K K-N 71.2



(98) -
member of
series XII

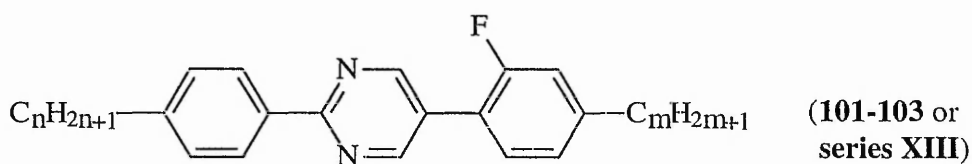
I 173.0 N 132.7 SA 103.2 SC 79.4 K K-SC 92.2



(84) -
member of
series IX

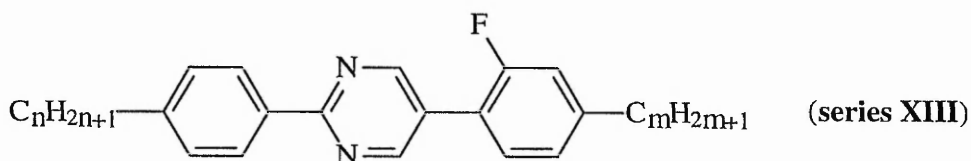
I 169.8 N 78.0 K K-N 89.8

3.2.11 2-(4-*n*-ALKYLPHENYL)-5-(2-FLUORO-4-*n*-ALKYLPHENYL)-PYRIMIDINES (series XIII)



Members (**101-103**) of **series XIII** were prepared in order to compare them with the analogous dialkyl-difluoro-compounds, i.e., 2-(4-*n*-alkylphenyl)-5-(2,3-difluoro-4-*n*-alkylphenyl)pyrimidines (**series VII**) and the mono-fluoro-compounds, i.e., the 2-(4-*n*-alkoxyphenyl)-5-(2-fluoro-4-*n*-alkylphenyl)pyrimidines (**series IX**). The mesomorphic transition temperatures for compounds (**101-103**) are listed in *Table 16*.

Table 16. Transition temperatures (°C) (**in bold**) and enthalpies ($\Delta H/kJ mol^{-1}$) (*in italics*) for the 2-(4-*n*-alkylphenyl)-5-(2-fluoro-4-*n*-alkylphenyl)pyrimidine (**series XIII**).

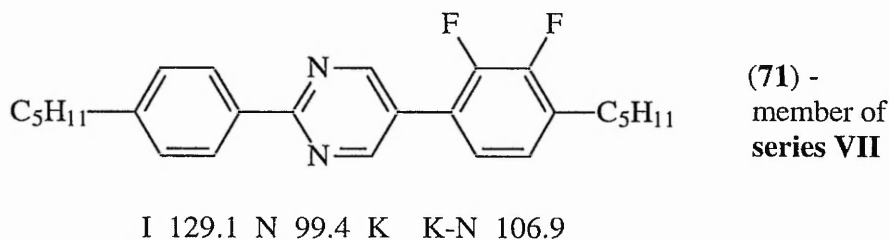
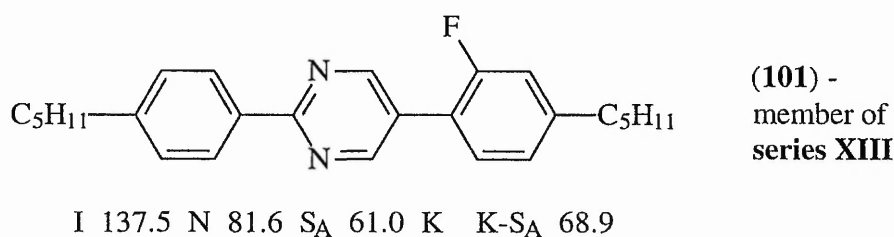
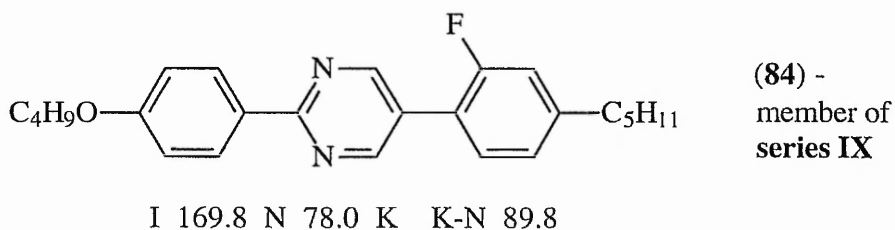


| No. | n | m | I-N | N-S _A | S _A -K | K-S _A |
|------------|---|---|---|-----------------------------|------------------------------|-----------------------------|
| 101 | 5 | 5 | 137.5 <i>0.59</i> | 81.6 ϕ | 61.0 <i>12.19</i> | 68.9 <i>11.78</i> |
| 102 | 7 | 7 | 153.2 <i>0.95</i> | 145.7 <i>0.84</i> | 57.7 <i>16.00</i> | 75.1 <i>19.42</i> |
| 103 | 9 | 9 | I-S _A 122.5 <i>1.48</i> | | 67.7 <i>18.40†</i> | 74.8 <i>21.10</i> |

ϕ Transition detected by optical microscopy, but not by DSC.

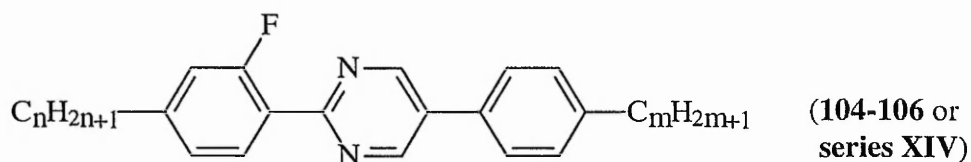
† Value includes the enthalpy of adjacent crystal-crystal transition(s).

Comparing the data for compound (**101**) with that of compound (**84**) shows that the replacement of the ether oxygen with a methylene unit as expected lowers thermal stability (32.3°C). Surprisingly, smectic properties are enhanced at the expense of nematic properties.



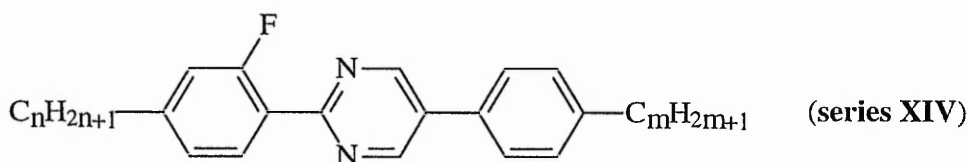
Reducing the number of fluoro-substituents from two to one for the dialkyl compounds (**101** vs **71**) shows an increase in the clearing point (8.4°C) with a nematic phase-range increase and unexpectedly the addition of some smectic character. The slight reduction in molecular breadth associated with the removal of the outer edge fluoro-substituent coupled with the effect of the 'more linear' terminal alkyl chains⁸⁸ may be significant in the emergence of smectic character.

3.2.12 2-(2-FLUORO-4-*n*-ALKYLPHENYL)-5-(4-*n*-ALKYLPHENYL)-PYRIMIDINES (series XIV)



To complete the study, a series (104-106) of 2-(2-fluoro-4-*n*-alkylphenyl)-5-(4-*n*-alkylphenyl)pyrimidines (series XIV) were prepared and their mesomorphic transition temperatures are listed in *Table 17*.

Table 17. Transition temperatures (°C) (**in bold**) and enthalpies ($\Delta H/\text{kJ mol}^{-1}$) (*in italics*) for the 2-(2-fluoro-4-*n*-alkylphenyl)-5-(4-*n*-alkylphenyl)pyrimidines (series XIV).



| No. | n | m | I-N | N-S _A | S _A -S _C | S _A -K | K-S _A |
|------------|---|---|---|--------------------------|--------------------------------|---|--|
| 104 | 5 | 5 | 148.7 <i>0.60</i> | 123.3 ϕ | | 100.6 <i>14.85</i> | 111.3 <i>15.22</i> |
| 105 | 7 | 7 | 141.0 <i>1.78§</i> | 139.6 α | | 98.7 <i>19.19</i> | 108.4 <i>18.71</i> |
| 106 | 9 | 9 | <u>I-S_A</u> 140.6 <i>6.54</i> | | 126.3 ϕ | <u>S_C-K</u> 93.3 <i>24.91</i> | <u>K-S_C</u> 103.4 <i>24.09</i> |

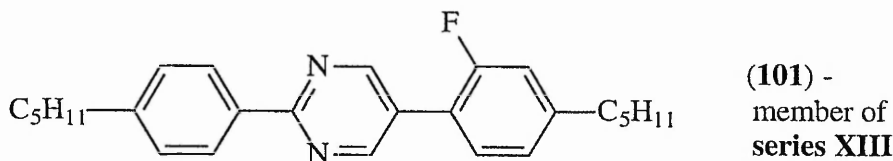
§ Combined enthalpy value for two unresolved peaks.

α The enthalpy of transition is concealed by an adjacent transition.

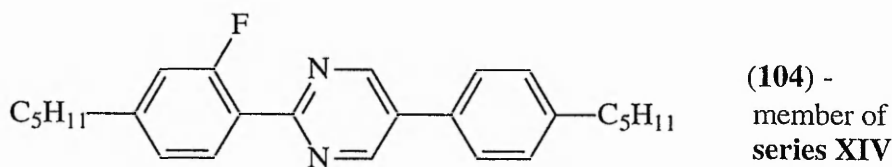
ϕ Transition detected by optical microscopy, but not by DSC.

Altering the disposition of the fluoro-substituent from the right-hand terminal ring (**101**) to the left-hand terminal ring (**104**) increases both the clearing point and melting point. Similar effects were reported on comparison of the dialkyl-difluoro-substituted compounds (**74** vs **71**).

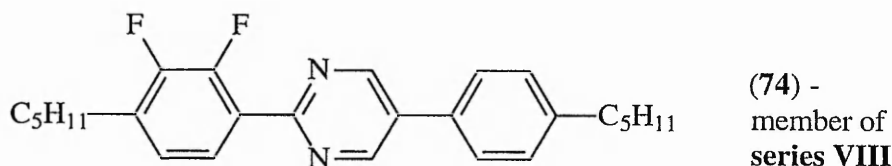
When 2-(2-fluoro-4-*n*-pentylphenyl)-5-(4-*n*-pentylphenyl)pyrimidine (**104**) and 2-(2,3-difluoro-4-*n*-pentylphenyl)-5-(4-*n*-pentylphenyl)pyrimidine (**74**) are compared it can be seen that the nematic phase is introduced at the expense of the S_A phase which is reduced by 20°C and, again, may be due to the removal of the outer edge fluoro-substituent although smectic thermal stability is, in fact, increased by 7.5°C.



I 137.5 N 81.6 S_A 61.0 K K-S_A 68.9



I 148.7 N 123.3 S_A 100.6 K K-S_A 111.3



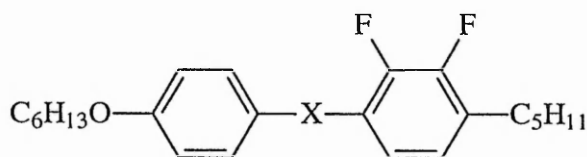
I 150.8 S_A 108.1 K K-S_A 121.3

3.3 COMPARATIVE STUDY OF FLUORINATED THREE-RING PYRIMIDINE-BASED COMPOUNDS WITH ANALOGOUS NON-HETEROCYCLIC COMPOUNDS

It is generally accepted that replacement of a CH group with a nitrogen atom slightly alters the shape of the ring, but drastically alters the electronic properties such that large electronic dipoles may be induced and hence alter the magnitude of intermolecular attraction. Therefore, changes are to be expected in the m.p., clearing point and the mesophase type depending upon the number and disposition of nitrogen atoms in the ring. To this effect, early studies by Zashcke⁸⁷ show that replacement of a 1,4-phenylene ring with a 2,5-pyrimidyl ring usually lowers both the m.p. and clearing point.

Similarly, a comparative study between mono- and di-fluoro-substituted pyrimidine with their analogous non-heterocyclic counterparts may be undertaken.

Table 18. Mesomorphic data (°C) for 2-(4-*n*-hexyloxyphenyl)-5-(2,3-difluoro-4-*n*-pentylphenyl)pyrimidine (**38a**) and 2,3-difluoro-4-*n*-pentyl-4''-*n*-hexyloxy-1,1':4',1''-terphenyl (**107**).⁶⁶




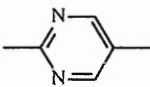
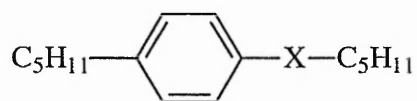
| X | melting point | clearing point | phase range | phase types |
|---|---------------|----------------|-------------|--|
|  (107) | 101.5 | 171.5 | 70.0 | S _C , S _A , N |
|  (38a) | 110.8 | 154.2 | 43.4 | S _C , N |

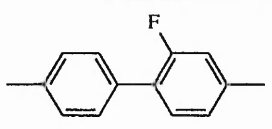
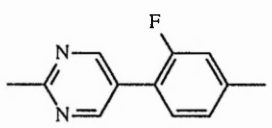
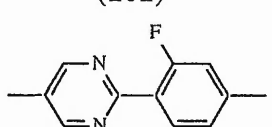
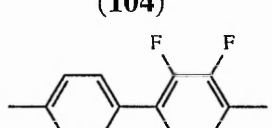
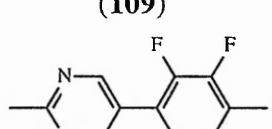
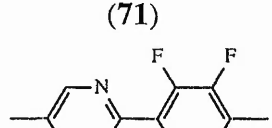
Table 18 (p.103) reports mesomorphic data for compounds with alkoxy-alkyl terminal substituents, i.e., compound (38a) versus (107), which reveals that, contrary to expectation, replacement of the central phenyl-ring with a pyrimidyl-ring increases the m.p. by a magnitude of 9.3°C. The thermal stability decreases by 17.3°C and the S_A phase is no longer observed. The combined effect of an increase in the m.p. and a lowering of the clearing point, reduces the mesophase range of compound (38a) as compared with that of compound (107).

A more detailed comparative study may be undertaken for the dialkyl mono- and dialkyl di-fluoro-substituted pyrimidines with respect to their non-heterocyclic counterparts in order to investigate the influence of the disposition of the nitrogen atoms in the central ring as shown in *Table 19*, p.105.

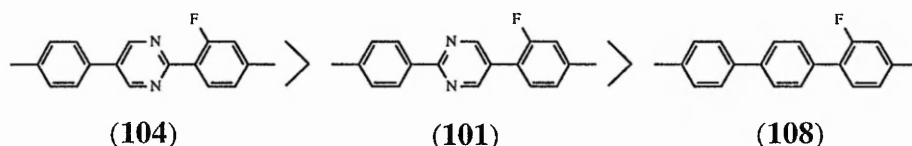
The data displayed in *Table 19* reveals that the mesomorphic properties are dependent upon the number of fluoro-substituents and the disposition of the nitrogen atoms in the central ring. For the mono-fluoro-substituted compounds, when compared with (108), the m.p. is lowered by 3.6°C when the nitrogen atoms are situated closer to the left-hand terminal alkylphenyl-ring, i.e., compound (101). However, the m.p. increases dramatically when the two nitrogen atoms are situated closer to the right-hand terminal alkylfluorophenyl-ring, i.e., compound (104). In this situation, the m.p. increases by 38.8°C. The variation in the clearing point is also contrary to expectation.

Table 19. Mesomorphic data (°C) for dialkyl mono- and difluoro-pyrimidines (**71**, **74**, **101**, **104**) and their corresponding -terphenyls (**108**, **109**).⁶⁸



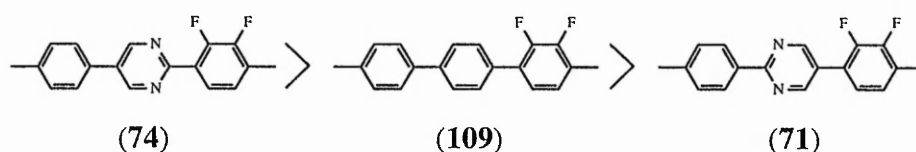
| X | melting point | clearing point | phase range | phase types |
|---|---------------|----------------|-------------|--|
|  (108) | 72.5 | 136.0 | 63.5 | S _C , N |
|  (101) | 68.9 | 137.5 | 68.6 | S _A , N |
|  (104) | 111.3 | 148.7 | 37.4 | S _A , N |
|  (109) | 81.0 | 142.0 | 61.0 | S _C , S _A , N |
|  (71) | 106.9 | 129.1 | 22.2 | N |
|  (74) | 121.3 | 150.8 | 29.5 | S _A |

As stated earlier, the replacement of a CH group by a nitrogen atom generally lowers the clearing point. However, comparison of compounds (108), (101) and (104) shows the following thermal stability order.



With respect to mesophase type, replacement of the central phenyl-ring with a pyrimidyl-ring (regardless of disposition of N atoms) extinguishes the S_C phase type which is replaced by the S_A phase.

Comparison of the difluoro-substituted pyrimidines (71) and (74) with the parent compound (109) shows an increase in the m.p. regardless of the N substitution pattern. The thermal stability order, as shown below, in this instance, shows that the disposition of two nitrogen atoms in the central ring can either increase or decrease mesophase thermal stability with respect to the non-heterocyclic compound.



Interestingly, the parent compound, (109), exhibits N, S_A and S_C phase types, whereas, compound (71) exhibits the nematic phase alone and compound (74) exhibits the S_A phase alone. It appears that the disposition of the nitrogen atoms controls both mesophase thermal stability and mesophase type.

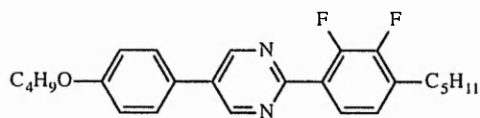
3.4 SUMMARY

The mesomorphic properties of three-ring pyrimidine-based compounds are extremely difficult to correlate with a single parameter. The properties are dependant upon:

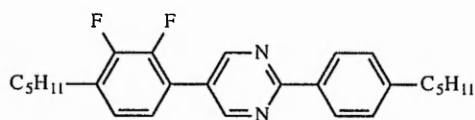
- number of fluoro-substituents;
- nature of terminal substituents and;
- disposition of the central pyrimidine.

Focusing on the shortest homologue of each series, i.e., either butyloxy-pentyl or pentyl-pentyl, reveals that:

- the most stable homologue is 2-(2,3-difluoro-4-*n*-pentylphenyl)-5-(4-*n*-butyloxyphenyl)pyrimidine (**68**), i.e., member of **series VI**;



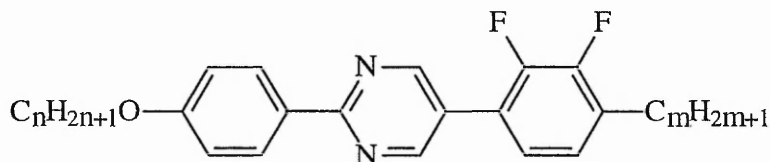
- the least stable homologue is 2-(4-*n*-pentylphenyl)-5-(2,3-difluoro-4-*n*-pentylphenyl)pyrimidine (**71**), i.e., member of **series VII**;



- dialkyl compounds either mono- or difluoro-substituted do not exhibit the S_C phase and;
- an increase in lateral fluorination of alkoxy-alkyl compounds from mono-fluoro- to difluoro-substituted enhances S_C thermal stability at the expense of the nematic phase.

3.5 EXPERIMENTAL

3.5.1 THE SYNTHESIS OF 2-(4-*n*-ALKOXYPHENYL)-5-(2,3-DIFLUORO-4-*n*-ALKYLPHENYL)PYRIMIDINES (series IIIa-d)



where $n=4$, $m=5-8$ (**51a-d** or **series IIIa**); $n=5$, $m=5-8$ (**52a-d** or **series IIIb**);
 $n=6$, $m=5-9$ (**38a-e** or **series IIIc**); $n=8$, $m=9$ (**53** or **series IIId**)

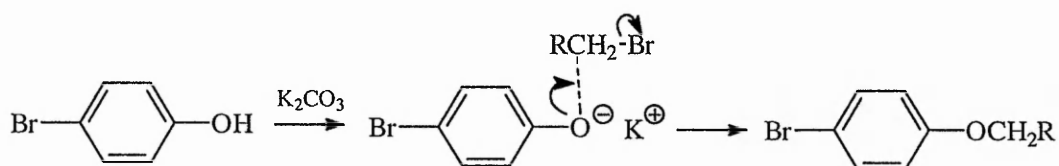
Initially, it was envisaged to prepare members of a series of 2-(4-*n*-alkoxyphenyl)-5-(2,3-difluoro-4-*n*-alkylphenyl)pyrimidines (**series IIIa-d**) using traditional ring closure (cyclisation) techniques,^{89,90} as shown in **scheme 2** (p 110), whereby the pyrimidine ring is formed in the final step. Although this methodology was successful, only the $n=6$, $m=7$ homologue (**38c**) of **series IIIc** was synthesised via this route because it was extremely troublesome and lengthy. Subsequently, members of the 2-(4-*n*-alkoxyphenyl)-5-(2,3-difluoro-4-*n*-alkylphenyl)pyrimidines (**series IIIa-d**) and, in fact, all the other three-ring pyrimidines were synthesised using the faster and higher yielding palladium-catalysed boronic acid cross-coupling methodology. Hence, this section is further sub-divided into two parts, namely: ring closure techniques and boronic acid cross-coupling.

3.5.1.1 RING CLOSURE TECHNIQUES - SYNTHETIC OVERVIEW

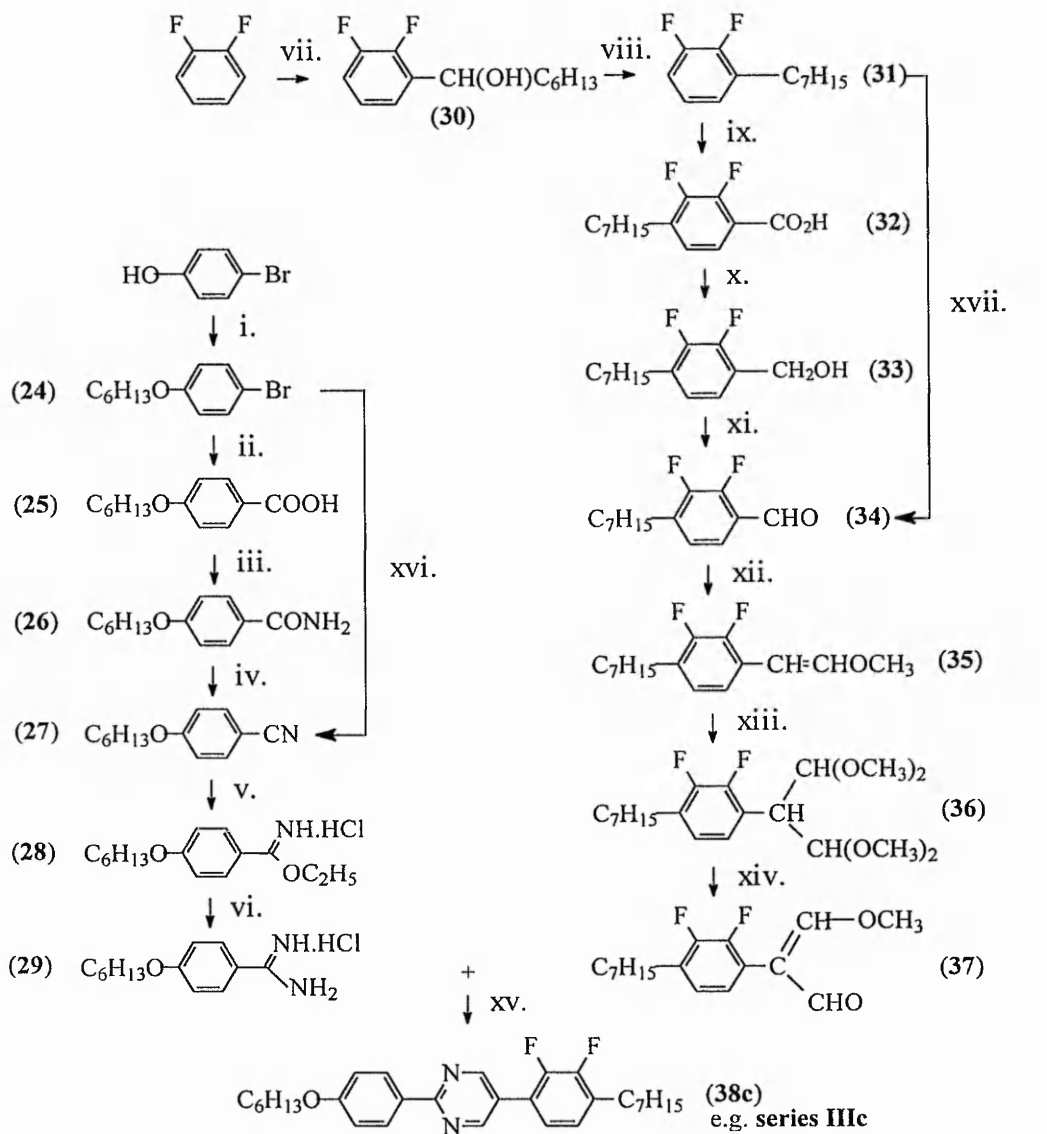
The $n=6$, $m=7$ (**38c**) homologue of **series IIIc**, i.e., 2-(4-*n*-hexyloxyphenyl)-5-(2,3-difluoro-4-*n*-heptylphenyl)pyrimidine was successfully prepared via ring closure

between the appropriate benzimidamide hydrochloride (**29**) and 2-(2,3-difluoro-4-*n*-heptylphenyl)-2-methoxymethylidene ethanal⁹⁰ (**37**) as outlined in **scheme 2** (p. 110).

Commercial 4-bromophenol was *O*-alkylated via the Williamson ether synthesis using 1-bromohexane in the presence of an excess of anhydrous potassium carbonate, as base, and acetone, as solvent, to afford the corresponding 4-*n*-hexyloxybromobenzene (**24**) in good yield (86%). The phenol is sufficiently acidic such that it readily generates the phenoxide anion, even in the presence of a mild base (K_2CO_3), which then replaces the bromide anion on the bromoalkane.



Low temperature ($-78^\circ C$) lithiation of compound (**24**) followed by treatment with solid carbon dioxide gave the desired 4-*n*-hexyloxybenzoic acid (**25**) in good yield (81%). Treatment of the intermediate acid chloride, (prepared by reacting (**25**) with oxalyl chloride), with ammonia solution (35% w/w) afforded the amide (**26**) which was subsequently dehydrated to furnish 4-*n*-hexyloxybenzotrile (**27**). Initial attempts to dehydrate (**26**) with phosphorous pentoxide gave black intractable tars and thus necessitated the use of a milder dehydrating agent. To this effect, (**26**) was dehydrated using a solution of trimethylsilyl polyphosphate⁹¹ prepared *in situ* by heating to reflux a mixture of phosphorous pentoxide and hexamethyldisiloxane in dry DCM, giving an excellent yield of the desired nitrile derivative (**27**).

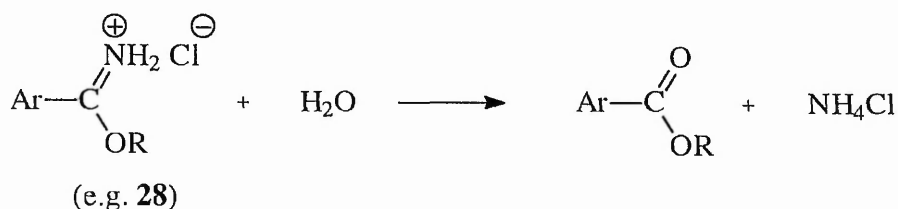


- | | | | |
|-------|---|-------|---|
| i. | $\text{C}_6\text{H}_{13}\text{Br}/\text{K}_2\text{CO}_3$, acetone, reflux. | ix. | a. 1.6M <i>n</i> -BuLi, -78°C , THF. |
| ii. | a. 1.6M <i>n</i> -BuLi, -78°C , THF. | | b. CO_2 . |
| | b. CO_2 . | x. | Borane-methyl sulfide complex, Et_2O , reflux. |
| iii. | a. $(\text{COCl})_2$, THF. | xi. | Pyridinium chlorochromate, DCM. |
| | b. NH_3 , DCM. | xii. | $\text{CH}_3\text{OCH}_2\text{P}^+(\text{Ph})_3\text{Cl}^-/\text{KOC}(\text{CH}_3)_3$, 0°C , <i>tert</i> -butylmethyl ether. |
| iv. | $\text{P}_2\text{O}_5/((\text{Me}_3)_3\text{Si})_2\text{O}$, DCM, reflux. | xiii. | $\text{HC}(\text{OCH}_3)_3$, $\text{BF}_3(\text{OC}_2\text{H}_5)_2$. |
| v. | HCl, 0°C , EtOH/toluene. | xiv. | <i>p</i> -Toluenesulfonic acid, water. |
| vi. | NH_3 , EtOH. | xv. | Na/MeOH. |
| vii. | a. 1.6M <i>n</i> -BuLi, -78°C , THF. | xvi. | ZnCN , $\text{Pd}(\text{PPh}_3)_4$, 80°C , DMF. |
| | b. $\text{C}_6\text{H}_{13}\text{CHO}$. | xvii. | a. 1.6M <i>n</i> -BuLi, -60°C , THF. |
| viii. | a. P_2O_5 , hexane. | | b. <i>N</i> -methylformanilide, -60°C , THF. |
| | b. $\text{H}_2/5\% \text{Pd/C}$. | | |

Scheme 2

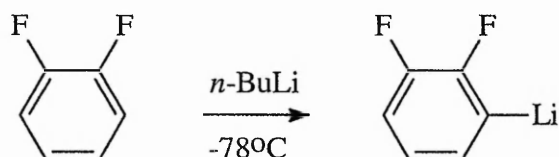
In an attempt to shorten the synthetic route leading to the formation of the nitrile intermediate (27), direct cyanation of 4-*n*-hexyloxybromobenzene was attempted. Direct cyanations typically employ either aryl-iodides or -triflates rather than aryl bromides because the latter are known to be substantially less reactive towards cyanation. However, despite using an improved procedure for aromatic cyanation reported by Tschaen *et al.*,⁹² whereby the 4-*n*-hexyloxybromobenzene (24) was treated with zinc cyanide in the presence of a catalytic amount of *tetrakis*(triphenylphosphine)palladium(0), only a low yield (24%) of compound (27) was effected.

The nitrile (27) was then converted to the corresponding benzimidazole ether hydrochloride (28) via the Pinner synthesis.⁹³ It is essential to use anhydrous conditions for the formation of the hydrochloride (28) otherwise hydrolysis occurs readily to produce the corresponding ester as a side-product as shown below.⁹⁴ The desired 4-*n*-hexyloxybenzimidazole hydrochloride (29) was prepared by ammonolysis of the benzimidazole ether hydrochloride (28) in the presence of ethanol.⁹⁰



The 2,3-difluoro-4-*n*-heptylacrolein intermediate (37) required for ring closure with the 4-*n*-hexyloxybenzimidazole hydrochloride (29) was also prepared via multi-stage synthesis. Starting from commercial *o*-difluorobenzene this route relies on the ability to lithiate at positions *ortho*- to the fluoro-substituents by virtue of *ortho*-directed metallation.⁹⁵ The presence of a highly electronegative substituent such as fluorine,

which exerts a strong electron withdrawing effect (-I), favours metal-hydrogen exchange of a hydrogen atom situated at an *ortho*-position. For successful lithiation it is of paramount importance to maintain the reaction temperature below -50°C to prevent the formation of highly reactive benzyne⁹⁶ due to the elimination of LiF.



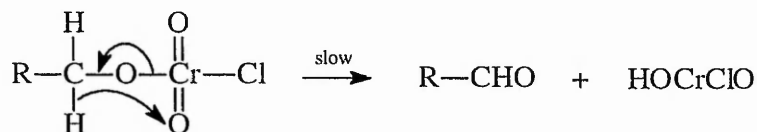
The addition of heptanal to lithiated *o*-difluorobenzene, maintained at low temperature (-78°C), produced the intermediate alcohol (**30**) which was subsequently dehydrated (P_2O_5) to the corresponding alkene. Room temperature, atmospheric pressure, catalytic hydrogenation (Pd/C) of the alkene afforded the desired 2,3-difluoro-1-*n*-heptylbenzene (**31**). A second *ortho*-metallation of (**31**) with *n*-butyllithium followed by treatment with solid carbon dioxide gave the corresponding carboxylic acid (**32**) in good yield (70%).

Reduction of (**32**) to the alcohol (**33**) was initially carried out using lithium aluminium hydride (LiAlH_4) but gave a low yield (37%). This may be attributed to the formation of side-products due to nucleophilic substitution of the fluoro-substituent by the hydride anion of LiAlH_4 .⁹⁷ Subsequently, borane-dimethylsulfide (BMS)⁹⁸ which, unlike LiAlH_4 , functions as an electrophilic reducing agent was employed to give 2,3-difluoro-4-*n*-heptylbenzyl alcohol (**33**) in good yield.

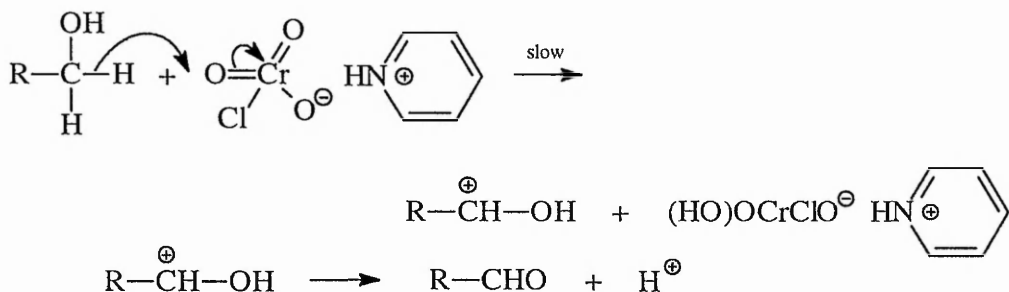
The alcohol (**33**) was then oxidised to the aldehyde (**34**) using pyridinium chlorochromate. The latter is an easily prepared oxidant which readily converts primary

alcohols exclusively to aldehydes.⁹⁹ On the basis of experimental data, Banerji^{100,101} has proposed two mechanistic pathways for this oxidation process as shown below.

Path a:



Path b:



At this stage the reaction scheme was once again reviewed and it was decided to prepare the aldehyde (**34**) directly from the 2,3-difluoro-1-*n*-heptylbenzene (**31**) via lithiation and treatment with *N*-methylformanilide. This 'one-pot' procedure was employed successfully to yield the aldehyde in reasonable yield (64%).

The aldehyde (**34**) was converted to the enol ether (**35**) via the Wittig reaction¹⁰² with the appropriate phosphonium salt. Although there are several methods for preparing enol ethers, the Wittig reaction was chosen because there is no ambiguity regarding the position of the double bond and also a wide variety of functional groups may be tolerated. The mechanism of the Wittig reaction is well documented and involves the formation of an intermediate betaine or phosphorane which then decomposes to give phosphine oxide and the desired alkene.

mixture was heated under reflux for 48 h., cooled, filtered, and the filtrate was evaporated to dryness. The crude residue was dissolved in diethyl ether and washed successively with water (2 x 50 ml), 5% aqueous sodium hydroxide (50 ml), water (50 ml) and dried over anhydrous magnesium sulfate (MgSO₄). The solvent was removed *in vacuo* and the crude residue was purified by vacuum distillation (Claisen) to give the pure 4-*n*-hexyloxy-1-bromobenzene (**24**), 19.3 g (86%), b.p. 122-124°C/0.15 mmHg, (Lit.⁶⁶ 100-110°C/0.1 mmHg), as a clear liquid.

¹H NMR (CDCl₃) δ: 0.86-0.93 (3H, t, CH₃), 1.25-1.47 (6H, m, CH₂), 1.68-1.78 (2H, quint, CH₂), 3.83-3.87 (2H, t, CH₂O), 6.70-6.75 (2H, dd, ArH), 7.29-7.34 (2H, dd, ArH) ppm.

i.r. ν_{\max} (Thin film): 2929, 2858, 1591, 1489, 1243, 820 cm⁻¹.

4-*n*-Hexyloxybenzoic acid (**25**) (scheme 2)

In an atmosphere of dry nitrogen, 1.6M *n*-butyllithium (35.3 ml, 0.056 mol) was added, dropwise, to a stirred solution of 4-*n*-hexyloxy-1-bromobenzene (**24**) (14.5 g, 0.056 mol) in dry THF (150 ml) maintained at -78°C. After the addition was complete the reaction mixture was maintained at -78°C for a further 3 h. The reaction mixture was then poured on to an excess of solid carbon dioxide and left to warm to room temperature overnight. The resultant residue was acidified with 4M HCl (200 ml) and extracted with diethyl ether (2 x 50 ml). The combined ethereal extract was dried (MgSO₄) and the solvent was removed *in vacuo*. The crude residue was recrystallised from cyclohexane to afford the pure 4-*n*-hexyloxybenzoic acid (**25**), 9.2 g (74%), m.p. 103-151°C (N-I) (Lit.¹⁰⁴ m.p. 105-153°C (N-I)), as white needles.

^1H NMR (CDCl_3) δ : 0.89-0.94 (3H, t, CH_3), 1.30-1.42 (4H, m, CH_2), 1.43-1.46 (2H, quint, CH_2), 1.78-1.83 (2H, quint, CH_2), 4.00-4.05 (2H, t, CH_2O), 6.91-6.95 (2H, d, ArH), 8.04-8.07 (2H, d, ArH), 11.08 (1H, s, COOH: disappears on D_2O shake) ppm.

i.r. ν_{max} (KBr): 3000-2500 (OH str.), 1682 (C=O str.), 1605, 1428, 1258, 646 cm^{-1} .

4-*n*-Hexyloxybenzamide (**26**) (scheme 2)

Oxalyl chloride (9.14 g, 0.072 mol) was added, dropwise, to a stirred solution of 4-*n*-hexyloxybenzoic acid (**25**) (8 g, 0.036 mol) in dry THF (100 ml). A few drops of pyridine were added to initiate the reaction and the mixture was left to stir overnight. The solvent was then removed *in vacuo* and the resultant crude 4-*n*-hexyloxybenzoyl chloride was immediately dissolved in dry DCM (150 ml). The solution was cooled to 0°C and ammonia solution (35% w/w) (20 ml) was added, dropwise, with stirring. The reaction mixture was stirred for 1 h. and the solvent was removed under reduced pressure. The crude amide was recrystallised from aqueous ethanol to furnish the pure 4-*n*-hexyloxybenzamide (**26**), 7.94 g (99%), m.p. $152\text{-}154^\circ\text{C}$ (Lit.¹⁰⁵ m.p. 154°C), as a white crystalline solid.

^1H NMR (CDCl_3) δ : 0.88-0.93 (3H, t, CH_3), 1.31-1.40 (4H, m, CH_2), 1.40-1.45 (2H, quint, CH_2), 1.75-1.81 (2H, quint, CH_2), 3.97-4.01 (2H, t, CH_2O), 6.57 (2H, s, NH_2 : disappears on D_2O shake), 6.84-6.92 (2H, dd, ArH), 7.84-7.89 (2H, dd, ArH) ppm.

i.r. ν_{max} (KBr): 3387-3180 (N-H str.), 2954, 2927, 1646 (C=O str.), 1422, 844 cm^{-1} .

4-*n*-Hexyloxybenzotrile (**27**) (Method 1) (scheme 2)

In an atmosphere of nitrogen, a mixture of phosphorous pentoxide (40 g, 0.28 mol),

hexamethyldisiloxane (90 ml, 0.42 mol) and dry DCM (200 ml) were heated under reflux until a clear solution was attained (approx. 30 min.). The reaction mixture was then cooled to room temperature and 4-*n*-hexyloxybenzamide (**26**) (7.7 g, 0.034 mol) was added. The reaction mixture was reheated under reflux for 2 h., cooled, and then quenched carefully with water (200 ml). The crude product was extracted with chloroform (3 x 100 ml) and the combined organic extract was dried (MgSO₄) and the solvent was removed *in vacuo*. Vacuum distillation (Claisen) of the crude residue gave the desired pure 4-*n*-hexyloxybenzotrile (**27**), 2.98 g (43%), b.p. 130-132°C/1 mmHg (Lit.¹⁰⁶ 155-157°C), as a colourless liquid.

¹H NMR (CDCl₃) δ: 0.88-0.93 (3H, t, CH₃), 1.31-1.40 (4H, m, CH₂), 1.41-1.53 (2H, quint, CH₂), 1.74-1.85 (2H, quint, CH₂), 3.97-4.01 (2H, t, CH₂O), 6.91-6.96 (2H, d, ArH), 7.55-7.59 (2H, d, ArH) ppm.

i.r. ν_{\max} (Thin film): 2929, 2858, 2224 (C≡N str.), 1605, 1508, 1257, 1170, 834 cm⁻¹.

4-*n*-Hexyloxybenzotrile (**27**) (Method 2) (scheme 2)

In an atmosphere of dry nitrogen, a mixture of 4-*n*-hexyloxy-1-bromobenzene (**24**) (4.12 g, 0.016 mol), zinc cyanide (1.13 g, 0.0096 mol), *tetrakis*(triphenylphosphine)palladium (0.73 g, 0.00064 mol) and dry DMF (20 ml) were heated at 80°C for 14 h. The mixture was then cooled to room temperature, diluted with toluene (50 ml), washed successively with 2M aqueous ammonium hydroxide solution (2 x 50 ml), brine (20 ml) and dried (MgSO₄). The solvent was removed *in vacuo* and the crude residue was subjected to column chromatography on silica gel eluting with 9 : 1 petroleum ether

(b.p. 60-80°C) : ethyl acetate. The solvent was removed from the desired fractions to furnish the pure 4-*n*-hexyloxybenzotrile (**27**), 0.98 g (24%), as a colourless liquid. Spectroscopic data as in Method 1 above.

4-*n*-Hexyloxybenzimidazole ether hydrochloride (**28**) (scheme 2)

A stirred solution of 4-*n*-hexyloxybenzotrile (**27**) (2.9 g, 0.014 mol) in dry ethanol (40 ml) and dry toluene (100 ml) was saturated with hydrogen chloride gas at 0°C and then stirred at room temperature for 48 h. The solvent was removed *in vacuo* and the crude residue shaken with dry ether (50 ml), filtered, washed with further portions of dry ether (2 x 20 ml) and then dried under vacuum to yield the pure 4-*n*-hexyloxybenzimidazole ether hydrochloride (**28**), 2.4 g (60%), m.p. 101-102°C, as a white solid.

¹H NMR (CDCl₃) δ: 0.88-0.93 (3H, t, CH₃), 1.31-1.49 (6H, m, CH₂), 1.55-1.61 (3H, t, CH₃), 1.75-1.83 (2H, quint, CH₂), 4.05-4.10 (2H, t, CH₂O), 4.70-4.78 (2H, q, CH₂), 7.01-7.05 (2H, d, ArH), 8.20-8.24 (2H, d, ArH), 11.4 (1H, br s), 12.0 (1H, br s) ppm.
i.r. ν_{max} (KBr): 3384, 3300-2500, 1605, 1443, 1267, 1184, 1070, 843 cm⁻¹.

4-*n*-Hexyloxybenzimidamide hydrochloride (**29**) (scheme 2)

A mixture of ethanol (70 ml), ammonia solution (35% w/w) (60 ml) and 4-*n*-hexyloxybenzimidazole ether hydrochloride (**28**) (2.3 g, 0.008 mol) was stirred at room temperature for 48 h. Subsequently, the solvent was removed under reduced pressure and the crude residue was shaken with ether (50 ml), filtered, washed with portions of ether (2 x 50 ml) and dried under vacuum to afford the desired 4-*n*-hexyloxybenzimidamide hydrochloride (**29**), 1.5 g (73%), m.p. 71-73°C, as a white solid.

^1H NMR (CDCl_3) δ : 0.88-0.93 (3H, t, CH_3), 1.34-1.48 (6H, m, CH_2), 1.75-1.82 (2H, quint, CH_2), 4.00-4.05 (2H, t, CH_2O), 6.65 (1H, s, NH_2), 6.99-7.02 (2H, d, ArH), 7.7 (1H, s NH_2), 7.87-7.90 (2H, d, ArH), 8.95 (1H, br s), 9.13 (1H, br s) ppm.

i.r. ν_{max} (KBr): 3400-2750, 1673, 1466, 1262, 839 cm^{-1} .

1-(2,3-Difluorophenyl)heptan-1-ol (**30**) (scheme 2)

In an atmosphere of nitrogen, 1.6M *n*-butyllithium (55 ml, 0.088 mol) was added, dropwise, to a stirred, cooled (-78°C) solution of *o*-difluorobenzene (10 g, 0.088 mol) in dry THF (80 ml). After the addition was complete, the reaction mixture was maintained at -78°C for a further 3 h. Subsequently, a solution of heptanal (10.05 g, 0.088 mol) in dry THF (50 ml) was added, dropwise, via a pressure-equalising funnel and the mixture was allowed to warm to room temperature overnight. The reaction mixture was quenched with saturated ammonium chloride solution (150 ml) and the product was extracted with diethyl ether (3 x 50 ml). The combined organic extract was washed with water (3 x 50 ml), dried (MgSO_4) and the solvent was removed *in vacuo*. The crude residue was purified by vacuum distillation (Kugelrohr) to furnish the pure 1-(2,3-difluorophenyl)heptan-1-ol (**30**), 10.37 g (52%), b.p. $118-120^\circ\text{C}/0.6$ mmHg (Lit.⁶⁶ $106-108^\circ\text{C}/0.1$ mmHg), as a colourless oil.

^1H NMR (CDCl_3) δ : 0.84-0.89 (3H, t, CH_3), 1.26-1.39 (8H, m, CH_2), 1.69-1.72 (2H, quint, CH_2), 3.13 (1H, s, OH: disappears on D_2O shake), 4.93-4.98 (1H, t, CH), 6.98-7.07 (2H, m, ArH), 7.13-7.19 (1H, m, ArH) ppm.

i.r. ν_{max} (Thin film): 3140-3540 (OH str.), 2930, 2858, 1625, 1595, 1275, 785, cm^{-1} .

1,2-Difluoro-3-*n*-heptylbenzene (**31**) (scheme 2)

Phosphorous pentoxide (19.8 g, 0.139 mol) was added to a stirred solution of 1-(2,3-difluorophenyl)heptan-1-ol (**30**) (10.6 g, 0.046 mol) in hexane (80 ml) at room temperature and allowed to stir overnight. The reaction mixture was then filtered to remove inorganic salts and the filtrate was evaporated to dryness *in vacuo*. Subsequently, hexane (80 ml) and 5% palladium-on-charcoal (0.98 g) were added to the residue which was subjected to room temperature atmospheric pressure hydrogenation. After hydrogenation was complete (no alkene peak at 1648 cm⁻¹ on i.r.), the solvent was removed *in vacuo* and the crude residue was purified by vacuum distillation (Claisen) to give the pure 1,2-difluoro-3-*n*-heptylbenzene (**31**), 6.8 g (70%), b.p. 75-77°C/0.8 mmHg (Lit.⁶⁶ 124-126°C/15 mmHg), as a colourless liquid.

¹H NMR (CDCl₃) δ: 0.85-0.89 (3H, t, CH₃), 1.27-1.34 (8H, m, CH₂), 1.54-1.65 (2H, quint, CH₂), 2.65 (2H, t, CH₂), 6.86-6.98 (3H, m, ArH) ppm.

i.r. ν_{\max} (Thin film): 2950, 2928, 2857, 1626, 1595, 1489, 1279, 779 cm⁻¹.

2,3-Difluoro-4-*n*-heptylbenzoic acid (**32**) (scheme 2)

In an atmosphere of dry nitrogen, 1.6M *n*-butyllithium (17.3 ml, 0.028 mol) was added, dropwise, to a stirred, cooled (-78°C) solution of 1,2-difluoro-3-*n*-heptylbenzene (**31**) (5.9 g, 0.028 mol) in THF (150 ml). The reaction was maintained at -78°C for 3 h., then poured on to an excess of solid carbon dioxide and allowed to warm to room temperature overnight. The resultant mixture was acidified (4M HCl) and extracted with ether (2 x 100 ml). The combined ethereal extract was dried (MgSO₄) and the

solvent was removed *in vacuo*. The crude product was purified by recrystallisation from cyclohexane to afford the desired 2,3-difluoro-4-*n*-heptylbenzoic acid (**32**), 5 g (70%), m.p. 116-118°C, as white crystalline plates.

¹H NMR (CDCl₃) δ: 0.88 (3H, t, CH₃), 1.28-1.33 (8H, m, CH₂), 1.63 (2H, quint, CH₂), 2.71 (2H, t, CH₂), 7.00-7.06 (1H, m, ArH), 7.67-7.73 (1H, m, ArH), ppm. No OH signal observed.

i.r. ν_{\max} (KBr): 3200-2500 (OH str.), 1678 (C=O str.), 1472, 1304, 930 cm⁻¹.

2,3-Difluoro-4-*n*-heptylbenzyl alcohol (**33**) (scheme 2)

In a dry nitrogen atmosphere, borane-methyl sulfide complex (2.1 ml, 0.022 mol) was added, dropwise, to a stirred solution of 2,3-difluoro-4-*n*-heptylbenzoic acid (**32**) (5 g, 0.019 mol) dissolved in dry diethyl ether (60 ml) at room temperature until gas evolution was complete. The reaction mixture was then heated under reflux for a further 2 h., cooled to room temperature, then poured into ice-cold methanol (100 ml). The resulting clear solution was allowed to stand overnight in a fume hood and then the methanol was removed under reduced pressure. The crude residue was purified by vacuum distillation (Kugelrohr) to give the pure 2,3-difluoro-4-*n*-heptylbenzyl alcohol (**33**), 3.3 g (72%), b.p. 138-139°C/0.1 mmHg, as a colourless liquid.

¹H NMR (CDCl₃) δ: 0.85-0.90 (3H, t, CH₃), 1.27-1.35 (8H, m, CH₂), 1.60 (2H, quint, CH₂), 2.10 (1H, s, OH: disappears on D₂O shake), 2.64 (2H, t, CH₂), 4.72 (2H, s, CH₂), 6.93-6.95 (1H, t, ArH), 7.03-7.06 (1H, t, ArH) ppm.

i.r. ν_{\max} (Thin film): 3540-3100 (OH str.), 2960, 2860, 1470, 1290, 1010, 930, 820 cm⁻¹.

2,3-Difluoro-4-*n*-heptylbenzaldehyde (**34**) (Method 1) (scheme 2)

2,3-Difluoro-4-*n*-heptylbenzyl alcohol (**33**) (3.3 g, 0.013 mol) was added to a stirred suspension of pyridinium chlorochromate (5.6 g, 0.026 mol) in dry DCM (70 ml) and allowed to stir at room temperature for 48 h. The progress of the reaction was monitored by tlc and when deemed complete, dry diethyl ether (50 ml) was added. The reaction mixture was then filtered through 'Hyflo super cell' and the solvent removed *in vacuo*. The crude residue was purified by flash column chromatography on silica gel eluting with a 3:1 mixture of light petroleum ether (b.p. 40-60°C) : DCM to furnish the pure 2,3-difluoro-4-*n*-heptylbenzaldehyde (**34**), 2.7 g (86%), 127-129°C/0.1 mmHg, as a clear yellow oil.

¹H NMR (CDCl₃) δ: 0.85-0.91 (3H, t, CH₃), 1.28-1.33 (10H, m, CH₂), 1.61-1.66 (2H, quint, CH₂), 2.70 (2H, t, CH₂), 7.07 (1H, t, ArH), 7.57 (1H, t, ArH), 10.29 (1H, s, CHO) ppm.

i.r. ν_{\max} (Thin film): 2960, 2930, 2855 (C-H str.), 1695 (C=O str.), 1465, 1400, 1255, 780 cm⁻¹.

2,3-Difluoro-4-*n*-heptylbenzaldehyde (**34**) (Method 2) (scheme 2)

In an inert atmosphere of nitrogen, 1.6M *n*-butyllithium (0.026 mol) was added, dropwise, to stirred, cooled (-60°C) solution of 1,2-difluoro-3-*n*-heptylbenzene (**31**) (5.5 g, 0.026 mol) in dry THF (100 ml). After the addition was complete, the reaction mixture was maintained at -60°C for a further 3 h. and then a solution of *N*-methylformanilide (3.5 g, 0.026 mol) in dry THF was added, dropwise, at such a rate

ensuring that the temperature did not exceed -50°C . Subsequently, the reaction mixture was allowed to warm to room temperature overnight. The reaction mixture was then quenched with 4M HCl, extracted with diethyl ether (2 x 50 ml), dried (MgSO_4) and the solvent was removed *in vacuo*. The crude residue was purified by vacuum distillation (Claisen) to afford the pure 2,3-difluoro-4-*n*-heptylbenzaldehyde (**34**), 6 g (64%), $127-129^{\circ}\text{C}/0.1\text{ mmHg}$, as a clear yellow oil.

Spectroscopic data as in Method 1 above.

2-(2,3-Difluoro-4-*n*-heptylphenyl)-1-methoxyethene (**35**) (scheme 2)

In an atmosphere of dry nitrogen, a mixture of 2,3-difluoro-4-*n*-heptylbenzaldehyde (**34**) (3.1 g, 0.013 mol) and *tert*-butylmethyl ether (40 ml) was added, dropwise, to a stirred mixture of methoxymethyl triphenylphosphonium chloride (7.5 g, 0.021 mol), potassium *tert*-butylate (2.3 g, 0.02 mol) and *tert*-butylmethyl ether (80 ml) at 0°C . The reaction mixture was then stirred at room temperature for 48 h. Water (100 ml) was then added and the reaction mixture was extracted with ether (3 x 50 ml). The combined organic extract was washed with water (2 x 50 ml), dried (MgSO_4) and the solvent removed *in vacuo*. The residue was purified* by column chromatography on silica gel eluting with light petroleum ether (b.p. $40-60^{\circ}\text{C}$) to give the desired 2-(2,3-difluoro-4-*n*-heptylphenyl)-1-methoxyethene (**35**), 1.2 g (67%), as a clear liquid.

* Prior to chromatography the residue may be treated with hexane which causes the triphenylphosphine oxide to precipitate from solution. This may be filtered and discarded whereas the filtrate is evaporated to dryness *in vacuo* and subjected to chromatography.

^1H NMR (CDCl_3) δ : 0.85-0.90 (3H, t, CH_3), 1.27-1.34 (8H, m, CH_2), 1.55-1.61 (2H, quint, CH_2), 2.60 (2H, t, CH_2), 3.78 (3H, s, CH_3), 5.40-5.43 (1H, d, CH), 6.20-6.23 (1H, d, CH), 6.80-6.87 (1H, t, ArH), 7.63-7.70 (1H, t, ArH) ppm.

i.r. ν_{max} (Thin film): 2930, 2850, 1696, 1645, 1465, 1435, 1255, 1225, 1105, 825 cm^{-1} .

2-(2,3-Difluoro-4-*n*-heptylphenyl)malonic anhydride-tetramethylacetal (**36**) (Scheme 2)
2-(2,3-difluoro-4-*n*-heptylphenyl)-1-methoxyethene (**35**) (4.5 g, 0.016 mol) was added, dropwise, to a cooled (0°C) solution of freshly distilled trimethyl orthoformate (42 ml) and boron trifluoride diethyl ether (1.1 ml, 0.0084 mol). After the addition was complete, the reaction mixture was allowed to warm to room temperature overnight. The reaction mixture was then diluted with toluene (40 ml), washed with saturated sodium bicarbonate solution (50 ml), water (2 x 50 ml) and then dried (MgSO_4). The solvent was removed *in vacuo* to afford the 2-(2,3-difluoro-4-*n*-heptylphenyl)malonic anhydride-tetramethylacetal (**36**), 4.17 g (74%), as a yellow oil.

^1H NMR (CDCl_3) δ : 0.85-0.90 (3H, t, CH_3), 1.28-1.31 (8H, m, CH_2), 1.59 (2H, quint, CH_2), 2.6 (2H, q, CH_2), 3.31 (3H, s, OCH_3), 3.34 (3H, s, OCH_3), 3.37 (3H, s, OCH_3), 3.43 (3H, s, OCH_3), 3.65 (1H, t, CH), 4.69 (2H, dd, CH), 6.8-7.2 (2H, m, ArH) ppm.

i.r. ν_{max} (Thin film): 2960, 2928, 2856, 1468, 1118, 1080 cm^{-1} .

2-(2,3-Difluoro-4-*n*-heptylphenyl)-2-methoxymethylidene ethanal (**37**) (Scheme 2)

A stirred mixture of 2-(2,3-difluoro-4-*n*-heptylphenyl)malonic anhydride-tetramethylacetal (**36**) (4.15 g, 0.011 mol), water (50 ml) and *p*-toluenesulfonic acid

(5 g, 0.0025 mol) was heated to 85°C for 3 h. After cooling to room temperature, sodium hydrogen carbonate (0.6 g) was added and the mixture was stirred for 2 h. The crude product was extracted with ether (50 ml) which was then washed with 3M aqueous sodium hydroxide solution (50 ml), water (50 ml), and dried (MgSO₄). The solvent was removed by rotary evaporation to give the crude 2-(2,3-difluoro-4-*n*-heptylphenyl)-2-methoxymethylidene ethanal (**37**) as a yellow oil. Purification was not achieved and (**37**) was used immediately in the next step.

i.r. ν_{\max} (Thin film): 2950, 2856, 1694 (C=O str.), 1628 (C=C str), 1468, 777 cm⁻¹.

2-(4-*n*-Hexyloxyphenyl)-5-(2,3-difluoro-4-*n*-heptylphenyl)pyrimidine (**38c**) (Scheme 2)

In an atmosphere of dry nitrogen, 2-(2,3-difluoro-4-*n*-heptylphenyl)-2-methoxymethylidene ethanal (**37**) (2.0 g, 0.0068 mol) was added to a stirred solution of 4-*n*-hexyloxybenzimidamide hydrochloride (**29**) (1.6 g, 0.0065 mol) previously dissolved in a solution of sodium metal (0.55 g) in methanol (20 ml). The reaction mixture was heated to and maintained at 50°C overnight, then cooled and the ensuing yellow suspension was acidified with 4M HCl. The residue was extracted with diethyl ether (2 x 50 ml), the combined ethereal extract was dried (MgSO₄) and the solvent removed *in vacuo*. The crude residue was purified by column chromatography on silica gel eluting with a 9:1 mixture of light petroleum ether (b.p. 40-60°C) : ethyl acetate followed by recrystallisation from ethanol to afford the desired 2-(4-*n*-hexyloxyphenyl)-5-(2,3-difluoro-4-*n*-heptylphenyl)pyrimidine (**38c**), 1.14 g (42%), as white crystals.

The m.p. and mesomorphic transition temperatures of compound **38c** are listed in *Table 4* (p. 68) of the results and discussion section.

Found: C, 74.78; H, 8.00; N, 6.12%. C₂₉H₃₆F₂N₂O requires C, 74.65; H, 7.78; N, 6.00%.

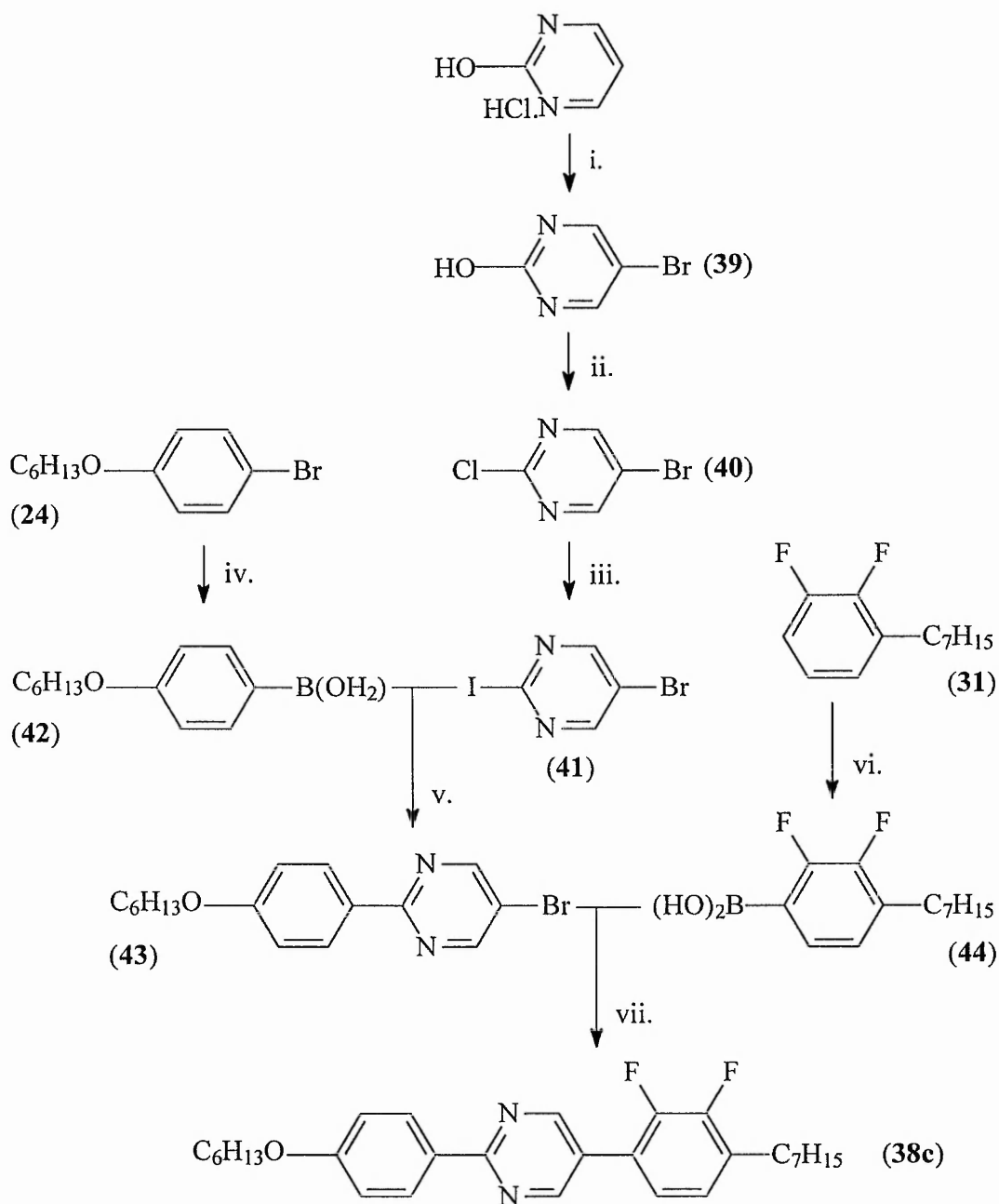
¹H NMR (CDCl₃) δ: 0.88-0.93 (3H, t, CH₃), 0.97-1.03 (3H, t, CH₃), 1.29-1.37 (14H, m, CH₂), 1.64-1.78 (2H, quint, CH₂), 1.81-1.86 (2H, quint, CH₂), 2.70-2.75 (2H, t, CH₂), 4.01-4.06 (2H, t, CH₂O), 6.98-7.03 (2H, dd, ArH), 7.03-7.18 (2H, m, ArH), 8.40-8.46 (2H, dd, ArH), 9.03 (2H, s, ArH) ppm.

i.r. ν_{max} (KBr): 2954, 2926, 2854, 1605, 1586, 1466, 1435, 1257, 1168, 1022, 798 cm⁻¹.

3.5.1.2. BORONIC ACID CROSS-COUPLING - SYNTHETIC OVERVIEW

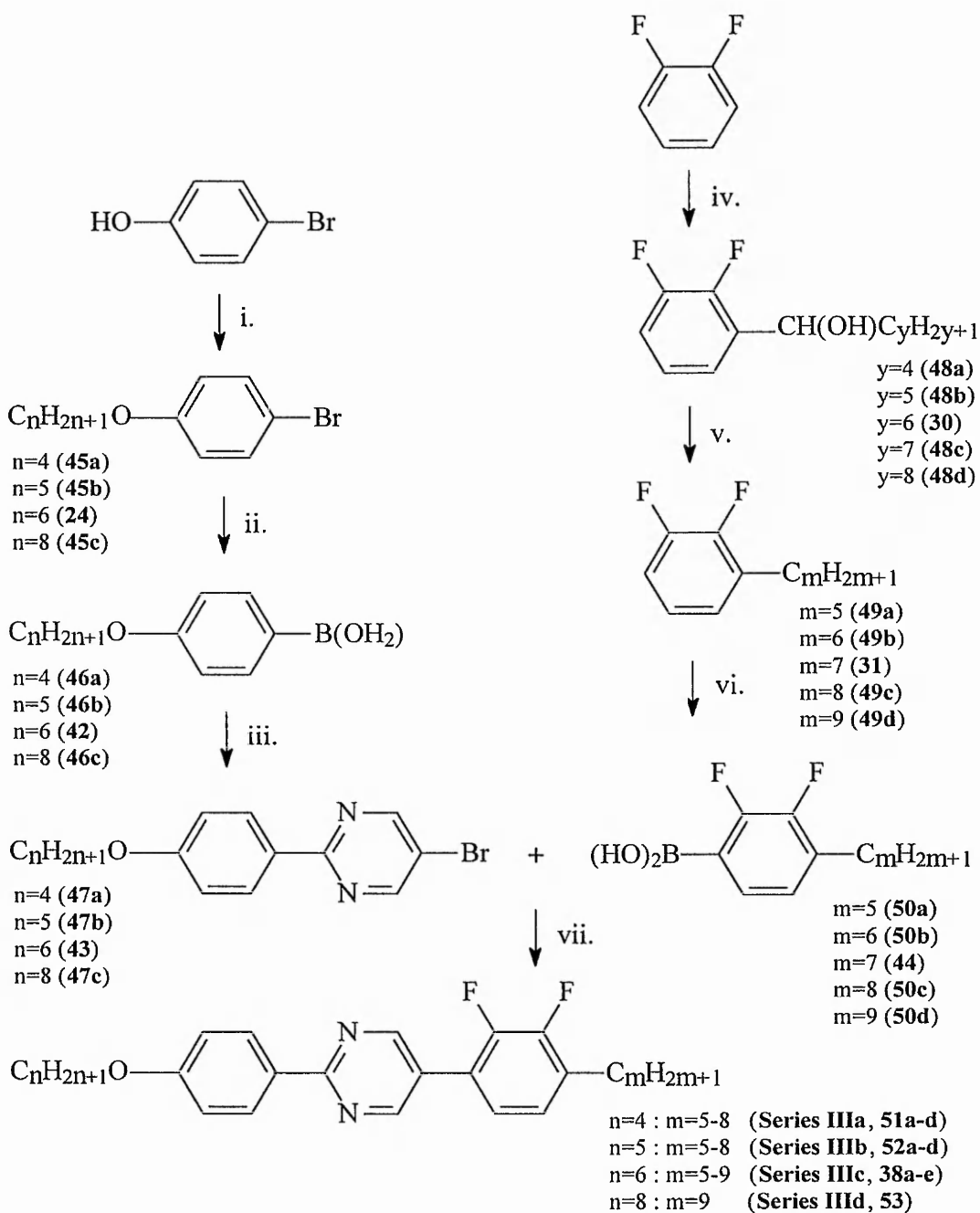
2-(4-*n*-Hexyloxyphenyl)-5-(2,3-difluoro-4-*n*-heptylphenyl)pyrimidine (**38c**) was readily prepared using the palladium-catalysed boronic acid cross-coupling (Suzuki coupling) methodology as depicted in **scheme 3** (p. 127). The success of this route relies on 5-bromo-2-iodopyrimidine¹⁰⁷ (**41**) as an important bifunctional precursor. In fact, this route was so successful compared to the tortuous ring closure techniques described previously, that the members of **series IIIa-d** were prepared in this manner as generalised in **scheme 3a** (p. 128).

The Suzuki coupling¹⁰⁸ is an important method for aromatic carbon-carbon bond formation as it employs readily accessible substrates and proceeds under mild conditions. In addition, the Suzuki coupling tolerates a wide range of functionalities and is generally high yielding. In order to synthesise the required three-ring pyrimidine compounds, two Suzuki couplings were carried out: an initial cross-coupling with (**41**) at the more



- i. Br_2 , water.
 ii. $\text{POCl}_3/N,N$ -dimethylaniline.
 iii. HI , DCM .
 iv. & vi. a. $1.6\text{M } n\text{-BuLi}$, -78°C , THF .
 b. Trimethyl borate, -78°C .
 c. 4M HCl , 20°C .
 v. Compound (41), $\text{Pd}(\text{PPh}_3)_4$,
 DME , $\text{aq. Na}_2\text{CO}_3$, reflux.
 vii. $\text{Pd}(\text{PPh}_3)_4$, DME ,
 $\text{aq. Na}_2\text{CO}_3$, reflux.

Scheme 3



i. $\text{C}_n\text{H}_{2n+1}\text{Br}$, K_2CO_3 , acetone, reflux.

ii & vi. a. 1.6M *n*-BuLi, -78°C, THF.
 b. Trimethyl borate, -78°C.
 c. 4M HCl, 20°C.

iii. Compound (41), $\text{Pd}(\text{PPh}_3)_4$, DME, aq. Na_2CO_3 , reflux.

iv. a. 1.6M *n*-BuLi, -78°C, THF.

b. $\text{C}_n\text{H}_{2n+1}\text{CHO}$, -78°C, THF.

c. NH_4Cl , 20°C.

v. a. P_2O_5 , hexane.

b. 5% Pd/C, H_2 , EtOH.

vii. $\text{Pd}(\text{PPh}_3)_4$, DME, aq. Na_2CO_3 , reflux.

Scheme 3a

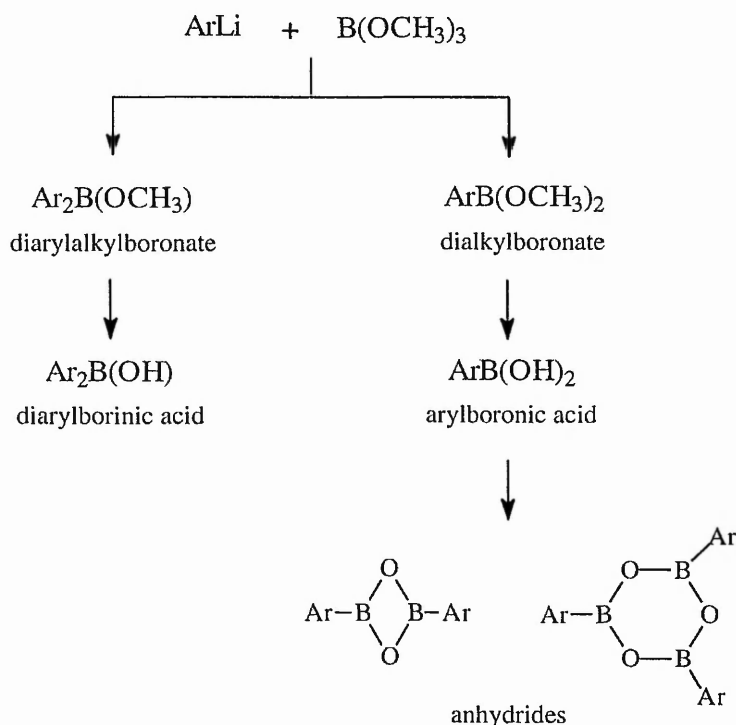
reactive iodo-position to give the desired two-ring intermediates (**43**; **47a-c**) followed by a second cross-coupling at the bromo-position to give the desired three-ring pyrimidines, i.e., members of series **IIIa-d**. It is important to emphasise that although two coupling reactions are required for each material synthesised this methodology is much more favourable and convenient than the original cyclisation-condensation method as the latter is tedious and gives poor yields.

Unactivated pyrimidines are very resistant to electrophilic aromatic substitution but the pyrimidine core may, however, be activated towards electrophilic attack by employing pyrimidones.¹⁰⁹ Therefore, commercial 2-hydroxypyrimidine, which exists exclusively in its tautomeric form as 2-pyrimidone, was readily brominated via electrophilic aromatic substitution using elemental bromine to afford the desired 5-bromo-2-hydroxypyrimidine (**39**). This reaction was carried out in water as this tends to increase the rate of reaction.¹¹⁰ Subsequently, chlorination of (**39**) was effected at the 2-position via nucleophilic aromatic substitution utilising phosphorous oxychloride to give the intermediate 5-bromo-2-chloropyrimidine (**40**).¹¹¹ Iodination of (**40**) using 57% hydriodic acid gave the desired 5-bromo-2-iodopyrimidine (**41**) in high yield (79%).

Once the desired 5-bromo-2-iodopyrimidine intermediate (**41**) had been successfully synthesised the next stage was to prepare the appropriate boronic acids required for palladium catalysed cross-coupling or 'Suzuki coupling'. The appropriate 4-*n*-alkoxybromobenzenes (**24**; **45a-c**) were prepared from commercial 4-bromophenol via the Williamson's ether synthesis as discussed earlier on p. 109. The required 4-*n*-alkoxyphenylboronic acids (**42**; **46a-c**) were then synthesised in excellent yield (76-100%) via low temperature lithiation (-78°C, 1.6M *n*-BuLi) at the bromo-position

of compounds (24; 45a-c) followed by treatment of the lithiated complex with trimethyl borate and subsequent acid (4M HCl) hydrolysis.

Although the formation of boronic acids is relatively straightforward, sometimes unwanted side-reactions can occur as shown below. The formation of borinic acids¹¹² is undesirable since, unlike boronic acids, they are inert to the Suzuki cross-coupling reaction. However, borinic acids may be easily removed by washing the crude boronic

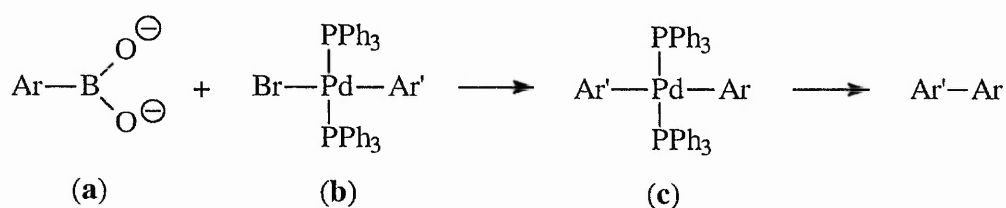


acid with hot petroleum ether. The borinic acid is readily soluble whereas the boronic acid is insoluble and can be isolated by filtration.

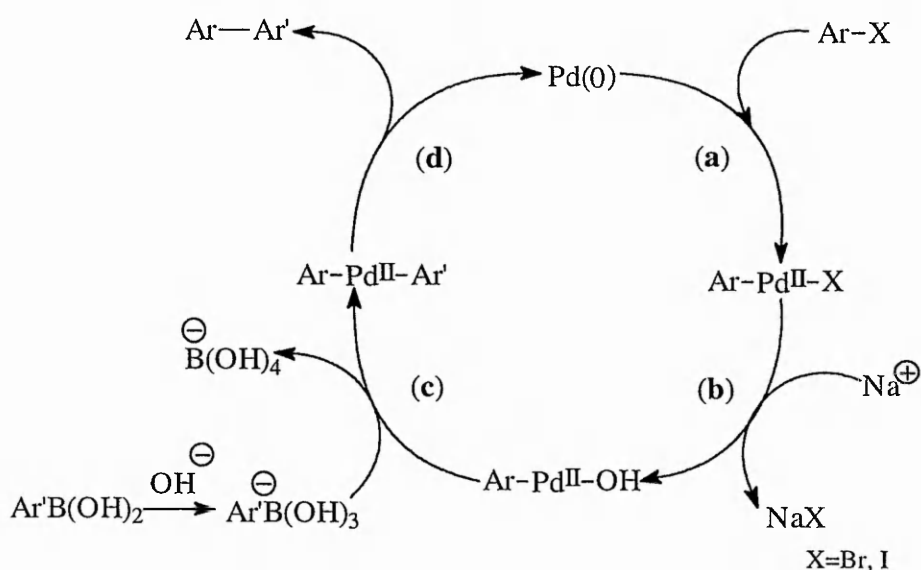
Boronic acids may also exist as various structures which include the monomeric, (ArB(OH)₂), and di- and tri-meric anhydrides. Hence, the m.p.s of boronic acids are not always reproducible and ¹H n.m.r. and i.r. spectroscopic data do not always show the presence of the hydroxyl group. Fortunately, the anhydride forms are equally as

reactive¹¹³ in cross-coupling reactions as the monomeric form.

Following the syntheses of the appropriate 4-*n*-alkoxyphenylboronic acids (**42**; **46a-c**) the appropriate two-ring phenylpyrimidine intermediates (**43**; **47a-c**) were prepared via palladium catalysed boronic acid cross-coupling methodology. The mechanism of boronic acid cross-coupling is rather vague but Thompson and Gaudino¹¹⁴ have proposed that the arylboronate dianion (**a**) appears to be the reactive organometallic intermediate which attacks the arylpalladium bromide complex (**b**) to form the diarylpalladium complex (**c**) during the reaction.

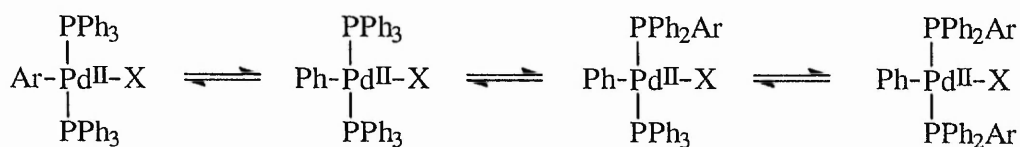


Recently, Martin and Yang¹¹⁵ have suggested the following catalytic cycle for the Suzuki coupling. The cycle involves the oxidative addition of the palladium(0)



complex to organic halides (ArX) (**a**), followed by transmetalation of the resulting complex to give the hydroxopalladium(II) complex (**b**). Subsequently, this complex reacts with an arylborane to give the biaryl organopalladium complex (**c**). The tetrahedral anion $\text{Ar}'\text{B}(\text{OH})_3^-$ in step (**c**) has been shown to be the more reactive species as opposed to the neutral boronic acid $\text{Ar}'\text{B}(\text{OH})_2$.¹¹⁶ Upon reductive elimination of the intermediate (**d**) the desired biaryl Ar-Ar' is formed and the catalyst is regenerated.

Two-ring phenyl pyrimidine intermediates (**43**; **47a-c**) were isolated generally in good yield (67-75%). The desired three-ring pyrimidines (**series IIIa-d**) were synthesised following a second Suzuki coupling with the appropriate 4-*n*-alkyl-2,3-difluorophenylboronic acid (**44** and **50a-d**). Occasionally, low yields were obtained and this may be due to the phenomenon of *aryl scrambling* reported by Segelstein *et al.*¹¹⁷ in palladium(0) catalysed cross-coupling reactions involving electron rich aryl halides. This phenomenon occurs when there is a significant amount of aryl-aryl exchange between the phenyl groups on the phosphine ligand with the oxidative intermediate of the aryl halide-palladium complex. In addition, Kong and Cheng¹¹⁸ ascertained that an equilibrium exists between the species as shown below and also that electron donating substituents, such as alkoxy ethers, on the boronic acid species promote the tendency



for migration. Alternatively, low yields may be due to proto-deboronation¹¹⁹ of the 4-*n*-alkyl-2,3-difluorophenylboronic acid (**44** and **50a-d**) in the presence of 2M aqueous

sodium carbonate solution to give the corresponding 4-*n*-alkyl-2,3-difluorobenzenes (e.g. **31** and **49a-d**).

Recently, Huff *et al.*¹²⁰ have reported modifications to the Suzuki cross-coupling reaction which may lead to an increase in yield. Firstly, catalytic amounts of palladium acetate and triphenylphosphine are added to the reaction vessel to generate palladium(0) *in situ* thus eliminating the need for *tetrakis*(triphenylphosphine)palladium(0) which is expensive and also air and light sensitive. Secondly, water miscible propanol, which allows the reaction mixture to remain homogeneous in the presence of aqueous base, is employed as an alternative solvent. In addition, Goodson *et al.*¹²¹ have reported Suzuki coupling via a ligandless palladium catalyst which is said to impart the following advantages: firstly, to eliminate aryl-aryl exchange as discussed earlier and; secondly, to give a marked improvement in reaction efficiency which allows for shorter reaction times, milder conditions and greater catalytic turnover.

3.5.1.2.1 Boronic Acid Cross-coupling - Experimental Procedures

5-Bromo-2-hydroxypyrimidine (**39**) (scheme 3)

Bromine (133 g, 0.838 mol) was added, dropwise, to a stirred solution of commercial 2-hydroxypyrimidine hydrochloride (100 g, 0.755 mol) in water (400 ml) at room temperature. The solution was stirred for 1 h. and then the water and excess of bromine were removed *in vacuo* to give the intermediate 5-bromo-2-hydroxypyrimidine (**39**) as a pale yellow solid which was dried in a vacuum oven at 80°C. The crude pyrimidine was

not purified and was used directly in the next reaction.

5-Bromo-2-chloropyrimidine (**40**) (scheme 3)

Dry crude 5-bromo-2-hydroxypyrimidine (**39**) was added to a mixture of phosphorous oxychloride (1000 ml) and *N,N*-dimethylaniline (20 ml) and heated under reflux for 4 h. The reaction was then cooled and poured into ice (CARE: VIOLENT REACTION!). The crude product was extracted with diethyl ether (2 x 1000 ml), washed with saturated sodium hydrogen carbonate solution (1000 ml), water (1000 ml) and then dried (MgSO₄). The solvent was removed *in vacuo* and the crude residue was recrystallised from ethanol to furnish the pure 5-bromo-2-chloropyrimidine (**40**), 87.8 g (61%), m.p. 77-79°C (Lit.¹¹¹ m.p. 77-79°C), as a white crystalline solid.

¹H NMR (CDCl₃) δ: 8.7 (2H, s, ArH) ppm.

i.r. ν_{\max} (KBr): 3010, 1532, 1396, 1360, 1165, 1008, 759, 631 cm⁻¹.

5-Bromo-2-iodopyrimidine (**41**) (scheme 3)

Cold 57% hydriodic acid (112 ml, 0.5 mol) was added, dropwise, to a vigorously stirred, cooled (ice-bath) solution of 5-bromo-2-chloropyrimidine (**40**) (32.5 g, 0.17 mol) in DCM (100 ml). After the addition was complete, the reaction mixture was stirred vigorously for a further 5 h. at approximately 0°C. The reaction was then neutralised with solid potassium carbonate and the iodine generated during the reaction was removed by the addition of aqueous sodium metabisulfite solution. The organic layer was isolated and the aqueous layer was extracted with DCM (2 x 100 ml). The

combined organic extract was dried (Na_2CO_3) and the solvent was removed *in vacuo*. The crude residue was crystallised from light petroleum ether (b.p. 60-80°C) to give 5-bromo-2-iodopyrimidine (**41**), 38.3 g (79%), m.p. 101-102°C (Lit.¹⁰⁷ m.p. 101-102°C), as white needles.

$^1\text{H NMR}$ (CDCl_3) δ : 8.54 (2H, s, ArH) ppm.

i.r. ν_{max} (KBr): 3000, 1514, 1373, 1129, 1003, 747, 623 cm^{-1} .

4-*n*-Alkoxy-1-bromobenzenes (**24**), (**45a-c**) (scheme 3 and 3a)

The appropriate 4-*n*-alkoxy-1-bromobenzenes (**45a-c**) were prepared according to the method described previously on p. 114 for 4-*n*-hexyloxy-1-bromobenzene (**24**). Each homologue was purified by vacuum distillation (Claisen) to give the desired 4-*n*-alkoxy-1-bromobenzene (**45a-c**), (67-84%), as a clear liquid. B.p.s: $\text{C}_4\text{H}_9\text{O}$ (**45a**), 101-103°/1; $\text{C}_5\text{H}_{11}\text{O}$ (**45b**), 140-142°/5; $\text{C}_8\text{H}_{17}\text{O}$ (**45c**), 126-128°C/0.05 mmHg (Lit.⁶⁶ 145°C/0.1 mmHg).

4-*n*-Alkoxyphenylboronic acids (**42**), (**46a-c**) (scheme 3 and 3a)

In an atmosphere of dry nitrogen, 1.6M *n*-butyllithium (0.066 mol) was added, dropwise, to a stirred, cooled (-78°C) solution of the appropriate 4-*n*-alkoxy-1-bromobenzene (**24** or **45a-c**) (0.066 mol) in dry THF (100 ml). The reaction mixture was maintained under these conditions for 3 h. and then trimethyl borate (22.5 ml, 0.198 mol) was added, dropwise, at -78°C. The reaction mixture was allowed to warm to room temperature overnight then stirred for 1 h. with 4M HCl (200 ml). The crude

product was extracted with diethyl ether (2 x 100 ml) and the combined ethereal extracts were washed with water (2 x 100 ml) and dried (MgSO₄). The solvent was removed *in vacuo* to yield the appropriate 4-*n*-alkoxyphenylboronic acid (**42** or **46a-c**), (79-85%), as a white solid. The boronic acids were not purified and were used directly in the next stage of the synthesis.

The following spectroscopic data refer to 4-*n*-octyloxyphenylboronic acid (**46c**) and are typical of the series:

¹H NMR (CDCl₃) δ: 0.90-0.92 (3H, t, CH₃), 1.32-1.48 (10H, m, CH₂), 1.75-1.84 (2H, quint, CH₂), 4.00 (2H, t, CH₂O), 6.97-7.00 (2H, dd, ArH), 8.12-8.15 (2H, dd, ArH) ppm. No OH signal observed.

i.r. ν_{\max} (KBr): 3400-3200 (O-H str.), 2950, 2930, 2860, 1600, 1414, 1247, 834 cm⁻¹.

2-(4-*n*-Alkoxyphenyl)-5-bromopyrimidines (**43**), (**47a-c**) (scheme 3 and 3a)

In an atmosphere of nitrogen, a solution of the appropriate 4-*n*-alkoxyphenylboronic acid (**42** or **46a-c**) (0.034 mol) dissolved in 1,2-dimethoxyethane (20 ml) was added, dropwise, to a vigorously stirred mixture of 5-bromo-2-iodopyrimidine (**41**) (8.8g, 0.031 mol), *tetrakis*(triphenylphosphine)palladium (0.48 g, 0.00042 mol), 1,2-dimethoxyethane (50 ml) and 2M aqueous sodium carbonate (80 ml). The mixture was heated under reflux until no remaining starting material was detected (monitored by tlc) and then cooled. The organic layer was separated and the aqueous layer was extracted with ethyl acetate (2 x 80 ml). The combined organic extract was washed with brine (80 ml), dried (MgSO₄) and the solvent was removed *in vacuo*. The crude residue was

purified by flash chromatography on silica gel eluting with 0.5 : 9.5 ethyl acetate : light petroleum ether (b.p. 60-80°C) followed by recrystallisation from ethanol to give the appropriate 2-(4-*n*-alkoxyphenyl)-5-bromopyrimidine (**43** or **47a-c**), (33-75%), as white crystals. M.p.s: C₄H₉O (**47a**), 116-118°; C₅H₁₁O (**47b**), 102-103°; C₆H₁₃O (**43**), 91-92°; C₈H₁₇O (**47c**), 101-102°C.

The following spectroscopic data refer to 2-(4-*n*-octyloxyphenyl)-5-bromopyrimidine (**47c**) and are typical of the series:

¹H NMR (CDCl₃) δ: 0.91 (3H, t, CH₃), 1.20-1.35 (8H, m, CH₂), 1.50-1.53 (2H, quint, CH₂), 1.80-1.86 (2H, quint, CH₂), 4.00 (2H, t, CH₂O), 6.99 (2H, dd, ArH), 8.34 (2H, dd, ArH), 8.77 (2H, s, ArH) ppm.

i.r. ν_{max} (KBr): 2926, 2858, 1605, 1523, 1419, 1257, 1164, 1028, 790 cm⁻¹.

1-(2,3-Difluorophenyl)alkan-1-ols (**30**), (**48a-d**) (scheme 3a)

The 1-(2,3-difluorophenyl)alkan-1-ols (**30** and **48a-d**) were prepared according to the method described previously for 1-(2,3-difluorophenyl)heptan-1-ol (**30**) on p. 119. Each homologue was purified by vacuum distillation (Claisen) to give the desired 1-(2,3-difluorophenyl)alkan-1-ol (**48a-d**), (62-72%), as a clear liquid. B.p.s: C₄H₉CHOH (**48a**), 130-132°/0.05, (Lit.⁶⁶ 182-184°C/0.1 mmHg); C₅H₁₁CHOH (**48b**), 160-162°/0.1; C₇H₁₅CHOH (**48c**), 175-177°/0.05; C₈H₁₇CHOH (**48d**), 150-152°/0.3 mmHg (Lit.⁶⁶ 118-122°C/0.1 mmHg).

1,2-Difluoro-3-*n*-alkylbenzenes (**31**), (**49a-d**) (scheme 3 and 3a)

The appropriate 1,2-difluoro-3-*n*-alkylbenzenes (**31** and **49a-d**) were prepared according to the method described previously for 1,2-difluoro-3-*n*-heptylbenzene (**31**) on p. 120. Each homologue was purified by vacuum distillation (Claisen) to give the desired 1,2-difluoro-3-*n*-alkylbenzene (**49a-d**), (57-69%), as a colourless liquid. B.p.s: C₅H₁₁ (**49a**), 70-72°/1, (Lit.⁶⁶ 206-208°C); C₆H₁₃ (**49b**), 75-77°/0.1; C₈H₁₇ (**49c**), 114-116°/0.4; C₉H₁₉ (**49d**), 124-126°C/1 mmHg, (Lit.⁶⁶ 146-148°C/15 mmHg).

2,3-Difluoro-4-*n*-alkylphenylboronic acids (**44**), (**50a-d**) (scheme 3 and 3a)

The appropriate 2,3-difluoro-4-*n*-alkylphenylboronic acids (**44** and **50a-d**) were prepared according to the method described previously on p. 135 for 4-*n*-alkoxyphenylboronic acids (**42** and **46 a-c**). The solvent was removed *in vacuo* to yield the appropriate 2,3-difluoro-4-*n*-alkylphenylboronic acid (**44** and **50a-d**), (71-91%), as a white solid. The boronic acids were not purified and were used directly in the next stage.

2-(4-*n*-Alkoxyphenyl)-5-(2,3-difluoro-4-*n*-alkylphenyl)pyrimidines (**38a-e** (series **IIIc**), **51a-d** (series **IIIa**), **52a-d** (series **IIIb**) and **53** (series **III d**)) (scheme 3 and 3a)

In an atmosphere of nitrogen, a solution of the appropriate 2,3-difluoro-4-*n*-alkylphenylboronic acid (**44** or **50a-d**) (0.0035 mol) dissolved in 1,2-dimethoxyethane (20 ml) was added, dropwise, to a vigorously stirred mixture of 2-(4-*n*-alkoxyphenyl)-5-bromopyrimidine (**43** or **47a-c**) (0.0032 mol), *tetrakis*(triphenylphosphine)palladium

(0.68 g, 0.0006 mol), 1,2-dimethoxyethane (50 ml) and 2M aqueous sodium carbonate (80 ml). The mixture was heated under reflux until no remaining starting material was detected (monitored by tlc) and then cooled. The organic layer was separated and the aqueous layer was extracted with ethyl acetate (2 x 80 ml). The combined organic extract was washed with brine (80 ml), dried (MgSO₄) and the solvent was removed *in vacuo*. The crude residue was purified by flash chromatography on silica gel eluting with 0.5 : 9.5 ethyl acetate : light petroleum ether (b.p. 60-80°C) followed by recrystallisation from ethanol to furnish the appropriate 2-(4-*n*-alkoxyphenyl)-5-(2,3-difluoro-4-*n*-alkylphenyl)pyrimidine (**38a-e** (series **IIIc**), **51a-d** (series **IIIa**), **52a-d** (series **IIIb**) and **53** (series **III d**)), (48-62%), as white crystals.

The m.p.s and mesomorphic transition temperatures of series **IIIa-d** are listed in **Table 4** (p. 68) of the results and discussion section.

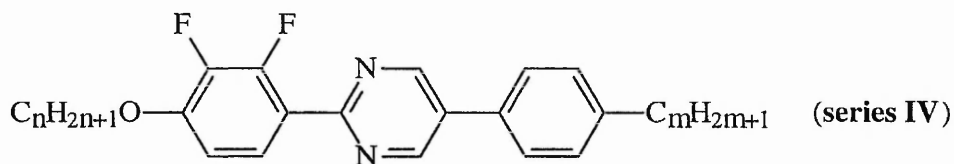
The following spectroscopic data refer to 2-(4-*n*-hexyloxyphenyl)-5-(2,3-difluoro-4-*n*-heptylphenyl)pyrimidine (**38c**) and are typical of the series:

Found: C, 74.78; H, 8.00; N, 6.12%. C₂₉H₃₆F₂N₂O requires C, 74.65; H, 7.78; N, 6.00%.

¹H NMR (CDCl₃) δ: 0.88-0.93 (3H, t, CH₃), 0.97-1.03 (3H, t, CH₃), 1.29-1.37 (14H, m, CH₂), 1.64-1.78 (2H, quint, CH₂), 1.81-1.86 (2H, quint, CH₂), 2.70-2.75 (2H, t, CH₂), 4.01-4.06 (2H, t, CH₂O), 6.98-7.03 (2H, dd, ArH), 7.03-7.18 (2H, m, ArH), 8.40-8.46 (2H, dd, ArH), 9.03 (2H, s, ArH) ppm.

i.r. ν_{max} (KBr): 2954, 2926, 2854, 1605, 1586, 1466, 1435, 1257, 1168, 1022, 798 cm⁻¹.

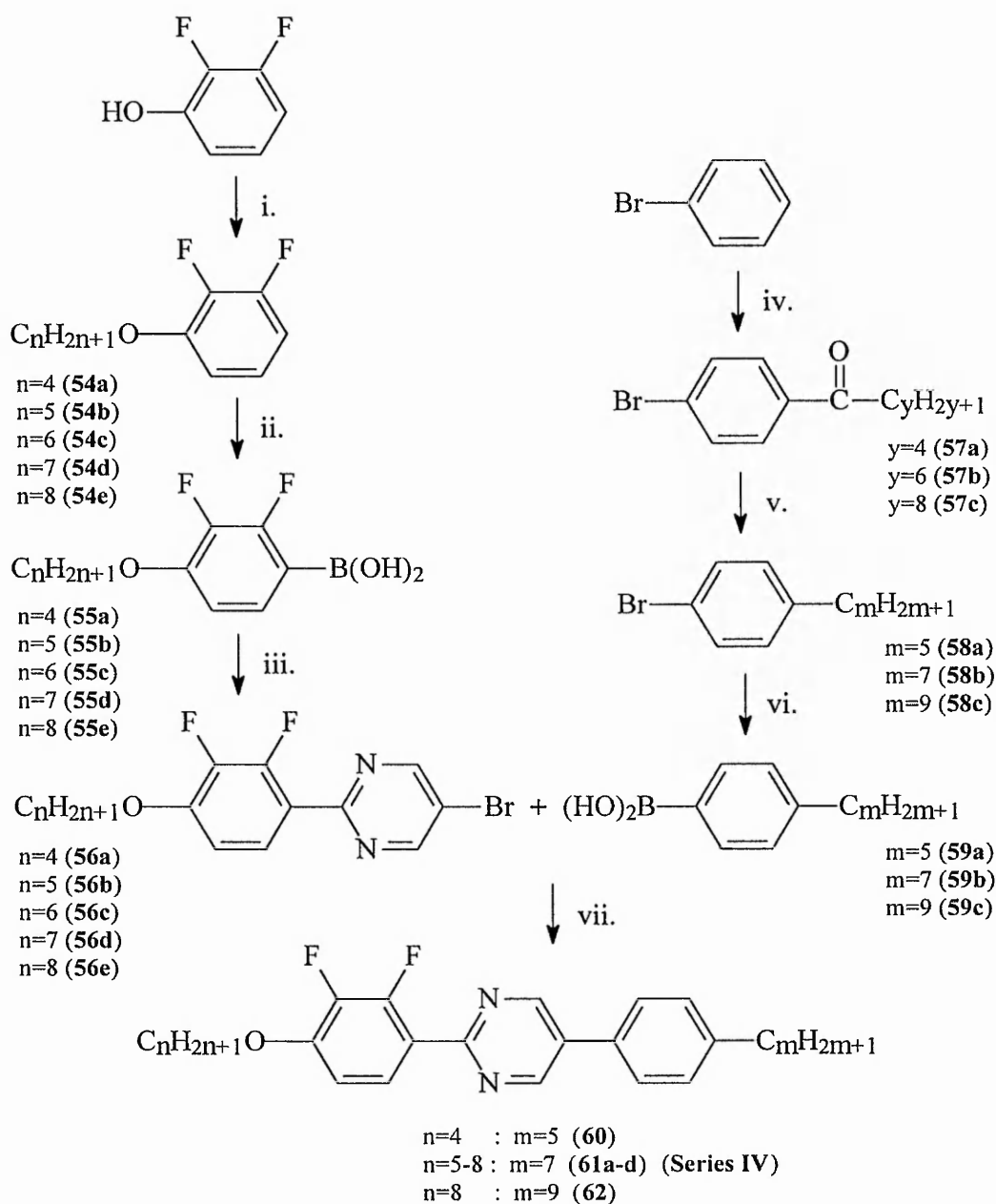
3.5.2 THE SYNTHESIS OF 2-(2,3-DIFLUORO-4-*n*-ALKOXYPHENYL)-5-(4-*n*-ALKYLPHENYL)PYRIMIDINES (series IV)



where $n=4$, $m=5$ (**60**); $n=5-8$, $m=7$ (**61a-d**) and; $n=8$, $m=9$ (**62**)

The members of **series IV**, i.e., the 2-(2,3-difluoro-4-*n*-alkoxyphenyl)-5-(4-*n*-alkylphenyl)pyrimidines, were synthesised as depicted in **scheme 4**, p. 141. Commercial 2,3-difluorophenol was *O*-alkylated with the appropriate 1-bromoalkane to give the alkoxy intermediates (**54a-e**) which in turn were *ortho*-lithiated to furnish the appropriate boronic acids (**55a-e**) in excellent yield (66-100%). Suzuki cross-coupling of (**55a-e**) with 5-bromo-2-iodopyrimidine (**41**) afforded the required two-ring pyrimidine intermediates (**56a-e**).

Friedel-Crafts acylation of commercial bromobenzene with the appropriate alkanoyl chloride using aluminium chloride as Lewis acid catalyst afforded the appropriate 4-*n*-alkanoyl-1-bromobenzenes (**57a-c**). Subsequent Wolff-Kishner reduction followed by low temperature lithiation and quenching with trimethyl borate afforded the necessary boronic acids (**59a-c**) which were, in turn, used in a second cross-coupling reaction with (**56a-e**) to furnish the desired 2-(2,3-difluoro-4-*n*-alkoxyphenyl)-5-(4-*n*-alkylphenyl)pyrimidines (**series IV**).



- i. $\text{C}_n\text{H}_{2n+1}\text{Br}$, K_2CO_3 , acetone, reflux.
- ii. & vi. a. 1.6M *n*-BuLi, -78°C , THF.
 b. Trimethyl borate, -78°C .
 c. 4M HCl.
- iii. Compound (41), $\text{Pd}(\text{PPh}_3)_4$, DME, aq. Na_2CO_3 , reflux.
- iv. a. $\text{C}_\gamma\text{H}_{2\gamma+1}\text{COCl}$, AlCl_3 , 80°C .
 b. 4M HCl, 20°C .
- v. $\text{NH}_2\text{NH}_2 \cdot \text{H}_2\text{O}$, KOH, digol, reflux.
- vii. $\text{Pd}(\text{PPh}_3)_4$, DME, aq. Na_2CO_3 , reflux.

Scheme 4

3.5.2.1 Experimental Procedures

1,2-Difluoro-3-*n*-alkoxybenzene (**54a-e**) (scheme 4)

Members of a series of 1,2-difluoro-3-*n*-alkoxybenzenes (**54a-e**) were prepared using a similar method to that described for 4-*n*-hexyloxy-1-bromobenzene (**24**) on p. 114. Each homologue was purified by vacuum distillation (Claisen) to give the desired 1,2-difluoro-3-*n*-alkoxybenzene (**54a-e**), (68-78%), as a clear liquid. B.p.s: C₄H₉O (**54a**), 70-72°/0.6; C₅H₁₁O (**54b**), 88-90°/0.1; C₆H₁₃O (**54c**), 80-82°/0.1, (Lit.⁶⁶ 122°C/15 mmHg); C₇H₁₅O (**54d**), 125-127°/3, (Lit.⁶⁶ 145°C/0.1 mmHg); C₈H₁₇O (**54e**), 135-137°C/2 mmHg (Lit.⁶⁶ 150°C/15 mmHg).

The following spectroscopic data refer to 1,2-difluoro-3-*n*-hexyloxybenzene (**54c**) and are typical of series:

¹H NMR (CDCl₃) δ: 0.88-0.94 (3H, t, CH₃), 1.26-1.38 (4H, m, CH₂), 1.40-1.51 (2H, quint, CH₂), 1.75-1.85 (2H, quint, CH₂), 3.98-4.03 (2H, t, CH₂O), 6.67-6.77 (2H, m, ArH), 6.89-6.99 (1H, m, ArH) ppm.

i.r. ν_{\max} (Thin film): 2932, 2860, 1620, 1514, 1480, 1253, 1076, 765 cm⁻¹.

1,2-Difluoro-3-*n*-alkoxyphenylboronic acids (**55a-e**) (scheme 4)

The appropriate 1,2-difluoro-3-*n*-alkoxyboronic acids (**55a-e**) were prepared according to the method described previously on p. 135 for 4-*n*-alkoxyphenylboronic acids (**42** and **46a-c**). The solvent was removed *in vacuo* to yield the appropriate 1,2-difluoro-3-*n*-alkoxyphenylboronic acid (**55a-e**), (66-100%), as a white solid. The boronic acids were not purified and were used directly in the next stage of the synthesis.

The following spectroscopic data refer to 2,3-difluoro-4-*n*-hexyloxyphenylboronic acid (**55c**) and are typical of series:

^1H NMR (CDCl_3) δ : 0.88-0.93 (3H, t, CH_3), 1.34-1.47 (6H, m, CH_2), 1.81-1.86 (2H, quint, CH_2), 4.05-4.10 (2H, t, CH_2O), 5.06 (2H, d, OH: disappears on D_2O shake), 6.78 (1H, t, ArH), 7.51 (1H, t, ArH) ppm.

i.r. ν_{max} (KBr): 3855-3330 (O-H str.), 2955, 2931, 2859, 1626, 1467, 1081, 789 cm^{-1} .

2-(2,3-Difluoro-4-*n*-alkoxyphenyl)-5-bromopyrimidines (**56a-e**) (scheme 4)

The 2-(2,3-difluoro-4-*n*-alkoxyphenyl)-5-bromopyrimidines (**56a-e**) were prepared according to the method described previously for 2-(4-*n*-alkoxyphenyl)-5-bromopyrimidine (**43** and **47a-c**) on p. 136. The crude residue was purified by flash chromatography on silica gel eluting with 0.5 : 9.5 ethyl acetate : light petroleum ether (b.p. 60-80°C) followed by recrystallisation from ethanol to give the appropriate 2-(2,3-difluoro-4-*n*-alkoxyphenyl)-5-bromopyrimidine (**56a-e**), (44-64%), as white crystals. M.p.s: $\text{C}_4\text{H}_9\text{O}$ (**56a**), 75-77°; $\text{C}_5\text{H}_{11}\text{O}$ (**56b**), 71-72°; $\text{C}_6\text{H}_{13}\text{O}$ (**56c**), 78-80°; $\text{C}_7\text{H}_{15}\text{O}$ (**56d**), 76-78°; $\text{C}_8\text{H}_{17}\text{O}$ (**56e**), 74-75°C.

The following spectroscopic data refer to 2-(2,3-difluoro-4-*n*-hexyloxyphenyl)-5-bromopyrimidine (**56c**) and are typical of the series:

^1H NMR (CDCl_3) δ : 0.91-0.93 (3H, t, CH_3), 1.33-1.37 (4H, m, CH_2), 1.41-1.49 (2H, quint, CH_2), 1.80-1.88 (2H, quint, CH_2), 4.08-4.13 (2H, t, CH_2O), 6.83 (1H, m, ArH), 7.83 (1H, m, ArH), 8.86 (2H, s, ArH) ppm.

i.r. ν_{\max} (KBr): 2945, 2867, 1626, 1535, 1420, 1305, 1080, 781 cm^{-1} .

4-*n*-Alkanoyl-1-bromobenzenes (**57a-c**) (scheme 4)

In an atmosphere of dry nitrogen, the appropriate alkanoyl chloride (0.382 mol) was added, dropwise, to a stirred, cooled (0°C) mixture of bromobenzene (170 ml) and anhydrous aluminium chloride (56 g, 0.42 mol). The mixture was stirred at 0°C for 1 h., heated at 80°C for 4 h., cooled to room temperature and then poured into 4M HCl. The crude residue was extracted with chloroform (2 x 200 ml) and the combined organic extract was washed with water and then steam distilled to remove chloroform and excess of bromobenzene. The crude material was again extracted with chloroform, washed with water (2 x 200 ml), dried (MgSO_4) and the solvent removed *in vacuo*. Purification was achieved by vacuum distillation (Claisen) to afford the appropriate pure 4-*n*-alkanoyl-1-bromobenzene (**57a-c**), (75-82%), as a clear liquid which solidified on standing. B.p.s: $\text{C}_4\text{H}_9\text{CO}$ (**57a**), $135-140^{\circ}/1$, (Lit.⁶⁶ $180-184^{\circ}\text{C}/20$ mmHg); $\text{C}_6\text{H}_{13}\text{CO}$ (**54b**), $134-138^{\circ}/0.2$, (Lit.⁶⁶ $130-135^{\circ}\text{C}/0.1$ mmHg); $\text{C}_8\text{H}_{17}\text{CO}$ (**54c**), $178-180^{\circ}\text{C}/0.5$ mmHg (Lit.⁶⁶ $138-140^{\circ}\text{C}/0.1$ mmHg).

The following spectroscopic data refer to 4-*n*-heptanoyl-1-bromobenzene (**57b**) and are typical of series:

^1H NMR (CDCl_3) δ : 0.87-0.91 (3H, t, CH_3), 1.33-1.37 (6H, m, CH_2), 1.69-1.72 (2H, quint, CH_2), 2.89-2.95 (2H, t, COCH_2), 7.57-7.61 (2H, dd, ArH), 7.80-7.83 (2H, dd, ArH), ppm.

i.r. ν_{\max} (KBr): 2924, 2853, 1686 ($\text{C}=\text{O}$ str.), 1564, 1456, 1305, 1004, 726 cm^{-1} .

4-*n*-Alkyl-1-bromobenzenes (**58a-c**) (scheme 4)

A mixture of the appropriate 4-*n*-alkanoyl-1-bromobenzene (**57a-c**) (0.12 mol), diethylene glycol (160 ml) and hydrazine hydrate (11.2 ml, 0.362 mol) was heated gently to reflux for 2 h. The excess of hydrazine hydrate was removed by distillation and the internal temperature was raised to 200°C. After cooling to room temperature, potassium hydroxide (20.4 g, 0.362 mol) was added and the reaction mixture was subsequently reheated to reflux for 4 h. The reaction was then quenched in 4M HCl/ice (200 ml), extracted with chloroform (3 x 100 ml), washed with water (2 x 100 ml), dried (MgSO₄) and the solvent removed *in vacuo*. The crude material was purified by vacuum distillation (Claisen) to furnish the appropriate pure 4-*n*-alkyl-1-bromobenzene (**58a-c**), (73-85%), as a clear liquid. B.p.s: C₅H₁₁ (**55a**), 109-111°/2, (Lit.⁶⁶ 145-148°C/20 mmHg); C₇H₁₅ (**55b**), 124-128°/1, (Lit.⁶⁶ 105-115°C/0.1 mmHg); C₉H₁₉ (**55c**), 138-140°C/1 mmHg (Lit.⁶⁶ 124-126°C/0.1 mmHg).

The following spectroscopic data refer to 4-*n*-heptyl-1-bromobenzene (**58b**) and are typical of series:

¹H NMR (CDCl₃) δ: 0.85-0.90 (3H, t, CH₃), 1.24-1.29 (8H, m, CH₂), 1.54-1.59 (2H, quint, CH₂), 2.50-2.56 (2H, t, CH₂), 7.00-7.03 (2H, dd, ArH), 7.34-7.38 (2H, dd, ArH), ppm.

i.r. ν_{max} (Thin film): 2955, 2926, 2855, 1488, 1011, 797 cm⁻¹.

4-*n*-Alkylphenylboronic acids (**59a-c**) (scheme 4)

The appropriate 4-*n*-alkylphenylboronic acids (**59a-c**) were prepared as previously described on p. 135 for the 4-*n*-alkoxyphenylboronic acids (**42** and **46 a-c**). The solvent

was removed *in vacuo* to yield the appropriate 4-*n*-alkylphenylboronic acid (**59a-c**) (73-79%), as a white solid. The boronic acids were not purified and were used directly in the next stage.

The following spectroscopic data refer to 4-*n*-heptylphenylboronic acid (**59b**) and are typical of series:

$^1\text{H NMR}$ (CDCl_3) δ : 0.85-0.94 (3H, t, CH_3), 1.27-1.31 (8H, m, CH_2), 1.61-1.65 (2H, quint, CH_2), 2.61-2.66 (2H, t, CH_2), 7.23-7.31 (2H, d, ArH), 8.11-8.14 (2H, d, ArH) ppm. No OH signal observed.

i.r. ν_{max} (KBr): 2955, 2927, 2856, 1609, 1407, 1344, 1181, 695 cm^{-1} .

2-(2,3-Difluoro-4-*n*-alkoxyphenyl)-5-(4-*n*-alkylphenyl)pyrimidines (**60**, **61a-d** and **62** (**series IV**)) (scheme 4)

The 2-(2,3-difluoro-4-*n*-alkoxyphenyl)-5-(4-*n*-alkylphenyl)pyrimidines (**series IV**) were prepared according to the method described for the 2-(4-*n*-alkoxyphenyl)-5-(2,3-difluoro-4-*n*-alkylphenyl)pyrimidines (**series IIIa-d**) on p. 138. The crude residue was purified by flash chromatography on silica gel eluting with 0.5 : 9.5 ethyl acetate : light petroleum ether (b.p. 60-80°C) followed by recrystallisation from ethanol to give the appropriate 2-(2,3-difluoro-4-*n*-alkoxyphenyl)-5-(4-*n*-alkylphenyl)pyrimidine (**60**, **61a-d** and **62** or **series IV**), (49-71%), as white crystals.

The m.p.s and mesomorphic transition temperatures of the members of **series IV** are listed in *Table 6* (p. 77) of the results and discussion section.

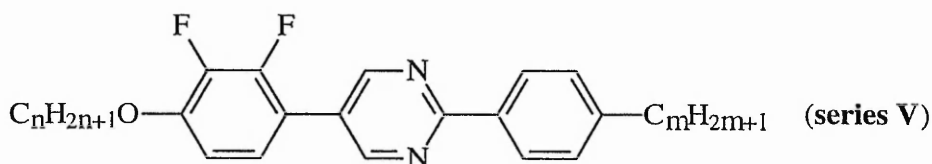
The following spectroscopic data refer to 2-(2,3-difluoro-4-*n*-butyloxyphenyl)-5-(4-*n*-pentylphenyl)pyrimidine (**60**) and are typical of the series:

Found: C, 73.38; H, 7.04; N, 6.90%. C₂₅H₂₈F₂N₂O requires C, 73.15; H, 6.87; N, 6.82%.

¹H NMR (CDCl₃) δ: 0.89-0.92 (6H, t, 2CH₃), 1.25-1.39 (4H, m, CH₂), 1.41-1.55 (2H, quint, CH₂), 1.63-1.69 (2H, quint, CH₂), 1.81-1.91 (2H, quint, CH₂), 2.65-2.70 (2H, t, CH₂), 4.10-4.18 (2H, t, CH₂O), 6.82-6.85 (1H, m, ArH), 7.33-7.38 (2H, dd, ArH), 7.53-7.56 (2H, dd, ArH), 7.86-7.93 (1H, m, ArH), 9.03 (2H, s, ArH) ppm.

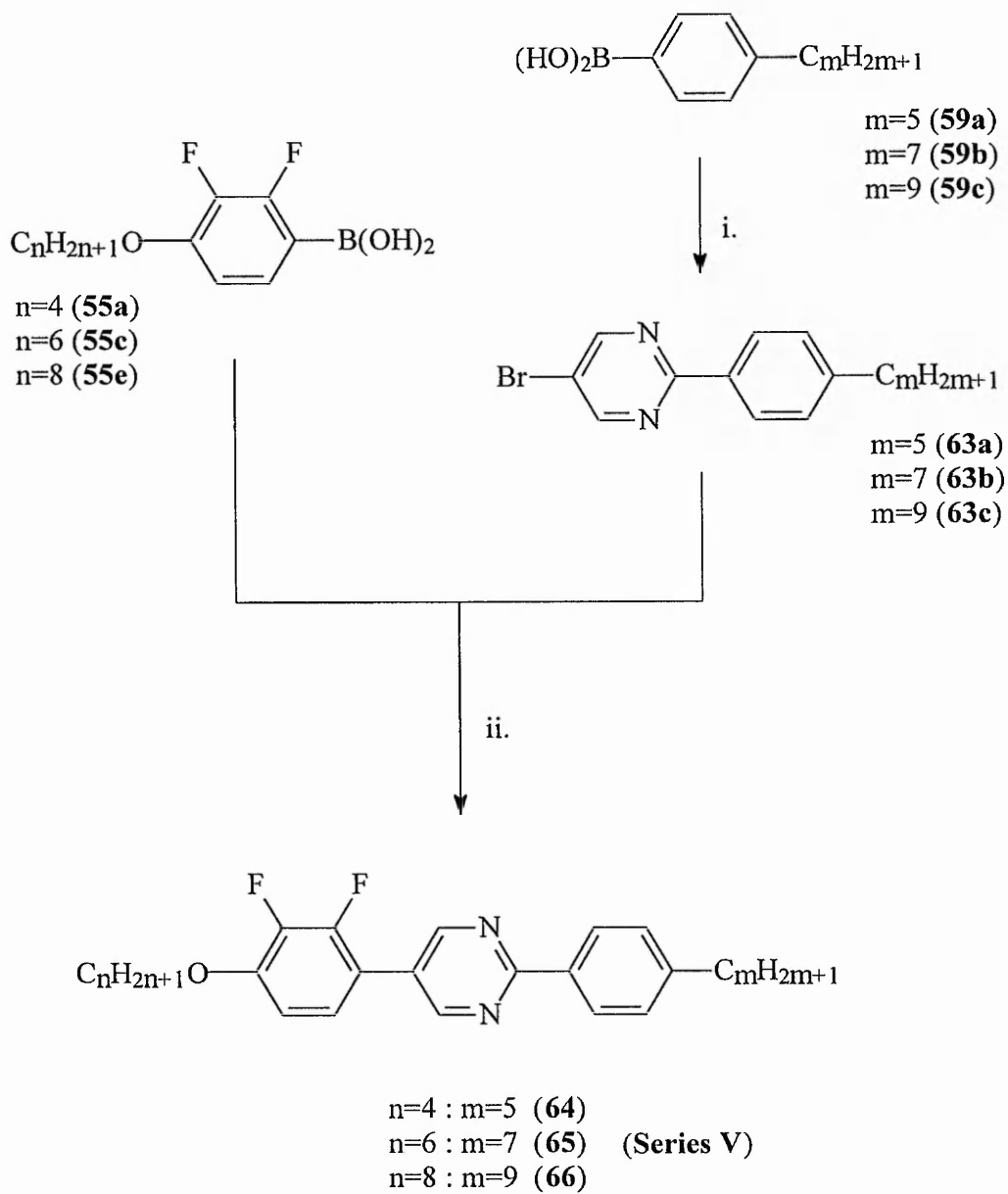
i.r. ν_{max} (KBr): 2954, 2926, 2854, 1628, 1537, 1435, 1300, 1205, 1085, 791 cm⁻¹.

3.5.3 THE SYNTHESIS OF 2-(4-*n*-ALKYLPHENYL)-5-(2,3-DIFLUORO-4-*n*-ALKOXYPHENYL)PYRIMIDINES (series V)



where n=4, m=5 (**64**); n=6, m=7 (**65**); and n=8, m=9 (**66**)

The 2-(4-*n*-alkylphenyl)-5-(2,3-difluoro-4-*n*-alkoxyphenyl)pyrimidines, i.e., members of **series V**, were synthesised with ease using the palladium catalysed cross-coupling methodology as shown in **scheme 5**, p. 148. Firstly, the appropriate 4-*n*-alkylphenylboronic acid (**59a-c**) was cross-coupled with 5-bromo-2-iodopyrimidine (**41**)



- i. Compound (**41**), $Pd(PPh_3)_4$, DME, aq. Na_2CO_3 , reflux.
 ii. $Pd(PPh_3)_4$, DME, aq. Na_2CO_3 , reflux.

Scheme 5

to furnish the two-ring pyrimidine intermediates (**63a-c**) which required a second cross-coupling with the appropriate 2,3-difluoro-4-*n*-alkoxyphenylboronic acid (**55a, c** and **e**) to afford the desired 2-(4-*n*-alkylphenyl)-5-(2,3-difluoro-4-*n*-alkoxyphenyl)pyrimidines (**64, 65** and **66**).

3.5.3.1 Experimental Procedures

2-(4-*n*-Alkylphenyl)-5-bromopyrimidines (**63a-c**) (scheme 5)

The appropriate 2-(4-*n*-alkylphenyl)-5-bromopyrimidines (**63a-c**) were prepared by the method previously described for the 2-(4-*n*-alkoxyphenyl)-5-bromopyrimidines (**43** and **47a-c**) on p. 136. The crude residue was purified by flash chromatography on silica gel eluting with 0.5 : 9.5 ethyl acetate : light petroleum ether (b.p. 60-80°C) followed by recrystallisation from ethanol to give the appropriate 2-(4-*n*-alkylphenyl)-5-bromopyrimidine (**63a-c**), (52-80%), as white crystals. M.p.s: C₅H₁₁ (**63a**), 83-85°; C₇H₁₅ (**63b**), 72-74°; C₉H₁₉ (**63c**), 77-79°C.

The following spectroscopic data refer to 2-(4-*n*-heptylphenyl)-5-bromopyrimidine (**63b**) and are typical of the series:

¹H NMR (CDCl₃) δ: 0.85-0.88 (3H, t, CH₃), 1.28-1.33 (8H, m, CH₂), 1.62-1.65 (2H, quint, CH₂), 2.64-2.70 (2H, t, CH₂), 7.26-7.31 (2H, dd, ArH), 8.29-8.32 (2H, dd, ArH), 8.80 (2H, s, ArH) ppm.

i.r. ν_{\max} (KBr): 2949, 2920, 2848, 1608, 1534, 1428, 1376, 1130, 785 cm⁻¹.

2-(4-*n*-Alkylphenyl)-5-(2,3-difluoro-4-*n*-alkoxyphenyl)pyrimidines (**64-66** or **series V**) (scheme 5)

The 2-(4-*n*-alkylphenyl)-5-(2,3-difluoro-4-*n*-alkoxyphenyl)pyrimidines (**series V**) were prepared in the manner previously described for the 2-(4-*n*-alkoxyphenyl)-5-(2,3-difluoro-4-*n*-alkylphenyl)pyrimidines (**series IIIa-d**) on p. 138. The crude residue was purified by flash chromatography on silica gel eluting with 0.5 : 9.5 ethyl acetate : light petroleum ether (b.p. 60-80°C) followed by recrystallisation from ethanol to give the appropriate 2-(4-*n*-alkylphenyl)-5-(2,3-difluoro-4-*n*-alkoxyphenyl)pyrimidine (**64-66** or **series V**), (50-61%), as white crystals.

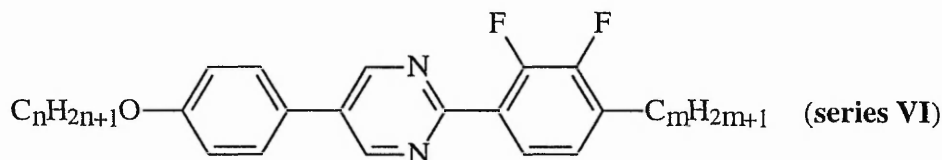
The m.p.s and mesomorphic transition temperatures of **series V** are listed in *Table 8* (p. 80) of the results and discussion section.

The following spectroscopic data refer to 2-(4-*n*-heptylphenyl)-5-(2,3-difluoro-4-*n*-hexyloxyphenyl)pyrimidine (**65**) and are typical of the series:

¹H NMR (CDCl₃) δ: 0.86-0.94 (6H, t, 2CH₃), 1.28-1.39 (12H, m, CH₂), 1.44-1.52 (2H, quint, CH₂), 1.60-1.67 (2H, quint, CH₂), 1.83-1.89 (2H, quint, CH₂), 2.66-2.71 (2H, t, CH₂), 4.08-4.13 (2H, t, CH₂O), 6.84-6.87 (1H, m, ArH), 7.12-7.19 (1H, m, ArH), 7.31-7.34 (2H, dd, ArH), 8.37-8.40 (2H, dd, ArH), 8.93 (2H, s, ArH) ppm.

i.r. ν_{max} (KBr): 2954, 2925, 2854, 1629, 1483, 1438, 1301, 1084, 791 cm⁻¹.

3.5.4 THE SYNTHESIS OF 2-(2,3-DIFLUORO-4-*n*-ALKYLPHENYL)-5-(4-*n*-ALKOXYPHENYL)PYRIMIDINES (series VI)



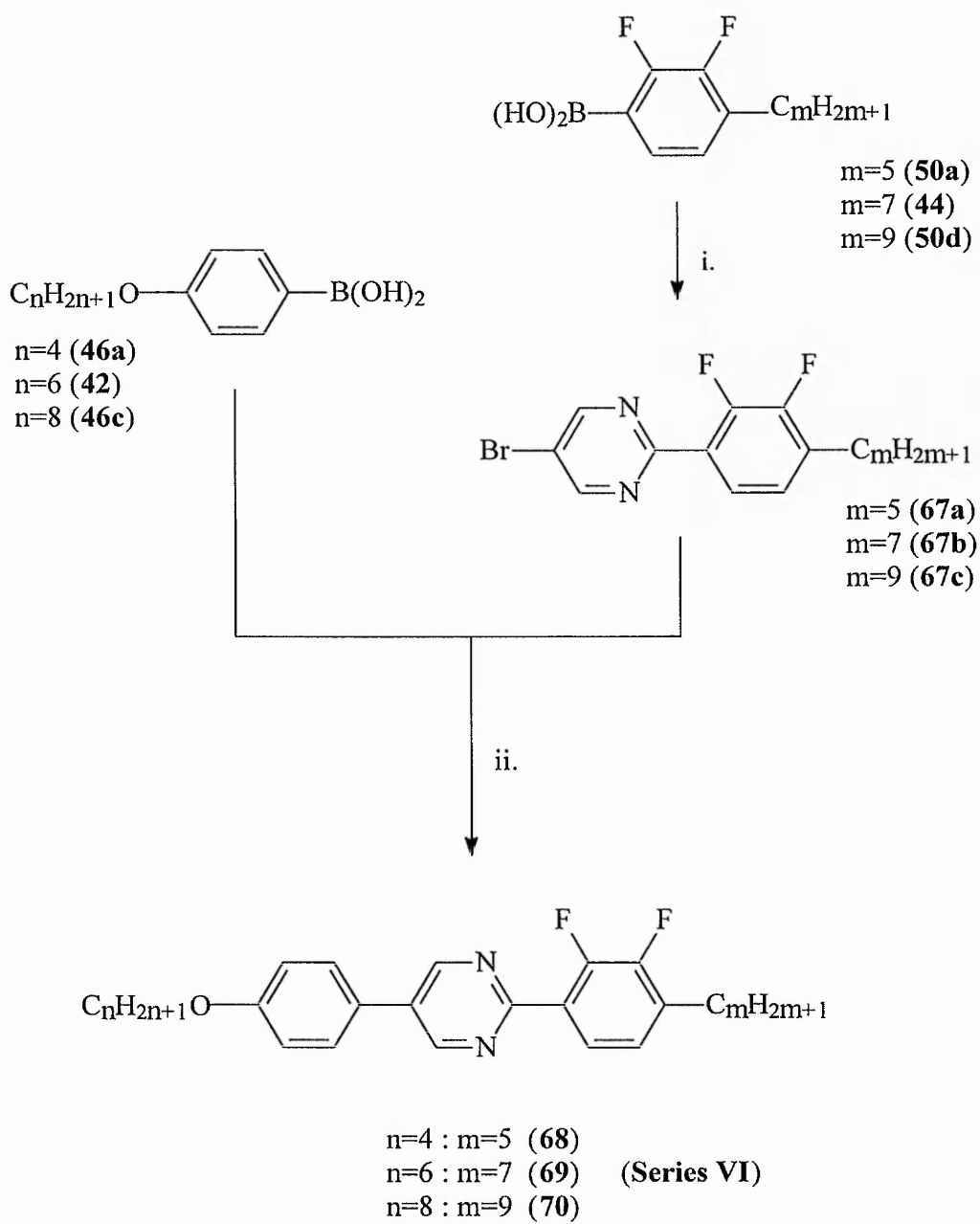
where $n=4$ $m=5$ (**68**); $n=6$ $m=7$ (**69**); $n=8$, $m=9$ (**70**)

The members of **series VI**, i.e., 2-(2,3-difluoro-4-*n*-alkylphenyl)-5-(4-*n*-alkoxyphenyl)pyrimidines, were prepared as shown in **scheme 6** (p. 152). Initially, the boronic acid intermediates (**44**; **50a** and **d**) were coupled with 5-bromo-2-iodopyrimidine (**41**) to give intermediates (**67a-c**) and subsequently, a further coupling reaction with the appropriate boronic acid (**42**; **46a** and **c**) gave the desired 2-(2,3-difluoro-4-*n*-alkylphenyl)-5-(4-*n*-alkoxyphenyl)pyrimidines (**68**, **69** and **70**).

3.5.4.1 Experimental Procedures

2-(2,3-Difluoro-4-*n*-alkylphenyl)-5-bromopyrimidines (**67a-c**) (scheme 6)

The appropriate 2-(2,3-difluoro-4-*n*-alkylphenyl)-5-bromopyrimidines (**67a-c**) were prepared according to the method described previously on p. 136 for 2-(4-*n*-alkoxyphenyl)-5-bromopyrimidines (**43** and **47a-c**). The crude residue was purified by flash chromatography on silica gel eluting with 0.5 : 9.5 ethyl acetate : light petroleum ether (b.p. 60-80°C) followed by recrystallisation from ethanol to furnish the appropriate 2-(2,3-difluoro-4-*n*-alkylphenyl)-5-bromopyrimidine (**67a-c**), (45-60%), as white crystals.



- i. Compound (**41**), $\text{Pd}(\text{PPh}_3)_4$, DME, aq. Na_2CO_3 , reflux.
 ii. $\text{Pd}(\text{PPh}_3)_4$, DME, aq. Na_2CO_3 , reflux.

Scheme 6

The following spectroscopic data refer to 2-(2,3-difluoro-4-*n*-heptylphenyl)-5-bromopyrimidine (**67b**) and are typical of the series:

$^1\text{H NMR}$ (CDCl_3) δ : 0.86-0.91 (3H, t, CH_3), 1.25-1.48 (8H, m, CH_2), 1.60-1.67 (2H, quint, CH_2), 2.71-2.75 (2H, t, CH_2), 7.02-7.08 (1H, m, ArH), 7.72-7.78 (1H, m, ArH), 8.90 (2H, s, ArH) ppm.

i.r. ν_{max} (KBr): 2957, 2921, 2853, 1630, 1531, 1482, 1426, 1374, 902, 785 cm^{-1} .

2-(2,3-Difluoro-4-*n*-alkylphenyl)-5-(4-*n*-alkoxyphenyl)pyrimidines (**68-70** or series **VI**) (scheme 6)

The 2-(2,3-difluoro-4-*n*-alkylphenyl)-5-(4-*n*-alkoxyphenyl)pyrimidines (series **VI**) were prepared according to the method described previously on p. 138 for 2-(4-*n*-alkoxyphenyl)-5-(2,3-difluoro-4-*n*-alkylphenyl)pyrimidines (series **IIIa-d**). The crude residue was purified by flash chromatography on silica gel eluting with 0.5 : 9.5 ethyl acetate : light petroleum ether (b.p. 60-80°C followed by recrystallisation from ethanol affording the appropriate 2-(2,3-difluoro-4-*n*-alkylphenyl)-5-(4-*n*-alkoxyphenyl)pyrimidine (**68-70** or series **VI**), (65-80%), as white crystals.

The m.p.s and mesomorphic transition temperatures of series **VI** are listed in *Table 9* (p. 82) of the results and discussion section.

The following spectroscopic data refer to 2-(2,3-difluoro-4-*n*-pentylphenyl)-5-(4-*n*-butyloxyphenyl)pyrimidine (**68**) and are typical of the series:

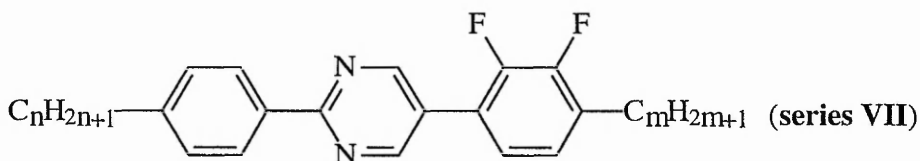
Found: C, 73.21; H, 70.2; N, 6.90%. $\text{C}_{25}\text{H}_{28}\text{F}_2\text{N}_2\text{O}$ requires C, 73.15; H, 6.87; N, 6.82%.

$^1\text{H NMR}$ (CDCl_3) δ : 0.86-0.94 (6H, t, 2CH_3), 1.29-1.39 (4H, m, CH_2), 1.41-1.54 (2H, quint, CH_2), 1.60-1.77 (2H, quint, CH_2), 1.79-1.87 (2H, quint, CH_2), 2.70-2.75 (2H, t,

CH₂), 4.00-4.05 (2H, t, CH₂O), 7.02-7.09 (3H, m, dd, ArH), 7.54-7.59 (2H, dd, ArH), 7.77-7.83 (1H, m, ArH), 9.03 (2H, s, ArH) ppm.

i.r. ν_{max} (KBr): 2954, 2923, 2853, 1608, 1464, 1436, 1252, 831 cm⁻¹.

3.5.5 THE SYNTHESIS OF 2-(4-*n*-ALKYLPHENYL)-5-(2,3-DIFLUORO-4-*n*-ALKYLPHENYL)PYRIMIDINES (series VII)



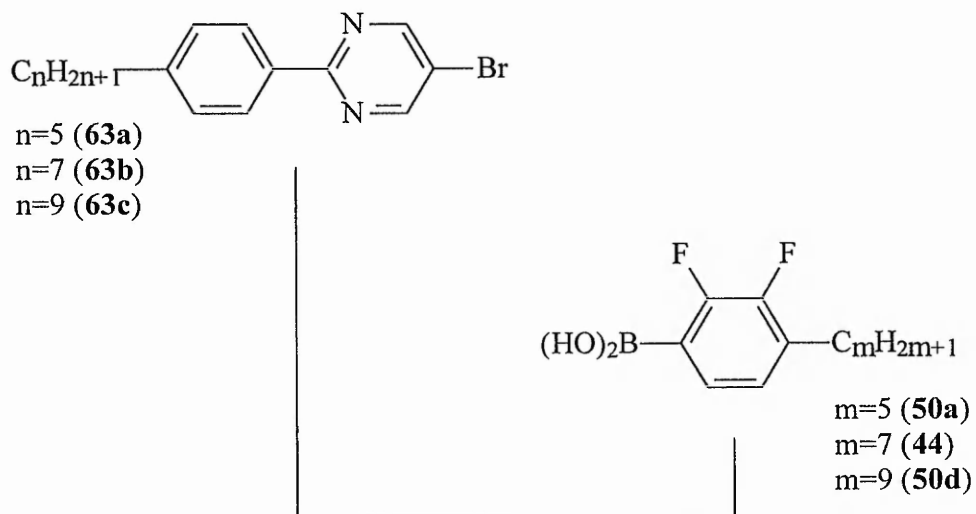
where $n=5, m=5$ (**71**); $n=7, m=7$ (**72**); $n=9, m=9$ (**73**)

The 2-(4-*n*-alkylphenyl)-5-(2,3-difluoro-4-*n*-alkylphenyl)pyrimidines, i.e., members of **series VII**, were synthesised using the previously prepared precursors (**44**; **50a** and **d**) and (**63a-c**) via a single cross-coupling reaction as shown in **scheme 7**, p.155.

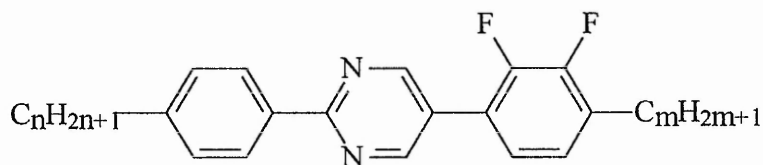
3.5.5.1 Experimental Procedures

2-(4-*n*-Alkylphenyl)-5-(2,3-difluoro-4-*n*-alkylphenyl)pyrimidines (**71-73** or **series VII**) (scheme 7)

The 2-(4-*n*-alkylphenyl)-5-(2,3-difluoro-4-*n*-alkylphenyl)pyrimidines (**series VII**) were prepared according to the method described earlier on p. 138 for 2-(4-*n*-alkoxyphenyl)-5-(2,3-difluoro-4-*n*-alkylphenyl)pyrimidines (**series IIIa-d**). The crude residue was purified by flash chromatography on silica gel eluting with 0.5 : 9.5 ethyl acetate : light



i.



n=5 : m=5 (**71**)
 n=7 : m=7 (**72**) (**Series VII**)
 n=9 : m=9 (**73**)

i. Pd(PPh₃)₄, DME, aq. Na₂CO₃, reflux.

Scheme 7

petroleum ether (b.p. 60-80°C) followed by recrystallisation from ethanol to give the appropriate 2-(4-*n*-alkylphenyl)-5-(2,3-difluoro-4-*n*-alkylphenyl)pyrimidine (**71-73** or **series VII**), (41-58%), as white crystals.

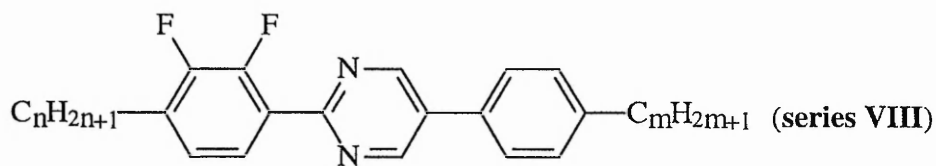
The m.p.s and mesomorphic transition temperatures of **series VII** are listed in *Table 10* (p. 85) of the results and discussion section.

The following spectroscopic data refer to 2-(4-*n*-heptylphenyl)-5-(2,3-difluoro-4-*n*-heptylphenyl)pyrimidine (**72**) and are typical of the series:

¹H NMR (CDCl₃) δ: 0.82-0.99 (6H, t, 2CH₃), 1.25-1.34 (16H, m, CH₂), 1.64-1.66 (4H, quint, 2CH₂), 2.63-2.78 (4H, t, 2CH₂), 7.05-7.19 (2H, m, ArH), 7.31-7.34 (2H, dd, ArH), 8.36-8.41 (2H, dd, ArH), 8.96 (2H, s, ArH) ppm.

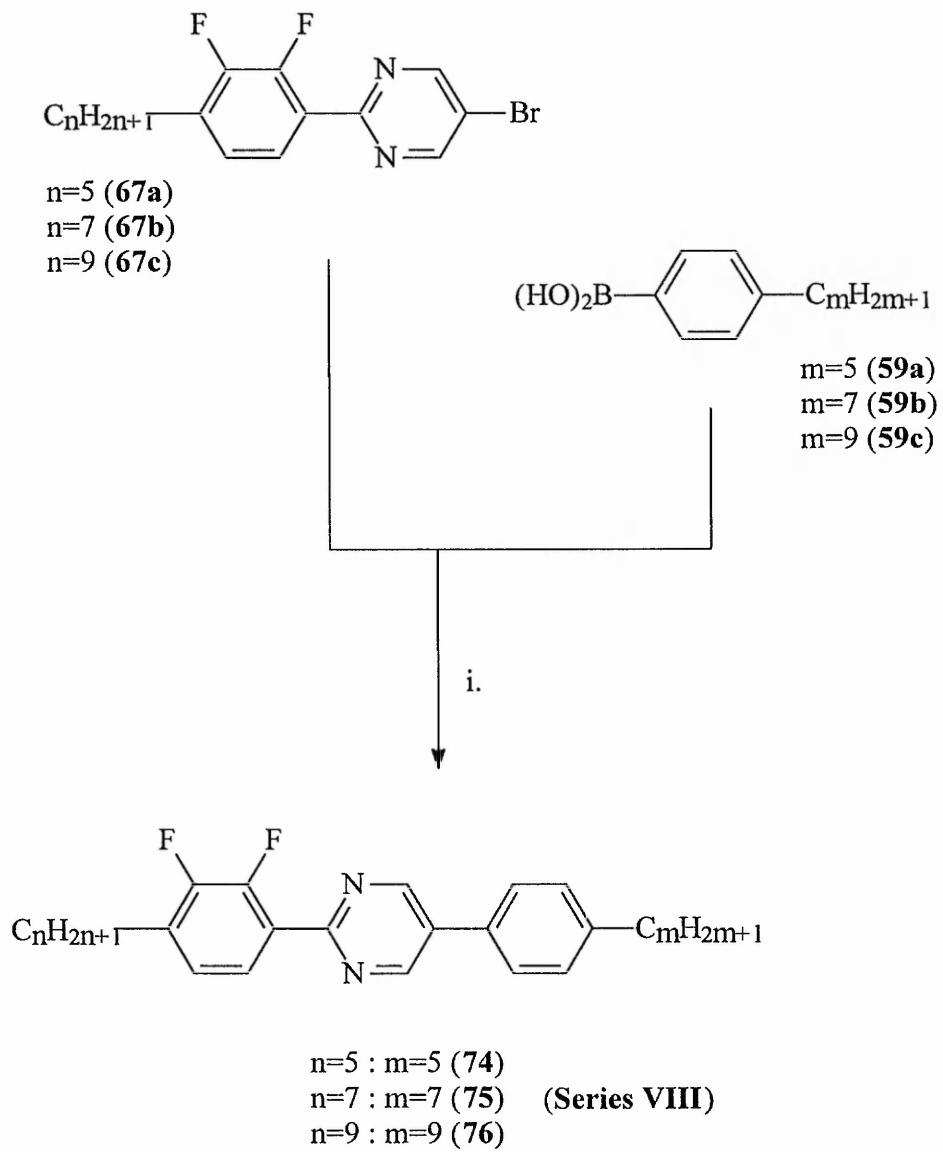
i.r. ν_{max} (KBr): 2954, 2925, 2853, 1583, 1468, 1438, 1377, 893, 792 cm⁻¹.

3.5.6 THE SYNTHESIS OF 2-(2,3-DIFLUORO-4-*n*-ALKYLPHENYL)-5-(4-*n*-ALKYLPHENYL)PYRIMIDINES (**series VIII**)



where $n=5$, $m=5$ (**74**); $n=7$, $m=7$ (**75**); $n=9$, $m=9$ (**76**)

The members of **series VIII**, i.e., 2-(2,3-difluoro-4-*n*-alkylphenyl)-5-(4-*n*-alkylphenyl)pyrimidines, were synthesised by Suzuki coupling of the appropriate two-ring 5-bromopyrimidine compounds (**67a-c**) and the appropriate single-ring boronic acid intermediate (**59a-c**) as shown in **scheme 8**, p. 157.



i. Pd(PPh₃)₄, DME, aq. Na₂CO₃, reflux.

Scheme 8

3.5.6.1 Experimental Procedures

2-(2,3-Difluoro-4-*n*-alkylphenyl)-5-(4-*n*-alkylphenyl)pyrimidines (**74-76** or **series VIII**) (scheme 8)

The 2-(2,3-difluoro-4-*n*-alkylphenyl)-5-(4-*n*-alkylphenyl)pyrimidines (**series VIII**) were prepared as previously described for the 2-(4-*n*-alkoxyphenyl)-5-(2,3-difluoro-4-*n*-alkylphenyl)pyrimidines (**series IIIa-d**) on p. 138. The crude residue was purified by flash chromatography on silica gel eluting with 0.5 : 9.5 ethyl acetate : light petroleum ether (b.p. 60-80°C) followed by recrystallisation from ethanol to give the appropriate 2-(2,3-difluoro-4-*n*-alkylphenyl)-5-(4-*n*-alkylphenyl)pyrimidine (**74-76** or **series VIII**), (47-49%), as white crystals.

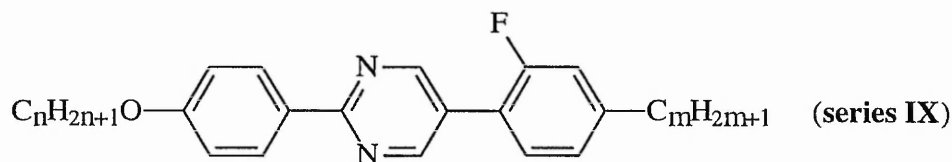
The m.p.s and mesomorphic transition temperatures of **series VIII** are listed in *Table 11* (p. 87) of the results and discussion section.

The following spectroscopic data refer to 2-(2,3-difluoro-4-*n*-heptylphenyl)-5-(4-*n*-heptylphenyl)pyrimidine (**75**) and are typical of the series:

$^1\text{H NMR}$ (CDCl_3) δ : 0.86-0.91 (6H, t, 2CH_3), 1.25-1.34 (16H, m, CH_2), 1.61-1.69 (4H, quint, 2CH_2), 2.65-2.75 (4H, t, 2CH_2), 7.03-7.10 (1H, m, ArH), 7.33-7.36 (2H, dd, ArH), 7.54-7.57 (2H, dd, ArH), 7.78-7.83 (1H, m, ArH), 9.06 (2H, s, ArH) ppm.

i.r. ν_{max} (KBr): 2954, 2922, 2852, 1534, 1466, 1435, 1375, 904, 799 cm^{-1} .

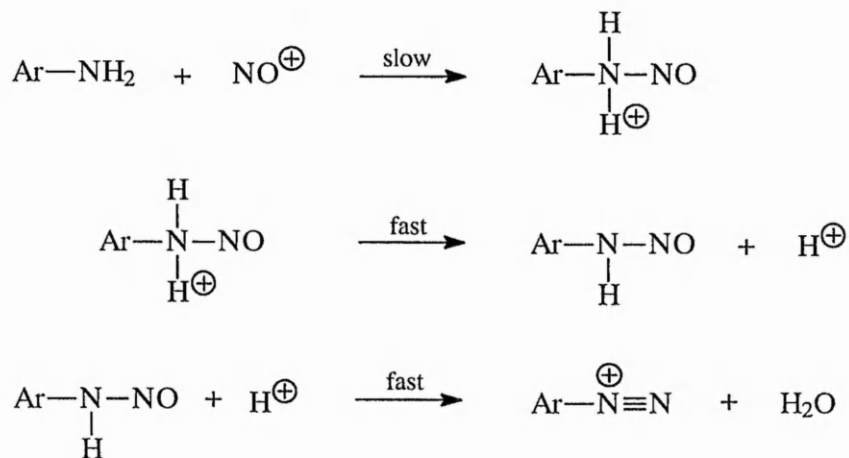
3.5.7 THE SYNTHESIS OF 2-(4-*n*-ALKOXYPHENYL)-5-(2-FLUORO-4-*n*-ALKYLPHENYL)PYRIMIDINES (series IX)

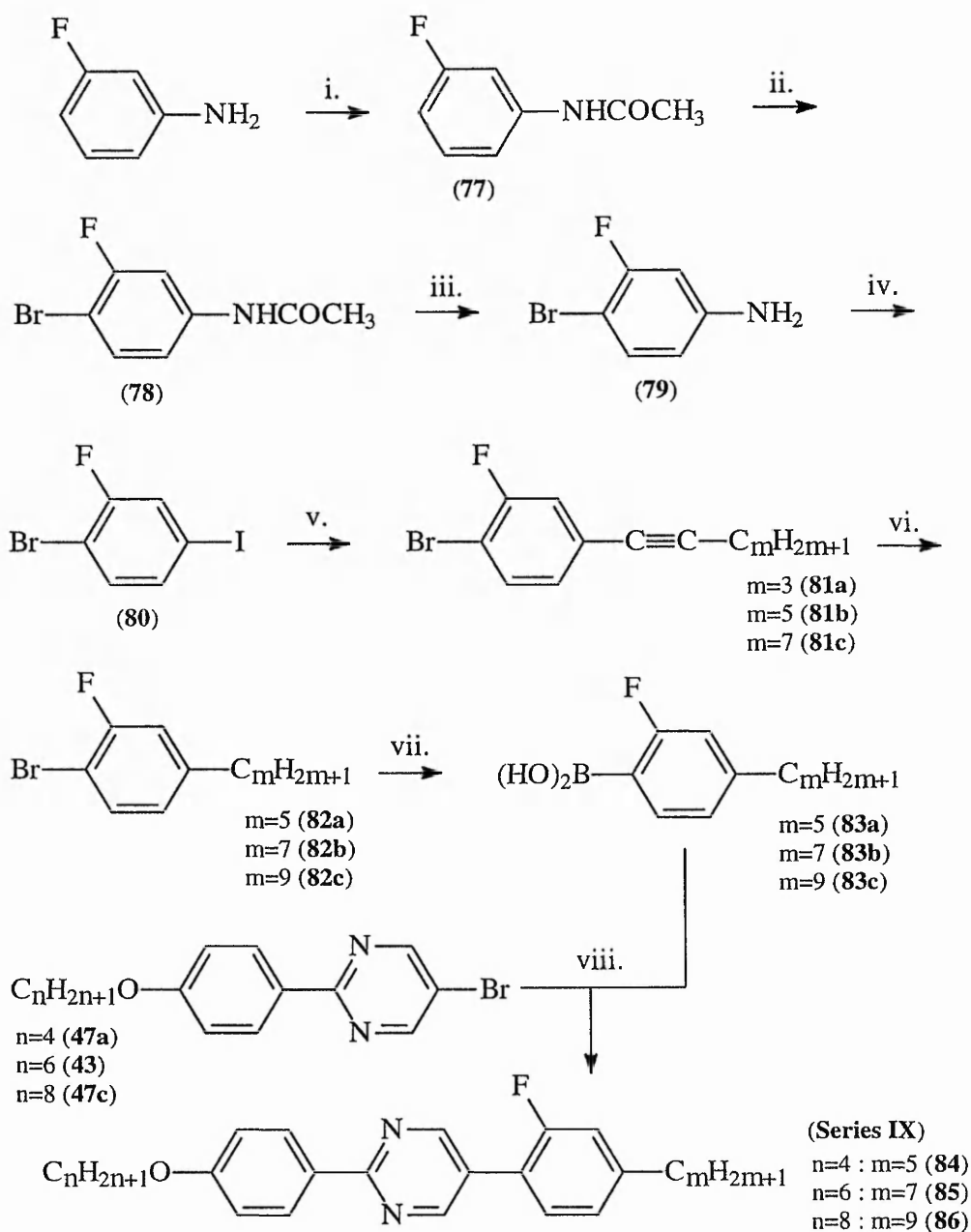


where $n=4$, $m=5$ (**84**); $n=6$, $m=7$ (**85**); $n=8$, $m=9$ (**86**)

The 2-(4-*n*-alkoxyphenyl)-5-(2-fluoro-4-*n*-alkylphenyl)pyrimidines (series IX) were synthesised as depicted in **scheme 9**, p.160. Initially, the important precursor 1-bromo-2-fluoro-4-iodobenzene (**80**)⁶⁸ was prepared in four steps starting from commercial 3-fluoroaniline which was protected as the ethanamide (**77**) and subsequently brominated via electrophilic substitution using *N*-bromosuccinimide to give compound (**78**) in excellent yield (89%). Deprotection of (**78**) released the amine which was diazotised and treated with iodine to furnish the desired 1-bromo-2-fluoro-4-iodobenzene (**80**).

The formation of the aromatic diazonium salt employing an NO^+ -donor proceeds in three steps as shown below.¹²²





- i. Glacial acetic acid, $(\text{CH}_3\text{CO})_2\text{O}$, reflux.
 ii. NBS, DCM, reflux.
 iii. Conc. HCl, EtOH, reflux.
 iv. a. Conc. HCl, water, 80°C .
 b. NaNO_2 , water, 0°C .
 c. KI, water, cyclohexane, 20°C .
 v. $\text{Pd}(\text{PPh}_3)_4$, compound (80), 1-alkynylzinc chloride, THF, 0°C .
 vi. PtO_2 , H_2 , EtOH.
 vii. a. 1.6M *n*-BuLi, THF, -78°C .
 b. Trimethyl borate, -78°C .
 c. 4M HCl, 0°C .
 viii. $\text{Pd}(\text{PPh}_3)_4$, DME, aq. Na_2CO_3 , reflux.

Scheme 9

Greiss¹²³ reported that replacement of the diazonium group with iodine is extremely facile upon the addition of alkaline iodide. The ease of which the reaction takes place may be attributed to the fact that the redox potential is near that of copper(I) and that the process involves generation of I_3^+ .

Room temperature palladium-catalysed cross-coupling of the appropriate alk-1-ynylzinc chloride to give compounds (**81a-c**) was achieved in good yield (70-79%). Hydrogenation of the triple bond at room temperature and atmospheric pressure using platinum(II) oxide as catalyst gave the desired intermediates (**82a-c**), which were then converted to boronic acids (**83a-c**) in the usual manner. Suzuki coupling with the appropriate two-ring bromo-compounds (**43**) and (**47a** and **c**) gave the desired 2-(4-*n*-alkoxyphenyl)-5-(2-fluoro-4-*n*-alkylphenyl)pyrimidines, i.e., members of **series IX**.

3.5.7.1 Experimental Procedures

N-(3-Fluorophenyl)ethanamide (**77**) (scheme 9)

A mixture of acetic anhydride (53.7 g, 0.526 mol) and glacial acetic acid (53 ml) was added to stirred 3-fluoroaniline (53 g, 0.477 mol) at room temperature and then heated under reflux for 20 min. After cooling to room temperature, the reaction mixture was poured on to ice and extracted with diethyl ether (2 x 150 ml). The combined ethereal extract was washed with water (2 x 150 ml), dried ($MgSO_4$) and the solvent was removed *in vacuo*. The crude residue was then recrystallised from aqueous glacial acetic acid to furnish the desired *N*-(3-fluorophenyl)ethanamide (**77**), 56 g (76%), m.p. 89-90°C (Lit.⁶⁸ 89-90°C), as colourless crystals.

^1H NMR (CDCl_3) δ : 2.17 (3H, s, CH_3), 6.79 (1H, t, ArH), 7.13-7.26 (2H, m, ArH), 7.45-7.51 (1H, m, ArH), 7.91 (1H, br s, NH: disappears on D_2O shake) ppm.

i.r. ν_{max} (KBr): 3255 (N-H str.), 3200, 3140, 3086, 1667(C=O), 1554, 1260, 786 cm^{-1} .

N-(4-Bromo-3-fluorophenyl)ethanamide (**78**) (scheme 9)

A vigorously stirred mixture of *N*-(3-fluorophenyl)ethanamide (**77**) (56 g, 0.366 mol), *N*-bromosuccinimide (65.4 g, 0.366 mol) and dry DCM (500 ml) was heated under reflux for 5 h. and then cooled to room temperature. The reaction mixture was then washed with water (2 x 200 ml), dried (MgSO_4) and the solvent was removed *in vacuo* to yield the desired *N*-(4-bromo-3-fluorophenyl)ethanamide (**78**), 65 g (89%), m.p. 151-152°C (Lit.⁶⁸ 151-152°C), as an off-white solid.

^1H NMR (CDCl_3) δ : 2.19 (3H, s, CH_3), 7.03-7.06 (1H, m, ArH), 7.42-7.48 (1H, t, ArH), 7.58-7.68 (1H, m, ArH) ppm. No NH signal observed.

i.r. ν_{max} (KBr): 3308 (N-H str.), 3200, 3131, 1674 (C=O str.), 1602, 1537, 1490, 1418, 1318, 1255, 855 cm^{-1} .

4-Bromo-3-fluoroaniline (**79**) (scheme 9)

Concentrated hydrochloric acid (82 ml) was added, dropwise, to a stirred solution of *N*-(4-bromo-3-fluorophenyl)ethanamide (**78**) (65 g, 0.28 mol) in ethanol (160 ml) and heated to reflux for 2 h. Water (500 ml) was added and the resultant mixture was distilled to remove ethyl acetate, water and ethanol. The crude residue was treated with 5% aqueous sodium hydroxide solution until just alkaline (universal pH paper) and the

product was extracted with DCM (2 x 300 ml). The combined organic extract was washed with water, dried (MgSO₄) and the solvent was removed *in vacuo* to give the desired 4-bromo-3-fluoroaniline (**79**), 45.9 g (87%), m.p. 68-69°C (Lit.⁶⁸ 63-65°C), as an off-white solid.

¹H NMR (CDCl₃) δ: 3.78 (2H, br s, NH₂: disappears on D₂O shake), 6.35 (1H, m, ArH), 6.45 (1H, m, ArH), 7.21-7.27 (1H, m, ArH) ppm.

i.r. ν_{\max} (KBr): 3436 (N-H str.), 3330, 3212, 1604, 1445, 1320, 1178, 844 cm⁻¹.

1-Bromo-2-fluoro-4-iodobenzene (**80**) (scheme 9)

A cold solution of sodium nitrite (11 g, 0.158 mol) in water (60 ml) was added, dropwise, to a cooled (-5°C) mixture of 4-bromo-3-fluoroaniline (**79**) (27.4 g, 0.144 mol), concentrated HCl (200 ml) and water (80 ml) which had been previously warmed to give a clear solution. Subsequently, a solution of potassium iodide (48 g, 0.29 mol) in water (80 ml) was added, dropwise, followed by cyclohexane (100 ml). The mixture was stirred at room temperature for 16 h. and the organic layer was isolated. The aqueous layer was extracted with diethyl ether (2 x 150 ml) and the combined organic extract was washed with water (300 ml), saturated sodium metabisulfite solution (300 ml), water (300 ml) and then dried (MgSO₄). The solvent was removed *in vacuo* and the crude residue was vacuum distilled (Claisen) to furnish the desired 1-bromo-2-fluoro-4-iodobenzene (**80**), 14.9 g (69%), b.p. 118-120°C/15 mmHg (Lit.⁶⁸ 118-120°C/15 mmHg), as a clear oil which solidified on standing.

^1H NMR (CDCl_3) δ : 7.23-7.29 (1H, m, ArH), 7.34-7.38 (1H, m, ArH), 7.45-7.48 (1H, m, ArH) ppm

i.r. ν_{max} (KBr): 2923, 2852, 1565, 1467, 1389, 1246, 1066, 859 cm^{-1} .

1-Bromo-2-fluoro-4-*n*-alk-1-ynylbenzenes (**81a-c**) (scheme 9)

In an atmosphere of dry nitrogen, 1.6M *n*-butyllithium (0.049 mol) was added, dropwise, to a stirred, cooled (0°C) solution of the appropriate alkyne (0.049 mol) in dry THF (25 ml). Subsequently, a solution of anhydrous zinc chloride (0.049 mol) dissolved in dry THF (50 ml) was added, dropwise, and the reaction mixture was then stirred for an additional 15 min. at room temperature. The resultant alkynylzinc chloride was then added, dropwise, to a second reaction vessel containing a cooled (0°C), stirred mixture of 4-bromo-3-fluoro-iodobenzene (**80**) (13.5 g, 0.045 mol), *tetrakis*(triphenylphosphine)palladium (0.53 g, 0.00046 mol) and dry THF (100 ml). The reaction mixture was stirred at room temperature for 3 h. Thereafter, the reaction mixture was quenched with 2M HCl (150 ml) and the product was extracted with diethyl ether (3 x 100 ml). The combined organic extract was washed with saturated sodium hydrogen carbonate solution (100 ml), dried (MgSO_4) and the solvent was removed *in vacuo*. The crude residue was vacuum distilled (Claisen) to yield the appropriate pure 1-bromo-2-fluoro-4-*n*-alk-1-ynylbenzene (**81a-c**), (70-79%), as a colourless liquid. B.p.s: $\text{C}_3\text{H}_7\text{C}\equiv\text{C}$ (**81a**), 132-134 $^\circ/15$, (Lit.⁶⁸ 132-134 $^\circ\text{C}/15$ mmHg); $\text{C}_5\text{H}_{11}\text{C}\equiv\text{C}$ (**81b**), 158-160 $^\circ/15$; $\text{C}_7\text{H}_{15}\text{C}\equiv\text{C}$ (**81c**), 158-160 $^\circ\text{C}/2$ mmHg.

The following spectroscopic data refer to 1-bromo-2-fluoro-4-*n*-hept-1-ynylbenzene (**81b**) and are typical of series:

^1H NMR (CDCl_3) δ : 0.90-0.95 (3H, t, CH_3), 1.34-1.45 (4H, m, CH_2), 1.56-1.63 (2H, quint, CH_2), 2.35-2.40 (2H, t, CH_2), 7.01-7.06 (1H, m, ArH), 7.10-7.15 (1H, m, ArH), 7.41-7.46 (1H, m, ArH), ppm.

i.r. ν_{max} (Thin film): 2956, 2930, 2859, 2234 ($\text{C}\equiv\text{C}$ str.), 1558, 1476, 1046, 815 cm^{-1} .

1-Bromo-2-fluoro-4-*n*-alkylbenzenes (**82a-c**) (scheme 9)

A mixture of the appropriate 1-bromo-2-fluoro-4-alk-1-ynylbenzene (**81a-c**) (0.031 mol), platinum(IV) oxide (0.2 g, 0.00088 mol) and ethanol (100 ml) was hydrogenated at room temperature and atmospheric pressure until the reaction was complete (i.r. spectroscopy: disappearance of alkyne peak at 2233 cm^{-1}). The solvent was removed *in vacuo* and the crude residue was vacuum distilled (Claisen) to furnish the desired 1-bromo-2-fluoro-4-*n*-alkylbenzene (**82a-c**), (63-75%), as a colourless liquid. B.p.s: C_5H_{11} (**82a**), 154-156°/20, (Lit.⁶⁸ 128-130°C/15 mmHg); C_7H_{15} (**82b**), 174-176°/15; C_9H_{19} (**82c**), 162-164°C/3 mmHg.

The following spectroscopic data refer to 1-bromo-2-fluoro-4-*n*-heptylbenzene (**82b**) and are typical of series:

^1H NMR (CDCl_3) δ : 0.85-0.90 (3H, t, CH_3), 1.27-1.30 (8H, m, CH_2), 1.55-1.61 (2H, quint, CH_2), 2.53-2.59 (2H, t, CH_2), 6.81-6.85 (1H, m, ArH), 6.91-6.96 (1H, m, ArH), 7.38-7.44 (1H, m, ArH), ppm.

i.r. ν_{max} (Thin film): 2960, 2855, 1603, 1578, 1484, 1418, 1241, 1152, 1041, 866 cm^{-1} .

2-Fluoro-4-*n*-alkylphenylboronic acids (**83a-c**) (scheme 9)

The 2-fluoro-4-*n*-alkylphenylboronic acids (**83a-c**) were prepared according to the method described for 4-*n*-alkoxyphenylboronic acids (**42** and **46a-c**) on p. 135. The solvent was removed *in vacuo* to yield the appropriate 2-fluoro-4-*n*-alkylphenylboronic acid (**83a-c**), (85-100%), as a white solid. The boronic acids were not purified and were used directly in the next stage.

The following spectroscopic data refer to 2-fluoro-4-*n*-heptylphenylboronic acid (**83b**), and are typical of series:

¹H NMR (CDCl₃) δ: 0.85-0.90 (3H, t, CH₃), 1.28-1.31 (8H, m, CH₂), 1.61-1.85 (2H, quint, CH₂), 2.59-2.65 (2H, t, CH₂), 5.13 (2H, br s, OH: disappears on D₂O shake), 6.85 (1H, d, ArH), 7.01-7.05 (1H, m, ArH), 7.69-7.75 (1H, t, ArH) ppm.

i.r. ν_{\max} (KBr): 3700-3100 (O-H str.), 2925, 2852, 1557, 1417, 1344, 1021, 812 cm⁻¹.

2-(4-*n*-Alkoxyphenyl)-5-(2-fluoro-4-*n*-alkylphenyl)pyrimidines (**84-86** or series **IX**) (scheme 9)

The 2-(4-*n*-alkoxyphenyl)-5-(2-fluoro-4-*n*-alkylphenyl)pyrimidines (series **IX**) were prepared according to the method described earlier on p. 138 for 2-(4-*n*-alkoxyphenyl)-5-(2,3-difluoro-4-*n*-alkylphenyl)pyrimidines (series **IIIa-d**). The crude residue was purified by flash chromatography on silica gel eluting with 0.5 : 9.5 ethyl acetate : light petroleum ether (b.p. 60-80°C) followed by recrystallisation from ethanol to furnish the appropriate 2-(4-*n*-alkoxyphenyl)-5-(2-fluoro-4-*n*-alkylphenyl)pyrimidine (**84-86** or series **IX**), (47-50%), as white crystals.

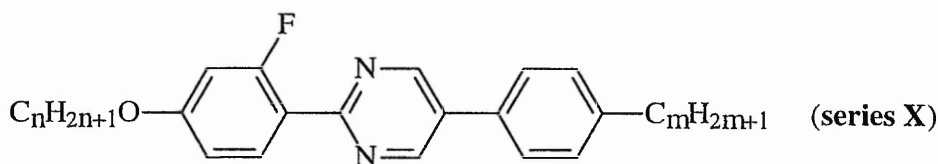
The m.p.s and mesomorphic transition temperatures of **series IX** are listed in *Table 12* (p. 90) of the results and discussion section.

The following spectroscopic data refer to 2-(4-*n*-hexyloxyphenyl)-5-(2-fluoro-4-*n*-heptylphenyl)pyrimidine (**85**) and are typical of the series:

$^1\text{H NMR}$ (CDCl_3) δ : 0.86-1.00 (6H, t, 2CH_3), 1.25-1.60 (6H, m, CH_2), 1.61-1.76 (2H, quint, CH_2), 1.79-1.86 (2H, quint, CH_2), 2.64-2.69 (2H, t, CH_2), 4.03-4.08 (2H, t, CH_2O), 6.98-7.03 (2H, dd, ArH), 7.05-7.12 (2H, m, ArH), 7.36-7.41 (1H, t, ArH), 8.40-8.45 (2H, dd, ArH), 8.94 (2H, s, ArH) ppm.

i.r. ν_{max} (KBr): 2924, 2852, 1606, 1582, 1432, 1256, 1168, 1023, 798 cm^{-1} .

3.5.8 THE SYNTHESIS OF 2-(2-FLUORO-4-*n*-ALKOXYPHENYL)-5-(4-*n*-ALKYLPHENYL)PYRIMIDINES (**series X**)



where $n=4$, $m=5$ (**91**); $n=6$, $m=7$ (**92**); $n=8$, $m=9$ (**93**)

The 2-(2-fluoro-4-*n*-alkoxyphenyl)-5-(4-*n*-alkylphenyl)pyrimidines, i.e., members of **series X**, were synthesised as outlined in **scheme 10**, p. 168. *O*-Alkylation of commercial 3-fluorophenol with the appropriate 1-bromoalkane afforded the intermediate alkoxy compounds (**87a-c**) which were then brominated¹²⁴ to yield the appropriate *n*-alkyl-4-bromo-3-fluorophenyl ethers (**88a-c**). Subsequently, treatment of

the lithiated complex of compounds (**88a-c**) with trimethyl borate followed by hydrolysis with 4M-aqueous hydrochloric acid afforded the appropriate 2-fluoro-4-*n*-alkoxyphenylboronic acids (**89a-c**). Palladium-catalysed cross-coupling between the appropriate boronic acid (**89a-c**) and 5-bromo-2-iodopyrimidine (**41**) gave the two-ring intermediates (**90a-c**) which were then subjected to a further coupling reaction with the appropriate boronic acids (**59a-c**) to furnish the desired 2-(2-fluoro-4-*n*-alkoxyphenyl)-5-(4-*n*-alkylphenyl)pyrimidines, i.e., members of **series X**.

3.5.8.1 Experimental Procedures

n-Alkyl-3-fluorophenyl ethers (**87a-c**) (scheme 10)

The *n*-alkyl-3-fluorophenyl ethers (**87a-c**) were prepared according to the method described previously on p. 114 for 4-*n*-hexyloxy-1-bromobenzene (**24**). The crude residue was purified by vacuum distillation (Claisen) to give the pure *n*-alkyl-3-fluorophenyl ethers (**87a-c**), (54-72%), as colourless liquids. B.p.s: C₄H₉O (**87a**), 66-67°/2; C₆H₁₃O (**87b**), 110-112°/0.1, (Lit.¹²⁵ 105-115°C/0.1 mmHg); C₈H₁₇O (**87c**), 115-116°C/0.3 mmHg (Lit.¹²⁵ 115°C/0.3 mmHg).

The following spectroscopic data refer to *n*-hexyl-3-fluorophenyl ether (**87b**) and are typical of the series:

¹H NMR (CDCl₃) δ: 0.88-0.93 (3H, t, CH₃), 1.30-1.46 (6H, m, CH₂), 1.72-1.82 (2H, quint, CH₂), 3.89-3.94 (2H, t, CH₂O), 6.57-6.74 (3H, m, ArH), 7.17-7.24 (1H, m, ArH) ppm.

i.r. ν_{\max} (Thin film): 2920, 2855, 1610, 1590, 1490, 1275, 1135, 760 cm⁻¹.

n-Alkyl-4-bromo-3-fluorophenyl ethers (**88a-c**) (scheme 10)

Bromine (0.037 mol) in dry chloroform (50 ml) was added dropwise over 3 h. to a stirred solution of the appropriate *n*-alkyl-3-fluorophenyl ether (**87a-c**) (0.037 mol) in dry chloroform (50 ml) at room temperature. After completion of the addition, the temperature of the reaction was raised to 30-40°C for 1 h. The mixture was then cooled and washed successively with brine (3 x 100 ml), 2M sodium hydroxide solution (2 x 100 ml) and dried (MgSO₄). The solvent was removed *in vacuo* and the crude residue was subjected to short path vacuum distillation (Kugelrohr) to furnish to desired *n*-alkyl-4-bromo-3-fluorophenyl ether (**88a-c**), (74-81%), as a colourless liquid. B.p.s: C₄H₉O (**88a**), 97-98°/0.6, (Lit.¹⁰⁴ 90°C/0.1 mmHg); C₆H₁₃O (**88b**), 134-135°/0.4, (Lit.¹²⁵ 135°C/0.4 mmHg); C₈H₁₇O (**88c**), 145-146°C/0.2 mmHg (Lit.¹²⁵ 155°C/0.3 mmHg).

The following spectroscopic data refer to *n*-hexyl-4-bromo-3-fluorophenyl ether (**88b**) and are typical of the series:

¹H NMR (CDCl₃) δ: 0.88-0.93 (3H, t, CH₃), 1.25-1.52 (6H, m, CH₂), 1.71-1.83 (2H, quint, CH₂), 3.87-3.92 (2H, t, CH₂O), 6.52-6.70 (2H, m, ArH), 7.34-7.42 (1H, t, ArH) ppm.

i.r. ν_{max} (Thin film): 2925, 2865, 1600, 1580, 1485, 1290, 1165, 830 cm⁻¹.

2-Fluoro-4-*n*-alkoxyphenylboronic acids (**89a-c**) (scheme 10)

The 2-fluoro-4-*n*-alkoxyphenylboronic acids (**89a-c**) were prepared according to the method described for 4-*n*-alkoxyphenylboronic acids (**42** and **46a-c**) on p. 135. The solvent was removed *in vacuo* to yield the appropriate 2-fluoro-4-*n*-alkoxy-

phenylboronic acid (**89a-c**), (86-89%), as a white solid. The boronic acids were not purified and were used directly in the next stage.

The following spectroscopic data refer to 2-fluoro-4-*n*-hexyloxyphenylboronic acid (**89b**) and are typical of the series:

^1H NMR (CDCl_3) δ : 0.86-0.91 (3H, t, CH_3), 1.29-1.45 (6H, m, CH_2), 1.73-1.86 (2H, quint, CH_2), 3.95-3.99 (2H, t, CH_2O), 5.5 (2H, d, OH: disappears on D_2O shake), 6.59-6.77 (2H, m, ArH), 7.69-7.76 (1H, t, ArH) ppm.

i.r. ν_{max} (KBr): 3600-3100 (O-H str.), 2950, 2875, 1620, 1350, 1220, 805, 650 cm^{-1} .

2-(2-Fluoro-4-*n*-alkoxyphenyl)-5-bromopyrimidines (**90a-c**) (scheme 10)

The 2-(2-fluoro-4-*n*-alkoxyphenyl)-5-bromopyrimidines (**90a-c**) were prepared by the method described previously for 2-(4-*n*-alkoxyphenyl)-5-bromopyrimidines (**43** and **47a-c**), p. 136. The crude residue was purified by flash chromatography on silica gel eluting with 0.5 : 9.5 ethyl acetate : light petroleum ether (b.p. 60-80°C) followed by recrystallisation from ethanol to give the appropriate 2-(2-fluoro-4-*n*-alkoxyphenyl)-5-bromopyrimidine (**90a-c**) (44-69%), as white crystals.

The following spectroscopic data refer to 2-(2-fluoro-4-*n*-hexyloxyphenyl)-5-bromopyrimidine (**90b**) and are typical of the series:

^1H NMR (CDCl_3) δ : 0.89-0.93 (3H, t, CH_3), 1.31-1.50 (6H, m, CH_2), 1.78-1.83 (2H, quint, CH_2), 3.98-4.03 (2H, t, CH_2O), 6.68-6.81 (2H, m, ArH), 8.02-8.08 (1H, t, ArH), 8.85 (2H, s, ArH) ppm.

i.r. ν_{\max} (KBr): 2949, 2925, 2866, 1618, 1579, 1418, 1342, 1272, 1127, 1023, 833 cm^{-1} .

2-(2-Fluoro-4-*n*-alkoxyphenyl)-5-(4-*n*-alkylphenyl)pyrimidines (**91-93** or **series X**) (scheme 10)

The 2-(2-fluoro-4-*n*-alkoxyphenyl)-5-(4-*n*-alkylphenyl)pyrimidines, i.e., members of **series X**, were prepared by the method previously described for 2-(4-*n*-alkoxyphenyl)-5-(2,3-difluoro-4-*n*-alkylphenyl)pyrimidines (**series IIIa-d**) on p. 138. The crude residue was purified by flash chromatography on silica gel eluting with 0.5 : 9.5 ethyl acetate : light petroleum ether (b.p. 60-80°C) followed by recrystallisation from ethanol to give the appropriate 2-(2-fluoro-4-*n*-alkoxyphenyl)-5-(4-*n*-alkylphenyl)pyrimidine (**91-93** or **series X**) (63-72%), as white crystals.

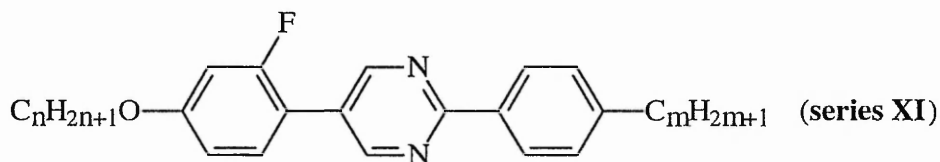
The m.p.s and mesomorphic transition temperatures of **series X** are listed in **Table 13** (p. 92) of the results and discussion section.

The following spectroscopic data refer to 2-(2-fluoro-4-*n*-hexyloxyphenyl)-5-(4-*n*-heptylphenyl)pyrimidine (**92**) and are typical of the series:

^1H NMR (CDCl_3) δ : 0.89-0.92 (6H, t, 2 CH_3), 1.29-1.53 (14H, m, CH_2), 1.60-1.69 (2H, quint, CH_2), 1.72-1.87 (2H, quint, CH_2), 2.65-2.71 (2H, t, CH_2), 4.00-4.04 (2H, t, CH_2O), 6.72-6.87 (2H, m, ArH), 7.32-7.35 (2H, dd, ArH), 7.53-7.56 (2H, dd, ArH), 8.12 (1H, t, ArH), 9.02 (2H, s, ArH) ppm.

i.r. ν_{\max} (KBr): 2954, 2922, 2854, 1622, 1581, 1440, 1342, 1271, 1170, 824 cm^{-1} .

3.5.9 THE SYNTHESIS OF 2-(4-*n*-ALKYLPHENYL)-5-(2-FLUORO-4-*n*-ALKOXYPHENYL)PYRIMIDINES (series XI)



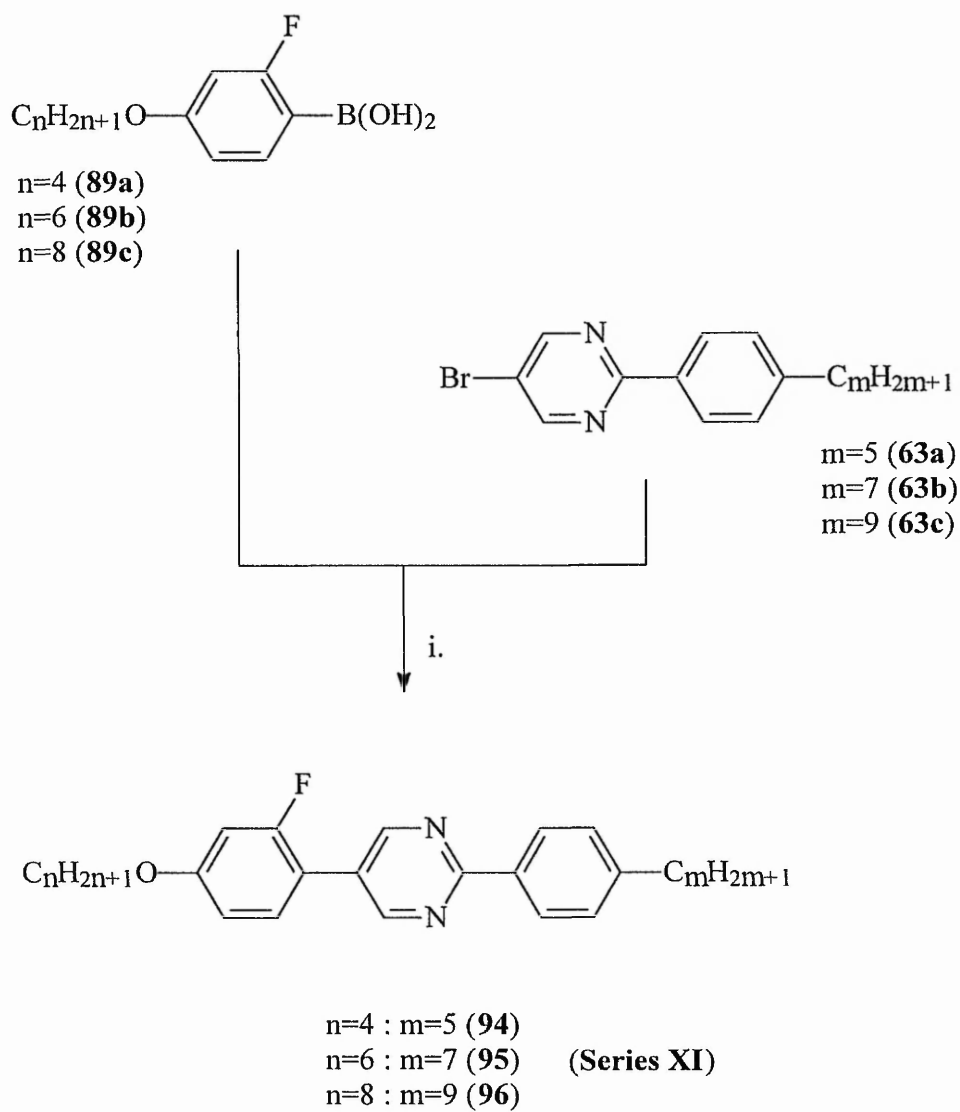
where $n=4$, $m=5$ (**94**); $n=6$, $m=7$ (**95**); $n=8$, $m=9$ (**96**)

The 2-(4-*n*-alkylphenyl)-5-(2-fluoro-4-*n*-alkoxyphenyl)pyrimidines, i.e., members of **series XI**, were synthesised via Suzuki coupling of the appropriate two-ring intermediates (**63a-c**) with the corresponding boronic acids (**89a-c**) as depicted in **scheme 11**, p.174.

3.5.9.1 Experimental Procedures

2-(4-*n*-Alkylphenyl)-5-(2-fluoro-4-*n*-alkoxyphenyl)pyrimidines (**94-96** or **series XI**) (scheme 11)

The 2-(4-*n*-alkylphenyl)-5-(2-fluoro-4-*n*-alkoxyphenyl)pyrimidines (**94-96**) were prepared according to the method described previously for 2-(4-*n*-alkoxyphenyl)-5-(2,3-difluoro-4-*n*-alkylphenyl)pyrimidines (**series IIIa-d**) on p. 138. The crude residue was purified by flash chromatography on silica gel eluting with 0.5 : 9.5 ethyl acetate : light petroleum ether (b.p. 60-80°C) followed by recrystallisation from ethanol to furnish the appropriate 2-(4-*n*-alkylphenyl)-5-(2-fluoro-4-*n*-alkoxyphenyl)pyrimidine (**94-96** or **series XI**), (54-64%), as white crystals.



i. $Pd(PPh_3)_4$, DME, aq. Na_2CO_3 , reflux.

Scheme 11

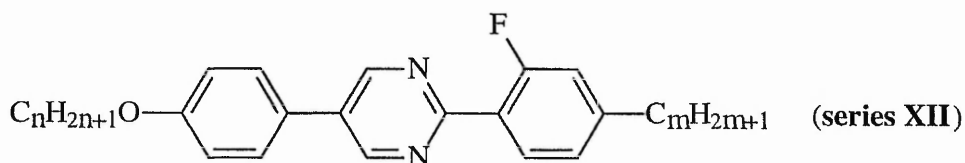
The m.p.s and mesomorphic transition temperatures of **series XI** are listed in *Table 14* (p. 94) of the results and discussion section.

The following spectroscopic data refer to 2-(4-*n*-heptylphenyl)-5-(2-fluoro-4-*n*-hexyloxyphenyl)pyrimidine (**95**) and are typical of the series:

$^1\text{H NMR}$ (CDCl_3) δ : 0.86-0.93 (6H, t, 2CH_3), 1.28-1.37 (12H, m, CH_2), 1.55-1.59 (2H, quint, CH_2), 1.61-1.72 (2H, quint, CH_2), 1.76-1.82 (2H, quint, CH_2), 2.65-2.71 (2H, t, CH_2), 3.98-4.02 (2H, t, CH_2O), 6.74-6.86 (2H, m, ArH), 7.30-7.36 (2H, dd, ArH), 7.39-7.42 (1H, t, ArH), 8.36-8.39 (2H, dd, ArH), 8.94 (2H, s, ArH) ppm.

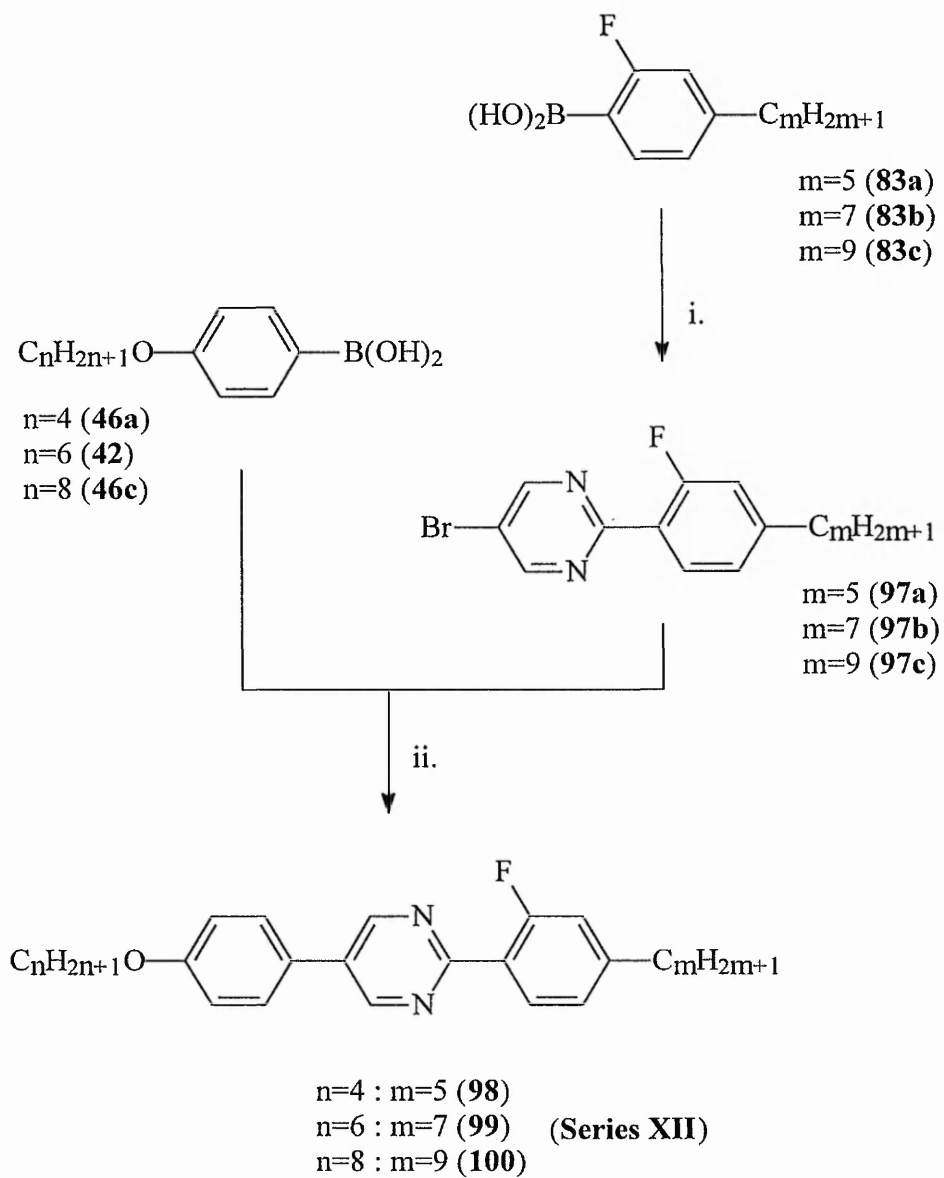
i.r. ν_{max} (KBr): 2953, 2923, 2847, 1622, 1434, 1290, 1130, 793 cm^{-1} .

3.5.10 THE SYNTHESIS OF 2-(2-FLUORO-4-*n*-ALKYLPHENYL)-5-(4-*n*-ALKOXYPHENYL)PYRIMIDINES (**series XII**)



where $n=4$, $m=5$ (**98**); $n=6$, $m=7$ (**99**); $n=8$, $m=9$ (**100**)

The members of **series XII**, i.e., 2-(2-fluoro-4-*n*-alkylphenyl)-5-(4-*n*-alkoxyphenyl)pyrimidines, were synthesised by the boronic acid cross-coupling methodology depicted in **scheme 12**, p.176. An initial cross-coupling of (**83a-c**) with 5-bromo-2-iodopyrimidine (**41**) gave the appropriate intermediates (**97a-c**) which were cross-coupled with the appropriate boronic acid (**42**; **46a** and **c**) to furnish the desired three-ring materials (**98-100**), i.e. members of **series XII**.



- i. Compound (**41**), $Pd(PPh_3)_4$, DME aq. Na_2CO_3 , reflux.
 ii. $Pd(PPh_3)_4$, DME aq. Na_2CO_3 , reflux.

Scheme 12

3.5.10.1 Experimental Procedures

2-(2-Fluoro-4-*n*-alkylphenyl)-5-bromopyrimidines (**97a-c**) (scheme 12)

The 2-(2-fluoro-4-*n*-alkylphenyl)-5-bromopyrimidines (**97a-c**) were prepared by the method previously described for 2-(4-*n*-alkoxyphenyl)-5-bromopyrimidines (**43** and **47a-c**) on p. 136. The crude residue was purified by flash chromatography on silica gel eluting with 0.5 : 9.5 ethyl acetate : light petroleum ether (b.p. 60-80°C) followed by recrystallisation from ethanol affording the appropriate 2-(2-fluoro-4-*n*-alkylphenyl)-5-bromopyrimidine (**97a-c**), (62-65%), as white crystals.

The following spectroscopic data refer to 2-(2-fluoro-4-*n*-heptylphenyl)-5-bromopyrimidine (**97b**) and are typical of the series:

¹H NMR (CDCl₃) δ: 0.85-0.90 (3H, t, CH₃), 1.27-1.32 (8H, m, CH₂), 1.59-1.67 (2H, quint, CH₂), 2.63-2.68 (2H, t, CH₂), 7.00-7.06 (2H, m, ArH), 7.97-8.00 (1H, t, ArH), 8.88 (2H, s, ArH) ppm.

i.r. ν_{\max} (KBr): 2950, 2922, 2850, 1621, 1572, 1430, 1375, 1140, 794 cm⁻¹.

2-(2-Fluoro-4-*n*-alkylphenyl)-5-(4-*n*-alkoxyphenyl)pyrimidines (**98-100** or series **XII**) (scheme 12)

The 2-(2-fluoro-4-*n*-alkylphenyl)-5-(4-*n*-alkoxyphenyl)pyrimidines (**98-100**) were prepared by the method described earlier for 2-(4-*n*-alkoxyphenyl)-5-(2,3-difluoro-4-*n*-alkylphenyl)pyrimidines (series **IIIa-d**) on p. 138. The crude residue was purified by flash chromatography on silica gel eluting with 0.5 : 9.5 ethyl acetate : light petroleum ether (b.p. 60-80°C) followed by recrystallisation from ethanol to give the appropriate

2-(2-fluoro-4-*n*-alkylphenyl)-5-(4-*n*-alkoxyphenyl)pyrimidine (**98-100** or **series XII**), (67-75%), as white crystals.

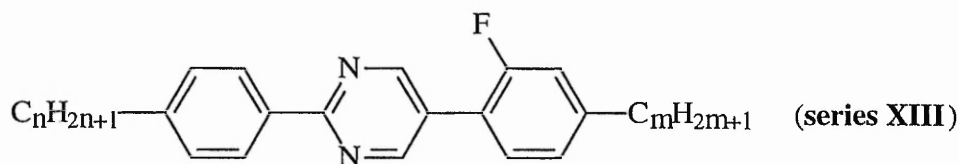
The m.p.s and mesomorphic transition temperatures of **series XII** are listed in *Table 15* (p. 97) of the results and discussion section.

The following spectroscopic data refer to 2-(2-fluoro-4-*n*-heptylphenyl)-5-(4-*n*-hexyloxyphenyl)pyrimidine (**99**) and are typical of the series:

$^1\text{H NMR}$ (CDCl_3) δ : 0.86-0.95 (6H, t, 2CH_3), 1.24-1.52 (14H, m, CH_2), 1.63-1.68 (2H, quint, CH_2), 1.77-1.85 (2H, quint, CH_2), 2.64-2.70 (2H, t, CH_2), 4.00-4.05 (2H, t, CH_2O), 7.02-7.11 (4H, dd, m, ArH), 7.55-7.58 (2H, dd, ArH), 8.00-8.03 (1H, t, ArH), 9.02 (2H, s, ArH) ppm.

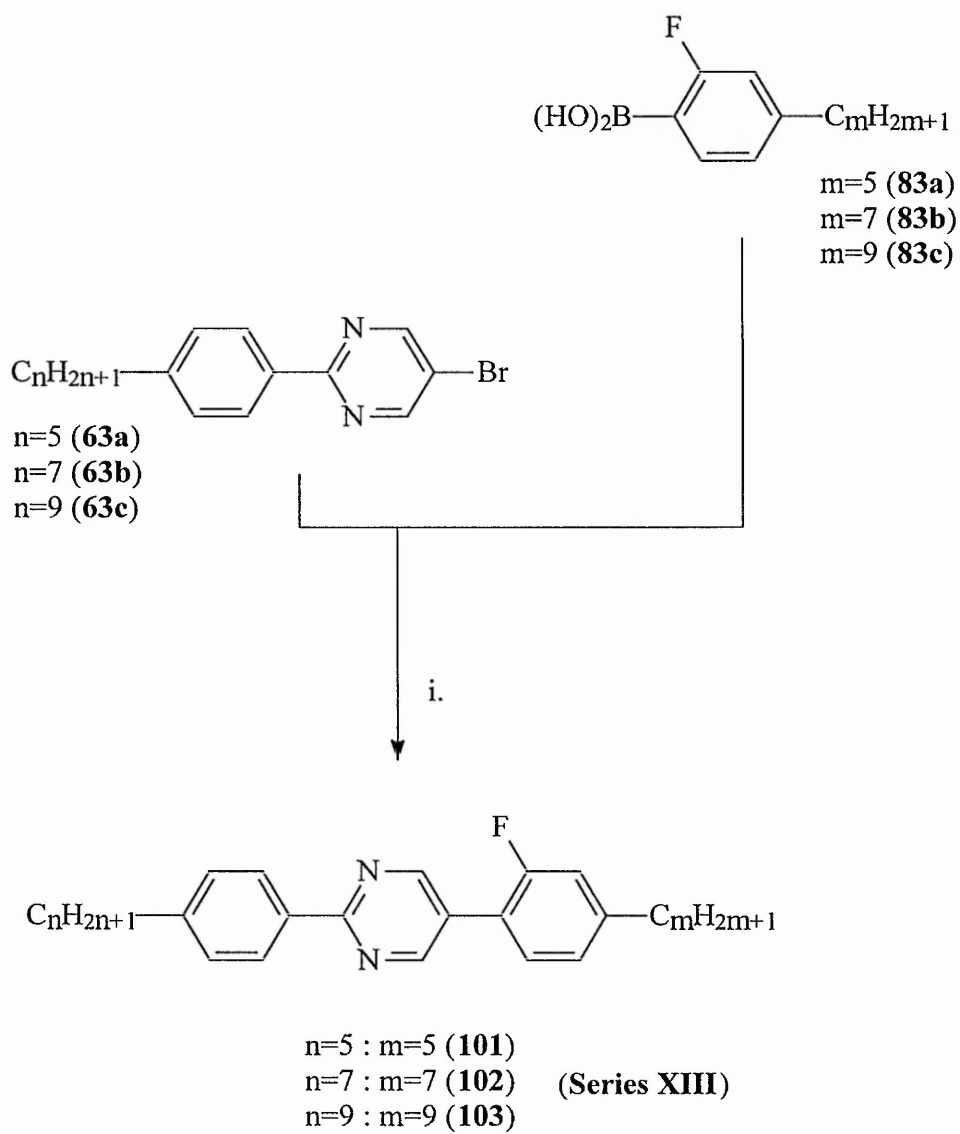
i.r. ν_{max} (KBr): 2951, 2922, 2854, 1610, 1516, 1438, 1249, 1186, 831 cm^{-1} .

3.5.11 THE SYNTHESIS OF 2-(4-*n*-ALKYLPHENYL)-5-(2-FLUORO-4-*n*-ALKYLPHENYL)PYRIMIDINES (**series XIII**)



where $n=5$, $m=5$ (**101**); $n=7$, $m=7$ (**102**); $n=9$, $m=9$ (**103**)

The 2-(4-*n*-alkylphenyl)-5-(2-fluoro-4-*n*-alkylphenyl)pyrimidines, i.e., members of **series XIII**, were synthesised as shown in **scheme 13**, p.179. Suzuki coupling of the appropriate two-ring intermediate (**63a-c**) with the appropriate mono-fluorinated



i. $\text{Pd}(\text{PPh}_3)_4$, DME, aq. Na_2CO_3 , reflux.

Scheme 13

boronic acid (**83a-c**) afforded the 2-(4-*n*-alkylphenyl)-5-(2-fluoro-4-*n*-alkylphenyl)-pyrimidines (**101-103**), i.e., members of **series XIII**.

3.5.11.1 Experimental Procedures

2-(4-*n*-Alkylphenyl)-5-(2-fluoro-4-*n*-alkylphenyl)pyrimidines (**101-103** or **series XIII**) (scheme 13)

The 2-(4-*n*-alkylphenyl)-5-(2-fluoro-4-*n*-alkylphenyl)pyrimidines (**101-103**) were prepared as described previously for 2-(4-*n*-alkoxyphenyl)-5-(2,3-difluoro-4-*n*-alkylphenyl)pyrimidines (**series IIIa-d**) on p. 138. The crude residue was purified by flash chromatography on silica gel eluting with 0.5 : 9.5 ethyl acetate : light petroleum ether (b.p. 60-80°C) followed by recrystallisation from ethanol to furnish the appropriate 2-(4-*n*-alkylphenyl)-5-(2-fluoro-4-*n*-alkylphenyl)pyrimidine (**101-103** or **series XIII**), (56-59%), as white crystals.

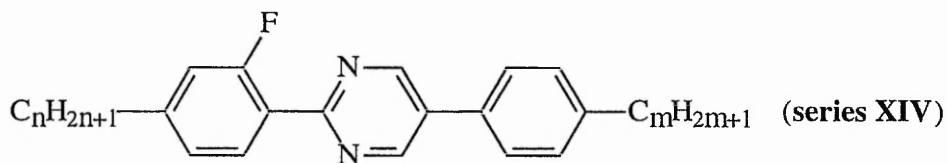
The m.p.s and mesomorphic transition temperatures of **series XIII** are listed in *Table 16* (p. 99) of the results and discussion section.

The following spectroscopic data refer to 2-(4-*n*-heptylphenyl)-5-(2-fluoro-4-*n*-heptylphenyl)pyrimidine (**102**) and are typical of the series:

¹H NMR (CDCl₃) δ: 0.90-0.92 (6H, t, 2CH₃), 1.22-1.38 (16H, m, CH₂), 1.60-1.69 (4H, quint, 2CH₂), 2.64-2.71 (4H, t, 2CH₂), 7.03-7.10 (2H, m, ArH), 7.12-7.13 (2H, dd, ArH), 7.31-7.34 (1H, t, ArH), 8.37-8.40 (2H, dd, ArH), 8.99 (2H, s, ArH) ppm.

i.r. ν_{max} (KBr): 2960, 2923, 2852, 1611, 1582, 1438, 1377, 1286, 1130, 793 cm⁻¹.

3.5.12 THE SYNTHESIS OF 2-(2-FLUORO-4-*n*-ALKYLPHENYL)-5-(4-*n*-ALKYLPHENYL)PYRIMIDINES (series XIV)



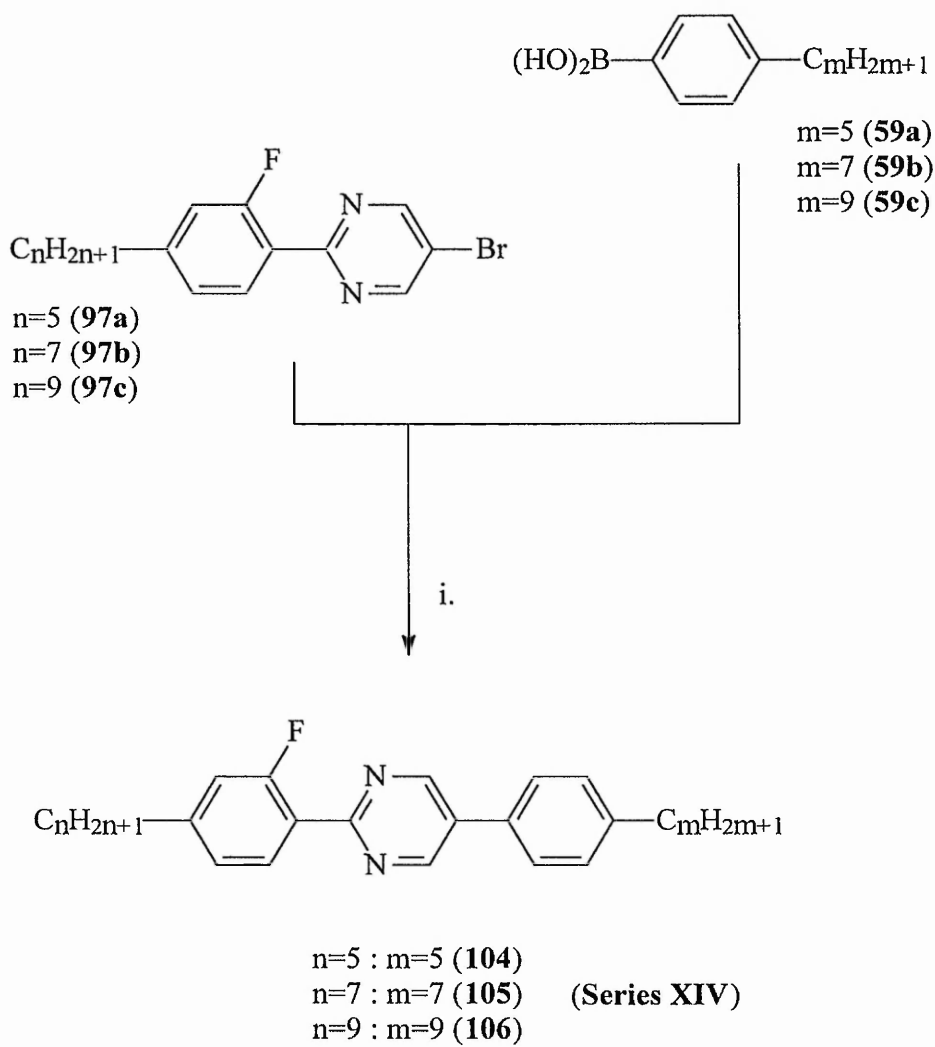
where $n=5$, $m=5$ (**104**); $n=7$, $m=7$ (**105**); $n=9$, $m=9$ (**106**)

The 2-(2-fluoro-4-*n*-alkylphenyl)-5-(4-*n*-alkylphenyl)pyrimidines (series XIV) were synthesised via the Suzuki cross-coupling methodology as shown in **scheme 14**, p. 182. The appropriate mono-fluorinated-phenyl-bromopyrimidine intermediate (**97a-c**) was cross-coupled with the appropriate boronic acid (**59a-c**) to give the desired 2-(2-fluoro-4-*n*-alkylphenyl)-5-(4-*n*-alkylphenyl)pyrimidines (**104**, **105** and **106**).

3.5.12.1 Experimental Procedures

2-(2-Fluoro-4-*n*-alkylphenyl)-5-(4-*n*-alkylphenyl)pyrimidines (**104-106** or series XIV) (scheme 14)

The 2-(2-fluoro-4-*n*-alkylphenyl)-5-(4-*n*-alkylphenyl)pyrimidines (**104-106**) were prepared according to the method described earlier for the 2-(4-*n*-alkoxyphenyl)-5-(2,3-difluoro-4-*n*-alkylphenyl)pyrimidines (series **IIIa-d**) on p. 138. The crude residue was purified by flash chromatography on silica gel eluting with 0.5 : 9.5 ethyl acetate : light petroleum ether (b.p. 60-80°C) followed by recrystallisation from ethanol to give the appropriate 2-(2-fluoro-4-*n*-alkylphenyl)-5-(4-*n*-alkylphenyl)pyrimidines (**104-106** or series XIV), (44-67%), as white crystals.



i. $Pd(PPh_3)_4$, DME, aq. Na_2CO_3 , reflux.

Scheme 14

The m.p.s and mesomorphic transition temperatures of series **XIV** are listed in *Table 17* (p. 101) of the results and discussion section.

The following spectroscopic data refer to 2-(2-fluoro-4-*n*-heptylphenyl)-5-(4-*n*-heptylphenyl)pyrimidine (**105**) and are typical of the series:

$^1\text{H NMR}$ (CDCl_3) δ : 0.86-0.91 (6H, t, 2CH_3), 1.27-1.33 (16H, m, CH_2), 1.59-1.66 (4H, quint, 2CH_2), 2.65-2.67 (4H, t, 2CH_2), 7.00-7.12 (2H, m, ArH), 7.33-7.36 (2H, dd, ArH), 7.54-7.57 (2H, dd, ArH), 8.04 (1H, t, ArH), 9.05 (2H, s, ArH) ppm.

i.r. ν_{max} (KBr): 2950, 2924, 2852, 1624, 1576, 1438, 1376, 1261, 1137, 811 cm^{-1} .

REFERENCES

REFERENCES

1. Reinitzer, F., *Monatsh. Chem.*, **9**, 421 (1888); *Liquid Crystals*, **5**, 7 (1989).
2. Lehmann, O., *Z. Krist.*, **18**, 464 (1890).
3. Quincke, F., *Annalen*, **53**, 613 (1894).
4. Tamman, G., *Ann. Physik.* **4**, 524 (1901); **8**, 103 (1902); **19**, 421 (1906).
5. Nernst, W., *Z. Electrochem.* **12**, 431 (1906).
6. Vorländer, D., 'Kristallinisch-flussige Substanzen', Enke, Stuttgart (1908); *Ber. Dtsch. Chem. Ges.*, **41**, 2033 (1908).
7. Friedel, G., *Ann. Physique*, **18**, 273 (1922).
8. Vorländer, D and Wilke, R., *Z. Physik. Chem.*, **57**, 361 (1906).
9. Bose, E., *Z. Phys.*, **10**, 32 (1909); **10**, 230 (1909).
10. Ornstein, L.S., and Zernicke, F., *Z. Phys.*, **19**, 134 (1918).
11. Zocher, H., *Z. Phys.*, **28**, 790 (1927).
12. Gray, G.W., 'Molecular Structure and the Properties of Liquid Crystals', Academic Press, London and New York (1962).
13. Gray, G.W., Harrison, K.J., and Nash, J.A., *Electron. Lett.*, **9**, 130 (1973).
14. Schadt, M and Helfrich, W., *Appl. Phys. Lett.*, **18**, 127 (1971).
15. Clark, N.A., and Lagerwall, S.T., *Appl. Phys. Lett.*, **36**, 899 (1980).
16. Meyer, R.B., Liebert, L., Strzelecki, L. and Keller, P., *J. Phys. Paris Lett.*, **36**, 669 (1975).
17. Shibaev, V.P., Kozlovsky, M.V., Bersnev, L.A., Blinov, L.M. and Plate, N.A., *Polym. Bull.*, **12**, 299 (1984).
18. Yuasa, K., Uchida, S., Sekiya, T., Hashimoto, K. and Kawasaki, K., *Ferroelectrics*, **122**, 53 (1991).
19. Naciri, J., Pfeiffer, S. and Shashidhar, R., *Liquid Crystals*, **10**, 585 (1991).

20. Chandani, A.D.L., Ouchi, Y., Takezoe, H., Fukuda, A., Terashima, K., Furukawa, K. and Kishi, A., *Jpn. J. Appl. Phys.*, **28**, L1261 (1989).
21. Chandani, A.D.L., Gorecka, E., Ouchi, Y., Takezoe, H. and Fukuda, A., *Jpn. J. Appl. Phys.*, **28**, L1265 (1989). For review; Fukada, A., Takaishi, Y., Isozaki, T., Ishikawa, K. and Takezoe, H., *J. Mater. Chem.*, **4**, 997 (1994).
22. Renn, S.R. and Lubensky, T.C., *Phys. Rev. A*, **38**, 2132 (1988).
23. Goodby, J.W., Waugh, M.A., Stein, S.M., Chin, E., Pindak, R. and Patel, J.S., *J. Am. Chem. Soc.*, **111**, 8119-8125 (1989).
24. Renn, S.R., *Phys. Rev. A*, **45**, 953 (1992)
25. Navailles, L., Barois, P. and Nguyen, H.T., *Phys. Rev. Lett.*, **71**, 545 (1993).
26. Collings, P.J. and Patel, J.S. (eds.), 'Handbook of Liquid Crystal Research', Oxford University Press, Oxford (1997).
27. Demus, D., Goodby, J., Gray, G.W., Spiess H.-W. and Vill V. (eds.), 'Handbook of Liquid Crystals, Vols. I-IV', Wiley-VCH (1998).
28. Tschierske, C., Brezesinski, G., Kuschel, F. and Zschke, H., *Mol. Cryst, Liq. Cryst. Lett.*, **7**, 131 (1990).
29. Dahn, U., Erdelen, C., Ringsdorf, H., Festag, R., Wendorff, J.H., Heiney, P.A. and Maliszewskyj, N.C., *Liquid Crystals*, **19**, 759 (1995).
30. Chandrasekhar, S., Sadashiva, B.K. and Suresh, K.A., *Pranama*, **9**, 471 (1977).
31. Andersch, J. and Tschierske, C., *Liquid Crystals*, **21**, 51 (1996).
32. Nguyen, H.T., Destrade, C. and Gasparoux, H., Fifth European Winter Liquid Crystal Conference on Layered and Columnar Mesomorphic Systems, Borovets, Bulgaria, Abstract A11 (1987).
33. Booth, C.J., Dunmur, D.A., Goodby, J.W., Haley, J. and Toyne, K.J., *Liquid Crystals*, **20**, 387 (1996).
34. Malthête, J., Nguyen, H.T. and Destrade, C., *Liquid crystals*, **13**, 171 (1993).
35. Nguyen, H.T., Destrade, C., Allouchi, H., Bideau, J.P., Cotrait, M., Guillon, D., Weber, P. and Malthête, J., *Liquid Crystals*, **15**, 435 (1993).
36. Bernal, J.D. and Crowfoot, D., *Trans. Faraday Soc.*, **29**, 1032 (1933).

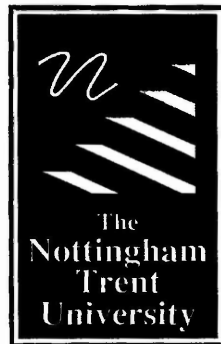
37. Leadbetter, A.J., Durrant, J.L.A. and Rugman, M., *Mol. Cryst. Liq. Cryst. Lett.*, **34**, 231 (1977).
38. Sage, I., 'Thermotropic Liquid Crystals - (Critical Reports on Applied Chemistry)', ed. Gray, G.W., John Wiley and Sons, Chichester, Vol. 22, Chap. 3 (1987).
39. Gray, G.W. and Goodby, J.W., 'Smectic Liquid Crystals', Leonard Hill, Glasgow and London (1984).
40. Demus, D. and Richter, L., 'Textures of Liquid Crystals', Verlag Chemie, Leipzig (1978).
41. Crooker, P.P., *Liquid Crystals*, **5**, 751 (1989).
42. Hückel, E., *Physik. Z.*, **22**, 561 (1921).
43. Sackmann, H. and Demus, D., *Mol. Cryst. Liq. Cryst.*, **21**, 239 (1973).
44. Cladis, P.E., *Phys. Rev. Lett.*, **35**, 48 (1975).
45. Byron, D.J., Matharu, A.S., Shirazi, S.N.R., Tajbakhsh, A.R. and Wilson, R.C., *Liquid Crystals*, **14**, 645 (1993).
46. Leadbetter, A.J., 'Thermotropic Liquid Crystals - (Critical Reports on Applied Chemistry)', ed. Gray, G.W., John Wiley and Sons, Chichester, Vol. 22, Chap. 1 (1987).
47. de Vries, A., *Mol. Cryst. Liq. Cryst.*, **10**, 361 (1970).
48. Levelut, A.M. and Lambert, M., *Compt. Rend. Acad. Sci. (Paris)*, **272**, 1018 (1971).
49. Goodby, J.W., *Mol. Cryst. Liq. Cryst. Lett.*, **75A**, 91 (1979).
50. Doucet, J. and Levelut, A.M., *J. Phys. (Paris)*, **38**, 1163 (1977).
51. Leadbetter, A.J., Gaughan, J.P., Kelly, B., Gray, G.W. and Goodby, J.W., *J. Phys. (Paris)*, **40**, 178 (1981).
52. Goodby, J.W., *Mol. Cryst. Liq. Cryst. Lett.*, **92**, 171 (1983).
53. Bowden, C.J., Herrington, T.M., Moseley, A.M. and Richardson, R., *Liquid Crystals*, **18**, 825 (1995).
54. Gray, G.W., Jones, B. and Marson, F., *J. Chem. Soc.*, 393 (1957).

55. Demus, D., Kunicke, G., Neelson, J. and Sackmann, H., *Z. Naturforsch.*, **23a**, **84** (1968).
56. Diele, S., Brant, P. and Sackmann H., *Mol. Cryst. Liq. Cryst.*, **17**, 163 (1972).
57. Lydon, J.E., *Mol. Cryst. Liq. Cryst.*, **72**, 79 (1981).
58. Levelut, A. and Clerc, M, *Liquid Crystals*, **24**, 105 (1998).
59. Demus, D. 'Handbook of Liquid Crystals', eds. Demus, D., Goodby, J., Gray, G.W., Spiess, H.-W. and Vill, V., Wiley, Vol. 1, Chap. 4 (1998).
60. Toyne, K.J., 'Thermotropic Liquid Crystals - (Critical reports on Applied Chemistry)', ed. Gray, G.W., John Wiley and Sons, Chichester, Vol. 22, Chap. 2 (1987).
61. Gray, G.W., 'Liquid Crystals and Plastic Crystals', eds. Gray, G.W. and Winsor, P.A., Ellis Horwood Ltd., Chichester, Vol. 1, Chap. 2 (1974).
62. Gray, G.W., Hartley, J.B. and Jones, B., *J. Chem. Soc.*, 1412 (1955).
63. Gray, G.W. and McDonnell, D.G., *Mol. Cryst. Liq. Cryst.*, **53**, 147 (1979).
64. Gray, G.W. and Worrall, B.M., *J. Chem. Soc.*, 1545 (1959).
65. Gray, G.W. and Jones, B., *J. Chem. Soc.*, 683 (1954).
66. Gray, G.W., Hird, M., Lacey, D. and Toyne, K.J., *J. Chem. Soc. Perkin Trans. 2*, 2041 (1989).
67. Gray, G.W., Hird, M., Lacey, D. and Toyne, K.J., *Mol. Cryst. Liq. Cryst.*, **172**, 165 (1989).
68. Gray, G.W., Hird, M. and Toyne, K.J., *Mol. Cryst. Liq. Cryst.*, **204**, 43 (1991).
69. Goulding, M.J. and Greenfield, S., *Liquid Crystals*, **13**, 345 (1993).
70. Hird, M., Toyne, K.J., Gray, G.W., McDonnell, D.G. and Sage, I.C., *Liquid Crystals*, **18**, 1 (1995).
71. Balkwill, P., Bishop, D., Pearson, A. and Sage, I.C., *Mol. Cryst. Liq. Cryst.*, **123**, 1 (1985).
72. Carr, N, Gray, G.W. and McDonnell, D.G., *Mol. Cryst. Liq. Cryst.*, **97**,

- 13 (1983).
73. Kelly, S.M., *Liquid Crystals*, **5**, 171 (1989).
74. Gray, G.W., Hird, M. and Toyne, K.J., *Mol. Cryst. Liq. Cryst.*, **195**, 221 (1991).
75. Uchida, T., *Mol. Cryst. Liq. Cryst.*, **104**, 1 (1984).
76. Scheffer, T.J. and Nehring, J., *Appl. Phys. Lett.*, **45**, 1021 (1984).
77. Valasek, J., *Phys. Rev.*, **17**, 475 (1921).
78. Demus, D., Demus, H. and Zschke, H., 'Flüssige Kristalle in Tabellen', VEB Deutscher Verlag Für Grundstoffindustrie, Leipzig, German Democratic Republic, Vol. II (1984).
79. Uhlenbroek, J.H. and Bijloo, J.D., *Rec. Trav. Chim. Pays-Bas.*, **79**, 1181 (1960).
80. Asano, T., Ito, S., Saito, N. and Hatakeda, K., *Heterocycles*, **6**, 317 (1977).
81. Jayasuriya, N. and Kagan, J. *Heterocycles*, **10**, 2901 (1986).
82. Crisp, G.T., *Synth. Commun.*, **19**, 307 (1989).
83. Seed, A.J., Toyne, K.J. and Goodby, J.W., *J. Mater. Chem.*, **5**, 653 (1995).
84. Tamao K., Kodama S., Nakajima I., Kumada M., Minato A. and Suzuki K., *Tetrahedron*, **38**, 3347 (1982).
85. Huang-Minlon, *J. Am. Chem. Soc.*, **68**, 2487 (1946).
86. Miller, R.L., Lykos, P.G. and Schmersing, H.N., *J. Am. Chem. Soc.*, **84**, 4623 (1962).
87. Zschke, H., *J. Prakt. Chem.*, **317**, 617 (1975).
88. Collings, P.J. and Hird, M., 'Introduction to Liquid Crystals Chemistry and Physics', Taylor and Francis Ltd, London (1997).
89. Kelly, S.M. and Fünfschilling, J., *J. Mater Chem.*, **4**, 1673 (1994).
90. Kelly, S.M. and Fünfschilling, J., *Liquid Crystals*, **19**, 519 (1995).
91. Yokoyama, M., Yoshida, S. and Imamoto, T., *Synthesis*, 591 (1982).

92. Tschaen, D.M., Desmond, R., King, A.O., Fortin, M.C., Pipik, B., King, S. and Verhoeven, T.R., *Synth. Commun.*, **24**, 887 (1994).
93. Sandler, S.R. and Karo, W., 'Organic Functional Group Preparation', Academic Press, New York, Vol. 3, Chap. 8 (1972)
94. Neilson, D.G., 'The Chemistry of Functional Groups -The Chemistry of Amidines and Imidates', John Wiley, and Sons, London, Ed. Patai, S., Chap. 9 (1975).
95. Snieckus, V.J., *Chem. Rev.*, **90**, 879 (1990).
96. Reiffenrath, V., Krause, J., Plach, H.J. and Weber, G., *Liquid Crystals*, **5**, 159 (1989).
97. Brooke, G.M., Burdon, J. and Tatlow, J.C., *J. Chem. Soc.*, 3253 (1962).
98. Lane, C.F., *Aldrichimica Acta*, **10**, 3 (1977).
99. Piancatelli, G., Scettri, A. and D'Auria, M., *Synthesis*, 245-258 (1982).
100. Banerji, K.K., *Bull. Chem. Soc. Jpn.*, **51**, 2732 (1978).
101. Banerji, K.K., *J. Chem. Soc. Perkin Trans. 2*, 639 (1978).
102. Walker, B.J., 'Organophosphorus Chemistry', William Clowes and Sons Limited, London, Chap. 4 (1972).
103. Oikawa, Y., Nishi, T. and Yonemitsu, O., *J. Chem. Soc. Perkin Trans. 1*, 7 (1985).
104. McSherry, I., The Nottingham Trent University, PhD Thesis (1996).
105. Partridge, M.W. and Turner, H.A., *J. Pharm. and Pharmacol.*, **5**, 111-116 (1953).
106. Partridge, M.W., *J. Chem. Soc.*, **44**, 3043-6 (1949).
107. Goodby, J.W., Hird, M., Lewis, R.A. and Toyne, K.J., *Chem. Commun.*, 2719 (1996)
108. Miyaura, N., Yanagi, T. and Suzuki, A., *Synth. Commun.*, **11**, 513 (1981).
109. Davies, D.T., 'Aromatic Heterocyclic Chemistry', Oxford University Press, Oxford (1995).

110. Taylor, R., 'Electrophilic Aromatic Substitution', John Wiley and Sons, Chichester, Chap. 9 (1990).
111. Hird, M., Toyne, K.J. and Gray, G.W., *Liquid Crystals*, **14**, 741 (1993).
112. Hawkins, R.T., Lennarz, W.J. and Synder, H.R., *J. Am. Chem. Soc.*, **82**, 3053 (1960).
113. Hird, M., Gray, G.W. and Toyne, K.J., *Mol. Cryst. Liq. Cryst.*, **206**, 187 (1991).
114. Thompson, W.J. and Gaudino, J., *J. Org. Chem.*, **49**, 5237 (1984).
115. Martin, A.R. and Yang, Y., *Acta. Chem. Scand.*, **47**, 221 (1993).
116. Kuivila, H.G., Reuwer, J.F. and Margravite, J.A., *Can. J. Chem.*, **41**, 3080 (1963).
117. Segelstein, B.E., Butler, T.W. and Chenard, B.L., *J. Org. Chem.*, **60**, 12 (1995).
118. Kong, K.-C. and Cheng, C.-H., *J. Am. Chem. Soc.*, **113**, 6313 (1991).
119. Hird, M., Toyne, K.J. and Gray, G.W., *Liquid Crystals*, **16**, 625 (1994).
120. Huff, B.E., Koenig, T.M., Mitchell, D. and Staszak, M.A., *Org. Synth.*, **75**, 53 (1997).
121. Goodson, F.E., Wallow, T.I. and Novak, B.M., *Org. Synth.*, **75**, 61 (1997).
122. Schank, K., 'The Chemistry of Functional Groups -The Chemistry of Diazonium and Diazo Groups', John Wiley, and Sons, London, Ed. Patai, S., Part 2, Chap. 14 (1978).
123. Wulfman, D.S., 'The Chemistry of Functional Groups -The Chemistry of Diazonium and Diazo Groups', John Wiley, and Sons, London, Ed. Patai, S., Part 1, Chap. 8 (1978).
124. Coates, D., *Liquid Crystals*, **2**, 423 (1987).
125. Shirazi, S.N.R., The Nottingham Trent University, Ph.D Thesis (1993).



Libraries & Learning Resources

The Boots Library: 0115 848 6343
Clifton Campus Library: 0115 848 6612
Brackenhurst Library: 01636 817049